UC San Diego

UC San Diego Electronic Theses and Dissertations

Title

Multimodal Neuroimaging Integration using fMRI and MEG in Youth with Autism Spectrum Disorder

Permalink

https://escholarship.org/uc/item/5kt6293p

Author

Wilkinson, Molly

Publication Date

2024

Peer reviewed|Thesis/dissertation

eScholarship.org Powered by the California Digital Library
University of California

UNIVERSITY OF CALIFORNIA SAN DIEGO

SAN DIEGO STATE UNIVERSITY

Multimodal Neuroimaging Integration using fMRI and MEG in Youth with Autism Spectrum Disorder

A dissertation submitted in partial satisfaction of the requirements
for the degree Doctor of Philosophy

in

Clinical Psychology

by

Molly Wilkinson

Committee in charge:

University of California San Diego

Professor Frank Haist
Professor Bradley Voytek

San Diego State University

Professor Ralph-Axel Müller, Chair
Professor Annika Linke
Professor Ksenija Marinkovic

2024

Copyright

Molly Wilkinson, 2024

All rights reserved.

The dissertation of Molly Wilkinson is approved, and it is acceptable in quality and form for publication on microfilm and electronically.

_____

_____

_____

_____

_____
Chair

University of California San Diego

San Diego State University

2024

TABLE OF CONTENTS

Dissertation Approval Page iii

Table of Contents iv

List of Figures vi

List of Tables vii

Acknowledgements ix

Vita x

Abstract of the Dissertation xii

Introduction 1

Chapter 1 Study 1 22

- Abstract 23
- Introduction 24
- Methods 26
- Results 35
- Discussion 39
- Supplemental Materials 53

Chapter 2 Study 2 102

- Abstract 103
- Introduction 105
- Methods 109
- Results 117
- Discussion 122
- Supplemental Materials 143

Chapter 3 Study 3 149

Abstract 150
Introduction 152
Methods 157
Results 162
Discussion 164
Supplemental Materials 185
Conclusion 197
References 206

LIST OF FIGURES

Figure 1.1 aMEG-derived and fMRI-derived ROIs in surface and volumetric space 47
Figure 1.2 Significant differences in theta power and BOLD signal in aMEG-and fMRI-derived ROIs 48
Figure 2.1 ROIs in surface and volumetric space 138
Figure 2.2 fMRI and MEG measures of activation in TD and ASD groups 139
Figure 2.3 fMRI and MEG laterality index in TD and ASD groups 141
Figure 3.1 Regions with significant group differences for Hurst exponent and aperiodic exponent 183
Figure 3.2 Regions with significant correlations between rs-fMRI HE and rs-MEG AE 184
Supplemental Figure 1.1 Group means of theta power 84
Supplemental Figure 1.2 Group means of BOLD signal 86
Supplemental Figure 1.3 Theta power and BOLD signal correlations 88
Supplemental Figure 1.4 Group means of theta power in sample with outliers removed 90
Supplemental Figure 1.5 Group means of BOLD signal in sample with outliers removed 92
Supplemental Figure 1.6 Group means of theta power in motion-matched sample 94
Supplemental Figure 1.7 Group means of BOLD signal in motion-matched sample 96
Supplemental Figure 1.8 Group means of theta power in sample with <150-day scan interval 98
Supplemental Figure 1.9 Group means of BOLD signal in sample with <150-day scan interval 100
Supplemental Figure 2.1 Lexicosemantic task performance by group for fMRI and MEG scans 144
Supplemental Figure 2.2 Pearson partial correlations for MEG N250m and N400m and fMRI BOLD signal 145

LIST OF TABLES

Table 1.1 Significant differences in theta power and BOLD signal in aMEG-and fMRI-derived ROIs 50
Table 1.2 ANOVA comparisons of event-related theta power and BOLD signal 51
Table 2.1 Participant demographics 135
Table 2.2 Demographics of high and low performers 136
Table 2.3 Pearson partial correlations for fMRI and MEG indices of activation 137
Table 3.1 Participant demographics for fMRI analyses 173
Table 3.2 Participant demographics for MEG analyses 174
Table 3.3 Participant demographics for fMRI-MEG correlations 175
Table 3.4 GLM analysis results for rs-fMRI Hurst exponent 176
Table 3.5 Pearson partial correlations for rs-fMRI HE and ASD symptomology (ADOS-2 Total & SRS-2 Total) 177
Table 3.6 GLM analysis results for rs-MEG aperiodic exponent 178
Table 3.7 Pearson partial correlations between rs-MEG AE and ASD symptomology 181
Table 3.8 Regions with significant Pearson partial correlations for rs-fMRI HE and rs-MEG AE 182
Supplemental Table 1.1 Medications and psychological conditions 58
Supplemental Table 1.2 Task stimuli word conditions 59
Supplemental Table 1.3 Participant demographics for fMRI-derived ROI selection 60
Supplemental Table 1.4 fMRI-derived ROIs 61
Supplemental Table 1.5 ROI modifications 62
Supplemental Table 1.6 Pearson partial correlations for BOLD signal and theta power in aMEG-derived ROIs 63
Supplemental Table 1.7 Pearson partial correlations for BOLD signal and theta power in fMRI-derived ROIs 64
Supplemental Table 1.8 ANOVA comparisons of theta power and BOLD signal in sample with outliers removed 66
Supplemental Table 1.9 Pearson partial correlations for BOLD signal and theta power in aMEG-derived ROIs in sample with outliers removed 68
Supplemental Table 1.10 Pearson partial correlations for BOLD signal and theta power in fMRI-derived ROIs in sample with outliers removed 70
Supplemental Table 1.11 Participant demographics in motion-matched sample 72
Supplemental Table 1.12 ANOVA comparisons of theta power and BOLD signal in motion-matched sample 73

Supplemental Table 1.13 Pearson partial correlations for BOLD signal and theta power in aMEG-derived ROIs in motion-matched sample 75

Supplemental Table 1.14 Pearson partial correlations for BOLD signal and theta power in fMRI-derived ROIs in motion-matched sample 76

Supplemental Table 1.15 Participant demographics in sample with <150-day scan interval 78

Supplemental Table 1.16 ANOVA comparisons of theta power and BOLD signal in sample with <150-day scan interval 79

Supplemental Table 1.17 Pearson partial correlations for BOLD signal and theta power in MEG-derived ROIs in sample with <150-day scan interval 81

Supplemental Table 1.18 Pearson partial correlations for BOLD signal and theta power in fMRI-derived ROIs in sample with <150-day scan interval 82

Supplemental Table 3.1 Medications and psychological conditions 186

Supplemental Table 3.2 Participant demographics for fMRI analyses - Male-only subgroup....188

Supplemental Table 3.3 Participant demographics for MEG analyses – Male-only subgroup ...189

Supplemental Table 3.4 Participant demographics for fMRI-MEG correlations – Male-only subgroup 190

Supplemental Table 3.5 GLM analysis results for rs-fMRI Hurst exponent – Male-only subgroup 191

Supplemental Table 3.6 Pearson partial correlations for rs-fMRI HE and ASD symptomology (ADOS-2 Total & SRS-2 Total) – Male-only subgroup.....191

Supplemental Table 3.7 GLM analysis results for rs-MEG aperiodic exponent – Male-only subgroup 193

Supplemental Table 3.8 Pearson correlations between rs-MEG AE and ASD symptomology – Male-only subgroup 195

Supplemental Table 3.9 Regions with significant Pearson partial correlations for rs-fMRI HE and rs-MEG AE – Male-only subgroup 196

ACKNOWLEDGEMENTS

I would like to acknowledge the chair of my committee, Dr. Ralph-Axel Müller, members of the SDSU Brain Development Imaging Labs, and my many supervisors for their support and guidance over the last six years.

Chapter 1, in full, is a reprint of the material as it appears in *Neuroimage: Reports, 2(4), 100134.* Wilkinson, M., Jao Keehn, R. J., Linke, A. C., You, Y., Gao, Y., Alemu, K., Correas, A., Rosen, B. Q., Kohli, J. S., Wagner, L., Sridhar, A., Marinkovic, K., & Müller, R.-A. (2022). The dissertation author was the primary investigator and author of this paper.

Chapter 2, in full, is currently being prepared for submission for publication of the material. Wilkinson, M., Linke, A. C., You, Y., Marinkovic, K., Müller, R.-A., & Jao Keehn, R. J. The dissertation author was the primary researcher and author of this paper.

Chapter 3, in full, is currently being prepared for submission for publication of the material. Wilkinson, M., Jao Keehn, R. J., You, Y., Preston, M., Marinkovic, K., Müller, R.-A, Voytek, B., & Linke, A. C. The dissertation author was the primary researcher and author of this material.

VITA

2018 Bachelor of Science in Behavioral Neuroscience
Northeastern University

2021 Master of Science in Clinical Psychology
San Diego State University
Thesis: fMRI BOLD and MEG theta power reflect complementary aspects of activity during lexicosemantic decision in adolescents with ASD
Chair: Ralph-Axel Müller, Ph.D.

2024 Clinical Psychology Pre-Doctoral Internship
Kennedy Krieger Institute / Johns Hopkins School of Medicine
Major Area of Study: Pediatric Neuropsychology / Behavioral Psychology

2024 Doctor of Philosophy in Clinical Psychology
San Diego State University / University of California San Diego
Major Area of Study: Clinical Neuropsychology
Emphasis: Child and Adolescent Psychopathology
Dissertation: Multimodal neuroimaging integration using fMRI and MEG in youth with autism spectrum disorder
Chair: Ralph-Axel Müller, Ph.D.

PUBLICATIONS

Kohli, J., Linke, A.C., Martindale, I., **Wilkinson, M.,** Kinnear, M.K., Lincoln, A., Hau, J., Shryock, I., Omaleki, V., Alemu, K., Pedrahita, S., Fishman I., Müller, R.-A., & Carper, R. (2024). Associations between atypical intracortical myelin content and neuropsychological functions in middle to older aged adults with ASD. *Brain and Behavior, 14*(6), e3594.

Wilkinson, M., Jao Keehn, R. J., Linke, A. C., You, Y., Gao, Y., Alemu, K., Correas, A., Rosen, B. Q., Kohli, J. S., Wagner, L., Sridhar, A., Marinkovic, K., & Müller, R.-A. (2022). fMRI BOLD and MEG theta power reflect complementary aspects of activity during lexicosemantic decision in adolescents with ASD. *Neuroimage: Reports, 2*(4), 100134.

Hau, J., Baker, A., Chaaban, C., Kohli, J. S., Jao Keehn, R. J., Linke, A. C., Mash, L. E., **Wilkinson, M.**, Kinnear, M. K., & Müller, R.-A. (2022). Reduced asymmetry of the hand knob area and decreased sensorimotor u-fiber connectivity in middle-aged adults with autism. *Cortex, 153*, 110-125.

Mash, L. E., Linke, A. C., Gao, Y., **Wilkinson, M.,** Olson, M. A., Jao Keehn, R. J., & Müller, R.-A. (2022). BOLD lag patterns differ between rest and task conditions, but are largely typical in autism. *Brain Connectivity, 12*(3). 234-245.

Pond, H. L., Heller, A. T., Gural, B. M., McKissick, O. P., **Wilkinson, M. K.,** Manzini, M. C. (2021). Digging behavior discrimination test to probe burrowing and exploratory digging in male and female mice. *Journal of Neuroscience Research, 99*(9), 2046-2058.

Linke, A. C., Mash, L. E., Fong, C., Kinnear, M. K., Kohli, J.S., **Wilkinson, M.,** Tung, R., Jao Keehn, R. J., Carper, R., Fishman, I., & Müller, R.-A. (2020). Dynamic time warping outperforms Pearson correlation in detecting atypical functional connectivity in autism spectrum disorders. *Neuroimage,* 117383.

Zamarbide, M., Mossa, A., Muñoz-Llancao, P., **Wilkinson, M. K.,** Pond, H. L., Oaks, A. W., & Manzini, C. (2019). Male-specific cAMP signaling in the hippocampus controls spatial memory deficits in a mouse model of autism and intellectual disability. *Biological Psychiatry*, *85*, 760-768.

Wang, R.*, **Wilkinson, M.***, Kane, T., & Takahashi, E. (2017). Convergence of cortical, thalamocortical, and callosal pathways during human fetal development revealed by diffusion MRI tractography. *Frontiers in Neuroscience*, *11*, 576. *co-first authors.

Wilkinson, M., Lim, A.R., Cohen, A.H., Galaburda, A.M., & Takahashi, E. (2017). Detection and growth pattern of arcuate fasciculus from newborn to adult. *Frontiers in Neuroscience*, *11*, 389.

Wilkinson, M., Kane, T., Wang, R., & Takahashi, E. (2017). Migration pathways of thalamic neurons and development of thalamocortical connections in humans revealed by diffusion MR tractography. *Cerebral Cortex, 27*(12), 5683-5695.

Cohen, A.H., Wang, R., **Wilkinson, M.**, MacDonald, P., Lim, A.R., & Takahashi, E. (2016). Development of human white matter fiber pathways: From newborn to adult ages. *International Journal of Developmental Neuroscience*, *50*, 26-38.

Wilkinson, M., Wang, R., van der Kouwe, A., & Takahashi, E. (2016). White and gray matter fiber pathways in autism spectrum disorder revealed by ex vivo diffusion MR tractography. *Brain and Behavior*, *6*(7), e00483.

ABSTRACT OF THE DISSERTATION

Multimodal Neuroimaging Integration Using fMRI and MEG in Youth with Autism Spectrum Disorder

by

Molly Wilkinson

Doctor of Philosophy in Clinical Psychology

University of California San Diego, 2024
San Diego State University, 2024

Professor Ralph-Axel Müller, Chair

Autism spectrum disorder (ASD) is a neurodevelopmental disorder that has been extensively studied using functional magnetic resonance imaging (fMRI). Studies have been mostly unimodal, with inconsistent findings. Combining fMRI with magnetoencephalography (MEG) is critical in accounting for dynamic aspects of brain activity, taking advantage of the high spatial vs. temporal resolution of each modality. The three-paper dissertation compares fMRI and MEG data from 12- to 21-year-olds with and without ASD. Study 1 (Wilkinson et al., 2022) compared fMRI BOLD signal and MEG event-related theta power in 33 ASD and 23

typically developing (TD) youth during a lexicosemantic task. Greater theta power was seen in the ASD group across several regions, whereas the BOLD signal was greater for the ASD group only in the anterior cingulate. No significant correlations were found between BOLD signal and theta power. Study 2 examined the relationship of N250m and N400m with fMRI BOLD signal in 30 ASD and 20 TD youth during lexicosemantic performance. The high-performing ASD subgroup had greater N250m in the inferior frontal region, and more bilateral N400m in inferior frontal and temporal regions. The low-performing ASD subgroup showed decreased N400m. fMRI BOLD signal did not show any significant group differences. Positive correlations between fMRI and MEG in multiple regions were seen predominantly in the low-performing ASD subgroup. Study 3 examined the relationship between two measures of the excitation:inhibition (E:I) ratio in adolescents with and without ASD. The Hurst exponent (HE) was estimated from resting-state fMRI data (34 ASD, 28 TD) and was found to be mostly increased in the ASD group. The aperiodic exponent (AE) was measured from resting-state MEG data (33 ASD, 22 TD) and was found to be greater in the ASD group across many brain regions. However, there was no clear relationship between fMRI HE and MEG AE. Overall findings from this dissertation indicate no clear relationship between fMRI and MEG, suggesting the two modalities are measuring distinct, yet complementary neural processes.

INTRODUCTION

Autism spectrum disorder (ASD) is a neurodevelopmental disorder defined by impaired social communication and the presence of restricted and/or repetitive behaviors (American Psychiatric Association, 2013). Prevalence is increasing with 1 in 36 children having a diagnosis of ASD (Maenner et al., 2023). ASD can be reliably diagnosed as early as 14 months (Pierce et al., 2019) and various hypotheses exist on the etiology, ranging from environmental to genetic causes (Amaral, 2017). Diagnostic measures remain exclusively behavioral, relying on reports and observations, and there are discrepancies in age of diagnosis across racial/ethnic, socioeconomic, and gender groups (Lord et al., 2018). Research examining objective indices as potential biomarkers (i.e., brain activity and organization) will enhance early and accurate diagnoses, rather than being forced to strictly rely on behavioral assessments that were created and normed without the use of diverse study populations.

ASD can affect several functional domains, such as sociability (American Psychiatric Association, 2013), language (Arunachalam & Luyster, 2016; Boucher, 2012; Loucas et al., 2008; Matson et al., 2012; Norbury et al., 2010; Tager-Flusberg, 2000), executive functioning (Berard et al., 2017; Craig et al., 2016; Hill, 2004; S. M. Hutchison et al., 2020; T. May et al., 2013; Robinson et al., 2009), motor control (Ming et al., 2007), and daily living skills/independence (Liss et al., 2001). The spectrum includes individuals with various levels of functioning, with each person demonstrating a unique profile of strengths and weaknesses (Masi et al., 2017). Early diagnosis and intervention are known to improve the long-term success of those with ASD (Elder et al., 2017).

Language and Executive Function

Although no longer included in the current diagnostic criteria for ASD, many individuals present with language delay and impairments, including lexicosemantic difficulties (Boucher, 2012; Condouris et al., 2003; Haebig et al., 2015; Henderson et al., 2011; Kamio et al., 2007; Löfkvist et al., 2014; Naigles & Tek, 2017; Salem et al., 2021). Lexicosemantic processing involves word meanings and relationships. Characteristics of lexicosemantic processing in the ASD population include smaller expressive and receptive vocabularies (Löfkvist et al., 2014), greater lexicosemantic than syntactic impairment (Naigles & Tek, 2017), and lower performance on neuropsychological assessments of lexicosemantics (Condouris et al., 2003). Lexicosemantic abilities and deficits vary across ages and functioning level of the ASD population (Boucher, 2012).

Another domain impacted in ASD is executive function (Craig et al., 2016; Hill, 2004; Robinson et al., 2009). Executive function, also referred to as cognitive control, is a cognitive domain focused on goal-directed behavior, and includes a number of functional skills such as inhibition, working memory, and shifting (Best & Miller, 2010; Lehto et al., 2003). Executive functioning difficulties are common in ASD and can exacerbate the effect of social communication difficulties and restrictive/repetitive behaviors on daily functioning.

There is a clear relationship between executive function and language, with higher executive function abilities coinciding with higher language skills in typically developing (TD) individuals (Friedman & Sterling, 2019; J. Hall et al., 2017; Joseph et al., 2005; Kaushanskaya et al., 2017; Weismer et al., 2018). To reflect the close relationship of language and executive functioning, many of the language tasks used in the neuroimaging literature include an executive function component that is necessary for successful performance on the task. Executive

functioning in children and adolescents with ASD is related to activation in inferior frontal and anterior cingulate gyri during inhibition, middle occipital gyrus during updating, and decreased activity in middle temporal gyrus during switching (Yerys et al., 2015; Zhang et al., 2020). There are inconsistencies in the literature regarding executive function in ASD due to studies often combining age groups, without taking developmental changes in executive functioning into consideration (Zhang et al., 2020). One must also bear in mind the diversity of cognitive processes that fall under the umbrella of executive functioning. Using tasks that clearly differentiate between the diverse subfunctions is critical for a clear understanding of neural activation. Without a clear differentiation, it is difficult to understand how executive function in individuals with ASD is different from TD peers.

Functional Magnetic Resonance Imaging

Functional magnetic resonance imaging (fMRI), which measures changes in the blood-oxygen-level-dependent (BOLD) signal, has been the method of choice in the study of task-related and resting-state brain activity for decades. fMRI has good spatial resolution, yet temporal resolution is poor, primarily because it relies on a slow hemodynamic response that peaks about five seconds after corresponding neuronal activity change. The BOLD signal provides information about task-related or spontaneous activity through measuring change in the deoxygenated hemoglobin concentration (Glover, 2011). Functional neuroimaging research on ASD has been dominated by fMRI, yet with inconsistent findings. Inconsistencies can be found in fMRI studies of task-related and resting-state activity and connectivity. Network dysfunction and abnormal connectivity are common features observed in ASD, but findings have varied, with reports of both over- and under-connectivity (Hull et al., 2018; Rane et al., 2015), preventing definitive conclusions on the direction and profile of atypicality. Most ASD studies examine only

resting-state fMRI, rather than integrating task and rest data, limiting understanding of neural activity.

fMRI Studies of Language in ASD

As described above, individuals with ASD often present with language difficulties. Deficits observed behaviorally through assessments and tasks are associated with atypical neural activity reflected in fMRI studies (Cermak et al., 2022). fMRI research on lexicosemantic processing and cognitive control in TD adolescents shows activation within a distributed network, involving inferior frontal, lateral temporal, prefrontal, and anterior cingulate regions (Blumenfeld et al., 2006; Chou et al., 2006; Moore-Parks et al., 2010). Similar regions, such as inferior frontal (Broca's area), temporal (Wernicke's area), and visual cortices, have also been observed to be activated in individuals with ASD during language and cognitive control tasks, yet activation patterns are atypical (Gaffrey et al., 2007; Herringshaw et al., 2016; Shen et al., 2012). There is consistent evidence for abnormally increased activity in the visual regions during language tasks (Gaffrey et al., 2007; Herringshaw et al., 2016; Shen et al., 2012) and decreased connectivity between frontal and temporal language regions during language processing and cognitive control in those with ASD (Y. Lee et al., 2017).

Despite many fMRI studies on lexicosemantics in individuals with ASD, findings are often not replicated or contradictory. For example, one study reported decreased connectivity between frontal and temporal language areas (Knaus et al., 2008), while another reported overconnectivity (Shen et al., 2012). Similar discrepancies in activity patterns are also seen in Broca's area, with studies reporting both increased (Knaus et al., 2008) and decreased activity (Gaffrey et al., 2007; Harris et al., 2006) in individuals with ASD when completing a language task. Conflicting reports of both increased (Gaffrey et al., 2007; Harris et al., 2006) and

decreased (Boddaert et al., 2004) activity in the temporal (Wernicke's) area have been published as well. Differences in activation may be a reflection of a number of variables, such as age of participants, task used, ASD symptom profile, or fMRI methodology. Nonetheless, it is still crucial to resolve the discrepancies in lexicosemantic processing in ASD studies, as it prevents understanding of neural networks which can provide critical information for diagnosis, biomarkers, and interventions.

Lateralization

An important aspect of functional brain organization for language, including lexicosemantics, is hemispheric lateralization. In most neurotypical individuals, language is predominantly lateralized to the left hemisphere, especially language processing regions such as Broca's and Wernicke's areas (Holland et al., 2007). Atypical language laterality is one of the few strongly replicated findings in ASD neuroimaging research, and both functional and structural differences have been found (Gage et al., 2009; Herringshaw et al., 2016; Jouravlev et al., 2020; Kleinhans et al., 2008; Knaus et al., 2008, 2010; Lindell & Hudry, 2013; Mody et al., 2013; Nielsen et al., 2014; Takeuchi et al., 2004).

With regard to functional lateralization, individuals with ASD frequently show atypical rightward or bilateral activity during language tasks. For example, Knaus et al. (2010) reported atypical language laterality was more prevalent in adolescents with ASD compared to TD peers, when completing a language task. Another study reported that differences in laterality between ASD and TD individuals may depend on the type of task. Kleinhans et al. (2008) examined laterality in adolescents with and without ASD during letter and category fluency tasks. During the letter fluency task, the ASD group showed more activity in the right frontal and temporal language areas, along with more impaired performance, compared to TD group. On the other

hand, the ASD and TD groups were similar in laterality during the category fluency task, with TD participants also showing right hemisphere activation. The ASD group did not show as great of an impairment during category fluency as they did during the letter fluency task. This study indicates that individuals with ASD may perform worse on language tasks that are strongly left lateralized in TD individuals, such as letter fluency. These differences in laterality can even be seen early in development, with toddlers (12- to 48-month-olds) with ASD showing decreased left hemisphere activity in response to speech sounds during natural sleep (Eyler et al., 2012a). This study also found rightward lateralization in the temporal cortex increased with age, with 3- to 4-year-old children showing the greatest atypical lateralization.

Despite atypical language lateralization being one of the most frequently replicated findings in ASD neuroimaging research, it is not fully established whether it is caused by decreased activity in the left hemisphere, increased activity in the right hemisphere, or both (Jouravlev et al., 2020). Instead of using group-level activation maps, such as many previous studies of laterality, Jouravlev and colleagues (2020) used a volume-based measure of lateralization at the individual level. Using this approach, the study supports atypical lateralization in ASD is a result of increased right hemispheric activity. Less lateralized responses were also found in neurotypical individuals with a high level of ASD traits, specifically in the communication domain. Additionally, they assessed for lateralization differences in the theory of mind network and an executive function network and found that atypical lateralization is specific to the language network. Although many studies look at functional activation in specific brain regions associated with language, laterality differences also exist at the functional connectivity level during resting-state (Cardinale et al., 2013; Nielsen et al., 2014).

fMRI Studies of Resting-State in ASD

Resting-state fMRI (rsfMRI) measures functional activity and neuronal network organization and connectivity in the absence of a task (Lv et al., 2018). rsfMRI studies have highlighted differences in organization and connectivity in ASD (Anderson, 2013; Guo et al., 2017; Hull et al., 2018; Maximo et al., 2013; Weng et al., 2010; Yao et al., 2021). Functional connectivity is one measure of neuronal organization that compares timeseries of different regions to understand connectivity of brain regions. Generally, studies support local overconnectivity and global underconnectivity in ASD (Anderson, 2013). Decreased connectivity is found within the default mode network, a network of regions active during rest, and has been replicated across many studies (Anderson, 2013; Hull et al., 2018; Maximo et al., 2013; Weng et al., 2010; Yao et al., 2021). The language network has also been studied using rsfMRI in individuals with ASD. Functional underconnectivity between Broca and Wernicke's areas has been linked to lower language abilities in youth with ASD (Verly et al., 2014). This study also found that a majority of ASD children in the sample lacked the arcuate fasciculus in the right hemisphere, a white matter tract connecting the two language regions. Compared with TD individuals, adolescents with ASD show decreased connectivity in Broca's area, while adults with ASD show decreased connectivity in Wernicke's area and increased connectivity in the left middle temporal gyrus (Y. Lee et al., 2017). When examining the relationship between language regions and other areas of the brain, children with ASD show increased functional connectivity between language and visual regions (Y. Gao et al., 2019). Increased connectivity between these two regions was related to lower language abilities.

Another measure of neuronal organization that can be obtained from rsfMRI is intrinsic neural timescales, a reflection of local neural dynamics indicating how long information is stored

in a neural region. Longer timescales are found in brain regions that integrate information and perform higher-order functions, such as frontal and parietal regions that are involved in decision making, memory, and emotions. This is in comparison to the shorter timescales found in sensory regions, involved in perception and movement (Gollo, 2018). One study found shorter timescales, which were correlated with ASD severity, in bilateral postcentral gyri and right inferior occipital gyrus and longer timescales, correlated with restricted/repetitive behaviors, in the right caudate in adolescents with ASD compared with TD peers (Watanabe et al., 2019).

Newer data science techniques have been used in rsMRI studies to classify individuals with ASD. One study examined resting-state data from individuals with ASD, their TD siblings, and TD peers (Yamagata et al., 2019). Using a machine learning approach, they identified functional connections between several regions that distinguished individuals with ASD and their siblings from TD peers, and one of these connections distinguished ASD from TD peers (connection between the right medial temporal gyrus and right anterior cingulate cortex). Yang et al. (2022) also used machine learning methods for ASD classification and reported underconnectivity in ASD between the frontal and temporal lobes. Another study used a deep neural network model to identify 32 functional connections in ASD adolescents, with 13 of these connections showing a significant difference in comparison to TD peers (Guo et al., 2017). There is clear potential for data science methods to be applied to ASD neuroimaging research.

fMRI Measure of E:I Imbalance in ASD

A balance of neuronal excitatory and inhibitory activity is necessary for typical brain development and processing. Excitatory and inhibitory activity rely on glutamate and GABA, respectively, with a balance represented as 2-6 times greater inhibitory activity compared to excitatory (Alvarez & Destexhe, 2004; Xue et al., 2014). Balance is achieved through several

factors, such as development of excitatory and inhibitory synapses, downstream signaling pathways, and cellular abnormalities (E. Lee et al., 2017). Imbalances in E:I activity have been linked to neuropsychiatric disorders, such as ASD (Bruining et al., 2020; Dani et al., 2005; Mariani et al., 2015; Rubenstein & Merzenich, 2003; R. X. Smith et al., 2018; Trakoshis et al., 2020), attention-deficit hyperactivity disorder (Mamiya et al., 2021), and schizophrenia (Molina et al., 2020). Studies have found individuals with ASD to have an increased level of excitatory activity, or decreased inhibitory abilities, resulting in an E:I imbalance (Bruining et al., 2020; R. X. Smith et al., 2018; Trakoshis et al., 2020). This imbalance relates to poor functional differentiation and increased noise in the brain, and may result from atypicalities at various levels of the nervous systems (Rubenstein & Merzenich, 2003; Sohal & Rubenstein, 2019). It is hypothesized that E:I imbalance in ASD is caused by either an increase in glutamatergic or a decrease in GABAergic neurotransmission (Uzunova et al., 2016). E:I imbalance is thought to be related to differences in functional connectivity and behavioral symptoms in ASD (Bruining et al., 2020; Hegarty et al., 2018; Nelson & Valakh, 2015; Rubenstein & Merzenich, 2003; Siegel-Ramsay et al., 2021; R. X. Smith et al., 2018; Sohal & Rubenstein, 2019). A recent study found that in children with ASD, a higher E:I ratio was correlated with higher symptom severity, as measured by the Social Responsiveness Scale (Bruining et al., 2020).

Mouse models of ASD have often been used to measure E:I imbalance due to the invasive nature of measuring excitatory and inhibitory activity (E. Lee et al., 2017; Sohal & Rubenstein, 2019). These studies have largely found that E:I imbalances are ameliorated by increasing inhibitory activity (Sohal & Rubenstein, 2019). For example, one study excited neurons in the medial prefrontal cortex, which led to atypical social behavior in the mice, as well as an increase in gamma power (Yizhar et al., 2011). Neuroimaging attempts to measure the E:I

ratio in humans have relied mostly on glutamate and GABA measures from magnetic resonance spectroscopy (MRS) and oscillations, particularly gamma band, measured from MEG (Dickinson et al., 2016; Port et al., 2019; Uzunova et al., 2016).

Hurst Exponent. There is a lack of non-invasive biomarkers for measuring the E:I ratio, as this has mostly been measured in animal models invasively. Mouse models and invasive measures traditionally used do not allow for studying the E:I ratio in humans and are typically restricted to studying a specific population of cells rather than E:I activity more globally. The Hurst exponent (HE), a measure obtained from the BOLD timeseries, measures the E:I ratio in a noninvasive manner, with decreases in HE reflecting increases in the E:I ratio (Lai et al., 2010; Trakoshis et al., 2020). Trakoshis and colleagues (2020) compared HE from rs-fMRI between adults with and without ASD. HE was found to be decreased in the ventromedial prefrontal cortex, reflecting an increased E:I ratio, in ASD males, but not in females with ASD. Gender differences in HE have also been identified in neurotypical adults (Dong et al., 2018). Another study found reduced HE in ASD participants in regions related to social function (amygdala, anterior insula, medial prefrontal cortex, and posterior cingulate cortex) when compared to TD individuals. They also reported a correlation between HE in multiple brain regions and ASD severity, with reduced HE correlated with increased severity (Lai et al., 2010). The fractal dimension, calculated from HE, was also found to be decreased in ASD adults during rs-fMRI, suggesting decreased signal complexity, and was also correlated with ASD symptom severity (Dona et al., 2017).

Summary of ASD fMRI Studies

fMRI has been a method of choice to study ASD functional activity and connectivity for decades. Findings have shown atypicalities in language regions, although with some

inconsistencies. Aside from atypical patterns of activation in specific brain regions during language tasks, typical patterns of language lateralization are often reversed or absent in ASD individuals. A measure of E:I ratio, H, is decreased in individuals with ASD during resting-state.

fMRI has excellent spatial resolution, allowing localization of multiple distributed foci of activation, but low temporal resolution due to the slow hemodynamic response. Combined use with techniques that measure neural activity more directly and at high temporal resolution is therefore ideal, as it unites both spatial and temporal benefits. However, the functional imaging literature in ASD (and beyond) has been almost exclusively single-modality studies and evidence capturing dynamics of neural activity at high spatial resolution remains sparse. The summarized findings in task-based language activation and lateralization and resting-state networks and E:I ratio, would benefit from integration of fMRI and MEG data to further solidify understanding of neural patterns in individuals with ASD.

Magnetoencephalography

Unlike fMRI, which measures neural activity indirectly through the hemodynamic response, MEG measures magnetic fields that are generated by the intracellular electrical currents in the brain (Singh, 2014). MEG has exquisite temporal resolution, detecting neural activity at the millisecond level, and allows reasonable spatial estimates (2-3 millimeters [mm]), compared to that of electroencephalography (EEG) (7-10mm) (Singh, 2014). Additionally, the magnetic fields measured through MEG are not impacted by the scalp, skull, cerebrospinal fluid, or brain, whereas the electrical fields detected by EEG are more vulnerable to distortion (Singh, 2014). MEG is therefore preferable to EEG in combined use with fMRI for comprehensive understanding of cognitive processing in the ASD brain. However, the following sections will

include background literature from multiple electrophysiological techniques [EEG/event-related potentials (ERP) and electrocorticography (ECoG), MEG] due to the small ASD MEG literature.

aMEG

Although MEG has higher spatial resolution compared to EEG, it does not compare to the spatial resolution of MRI. An anatomically-constrained MEG (aMEG) approach is used to address the lower spatial resolution of MEG. aMEG combines distributed source modeling of the MEG signal with structural MRI, providing insight into spatiotemporal stages of processing by yielding "brain movies" that dynamically map activity estimates in both time- and time-frequency domains across different frequency bands (Dale et al., 2000; Marinkovic et al., 2003, 2019). aMEG is advantageous over traditional MEG because the combination with structural MRI allows for estimations of both spatial and temporal components of neural activity.

Electrophysiological Studies of Language in ASD

Theta

Theta power (4-7 Hz) has been found to be associated with memory, cognitive control, and language processes (Bakker-Marshall et al., 2018; Bastiaansen et al., 2005; Beaton et al., 2018; Doesburg et al., 2015; Gaudet et al., 2020; Green et al., 2020; Halgren et al., 2015; Kovacevic et al., 2012; Marinkovic et al., 2012, 2019; Pu et al., 2020; Rosen et al., 2016). You et al. (2021) compared event-related theta power as measured by MEG during a lexicosemantic task in ASD and TD youth, in a sample partially overlapping with this dissertation. Atypically increased event-related theta power in adolescents with ASD compared to TD adolescents was found in multiple fronto-temporal brain regions. Aside from this study, few EEG/MEG studies have investigated the role of theta during language processing in individuals with ASD. Jochaut et al. (2015) reported atypically increased theta during movie watching, a passive language processing activity. Bloy et al. (2019) found that the event-related desynchronization during 5-20

Hz (not specific to the 4-7 Hz theta range) over 200-1000 millisecond (ms) post-stimulus period in the auditory cortex was correlated with language abilities in ASD and TD participants. An ERP study reported decreased theta power and theta phase coherence in the occipital region during a visual-auditory task compared to TD children (Ortiz-Mantilla et al., 2019). Interestingly, a recent EEG study found that theta power (as well as delta, beta, and gamma) was important for predicting language abilities in infants at high-risk for developing autism (C. L. Wilkinson et al., 2020).

N250(m) and N400(m)

In addition to theta power, N250(m) and N400(m) components are important for evaluating language processes, with N250(m) related to lexical access and N400(m) involved in semantic processing and integration (Carreiras et al., 2014; Halgren et al., 2002; Kotchoubey, 2002; Kutas & Federmeier, 2000; Kutas & Hillyard, 1980; Leminen et al., 2019; Marinkovic, 2004a; Marinkovic et al., 2014; Parkes et al., 2016; Pylkkänen & Marantz, 2003). N250(m) has been much less studied in ASD language paradigms than N400(m).

With regard to lexical access as measured by N250(m), one study did not find any effect of group for the N250 during an auditory speech task (Galilee et al., 2017). This contrasts with an earlier study, which identified ASD participants as having stronger N250 for incongruous words compared to congruous words (Braeutigam et al., 2008). Neurotypical participants did not have any differences in N250 amplitude between the two categories. Additional studies of N250(m) are needed for understanding of lexical processes in individuals with ASD.

Lexicosemantic processing in ASD individuals is largely associated with atypical N400(m), demonstrated as increased latency, reduced amplitude, or total lack of N400(m) (Cantiani et al., 2016; DiStefano et al., 2019; M. Dunn et al., 1999; M. A. Dunn & Bates, 2005;

Fishman et al., 2011; McCleery et al., 2010; McFadden & Rojas, 2013; Pijnacker et al., 2010; Russo et al., 2012). In one ERP study, children were instructed to passively listen to a list of animal and non-animal words (Dunn & Bates, 2005). TD children showed increased N400 amplitude when viewing non-animal words compared to animal words. Children with ASD did not show any difference in the N400 amplitude between words of different categories. Some studies have identified a relationship between atypical N400 activity and language skills. Strandburg et al. (1993) administered an idiom recognition task where adults had to determine if literal, idiomatic, and nonsense phrases were meaningful or not. Compared to neurotypical adults, adults with ASD had significantly less, and almost a complete absence of, N400 activity for idioms. The smaller N400 was correlated with poorer task performance. In another EEG study, adults with ASD lacked the typical N400 response during a task consisting of semantically congruent and incongruent sentences (Pijnacker et al., 2010). The ASD adults were matched with the neurotypical adults on IQ and did not differ on task performance (Pijnacker et al., 2010). It is important to note that in this study the ASD group was divided into subgroups based on DSM-IV diagnoses – Asperger's and high-functioning autism – and there was no neurotypical group for comparison. Only the high-functioning autism subgroup lacked the typical N400 activity. This is similar to the ASD subgroup findings by (Valdizán et al., 2003). While listening to congruent and incongruent words, an increased N400 latency was found in children with autism, but not in those with Asperger's. There were no differences in the N400 amplitude between the autism, Asperger's, and TD children. This finding was similar to another study, which did not find any evidence of atypical M400 amplitude in adults with ASD during semantic processing, although they did report different in lateralization (discussed below) (Braeutigam et al., 2008). However, Gold et al. (2010) identified differences in the N400 amplitude in adults with Asperger's

compared to neurotypical adults during semantic processing. Even though distinctions between subgroups of ASD are no longer made in the DSM-5, it is important to recognize the heterogeneity of the N400 in response to language tasks in ASD.

Lateralization

As described above, language abilities are typically lateralized, with the left hemisphere demonstrating increased activation compared to the right hemisphere. Similar to fMRI findings, EEG/MEG studies of individuals with ASD support atypical language lateralization (Braeutigam et al., 2008; Curl & Coderre, 2022; Flagg et al., 2005; Liang et al., 2021; Matsuzaki et al., 2020; Yoshimura et al., 2013). Yoshimura and colleagues (2013) reported significantly reduced leftward lateralization for ASD children in the P50m component during a passive auditory recording compared to TD children. In another study, ASD participants had greater theta coherence in the right hemisphere when looking at related words compared to unrelated words (Curl & Coderre, 2022). TD participants did not show a significant effect for the right hemisphere activity. In a small MEG study of 6 ASD and 6 TD children, increasing rightward dominance of the 300 ms late field window during a passive auditory task with age was identified in the ASD group (Flagg et al., 2005), whereas TD children showed increasing leftward dominance with age. In a study of ASD adults, participants were presented sentences with congruous or incongruous endings (Braeutigam et al., 2008). The ASD adults demonstrated right hemisphere dominance, specifically in the anterior temporal cortex, for N400 activity when viewing incongruous sentences. This rightward lateralization was not observed in the neurotypical adults. In a sample overlapping with this dissertation, You et al. (2023) found that N250m in the prefrontal cortex was left lateralized only in the TD participants, whereas the ASD group showed bilateral activity during the lexicosemantic task.

Other studies provide evidence for atypical lateralization beyond language processing, such as during non-language tasks and rest (Hiraishi et al., 2015; O'Reilly et al., 2017; Wang et al., 2013; Yuk et al., 2020). At rest, studies typically see greater power in the left hemisphere compared to the right in individuals with ASD across all frequency bands; whereas TD individuals show much milder hemispheric asymmetries (Wang et al., 2013). Atypical lateralization in the theta band was reported for adult males with ASD during response inhibition (Yuk et al., 2020). While neurotypical participants showed activation in the right hemisphere, ASD participants were more left lateralized. Another study measured laterality in children with ASD while watching a 6-minute video (Hiraishi et al., 2015). MEG results indicated rightward lateralization in the TD group for delta, theta, and alpha band oscillations; this lateralization pattern was not present for ASD children.

Electrophysiological Studies of Resting-State in ASD

Lajiness-O'Neill et al. (2014) reviewed the four ASD resting-state MEG studies that had been published at that time. Among those studies, there is support for increased alpha power in temporal, parietal, and occipital regions; and increased theta power in central regions during rest (Lajiness-O'Neill et al., 2014). An ASD resting-state MEG study published after that review show higher peak alpha frequency in ASD children (6-10 years) compared to TD children, but no significant difference was found between TD and ASD adolescents (10-18 years) (Edgar et al., 2019). A higher peak alpha frequency in the TD group, especially for the younger children, was correlated with faster processing speed, whereas a higher peak frequency in the ASD adolescents was correlated with higher non-verbal IQ (Edgar et al., 2019). Ye et al. (2014) examined coherence during resting-state MEG in adolescents and found decreased connectivity compared to TD participants for lower frequencies (delta, theta, and alpha) between parietal and occipital

regions and other areas of the brain. Among EEG studies, individuals with ASD generally show increased power at low and high frequency bands (delta, theta, beta, and gamma), but decreased power in the mid-range (beta) throughout the cortex (Wang et al., 2013). However, there are some inconsistencies; other studies have found decreases in delta and theta, and increases or no differences in alpha power (Wang et al., 2013).

Electrophysiological Measurement of E:I Imbalance in ASD

As described above, there is evidence supporting E:I imbalance in ASD. While most measures of E:I ratio are invasive and have been performed in animal models, there is recent research exploring the relationship of aperiodic neural activity, a noninvasive measurement, to excitatory and inhibitory activity in the brain.

Aperiodic Exponent. Neural activity can be separated into two components – periodic and aperiodic (Donoghue et al., 2020; He, 2014; He et al., 2010). Periodic activity, the more researched of the two, is measured by the power or oscillations of frequency bands (i.e., alpha, delta, theta, beta, gamma), such as in the studies described above. Historically the aperiodic component has been pushed aside as spontaneous neural noise until more recently. Aperiodic neural activity, also referred to as 1/*f* activity, 1/*f* noise, or scale-free activity, follows a 1/*f*-like pattern. Recent advances have been made to separate periodic and aperiodic activity in the brain, so that the aperiodic activity can be more easily studied. Donoghue et al. (2020) created a toolbox that applies a Fourier transform to raw neural data, splitting the aperiodic activity into waves at different frequencies. A plot of the wave amplitudes across frequencies results in a power spectrum. Donoghue et al. (2020) found that neural data follows a pattern of lower frequencies with higher amplitudes, with exponentially decreasing power with increases in frequency, resulting in a 1/*f* shape. The slope of the 1/*f*-like distribution, also known as the

aperiodic exponent, in neural data is negative (Donoghue et al., 2020; Podvalny et al., 2015) and is significantly different from true random white noise, which has a flat slope. Studies have found changes in the aperiodic exponent to be related to age, processing of stimuli, memory, and sleep/wake stages (Lendner et al., 2020; Maniscalco et al., 2018; Thuwal et al., 2021; Voytek et al., 2015).

Aperiodic activity is hypothesized to be a reflection of the E:I ratio in the brain (Colombo et al., 2019; R. Gao et al., 2017; Gerster et al., 2022; Lendner et al., 2020; Miskovic et al., 2018; Waschke et al., 2021). Similar to the rsfMRI HE, aperiodic activity is thought to be a noninvasive way to assess the balance of excitatory and inhibitory activity in the brain, which is thought to be unbalanced in ASD. To determine the relationship between aperiodic activity and the E:I ratio, Gao et al. (2017) used a simulation to alter excitatory and inhibitory activity while measuring aperiodic activity in local field potential (LFP) data. They found that the E:I ratio was positively correlated with the aperiodic slope, and that increasing the E:I ratio resulted in a flatter slope. When exploring the relationship between the aperiodic slope and activity in a rat model, they found that the slope was again correlated with the E:I ratio (measured as excitatory and inhibitory synaptic density) (Gao et al., 2017). These results support aperiodic activity as a noninvasive measure of E:I ratio in the brain.

There are a few recent studies that have examined aperiodic activity in children with ASD and related neurodevelopmental disorders. One study used resting-state EEG data from a small sample of boys with Fragile X Syndrome (FXS) (Wilkinson & Nelson, 2021). Although not all children with FXS have ASD, it is estimated that 30-54% of males with FXS meet criteria for ASD (Kaufmann et al., 2017). The FXS boys group showed a marginally significant reduction in the aperiodic exponent in frontal and central compared to TD boys. The flatter slope

was caused by an increase in higher frequencies, such as gamma power. The increased gamma was found to be correlated with better language abilities. The aperiodic offset, another part of the aperiodic component, did not show significant differences between groups. Another study in Rett Syndrome found a steeper aperiodic slope, with higher power in low frequency bands (delta, theta) and lower power in middle frequency bands, compared to TD girls. The steeper slope was associated with lower cognitive abilities (Roche et al., 2019). Levin et al. (2020) analyzed resting-state EEG scans about a week apart in ASD and TD children using the toolbox described in Donoghue et al. (2020). While the study generally demonstrates test-retest reliability of the power spectrum and aperiodic activity, they suggest that changes in these measures may arise from individual changes, such as mood, task, and epileptic activity (Levin et al., 2020). It is important to note that the slope was stable across the two scans in the ASD participants, but less so in the TD group, without a clear explanation for the cause.

Summary of ASD Electrophysiological Studies

The MEG literature on ASD is small compared to fMRI and there is a need for further studies. Similar to findings of altered neural activity during language tasks in fMRI for ASD, there is evidence to support atypical activity in EEG/MEG studies. For example, theta synchronization is altered in ASD relative to TD during cognitive control tasks (Doesburg et al., 2013), and the minimal studies that exist support atypical N250(m) and N400(m) amplitude and latency in ASD individuals, compared to TD peers, during lexical processing. Aside from one study from members of our group, which found atypical early theta in fusiform cortex and increased theta in fronto-temporal and anterior cingulate cortices during a lexico-semantic decision task, there are no studies examining theta during language processing in individuals with ASD. Similar to fMRI, there is a need to study excitatory and inhibitory activity in the brain

using MEG. Novel research studying the aperiodic activity at the brain at rest has found the slope of the power spectrum to be a good indication of the E:I balance. Examining the aperiodic slope in individuals with ASD will be crucial based on the E:I imbalance hypothesis behind the disorder.

Limitations of Previous Research

Functional neuroimaging research has been dominated by fMRI for decades, yet combining fMRI with electrophysiological methods is critical in accounting for dynamic aspects of brain activity. Integrating fMRI with aMEG takes advantage of the high spatial and temporal resolution of each modality, yet fMRI and MEG literatures have developed largely in isolation. Combining these techniques in a comprehensive approach to brain function and connectivity that captures brain dynamics is necessary for a clear understanding of neural abnormalities in ASD and the potential identification of ASD neural biomarkers. Integration will allow for improved understanding of links between spatial organization of brain function and dynamics.

Advances in neuroimaging provide a variety of non-invasive techniques to study anatomical and functional brain organization, but most research continues to be limited to the use of a single neuroimaging method. Functional connectivity MR (fcMRI) identifies the temporal relationship between brain regions measured by changes in BOLD signal (Fox & Raichle, 2007), which can reveal important details of ASD brain organization. Yet most fcMRI studies have utilized static techniques to examine functional relationships, which cannot account for the dynamic properties of neural networks (Ciric et al., 2017). Attempts in using dynamic fcMRI has been a first step in solving the ASD inconsistency problem, but is severely limited due to the poor temporal resolution of fMRI (Hutchison et al., 2013). Despite the important spatial information MRI reveals, conventional fMRI and fcMRI methods cannot well account for

dynamic aspects of brain activity, which leaves out critical data in understanding neural activity and networks of ASD individuals. Lack of integration between modalities inhibits the development of comprehensive models of brain function. Neglect of the temporal dynamics of brain activity is a serious limitation. It is critical to combine fMRI with methods that reflect electrophysiology directly, such as MEG. Method integration is critical for advances in cognitive neuroscience that will result in a better understanding of activity in the ASD brain during task and rest (Mash et al., 2018).

The overall aim of this dissertation was to use multimodal neuroimaging integration to study neural activation differences in adolescents with ASD through fMRI and MEG task and resting-state measures. A lexicosemantic task was chosen based on the extensive literature documenting language and executive function skill difficulties in ASD. The design of this task is well suited to broadly assess spatiotemporal dynamics of neural activity from visual input to cognitive lexicosemantic processing to executive function and motor output. The lexicosemantic neural network is highly distributed, allowing for multiple areas of regional activation and functional connectivity to be studied in this dissertation. Resting-state data was also examined in order to evaluate measures of excitatory and inhibitory activity in the brain, which has been implicated as imbalanced in ASD.

This dissertation aimed to integrate fMRI and MEG and take a more comprehensive approach to brain function and connectivity, capturing brain dynamics. This approach is necessary for understanding brain differences in ASD and takes a step toward filling a critical gap in the neuroimaging literature, bringing improved understanding of links between spatial organization of brain function and its dynamics in regard to ASD.

Chapter 1 Study 1

fMRI BOLD and MEG theta power reflect complementary aspects of activity during lexicosemantic decision in adolescents with ASD

Wilkinson, M.[1,2], Jao Keehn, R. J.[2], Linke, A. C.[2], You, Y.[3], Gao, Y.[1,2], Alemu, K.[2], Correas, A.[3], Rosen, B. Q.[3], Kohli, J. S.[1,2], Wagner, L.[3], Sridhar, A.[2], Marinkovic, K.[1,3,4], & Müller, R.-A[1,2].

[1]San Diego State University / University of California San Diego Joint Doctoral Program in Clinical Psychology, San Diego, CA, United States

[2]Brain Development Imaging Laboratories, Department of Psychology, San Diego State University, San Diego, CA, United States

[3]Spatiotemporal Brain Imaging Laboratory, Department of Psychology, San Diego State University, San Diego, CA, United States

[4]Radiology Department, University of California San Diego, CA, United States

Abstract

Neuroimaging studies of autism spectrum disorder (ASD) have been predominantly unimodal. While many fMRI studies have reported atypical activity patterns for diverse tasks, the MEG literature in ASD remains comparatively small. Our group recently reported atypically increased event-related theta power in individuals with ASD during lexicosemantic processing. The current multimodal study examined the relationship between fMRI BOLD signal and anatomically-constrained MEG (aMEG) theta power. Thirty-three adolescents with ASD and 23 typically developing (TD) peers took part in both fMRI and MEG scans. During which they distinguished between standard words (SW), animal words (AW), and pseudowords (PW). Regions-of-interest (ROIs) were derived based on task effects detected in BOLD signal and aMEG theta power. BOLD signal and theta power were extracted for each ROI and word condition. Compared to TD participants, increased theta power in the ASD group was found across several time windows and regions including left fusiform and inferior frontal, as well as right angular and anterior cingulate gyri, whereas BOLD signal was significantly increased in the ASD group only in right anterior cingulate gyrus. No significant correlations were observed between BOLD signal and theta power. Findings suggest that the common interpretation of increases in BOLD signal and theta power as 'activation' require careful differentiation, as these reflect largely distinct aspects of regional brain activity. Some group differences in dynamic neural processing detected with aMEG that are likely relevant for lexical processing may be obscured by the hemodynamic signal source and low temporal resolution of fMRI.

Keywords: Functional magnetic resonance imaging (fMRI), magnetoencephalography (MEG), multimodal integration, autism spectrum disorder (ASD), lexicosemantic processing, executive function

Introduction

Autism spectrum disorder (ASD) is a neurodevelopmental disorder characterized by socio-communicative impairments and restricted, repetitive behaviors (American Psychiatric Association, 2013). Many individuals with ASD show delays, impairment, or complete lack of language (Boucher, 2003). A language domain often impacted in ASD is lexicosemantic processing (Bavin et al., 2016; Boucher, 2012; Groen et al., 2008; Kamio et al., 2007; McGregor et al., 2012; Naigles & Tek, 2017). Some previous functional magnetic resonance imaging (fMRI) studies examining lexicosemantic processing reported greater temporo-occipital activation but reduced frontal activity in ASD compared to typically developing (TD) groups (Gaffrey et al., 2007; Harris et al., 2006; Knaus et al., 2017; Lo et al., 2013).

fMRI detects neural activity through changes in blood oxygenation at good spatial, but low temporal, resolution (due primarily to a late in the hemodynamic response), which has resulted in a predominant neglect of brain dynamics in the fMRI literature and a movement toward multimodal integration (Bolton et al., 2020; S. Liu et al., 2015; Mash et al., 2018; Padmanabhan et al., 2017). Multimodal studies capturing both temporal dynamics and spatial localization are indispensable for comprehensive models of cognitive and language processing. Some studies attempting to link localized task-related neural activity detected with fMRI with measures derived from neuroimaging modalities with high temporal resolution, such as electroencephalography (EEG) and magnetoencephalography (MEG), have yielded strong associations (including both positive and negative correlations; (Ekstrom et al., 2009; Meltzer et al., 2007; Scheeringa et al., 2009a; Scheeringa & Fries, 2019; Winterer et al., 2007). Methods that detect postsynaptic currents, such as EEG and MEG, have exquisite temporal resolution suitable for the study of brain dynamics. Event-related theta power (4-7 Hz) detected with these techniques is considered the standard for detecting neural activity changes related to cognitive

control, working memory, and language processing (Audrain et al., 2020; Bakker-Marshall et al., 2018; Bastiaansen et al., 2005; Begus & Bonawitz, 2020; Halgren et al., 2015; Kovacevic et al., 2012; Marinkovic et al., 2012, 2019; Pu et al., 2020), as well as the transfer of information between brain regions (Begus & Bonawitz, 2020; Marinkovic et al., 2019).

Studies relating BOLD signal to theta power have remained primarily limited to neurotypical adults and the use of EEG (rather than MEG). One resting-state EEG study in children revealed decreased theta power in ASD compared to TD children, which was associated with greater ASD symptomology (Hornung et al., 2019). Another EEG study reported that a neurotypical increase in theta power associated with increasing working memory load was absent in adults with ASD (Larrain-Valenzuela et al., 2017), and furthermore, that this lack of theta power increase was associated with greater ASD symptomology. Research using MEG to examine theta power in ASD had been minimal. In one of the few MEG studies on lexicosemantic processing in ASD, members of our group recently reported atypically increased event-related theta power in adolescents with ASD in multiple fronto-temporal brain regions (You et al., 2021). This appears to be in partial contract to BOLD fMRI findings of atypically *reduced* frontal activity in ASD (Gaffrey et al., 2007; Harris et al., 2006; Just et al., 2004; Knaus et al., 2017), which raises the question whether MEG and fMRI, when implemented in isolation (as has been standard practice), can provide comprehensive assays of neurofunctional differences between ASD and TD samples.

Following up on our unimodal (anatomically constrained MEG [aMEG]) report (You et al., 2021), the current study, which included an expanded, but partially overlapping sample, investigated the relation between BOLD signal and event-related theta power during

lexicosemantic decision in two sets of regions that were (1) reported to show aMEG activity by You et al. (2021), and (2) identified based on increases in task-driven fMRI BOLD signal.

Methods

Participants

Thirty-three ASD and 23 TD participants (aged 12-21 years) were selected from an initially screened sample of 156 ASD and 120 TD adolescents (see supplement for details on exclusions and data loss). ASD diagnoses were based on DSM-5 criteria (American Psychiatric Association, 2013), the Autism Diagnostic Observation Schedule, 2nd Edition (ADOS-2; Lord et al., 2012), and the Autism Diagnostic Interview-Revised (ADI-R; (Rutter et al., 2003), as well as expert clinical judgement. Twelve ASD participants were currently taking psychotropic medications (Supplemental Table S1.1). Fourteen ASD individuals reported comorbidities: 4 with attention-deficit/hyperactivity disorder, 7 with anxiety, and 4 and with depression; 2 of these adolescents reported multiple comorbidities (Supplemental Table S1.1). Presence of comorbidities and use of psychotropic medications were not considered exclusionary as they are common in adolescents with ASD and their exclusion would have rendered the sample less representative of the broader ASD population (Gurney et al., 2006). There was some overlap between these study and You et al. (2021). Fourteen ASD and 16 TD participants were included in both You et al. (2021) and the current study. Five ASD and 4 TD participants were included in You et al. (2021), but not in the current study. Nineteen ASD and 7 TD participants were new to the current study. Informed assent and consent were obtained from all participants and their parents/guardians in accordance with the San Diego State University (SDSU) and the University of California San Diego (UCSD) Institutional Review Boards. Groups did not differ on age, gender, IQ, or handedness (Table 1.1). As expected, groups differed on task accuracy. Only participants with usable data in *both* fMRI and aMEG modalities were included in analyses.

Experimental design

Participants completed the Word Reading subtest of the Wechsler Individual Achievement Test, 3rd Edition (WIAT-III; Wechsler, 2009) to assess reading level. Those who received a standard score below 80, which is the average based on 12-year-old reading norms (i.e., a 6th-grade reading level), were excluded. Participants were administered the Edinburgh Handedness Inventory (Oldfield, 1971), the Wechsler Abbreviated Scale of Intelligence, 2nd Edition (WASI-II; Wechsler, 2011), the Beery-Buktenica Developmental Test of Visual-Motor Integration, 6th Edition (Beery VMI-6; Beery et al., 2010), and the Clinical Evaluation of Language Fundamentals, 5th Edition (CELF-5; Semel et al., 2013). MEG and MRI scans were completed in subsequent sessions with a counterbalanced order of scans. MEG and MRI data were collected within 150 days of one another, except for 2 ASD participants (174 and 184 days) and 1 TD participant (252 days). To address any potential sensory sensitivities and overall anxiety, participants underwent a mock scan prior to the actual MRI scan to familiarize themselves with the environment. During the mock and MRI scans participants were given ear plugs to reduce noise, had cushions surrounding their ears and under their legs for sound reduction and comfort, and were offered a blanket for warmth. MRI operators were in frequent contact with participants throughout the scan and assessed the participants' wellbeing. Similar steps were taken to ensure comfort during the MEG scan. Refer to supplement for additional scan environment information.

During the task, participants were asked to respond differentially to three conditions: real non-animal standard words (SW), animal words (AW), and pseudowords (PW). The task was adapted from an aMEG study in neurotypical adults by Marinkovic and colleagues (Marinkovic et al., 2012, 2014). PW trials were orthographically and phonologically legal letter strings with

no meaning (e.g., “blont”). Participants used their left hand to respond on a 2-button fORP 904 response pad (Cambridge Research Systems Ltd., Rochester, UK, https://www.crsltd.com), and were instructed to press the button under their index finger for SW, the button under their middle finger for AW, and to withhold pressing any button for PW. Conditions did not significantly differ on word length or number of syllables; SW and AW conditions did not differ on the frequency of occurrence based on the Zipf scale (Brysbaert & New, 2009; van Heuven et al., 2014) or age of acquisition (Supplemental Table S1.2; Kuperman et al., 2012). A practice test was administered while participants lay supine in a mock MRI scanner to simulate the actual MRI scan. Words used during practice differed from those presented during the fMRI and MEG scans.

In the fMRI task, each word was visually presented for 500 ms, followed by a fixation string (“xxxxxx”) for 1500 ms (given insertion of additional null trials in fMRI, see below). For the MEG trials, stimuli were also presented for 500 ms in a randomized order, followed by a fixation string for 2000 ms, with no jitter. Stimuli were presented using Presentation ® software (Version 22.2, Neurobehavioral Systems, Inc., Berkeley, CA, www.neurobs.com) in white lower-case letters on a black background. Trials were presented in the same order to all participants except 2 ASD and 2 TD adolescents who were scanned a second time due to technical issues and were presented with a different sequence to avoid practice effects. Different stimuli sets were used during MEG and fMRI scans. During MEG scans, task stimuli were presented in a randomized order during an approximately 25-min run, with short breaks every 4 min; 100 words were presented and analyzed for each word condition. An additional 180 SW words were presented as fillers to establish a prepotent response tendency. For fMRI scans, the

task was split into two 7-min runs with a 3-min break between runs. Each fMRI run consisted of 90 SW trials, and 30 trials each for AW and PW conditions.

Experimental stimulus trial structure

RSFgen, a random stimulus function generation in Analysis of Functional NeuroImages (AFNI; Cox, 1996; https://afni.nimh.gov), was used to create the trial sequence in the event-related design. During null trials (in fMRI only), a fixation string ("xxxxxx") was shown. There were 124 1-s null trials ("xxxxxx") per run. Refer to supplement for additional information.

MEG acquisition and processing

MEG scans were acquired at the UCSD Radiology Imaging Laboratory. Data were acquired from 204 planar gradiometers (102 pairs) using a whole-head Neuromag Vectorview system (Elekta AB, Stockholm, Sweden). To co-register MEG with structural MRI scans, a 3Space Isotrak II (Polhemus Inc., Colchester, VT) was used to digitize fiduciary points (naison and periauricular points), head position indicator coils, and many other random points on the scalp. A 1000 Hz sampling rate and minimal filtering (0.1-300 Hz) were used to record signals continuously. Matlab scripts (Mathworks Inc., Natick, MA, USA) utilizing Fieldtrip (Oostenveld et al., 2011), EEGLab (Delorme & Makeig, 2004), and MNE (Gramfort et al., 2013), were used for processing and analyzing MEG data as previously described (Beaton et al., 2018; Correas et al., 2019; Kovacevic et al., 2012; Marinkovic et al., 2012, 2019; Rosen et al., 2016). Data were downsampled to 250 Hz, bandpass filtered (0.1-100 Hz), epoched from -300 to 1100 ms for stimulus-locked analysis, and baseline-corrected using the prestimulus period (-300 to 0 ms). Artifacts, such as eyeblinks and heartbeat, were removed using ICA (Delorme & Makeig, 2004), with additional artifacts identified by visual inspection and removed using threshold rejection

(Oostenveld et al., 2011). Analyses were conducted on artifact-free trials with correct task response.

Complex wavelet power spectra were calculated across all epochs by convolving them with Morlet wavelets (Lachaux et al., 1999) for the theta band (4-7 Hz, in 1 Hz increments), with a frequency resolution of 2 Hz and time resolution of 80 ms. To remove edge artifacts, padding of 300 ms was added to the two ends of each epoch and subsequently removed after wavelet analysis. Source power estimates were calculated with an aMEG approach (Dale et al., 2000; Marinkovic, 2004a), by applying cortically constrained minimum norm estimation to the complex wavelet power spectrum (Kovacevic et al., 2012; Marinkovic et al., 2012, 2019). Noise covariance matrix was estimated by pooling empty room data across sessions, which were band-pass filtered (3-50 Hz). For each participant, total theta source power was estimated at each location on the cortical surface, averaging across theta frequency (4-7 Hz) and artifact-free, correct trials for each condition. Finally, event-related theta power estimates were calculated as percent signal change from the pre-stimulus baseline (-300 to 0 ms). Structural MRI scans obtained for all participants were analyzed with Freesurfer (Dale et al., 2000; Fischl et al., 1999). Each participant's reconstructed cortical surface served to constrain inverse solutions (Dale et al., 2000; Marinkovic et al., 2003). Inner skull surface derived from segment MRI data was used for a boundary element model of the volume conductor. To conduct the group analysis, the reconstructed individual surfaces were morphed into an average representation by aligning their sulcal-gyral patterns (Fischl et al., 1999) and decimated, defining the solution space with 5124 free-rotating dipoles spaced ~7 mm apart. Group average maps were then computed by averaging individual source power estimates for each group and word condition.

MRI acquisition and processing

MRI scans were acquired at the UCSD Center for fMRI with a General Electric Discovery MR750 3.0 T scanner (GE Healthcare, Milwaukee, WI) and a Nova Medical 32-channel head coil. Structural scans were acquired using a Fast Spoiled Gradient Recalled T1-weighted sequence (TW: 8.136 ms; TE: 3.172 ms; flip angle: 8°; FOV: 25.6 cm; acquisition matrix: 256x256; slices: 172; voxel size: 1 mm^3; duration: 5 min). Functional scans were acquired using a multi-echo simultaneous multi-slice (MESMS) T2*-weighted echo planar imaging (EPI) sequence (volumes: 240; TR: 1250 ms: TEs: 13.2, 30.3, 47.4 ms; flip angle: 60°; FOV: 21.6 cm; acquisition matrix: 72x36; acceleration factor [R]: 2; slices: 54; voxel size: 3 mm^3). Data from ten participants (9 TD, 1 ASD) were collected using a slightly different protocol due to a technical error at early stages of the study (all parameters identical except volumes: 386; TR: 1100; slices: 45). The first 9 volumes were discarded to allow for magnetization to reach equilibrium. The MESMS protocol includes simultaneous acquisition of multiple slices at multiple echo times, with increased signal-to-noise ratio (Kundu et al., 2012, 2013; Olafsson et al., 2015). fMRI data were preprocessed and analyzed using AFNI (Version 19.0.00), FSL (Version 5.0), and Matlab (2013b). Echo-planar images (EPI) for each echo time were corrected for susceptibility-induced distortions with FSL's TOPUP tool, using two spin-echo acquisitions with opposite phase encoding directions (Smith et al., 2004). Rigid-body realignment of each functional volume to the middle volume was performed using AFNI and head motion quantified as the root mean square difference (RMSD) from the six motion parameters of the 30.3 ms echo time data. EPIs from the three echoes were optimally combined (Kundu et al., 2013). Data were denoised with multi-echo ICA (ME-ICA; (Olafsson et al., 2015) using meica.py (openly available on Github, https://github.com/ME-ICA/me-ica). ME-ICA has

been shown to be superior to standard denoising processes (Lynch et al., 2020), allowing for removal of artifacts (non-BOLD components) from the BOLD signal (Kundu et al., 2013). FSL FLIRT was used to co-register functional and structural scans, and FNIRT to reorient images to MNI-152 space. Data were spatially smoothed using a Gaussian kernel of 6 mm KWHM in AFNI's 3dBlurToFWHM and scaled to percent signal change. Functional data of the two runs were concatenated for each participant and analyzed in AFNI using 3dBandPass for temporal filtering (f > .008 Hz).

General linear model

3dDeconvolve was used to perform an ordinary least squares (OLS) regression on the functional data. Regressors included the three word conditions of interest (SW, AW, and PW). A two-parameter statistical parametric mapping (SPM) gamma variate basis function approximated the canonical hemodynamic response function. 3dREMLfit was used to conduct a residual maximum likelihood estimation, which takes into consideration the residuals of the time series and uses an autoregressive moving average (ARMA[1,1]) model, for each participant on a voxel-wise basis through a generalized least squares time series fit. The estimates of effect size (beta coefficients) were output and used for subsequent group comparisons.

ROI identification

fMRI-derived and MEG-derived ROIs were two separate sets in largely different brain regions. Regions of activation were identified from MEG scans that were based on cortical surfaces reconstructed with FreeSurfer, serving to constrain inverse estimates. These MEG-derived ROIs were then transformed into volumetric space to be used with fMRI data. Regions of activation were also identified from fMRI scans, and these fMRI-derived ROIs were then

transformed into surface space for use with MEG data. Refer to the aMEG and fMRI sections below, as well as the supplement, for further details on ROI identification and transformation.

aMEG

aMEG-derived ROIs were adopted from You et al. (2021) and consisted of regions with significant source power based on an average of all participants and word conditions. aMEG-derived ROIs were transformed into volumetric space using FreeSurfer (Dale et al., 1999) to test if prominent group differences in event-related theta power between ASD and TD adolescents in the previous unimodal analysis correspond to BOLD differences within the same regions. Given the uncertain spatial precision associated with aMEG findings (Lütkenhöner, 2003) and with transformation from surface to volumetric space, ROIs from the Scaefer-400 atlas (Schaefer et al., 2018) that most closely aligned with the aMEG-derived ROIs were identified as volumetric aMEG-derived ROIs (Figure 1.1).

fMRI

A one-sample linear contrast (SW + AW + PW > Null) across all ASD and TD participants was used to identify ROIs from fMRI data. Four additional participants with usable fMRI but no MEG data were included in the ROI identification sample (Supplemental Table S1.3). ASD and TD participants were combined in this step. Note that ROIs determined for ASD and TD separately by group were largely similar. 3dMEMA was used to perform a mixed-effects multilevel analysis (MEMA; Chen et al., 2012) for selection of ROIs, while controlling for age, RMSD, and task accuracy. As the current version of 3dMEMA does not support permutation testing for cluster-correction, randomization and permutation simulation were performed using 3dttest++ to obtain cluster sizes with alpha $\leq$ .05 on the same contrast (SW + AW + PW > Null). Clusters of increased activity in $\geq$ 56 contiguous voxels at $p \leq .001$, with most from more

stringent thresholds, resulted in eleven fMRI-derived ROIs. These fMRI-derived ROIs were then transformed into surface-space ROIs using FreeSurfer (Version 7.1.1). For three ROIs (Rolandic operculum, post-central gyrus, and temporal pole), a MEG data could not be extracted after transformation to surface space due to ROI fragmentation caused by the transformation process, or an insufficient number of vertices required for the extraction of theta power. This resulted in eight fMRI-derived ROIs with $\geq$ 524 vertices (Figure 1.1, Supplemental Table S1.4). ROIs were dilated to a minimum degree to permit aMEG data extraction from non-fragmented ROIs. For details, see Supplemental Table S1.5.

Data extraction and analysis

The goal of ROI identification was to derive ROIs from areas with the strongest activation effects related to the lexical decision task for: (1) event-related theta power from MEG scans and (2) BOLD response from fMRI scans.

For MEG, the signal sequence was segmented based on stimulus-presentation triggers denoting zero time point for each trial. Trials were epoched from -300 to 1100 ms and baseline-corrected. Artifact-free trials with correct responses were analyzed with Morlet waves to estimate event-related theta total power averaged across 4-7 Hz at each location on the cortical surface, and presented as percent change from the baseline. MEG theta activity progressed in the posterior-to-anterior direction from sensory-specific to supramodal regions in accordance with the expected spatio-temporal processing stages. Time windows of interest were determined based on the largest theta activity across all participants for each processing stage. For each ROI, the time window of maximal event-related increase in theta power (compared with baseline) was analyzed, as previously reported by You et al. (2021). More specifically, the time windows and the corresponding regions were as follows: 150-200 ms (fusiform cortex), 250-350 ms (lateral

temporal cortex), 450-650 ms (inferior frontal gyrus, lateral temporal cortex), and 700-1000 ms (anterior cingulate cortex, inferior frontal gyrus, motor cortex). For determination of MEG-derived ROIs and extraction of theta power age, sex, and handedness were not included in the model. An identical process was used to identify the MEG time windows to be analayzed for the fMRI-derived ROIs.

BOLD beta coefficients were extracted for each participant, ROI, and word condition (compared with baseline). Two (Group: ASD vs. TD) x 3 (Word Condition: SW vs. AW. Vs. PW) ANOVAs were used to test for the effects of group, word condition, and the interaction on event-related theta power and BOLD signal in the two sets of ROIs. Significant results from the ANOVAs were followed up with Tukey post hoc analyses to examine pairwise comparisons. Pearson partial correlations, controlling for age and fMRI RMSD, were used to examine the relationship between BOLD beta coefficients and event-related theta power in aMEG- and fMRI-derived ROIs by group.

Results

Event-related theta power

For aMEG-derived ROIs, a 2 x 3 ANOVA revealed a significant main effect of group with increased event-related theta power in the ASD group compared to the TD group in the following ROIs (Figure 1.2A): L fusiform for the 150-200 ms time window ($F(1, 162) = 5.57$, $p = .02$), R ACC for the 700-1000 ms time window ($F(1, 162) = 5.11$, $p = .03$), L IFGop for the 700-1000 ms time window ($F(1, 162) = 10.00$, $p = .002$), and L IFGtri for the 700-1000 ms time window ($F(1, 162) = 7.05$, $p = .009$). The ANOVA also revealed a significant main effect of word condition for event-related theta power in L IFGop for the 450-650 ms time window ($F(2, 162) = 7.39$, $p = .0009$), L IFGtri for the 450-650 ms time window ($F(2, 162) = 9.64$, $p = .0001$),

and L LTC for the 450-650 ms time window ($F(2, 162) = 5.00$, $p = .008$). Tukey post hoc tests revealed significantly increased theta power for SW compared to AW [L IFGtri for the 450-650 ms time window ($p = .001$) and L LTC for the 450-650 ms time window ($p = .007$)] conditions. No significant interaction between group and word condition was identified for theta power in the aMEG-derived ROIs (Table 1.2, Supplemental Figure S1.1).

In fMRI-derived ROIs, a significant main effect of group (ASD > TD) for theta power was detected (Figure 1.2B) in R AG for the 110-170 ms time window ($F(1, 162) = 7.16$, $p = .008$) and in L IFG for the 450-650 ms ($F(1, 162) = 5.01$, $p = .03$) and 700-1000 ms time windows ($F(1, 162) = 14.15$, $p = .0002$). An inverse effect of significantly greater theta power in the TD compared to the ASD group was observed in L MTG for the 250-350 ms time window ($F(1, 162) = 4.69$, $p = .03$). Significant main effects of word condition included: L IFS for the 450-650 ms time window ($F(2, 162) = 10.66$, $p < .0001$), L SMA/MCC for the 450-650 ms time window ($F(2, 162) = 4.65$, $p = .01$), L IFG for the 450-650 ms time window ($F(2, 162) = 4.75$, $p = .009$), L motor for the 450-650 ms time window ($F(2, 162) = 5.93$, $p = .003$), L IFG for the 700-1000 ms window ($F(2, 162) = 20.95$, $p < .0001$). Tukey post hoc tests showed theta power was significantly increased for SW [L IFG for the 700-1000 ms time window ($p = .02$) and R motor for the 700-1000 ms time window ($p = .001$), L SMA/MCC for the 450-650 ms time window ($p = .008$), L IFG for the 450-650 ms time window ($p = .01$), L motor for the 450-650 ms time window ($p = .004$), and R motor for the 700-1000 ms time window ($p = .001$)] conditions when compared to PW condition. Theta power was significantly increased for AW when compared to SW in L IFG for the 450-650 ms time window ($p = .02$). A significant interaction was found between group and word condition for L IFG for the 700-1000 ms time window ($F(2, 162) = 3.08$, $p = .05$). Tukey post hoc analyses showed that theta power was

significantly increased in the ASD group compared to the TD group for both SW (p = .03) and AW (p = .02) conditions in the L IFG for the 700-1000 ms time window (Table 1.2; Supplemental Figure S1.1).

BOLD signal

For aMEG-derived ROIs, a 2 x 3 ANOVA showed a significant main effect of group, with increased BOLD signal for the ASD group compared to the TD group for BOLD signal in R ACC (F(1, 162) = 4.80, p = .03; Fig. 2C). There were significant main effects of word condition in L fusiform (F(2, 162) = 25.19, p < .0001), L LTC (F(2, 162) = 10.61, p < .0001), L IFGop (F(2, 162) = 8.35, p = .0004), L IFGtri (F(2, 162) = 4.04, p = .02), and L Motor (F(2, 162) = 7.92, p = .0005). Tukey post hoc tests showed significantly increased BOLD signal for SW compared to AW [L fusiform (p = .001), L LTC (p = .001), L IFGop (p = .001), and L IFGtri (p = .01)] and compared to PW [L fusiform (p = .001), L LTC (p = .008), and L IFGop (p = .005)]. The BOLD signal was also increased for the PW condition compared to AW for L motor (p = .001). No significant interaction between group and word condition was identified for BOLD signal in the aMEG-derived ROIs (Table 1.2; Supplemental Figure S1.2).

For fMRI-derived ROIs, there was no significant main effect of group for BOLD signal. There was a significant main effect of word condition for L SPL/IPL/MOG (F(2, 162) = 10.65, p < .0001), R AG (F(2, 162) = 4.49, p = .01), L IFG (F(2, 162) = 6.89, p = .001), L MTG (F(2, 162) = 12.16, p < .0001), L IFS (F(2, 162) = 8.17, p = .0400), L SMA/MCC (F(2, 162) = 24.00, p < .0001), L motor (F(2, 162) = 10.76, p < .0001), and R motor (F(2, 162) = 69.48, p < .0001). Results of Tukey post hoc analyses showed significantly increased BOLD signal for SW compared to AW [L SPL/IPL/MOG (p = .001), R AG (p = .01), L IFG (p = .001), L MTG (p = .001), L IFS (p = .001), L SMA/MCC (p = .001), L motor (p = .001), and R motor (p = .001)]

and SW compared to PW [L SPL/IPL/MOG (p = .005), L IFG (p = .03), L MTG (p = .001), L SMA/MCC (p = .001), and R motor (p = .001)]. BOLD signal was significantly greater for PW compared to AW in L motor (p = .002) and for AW compared to PW in R motor (p = .001). A significant interaction was found between group and word condition for L IFS (F(2,162) = 3.18, p = .04). Tukey post hoc analyses for L IFS did not show significant group differences for any of the word conditions (Table 1.2; Supplemental Figure S1.2).

MEG-fMRI correlations

None of the partial correlations (controlling for fMRI RMSD and age) between theta power and BOLD signal survived FDR-adjustment (alpha = .05; Benjamini & Hochberg, 1995), with only a few reaching an uncorrected threshold $p \leq .05$. For MEG-derived ROIs (Supplemental Table S1.6; Figure S1.3), correlations were found in the TD group in L LTC for the 250–350 ms time window for AW (r(19) = -.46, p = .05), and in the ASD group in R ACC for the 700–1000 ms time window for PW (r (27) = 0.46, p = .02). For fMRI-derived ROIs, a correlation was found in the TD group in L MTG for the 250–350 ms time window for the AW condition (r(27) = -.62, p = .004; Supplemental Table S1.7; Figure S1.3). To account for any effect of time between scans on the relationship, partial correlations were also examined with the addition of the number of days between scans as a covariate. The length of time between fMRI and MEG scans did not have a significant impact on the results of the partial correlation.

Supplementary analyses

Three sets of supplementary analyses were conducted to account for outliers, participants with high motion, and those with >150 days between fMRI and MEG scans. See supplement for additional analyses (Supplemental Tables S1.8-S1.18; Figures S1.4-S1.9).

Discussion

In this study, we examined the relation between event-related theta power measured with aMEG and fMRI BOLD signal during lexico-semantic processing in adolescents with ASD and TD peers. We found that correspondence between task related changes in BOLD signal and theta power was generally weak. Atypically increased theta power in ASD across several ROIs was mostly not reflected in corresponding BOLD group differences, suggesting that the two imaging methods are differentially sensitive to at least some ASD-specific alterations and capturing different aspects of the neural signal.

Task-induced signal changes in MEG and fMRI

Marinkovic et al. (2012) previously tested this lexicosemantic task in neurotypical adults using aMEG data. ROIs from that study included the occipital cortex, left lateral and inferior frontal regions, anterior cingulate, and motor cortex. Most of the ROIs in the present study overlap with these previous findings. Refer to the supplement for additional details on the background literature on identified ROIs and their relation to the different processing stages involved in the task.

Multiple frontal and temporal ROIs (both aMEG and fMRI-derived) showed greater increase in event-related theta power in the ASD than the TD group. This is consistent with the overall pattern of increased theta power reported in (You et al., 2021), which included a smaller, partially overlapping sample. However, only one region (R ACC) showed a concordant group difference for the BOLD signal, whereas no group differences in BOLD signal were detected for any other of the 14 ROIs.

It is interesting that both theta power and BOLD signal in the ACC were significantly greater in the ASD group compared to the TD group. The ACC is known to play a role in

decision making, as described above (Kovacevic et al., 2012; Marinkovic et al., 2012; Posner et al., 2007; Ruff et al., 2008). Atypically increased activation in the ASD group in this region may be due to greater attentional engagement in adolescents with ASD during the final stage of task processing. Participants needed to decide what word category the presented word falls in, recall what finger to press for that word category, and then execute the button press or inhibit a response in case of a pseudoword. The planning and organization required during this step calls on the individual's executive functioning skills. It has been widely found that individuals with ASD have deficits in this domain, with many studies pointing to the relationship between executive functioning and the ACC in ASD (Braconnier & Siper, 2021; Demetriou et al., 2019; Hill, 2004; K. E. May & Kana, 2020; Zhang et al., 2020).

The lack of group differences in BOLD signal for a majority of the ROIs appears to be in contrast to previous reports of atypical BOLD signal in ASD during lexicosemantic processing (Gaffrey et al., 2007; Harris et al., 2006; Just et al., 2004; Knaus et al., 2017; Lo et al., 2013; Moseley et al., 2013; Sahyoun et al., 2010; Shen et al., 2012). Several reasons may account for this finding in our study. fMRI-derived ROIs were based on data pooled from both ASD and TD groups. Given our study's focus on the relation between BOLD signal and theta power, fMRI-derived ROIs were limited to those showing the greatest task-induced increases across the entire sample. However, as suggested by some previous lexicosemantic studies, atypical activity patterns may occur in regions *outside* the neurotypical language network (Gaffrey et al., 2007; Y. Gao et al., 2019; Kana et al., 2006; Knaus et al., 2008; Shen et al., 2012). Therefore, heterogeneity and ASD variants with diverging patterns of atypical language networks may obscure differences from TD comparison groups (Y. Gao et al., 2019; Lombardo et al., 2019).

Notably, within some of these regions of shared activation, group differences in event-related theta power could nonetheless be detected.

Relation between BOLD signal and theta power

The results of this study show a significant correlation in the positive direction between theta power and BOLD signal in the ACC for the ASD group. As described above, the ACC plays an important role in cognitive control, decision making, and attention (Carter & Van Veen, 2007; Heilbronner & Hayden, 2016; Posner et al., 2007; Ruff et al., 2008). Theta power is also linked to these domains (Klimesch, 1999; Kovacevic et al., 2012, p. 20; Marinkovic et al., 2012). Previous studies suggest that the ACC may be a major generator of theta oscillation (Holroyd & Umemoto, 2016; Kouijzer et al., 2010; Luu & Tucker, 2001; Rajan et al., 2019; Tsujimoto et al., 2006).

Aside from the ACC, no other distinct pattern was detected in the relationship between event-related BOLD and theta signal changes. One might expect to see some correspondence between BOLD signal and theta power, since each measure is considered an index of choice in studies testing for task- or stimulus-related regional 'activation' (Audrain et al., 2020; Bakker-Marshall et al., 2018; Bastiaansen et al., 2005; Begus & Bonawitz, 2020; Gaffrey et al., 2007; Halgren et al., 2015; Harris et al., 2006; Just et al., 2004; Knaus et al., 2017; Kovacevic et al., 2012; Lo et al., 2013; Marinkovic et al., 2012, 2019; Moseley et al., 2013; Pu et al., 2020; Sahyoun et al., 2010; Shen et al., 2012). Indeed, event-related theta oscillations are particularly relevant to the double-duty lexical decision task employed in the current study that combined demands on both lexicosemantic processing and cognitive control. It has been well established that event-related theta power is sensitive to the retrieval of lexicosemantic information (Bastiaansen et al., 2005; Halgren et al., 2015), cognitive control (Cavanagh & Frank, 2014;

Correas et al., 2019; Kovacevic et al., 2012), and the integration of task-relevant representations across long-range functional networks (Bastiaansen et al., 2005; Halgren et al., 2015; Marinkovic et al., 2012).

To critically evaluate the relationship between fMRI and MEG, it is important to understand neurovascular coupling, that is, how local neuronal activity relates to increases in blood flow. For fMRI, the BOLD effect – conventionally considered the sole available (though indirect) assay of neuronal activity changes – measures changes in blood oxygenation that begin within 500 ms of stimulus onset and peak with a c.5 s delay (Hillman, 2014). When a stimulus is presented, there is an increase in oxygenation in activated brain regions, resulting in a local BOLD signal increase (Buxton, 2009; Hillman, 2014). The relationship between hemodynamics and brain activation has allowed the field to use vascular changes as an index of neural activity. Other metabolic and physiological processes that may impact the spatiotemporal processes of the BOLD signal include differences in the timing of blood vessel dilation and constriction, residual neurochemical changes post stimulus, and changes in the amount of neurotransmitters (Hillman, 2014). The relationship between neurovascular coupling and BOLD signal changes also depends on region and cortical depth (Devonshire et al., 2012; Goense et al., 2012). Neurovascular coupling differences may exist in ASD due to neurophysiological changes such as decreased inhibition that can increase blood flow and nitric oxide activity, which can in turn lead to an increased hemodynamic response (Reynell & Harris, 2013).

Unlike the reliance on hemodynamics in fMRI, the MEG signal is directly sensitive to neuronal activity, with a temporal resolution at the millisecond level (Ahlfors & Mody, 2019; Baillet, 2017). Previous work in monkeys has shown a strong relationship between MEG and local field potentials (LFP), providing support that MEG activity measures postsynaptic events

(E. L. Hall et al., 2014). Neural oscillations can be analyzed in time domain by averaging event-related fields per time unit, or in time-frequency domain by decomposing oscillatory signals into different frequency bands in a time-sensitive manner. These analyses provide different insights into the underlying spatio-temporal signal characteristics (Marinkovic et al., 2012, 2014). Despite the obvious benefits of MEG, such as its direct sensitivity to neural activity with excellent temporal resolution, its spatial estimates depend on the source modeling used to solve the inverse problem (Dale & Halgren, 2001). In the present study, we employed an aMEG method that combines distributed source modeling of the MEG signal with structural MRI. It constrains inverse solutions to each participant's cortical mantle based on real-shape head models.

The lack of relation between the two measures in the current study is not surprising given inconsistent findings in previous multimodal task-based neuroimaging studies reporting both positive and negative correlations (Ekstrom et al., 2009; Meltzer et al., 2007; Scheeringa et al., 2009a; Scheeringa & Fries, 2019; K. D. Singh et al., 2002; Winterer et al., 2007). Singh et al. (2002) reported an inverse relationship between fMRI response and event-related desynchronizations in the 5–15 Hz band, which includes theta power. However, this study included a small sample, with participants differing between the two modalities, and did not specifically focus on the 4–7 Hz range. A negative correlation between BOLD signal and theta power (measured with EEG) was also found within the default mode network in two studies of neurotypical adults (Meltzer et al., 2007; Scheeringa et al., 2009a). By contrast, the relationship between BOLD signal and event-related theta power during a visual decision task was found to be positive in motor cortex, but negative in ACC (Winterer et al., 2007). Although some of the seemingly inconsistent results may be attributed to differences in task and regions tested, the

relation between BOLD signal and theta power is clearly complex and incompletely understood, and findings in ASD from the current study are therefore not unexpected. Such a complex and seemingly intransparent relationship can be viewed in a positive light, according to Hari and Salmelin (2012) who argue that differences in findings may be more informative than similarities. Indeed, as fMRI and MEG detect neural activity in fundamentally different ways, differential findings may be considered complementary rather than inconsistent.

Limitations

fMRI analyses are conventionally volume-based, whereas they are surface-based in MEG. Due to some inherent limitations of volume to surface transformation, a few fMRI-derived ROIs could not be transformed into usable surface ROIs. Additionally, although MEG analyses focused on theta power in the present study given the established sensitivity of this frequency band to language processing and cognitive control, the MEG signal is inherently oscillatory and multiplexed, and future investigations of changes in other frequency bands may be useful. Slight differences in task presentation between MEG and fMRI scans were unavoidable due to differences in neuroimaging techniques, such as the need for null trials and jittering in fMRI.

While there are potential confounds that can lead to differences between scans over time, such as seasonal changes, menstrual cycles, or circadian rhythms, efforts were taken to reduce the possible impact of external circumstances. The number of days between MEG and fMRI scans was kept at a minimum to limit effects of maturational changes in adolescents. A large majority of the participants (85% ASD, 78% TD) in the analysis completed scans within a 3-month time frame. Although the results presented here are from a group of participants with a scan interval range of 1–252 days, supplemental analyses conducted in participants who completed the scans within 150 days did not alter the overall findings. In this supplemental

analysis most participants (90% ASD, 82% TD) were in the 3-month timeframe. There was no significant difference in scan intervals between ASD and TD groups. ($t(53) = -1.31$, $p = .19$). When days between scans was added as a covariate, there was no impact on the correlation between BOLD signal and event-related theta power. Additionally, most of the participants were above 15 years of age, rather than in a younger range when the brain is more rapidly developing and changing. Finally, due to lengthy fMRI and MEG scans and the moderately challenging lexicosemantic task, our ASD sample was limited to relatively high-functioning adolescents and findings may therefore not represent the broader autism spectrum, including minimally verbal and nonverbal individuals.

Conclusion

Comparing two metrics of choice for the detection of brain regional activity changes during lexicosemantic decision in adolescents with ASD and TD peers, we found no clear relationship between event-related fMRI BOLD signal and aMEG theta power. This indicates that reports of atypical "activation" patterns in ASD can only be interpreted with respect to the specific neuroimaging modality used. Group differences detected with aMEG, but not fMRI, further suggest that some neurofunctional differences in ASD may occur at the level of dynamic processing that is not detected at the limited temporal resolution of the hemodynamic response in fMRI. More generally, differential findings emphasize the need for integration between imaging modalities that have thus far been implemented largely in isolation in ASD research and beyond.

Acknowledgements

Chapter 1, in full, is a reprint of the material as it appears in *Neuroimage: Reports, 2(4), 100134.* Wilkinson, M., Jao Keehn, R. J., Linke, A. C., You, Y., Gao, Y., Alemu, K., Correas,

A., Rosen, B. Q., Kohli, J. S., Wagner, L., Sridhar, A., Marinkovic, K., & Müller, R.-A. (2022).

The dissertation author was the primary investigator and author of this paper.

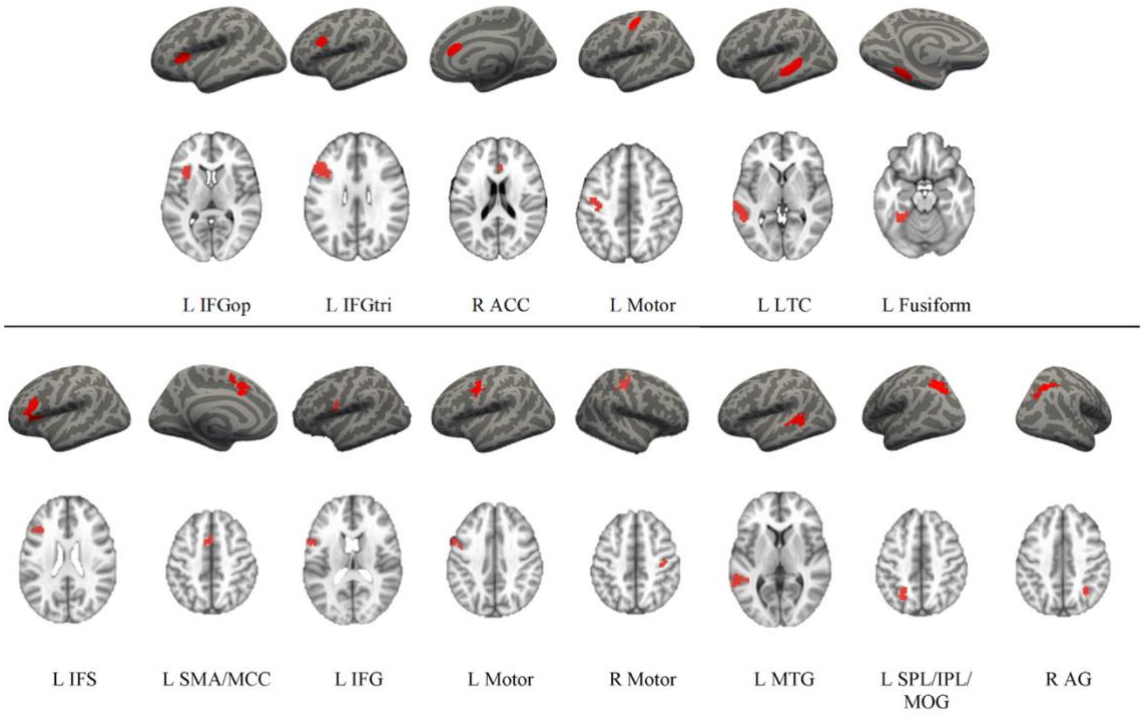

Figure 1.1 aMEG-derived and fMRI-derived ROIs in surface and volumetric space

Note: aMEG-derived surface space ROIs depicted in the top row and volumetric ROIs in the second row. Volumetric ROIs that closely aligned with aMEG-derived surface space ROIs were selected from the Schaefer-400 atlas. aMEG-derived ROIs: left inferior frontal gyrus pars opercularis (L IFGop), left inferior frontal gyrus pars triangularis (L IFGtri), right anterior cingulate cortex (R ACC), left precentral gyrus (L Motor), left lateral temporal cortex (L LTC), and left fusiform gyrus. fMRI derived-surface space ROIs depicted in the third row and volumetric ROIs in the fourth row. fMRI-derived ROIs: left inferior frontal sulcus (L IFS); left SMA and middle cingulate cortices (L SMA/MCC); left inferior frontal gyri (L IFG); left precentral gyrus (L Motor); right precentral gyrus (R Motor); left middle temporal gyrus (L MTG); left superior parietal, inferior parietal, and middle occipital cortices (L SPL/IPL/MOG); right angular gyrus (R AG).

Figure 1.2 Significant differences in theta power and BOLD signal in aMEG-and fMRI-derived ROIs

Note: Mean percent change from baseline in event-related theta power (top; A and B) and BOLD signal (bottom; C) by group for ROIs with significant group differences. Figure 1.2A – Theta power was significantly increased in ASD group compared to TD group for aMEG-derived ROIs: L fusiform for the 150-200 ms time window, R ACC for the 700-1000 ms time window, and L IFGtri for the 700-1000 ms time window. Figure 1.2B – Theta power was significantly increased in ASD group compared to TD group for fMRI-derived ROIs: R AG for the 110-170 ms time window, L IFG for the 450-650 ms time window, and L IFG for the 700-1000 ms time window. Figure 1.2C – Theta power was significantly increased in TD group compared to ASD group for fMRI-derived ROI L MTG for the 250-350 ms time window. BOLD signal was significantly increased in aMEG-derived ROI R ACC for ASD group compared to TD group. There were no group differences for BOLD signal in fMRI-derived ROIs.

ASD = autism spectrum disorder
L IFG = left inferior frontal gyri
L IFGop = left inferior frontal gyrus pars opercularis
L IFGtri = left inferior frontal gyrus pars triangularis
L MTG = left middle temporal gyrus
ms = millisecond
R ACC = right anterior cingulate cortex
R AG = right angular gyrus
ROI = region-of-interest
TD = typically developing

A.

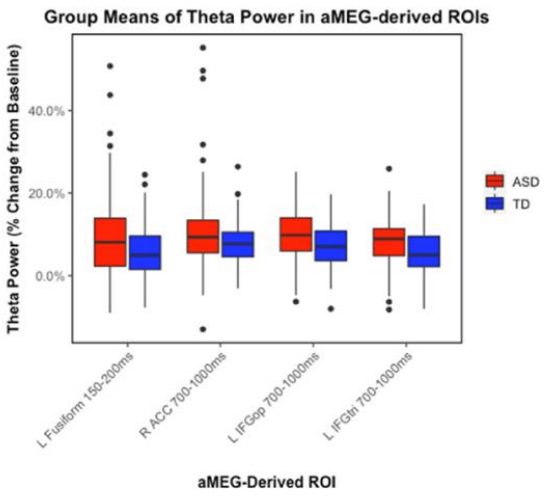
Group Means of Theta Power in aMEG-derived ROIs
Theta Power (% Change from Baseline)
40.0%
20.0%
0.0%
ASD
TD
L Fusiform 150-200ms
R ACC 700-1000ms
L IFGop 700-1000ms
L IFGtri 700-1000ms
aMEG-Derived ROI

B.

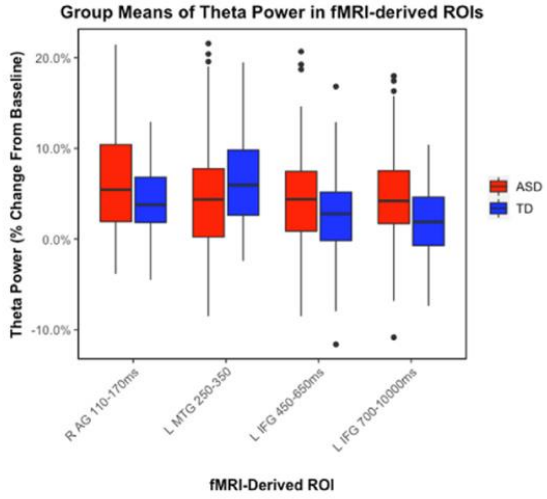
Group Means of Theta Power in fMRI-derived ROIs
Theta Power (% Change From Baseline)
20.0%
10.0%
0.0%
-10.0%
ASD
TD
R AG 110-170ms
L MTG 250-350
L IFG 450-650ms
L IFG 700-10000ms
fMRI-Derived ROI

C.

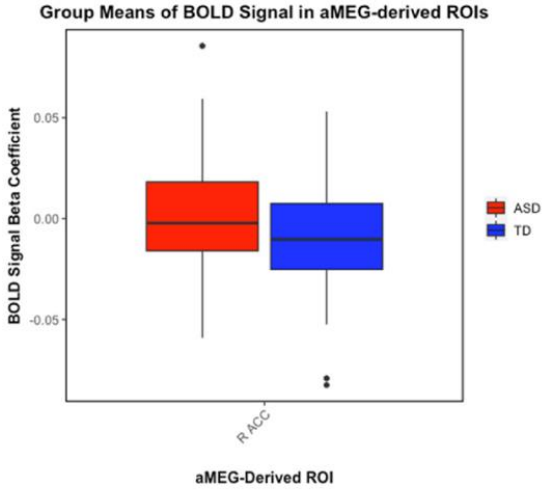
Group Means of BOLD Signal in aMEG-derived ROIs
BOLD Signal Beta Coefficient
0.05
0.00
-0.05
ASD
TD
R ACC
aMEG-Derived ROI

Table 1.1 Significant differences in theta power and BOLD signal in aMEG-and fMRI-derived ROIs

Note: Means, standard deviations (SD), and ranges for each group. Chi-square tests (gender, handedness) and *t*-tests were performed to determine if groups were significantly different on demographic variables. Non-standard degrees of freedom are attributed to Levene's test for homogeneity of variance, and thus reject the null hypothesis of equal variance. * denotes $p \leq .05$, ** $p \leq .01$, *** $p \leq .001$

ASD = autism spectrum disorder
RMSD = root mean square difference
TD = typically developing

	ASD (n = 33)		**TD (n = 23)**			**χ2 (df)**	***p***
Gender	24 male, 9 female		18 male, 5 female			.22 (1)	.64
Handedness	31 right, 1 left, 1 ambidextrous		21 right, 2 left			1.52 (2)	.47
	Mean (SD)	**Range**	**Mean (SD)**	**Range**	**Cohen's d**	***t*-stat (df)**	***p***
Age (years)	15.77 (2.30)	12.25–20	15.28 (1.93)	12.33–21.42	.23	1.02 (54)	.31
MRI Task Accuracy (%)	88 (8)	71–99	94 (3)	85–99	−.93	3.70 (47.08)	.0006***
MEG Task Accuracy (%)	87 (8)	68–99	92 (6)	70–98	−.69	2.08 (54)	.04*
MRI RMSD	.07 (.03)	.03–.14	.06 (.02)	.03–.13	.38	2.24 (54)	.03*
WASI-II							
Full Scale IQ	107.64 (17.86)	59–136	112.35 (12.94)	88–135	−.29	1.08 (54)	.28
Verbal IQ	105.33 (16.51)	68–134	111.26 (13.08)	85–135	−.39	1.43 (54)	.16
Non-Verbal IQ	109.97 (21.70)	54–156	110.30 (12.31)	80–128	−.02	.07 (52.19)	.94
ADOS-2							
Total	11.06 (3.37)	6–20	–	–	–	–	–

Table 1.2 ANOVA comparisons of event-related theta power and BOLD signal

Note: 2 x 3 ANOVA tests looked at the effect of group (ASD, TD) and word condition (SW, AW, PW) and the interaction on event-related theta power and BOLD beta coefficients in both sets of ROIs. Group differences in theta power were observed across multiple regions for both sets of ROIs. One group difference in BOLD signal was observed. The interaction was mostly nonsignificant, except for theta power in fMRI-derived ROI L IFG for the 700-1000 ms time window. * denotes $p \leq .05$, ** $p \leq .01$, *** $p \leq .001$

ASD = autism spectrum disorder
AW = animal word
L IFG = left inferior frontal gyri
L IFGop = left inferior frontal gyrus pars opercularis
L IFGtri = left inferior frontal gyrus pars triangularis
L IFS = left inferior frontal sulcus
L LTC = left lateral temporal cortex
L MTG = left middle temporal gyrus
L SMA/MCC = left SMA and middle cingulate cortices
L SPL/IPL/MOG = left superior parietal, inferior parietal, and middle occipital cortices
ms = millisecond
PW = pseudoword
R ACC = right anterior cingulate cortex
R AG = right angular gyrus
ROI = region-of-interest
SW = standard word
TD = typically developing

Theta Power in aMEG-derived ROIs

Time Window (ms)	ROI	Group		Condition		Group x Condition	
		F(1,162)	*p*	*F*(1,162)	*p*	*F*(1,162)	*p*
150–200	L Fusiform	5.57	0.02*	0.09	0.91	0.11	0.90
250–350	L LTC	1.96	0.16	0.96	0.39	0.45	0.64
450–650	L IFGop	0.88	0.35	7.39	0.0009**	1.50	0.23
	L IFGtri	2.37	0.13	9.64	0.0001***	1.09	0.34
	L LTC	0.00005	0.99	5.00	0.008**	1.70	0.19
700–1000	R ACC	5.11	0.03*	1.61	0.20	1.02	0.36
	L IFGop	10.00	0.002**	1.91	0.15	1.39	0.25
	L IFGtri	7.05	0.01**	1.20	0.31	2.70	0.07
	L Motor	2.84	0.09	2.48	0.09	1.12	0.33

Theta Power in fMRI-derived ROIs

Time Window (ms)	ROI	Group		Condition		Group x Condition	
		F(1,162)	*p*	*F*(1,162)	*p*	*F*(1,162)	*p*
110–170	L SPL/IPL/MOG	3.06	0.08	0.04	0.96	0.03	0.97
	R AG	7.08	0.008**	0.68	0.51	0.07	0.93
250–350	L IFG	0.49	0.48	0.94	0.39	0.69	0.50
	L MTG	4.69	0.03*	0.47	0.62	0.11	0.89
450–650	L IFS	2.09	0.15	10.66	<0.0001***	1.67	0.19
	L SMA/MCC	0.95	0.33	4.65	0.01*	0.38	0.69
	L IFG	5.01	0.03*	4.75	0.009**	0.24	0.79
	L Motor	1.08	0.30	5.93	0.003**	1.14	0.32
700–1000	L IFG	14.15	0.0002***	4.57	0.01*	3.08	0.05*
	R Motor	3.07	0.08	20.95	<0.0001***	0.71	0.49

BOLD Signal in aMEG-derived ROIs

ROI	Group		Condition		Group x Condition	
	F(1,162)	*p*	*F*(1,162)	*p*	*F*(1,162)	*p*
L Fusiform	0.28	0.60	25.19	<0.0001***	2.80	0.06
L LTC	1.49	0.22	10.61	<0.0001***	0.82	0.44
L IFGop	0.58	0.45	8.35	0.0004***	1.46	0.24
L IFGtri	0.64	0.42	4.04	0.02*	2.13	0.12
R ACC	4.80	0.03*	1.42	0.25	0.80	0.45
L Motor	1.19	0.28	7.92	0.0005***	0.30	0.74

BOLD Signal in fMRI-derived ROIs

ROI	Group		Condition		Group x Condition	
	F(1,162)	*p*	*F*(1,162)	*p*	*F*(1,162)	*p*
L SPL/IPL/MOG	0.06	0.81	10.65	<0.0001***	1.78	0.17
R AG	0.04	0.84	4.49	0.01**	0.96	0.39
L IFG	0.03	0.85	6.89	0.001**	0.07	0.93
L MTG	2.57	0.11	12.16	<0.0001***	0.82	0.44
L IFS	0.001	0.97	8.17	0.0004***	3.18	0.04*
L SMA/MCC	0.52	0.47	24.00	<0.0001***	1.00	0.37
L Motor	0.01	0.91	10.76	<0.0001***	0.09	0.91
R Motor	0.01	0.93	69.48	<0.0001***	0.70	0.50

Supplemental Materials

Participant recruitment and exclusion

Of the initial 156 recruits screened for the ASD cohort, 78 adolescents were excluded due to contraindications for MRI/MEG scanning (e.g., braces, permanent retainer) or history of neurological or other autism-related medical conditions (e.g., Fragile X syndrome, tuberous sclerosis, epilepsy). Fifty-nine of the initial 120 recruits for the TD sample were excluded due to contraindications for MRI/MEG scanning or personal/family history of ASD or other developmental, neurological, or psychological conditions. An additional 11 ASD and 8 TD participants dropped from the study after screening. Sixty-seven ASD and 53 TD participants were inducted into the study. Of these, 3 ASD and 3 TD adolescents could not be reached for scheduling, 2 ASD participants were no longer interested, 1 ASD and 3 TD participants were excluded for exposure to another language before age 5, 1 ASD participant was uncooperative during neuropsychological testing, 2 ASD participants performed below a sixth-grade reading level, 5 ASD and 2 TD participants performed below 60% on the lexicosemantic decision task during practice, 2 ASD participants were unable to follow task instructions, 1 ASD and 2 TD participants could not fit into the MRI head coil due to large head size, 1 ASD participant was hospitalized during the study, and 1 ASD and 8 TD participants did not complete all study components due to COVID-19 research shutdown in March 2020. Of the remaining 48 ASD and 35 TD participants who were scanned, 2 ASD and 4 TD adolescents completed a scan in only one of the modalities, 4 ASD and 4 TD participants were subject to unexpected data loss or scanner malfunction, 1 ASD participant had a left temporal abnormality, 8 ASD and 3 TD participants had excessive head motion ($\geq$2 standard deviations from the mean) during the fMRI scan, and 1 TD participant had unusable MEG data.

Scan environment

The environment was carefully considered to ensure success for ASD participants. Sensory sensitivities and overall anxiety were taken into account when conducting the study. All participants completed at least 1 extensive mock scan in an MRI simulator prior to the actual fMRI scan. Participants were able to familiarize themselves with the MR environment during this session. If the participant was not comfortable at any point, they were given the option to try again at a different time or to withdraw from the study. Mock scans lasted approximately 30 minutes in comparison to the 45-60-minute fMRI scan. During the mock scan, participants were exposed to the various types of scan sequences used during the MRI scan – auditory recordings from the MRI scan sequences were played to acclimate the participants. During the fMRI scan, great care was taken to ensure that the MRI environment was comfortable for all participants. In both the mock and MRI scans, foam cushions were used to pad and stabilize the participant's head, blankets were offered, and earplugs were provided to minimize noise. The participant was made aware that at any point during the scan they could speak to the MRI operators. Participants also held onto a squeeze ball to use in the case of emergency and/or if they felt an immediate need to be removed from the scanner environment. If a participant found the scan to be intolerable, they were allowed to stop at any point. MRI operators were in frequent contact with participants throughout the session and checked in with the participant between each scan sequence (i.e., at least every 5-10 minutes).

Regarding the MEG, there is no noise from the scanner and the participant was sitting with only part of their head inside the dewar. Many of the steps taken to aide with comfort during the MRI scan were employed during the MEG scan. The participant was comfortably seated in the scanner, with cushions and other reasonable accommodation provided if asked.

There were constant breaks in between tasks (every 5-7 minutes), allowing them to move about and rest their eyes. If the participant was not comfortable, they were made aware that at any point during the scan they could speak to the operators to stop the experiment. Frequent check-ins (every 5-7 minutes) occurred to ensure the participant was comfortable.

Experimental stimulus trial structure

The program produced 10,000 random permutations of the experimental stimulus order. In AFNI, the 3dDeconvolve function was run to generate and evaluate the normalized standard deviation for each randomized order. An optimal sequence was selected based on the smallest normalized standard deviation, with maxima set to 5 sequential word trials and 3 sequential null trials.

ROI identification and transformation

The transformation of ROIs between modalities was necessary for both the MEG-derived ROIs and the fMRI-derived ROIs. These two sets of ROIs were each derived from their respective modality and then transformed for the other modality. We performed this transformation so that we could use ROIs directly derived from the data, and to accommodate for any dislocations that occurred.

MEG-derived ROIs

First, the MEG-derived ROIs were identified using event-related theta power from MEG scans. These MEG-derived ROIs were transformed from surface to volumetric space using FreeSurfer. As the transformation between a surface space ROI and a volumetric ROI is not perfect, this resulted in holes in the volumetric ROIs. To ensure the BOLD response was able to be appropriately extracted from the MEG-derived ROIs, the Schaffer atlas was used as an alternative (i.e., a way to use the same region, but without any holes in the ROIs). We identified

volumetric ROIs from the Schaffer atlas that overlapped with the volumetric versions of the MEG-derived ROIs. The use of the Schaffer atlas was not related to aligning MEG-fMRI activations. Moreover, the Schaffer-400 atlas was selected due to its finer grained parcellation compared to other Schaeffer atlases (e.g., 100, 200, 300); this atlas provides an appropriate level of detail based on the MEG-derived ROIs. The MEG-derived ROIs (using the Schaffer atlas ROI files) were then used to extract the fMRI BOLD response.

fMRI-derived ROIs

Next, a set of fMRI-derived ROIs were identified using fMRI BOLD data. Areas of BOLD activation across both TD and ASD groups combined were used as the ROIs. The fMRI-derived ROIs were then transformed from volumetric space to surface space (using FreeSurfer). The transformation from volumetric to surface space also left some small holes in the ROIs, but these were able to be filled in using FreeSurfer. There were some regions (noted in the manuscript) that were identified as fMRI-derived ROIs, but were unable to be used because MEG does not have sufficient enough ability to extra data from these regions. Once in surface space, MEG theta power was extracted from these fMRI-derived ROIs.

Relationship of ROIs and task paradigm

The participant goes through several processing stages when engaging in this task, which activate specific brain regions. The first stage requires reading a word presented visually – a task which calls upon the middle occipital gyrus (Eigsti et al., 2015; Fiebach et al., 2002). Next, as the participant reads and comprehends the presented word, the prefrontal, temporal, and parietal regions are expected to be involved (Cabeza & Nyberg, 2000; Davis & Gaskell, 2009; Marinkovic, 2004a; Marinkovic et al., 2003, 2012; Price, 2010; Seghier, 2013). The lateral/middle temporal, inferior frontal, and fusiform ROIs identified as regions of activation

during this task fall into this category. Specifically, the IFG was expected based on previous findings that demonstrate its role in lexicosemantic tasks, and many ASD language studies have discussed the importance of this region (Cermak et al., 2022; Gaffrey et al., 2007; Huang et al., 2012; Tesink et al., 2011). After reading and comprehending the word, the participant starts to engage in a decision-making process to determine if the word is an existing word and if so, if it is an animal word. Alternatively, the word may be a pseudoword. The ACC is known to play a role in decision making, as is the prefrontal cortex, so it is expected that ROIs in these areas were activated during the task (Kovacevic et al., 2012; Marinkovic et al., 2012; Posner et al., 2007; Ruff et al., 2008). Lastly, the participant must then make a motor response appropriate to the presented word, and the parietal lobule assists with the required visual-motor integration (Fogassi & Luppino, 2005; Wise, 1985). While the right motor region was identified as an fMRI-derived ROI, the left motor region was identified as an MEG-derived ROI. It is not surprising that even though the participants responded with a button box in their left hand, that the left motor region was activated. A previous study in TD individuals found that for right-handed people (which is most of the sample in this paper) ipsilateral activation was quite pronounced when they used their left hand for motor tasks (Verstynen et al., 2005). Specific to ASD, research suggests that individuals with ASD may show more ipsilateral activation due to a less lateralized motor network (Carper et al., 2015; Gowen & Hamilton, 2013; Hau et al., 2022; Jansiewicz et al., 2006; Mostofsky & Ewen, 2011; Nebel et al., 2014).

Supplemental Table 1.1 Medications and psychological conditions

Note. Current psychotropic medication and psychological comorbidities for participants in autism spectrum disorder (ASD) group. Medication data were not available for 1 ASD participant.

SSRI = selective serotonin reuptake inhibitor
ADHD = attention deficit/hyperactivity disorder
[a]Mood stabilizers include antipsychotics and anticonvulsants
[b]Other includes sympatholytics and an antihistamine (used as an anxiolytic)

	List of medications	Stimulants	Mood Stabilizers[a]	SSRI/ Antidepressants	Anxiolytics/ Other[b]	Co-occurring Disorders
1.	Mirtazapine, Escitalopram oxalate, Aripiprazole, Methylphenidate hydrochloride	+	+	+	+	
2.	Methylphenidate hydrochloride, Guanfacine	+			+	
3.	Methylphenidate hydrochloride	+				ADHD
4.	Lamotrigine		+			ADHD
5.	Methylphenidate Hydrochloride	+				ADHD
6.	Oxcarbazepine, Guanfacine, Aripiprazole, Escitalopram oxalate, Alprazolam	+	+	+	+	Anxiety, Depression
7.	Methylphenidate hydrochloride	+				Anxiety
8.	Inderal				+	Anxiety
9.	Aripiprazole		+			Depression
10.	Guanfacine, Aripiprazole, Bupropion Hydrochloride		+	+	+	
11.	Aripiprazole, Lisdexamfetamine, Dextroamphetamine, Fluoxetine, Citalopram	+	+	+		Anxiety
12.	Quetiapine, Sertraline, Duloxetine, Amantadine, Prazosin		+	+	+	Depression
13.	None					Anxiety
14.	None					Anxiety
15.	None					Anxiety
16.	None					Depression
17.	None					ADHD, Depression
18.	Not Reported					Not Reported
	Total	7	7	5	6	14

Supplemental Table 1.2 Task stimuli word conditions

Note: SW, AW, and PW conditions did not significantly differ on number of letters or syllables between MRI and MEG stimuli sets. SW and AW conditions did not differ on the frequency of occurrence based on the Zipf scale or age of acquisition between MRI and MEG stimuli sets. Frequency of word occurrence is based on the Zipf scale. Age of acquisition is measured in years.

	MRI mean	**MEG mean**	***t*-stat (df)**		***p*-value**
Letters	6.04	5.96	0.55	(531.76)	0.79
Syllables	1.92	1.85	1.16	(556.77)	0.25
Frequency	3.73	3.70	0.63	(618)	0.53
Age of Acquisition	6.72	6.75	0.24	(618)	0.81

Supplemental Table 1.3 Participant demographics for fMRI-derived ROI selection

Note: Means, standard deviations (SD), and ranges for each group. Chi-square tests (gender, handedness) and *t*-tests were performed to determine if groups were significantly different on demographic variables. Non-standard degrees of freedom are attributed to Levene's test for homogeneity of variance, and thus reject the null hypothesis of equal variance. * denotes $p \leq .05$, ** $p \leq .01$, *** $p \leq .001$

ASD = autism spectrum disorder
RMSD = root mean square difference
TD = typically developing

	ASD (n=34)		**TD (n=26)**			**χ2 (df)**	***p***
Gender	25 male, 9 female		19 male, 7 female			.002 (1)	.97
Handedness	31 right, 2 left, 1 ambidextrous		23 right, 3 left			1.34 (2)	.51
	Mean (SD)	**Range**	**Mean (SD)**	**Range**	**Cohen's d**	***t*-stat (df)**	***p***
Age (years)	15.90 (2.27)	12.25-20	15.22 (1.89)	12.33-21.42	.32	1.24 (58)	.22
MRI Task Accuracy (%)	89 (8)	71-99	94 (3)	85-99	-.79	3.78 (46.88)	.0004***
MRI RMSD	.07 (.03)	.03-.14	.06 (.03)	.03-.13	.33	1.78 (58)	.08
WASI-II							
Full Scale IQ	107.50 (17.60)	59-136	111.73 (12.26)	88-136	-.27	1.05 (58)	.30
Verbal IQ	105.29 (16.26)	68-134	110.23 (12.67)	85-135	-.33	1.27 (58)	.21
Non-Verbal IQ	109.71 (21.42)	54-156	110.31 (11.63)	80-128	-.03	.14 (52.95)	.89
ADOS-2							
Total	10.79 (3.67)	2-20	--	--	--	--	--

Supplemental Table 1.4 fMRI-derived ROIs

Note: Number of voxels and peak MNI coordinates (RAI) for each MRI-derived ROIs.

L IFG = left inferior frontal gyri
L IFS = left inferior frontal sulcus
L MTG = left middle temporal gyrus
L SMA/MCC = left SMA and middle cingulate cortices
L SPL/IPL/MOG = left superior parietal, inferior parietal, and middle occipital cortices
R AG = right angular gyrus

MEG-Derived ROI	**Number of Voxels**	**Peak Coordinates**
L IFS	64	36.5, -27.5, 9.5
L SMA/MCC	62	6.5, -15.5, 36.5
L IFG	64	51.5, -6.5, 9.5
L Motor	63	36.5, 2.5, 30.5
R Motor	88	-38.5, 26.5, 45.5
L MTG	65	54.5, 44.5, 3.5
L SPL/IPL/MOG	64	30.5, 65.5, 27.5
R AG	56	-35.5, 65.5, 24.5

Supplemental Table 1.5 ROI modifications

Note. Modifications made to surface space ROIs after transformed from volumetric space. ROIs were fragmented and not large enough, resulting in not enough vertices to extract data. ROIs were manually dilated and eroded in FreeSurfer's Freeview. ROIs were dilated to fill in holes and connect fragmented pieces and were then eroded to maintain the initial shape of the ROI.

L IFG = left inferior frontal gyri
L IFS = left inferior frontal sulcus
L MTG = left middle temporal gyrus
L SMA/MCC = left SMA and middle cingulate cortices
L SPL/IPL/MOG = left superior parietal, inferior parietal, and middle occipital cortices
R AG = right angular gyrus

ROIs	Modifications
L IFG	Dilate 13, Erode 12
L SMA, MCC	None
L IFG, Motor	None
L Motor	Erode 1, Dilate 6, Erode 4
R Motor	Dilate 4, Erode 3
L MTG	Dilate 1
L SPL, IPL, MOG	Dilate 3, Erode 2
R AG	Dilate 2, Erode 1

Supplemental Table 1.6 Pearson partial correlations for BOLD signal and theta power in aMEG-derived ROIs

Note: Pearson partial correlations between event-related theta power and BOLD beta coefficients controlling for RMSD and age by group. Correlations were mostly insignificant, in both positive and negative directions for both autism spectrum disorder (ASD) and typically developing (TD) adolescents. * denotes $p \leq .05$

AW = animal word
L IFGop = left inferior frontal gyrus pars opercularis
L IFGtri = left inferior frontal gyrus pars triangularis
L LTC = left lateral temporal cortex
ms = millisecond
PW = pseudoword
R ACC = right anterior cingulate cortex
ROI = region-of-interest
SW = standard word

Theta Time Window (ms)	ROI	Word Condition	TD			ASD		
			r	*p*	FDR-adjusted	*r*	*p*	FDR-adjusted
150-200	L Fusiform	SW	0.15	0.54	0.97	0.07	0.74	0.99
		AW	-0.18	0.45	0.96	0.23	0.24	0.89
		PW	-0.01	0.96	0.99	0.04	0.84	0.99
250-350	L LTC	SW	-0.19	0.42	0.96	0.07	0.73	0.99
		AW	-0.46	0.05**	0.67	-0.01	0.95	0.99
		PW	-0.27	0.27	0.96	0.08	0.68	0.99
450-650	L IFGop	SW	-0.02	0.95	0.99	0.19	0.34	0.99
		AW	0.21	0.40	0.96	-0.15	0.45	0.99
		PW	-0.12	0.63	0.99	-0.004	0.99	0.99
	L IFGtri	SW	0.16	0.50	0.96	0.10	0.64	0.99
		AW	0.20	0.41	0.96	0.08	0.69	0.99
		PW	0.05	0.83	0.99	-0.22	0.26	0.89
	L LTC	SW	-0.07	0.78	0.99	0.01	0.97	0.99
		AW	-0.37	0.12	0.67	0.10	0.63	0.99
		PW	-0.07	0.77	0.99	0.24	0.22	0.89
700-1000	R ACC	SW	-0.34	0.15	0.67	0.01	0.94	0.99
		AW	0.08	0.75	0.99	0.16	0.44	0.99
		PW	-0.03	0.89	0.99	0.46	0.02*	0.46
	L IFGop	SW	0.19	0.43	0.96	0.06	0.78	0.99
		AW	0.35	0.14	0.67	0.02	0.93	0.99
		PW	-0.17	0.49	0.96	0.14	0.48	0.99
	L IFGtri	SW	0.00	0.99	0.99	0.22	0.27	0.89
		AW	0.39	0.10	0.67	0.26	0.19	0.89
		PW	0.01	0.98	0.99	-0.08	0.71	0.99
	L Motor	SW	-0.06	0.80	0.99	0.31	0.11	0.89
		AW	-0.06	0.82	0.99	0.14	0.49	0.99
		PW	0.42	0.07	0.67	0.27	0.18	0.89

Supplemental Table 1.7 Pearson partial correlations for BOLD signal and theta power in fMRI-derived ROIs

Note: Pearson partial correlations between event-related theta power and BOLD beta coefficients controlling for RMSD and age by group. Correlations were mostly insignificant, in both positive and negative directions for both autism spectrum disorder (ASD) and typically developing (TD) adolescents. ** denotes $p \leq .01$

AW = animal word
L IFG = left inferior frontal gyri
L IFS = left inferior frontal sulcus
L MTG = left middle temporal gyrus
L SMA/MCC = left SMA and middle cingulate cortices
L SPL/IPL/MOG = left superior parietal, inferior parietal, and middle occipital cortices
ms = millisecond
PW = pseudoword
R AG = right angular gyrus
ROI = region-of-interest
SW = standard word

Theta Time Window (ms)	ROI	Word Condition	TD			ASD		
			r	*p*	FDR-adjusted	*r*	*p*	FDR-adjusted
110-170	L SPL/IPL/ MOG	SW	-0.38	0.11	0.90	0.07	0.72	0.97
		AW	0.19	0.44	0.90	0.03	0.89	0.97
		PW	0.09	0.70	0.90	-0.12	0.54	0.97
	R AG	SW	-0.29	0.23	0.90	-0.07	0.74	0.97
		AW	-0.01	0.97	0.99	0.18	0.37	0.97
		PW	0.08	0.75	0.90	-0.26	0.19	0.97
250-350	L IFG	SW	-0.10	0.67	0.90	0.13	0.51	0.97
		AW	0.09	0.72	0.90	-0.15	0.45	0.97
		PW	-0.20	0.40	0.90	0.11	0.59	0.97
	L MTG	SW	-0.32	0.18	0.90	0.14	0.50	0.97
		AW	-0.62	0.004**	0.13	-0.01	0.95	0.97
		PW	-0.30	0.22	0.90	-0.15	0.44	0.97
450-650	L IFS	SW	-0.16	0.50	0.90	-0.13	0.52	0.97
		AW	0.10	0.67	0.90	-0.08	0.69	0.97
		PW	-0.12	0.63	0.90	0.04	0.86	0.97
	L SMA/MCC	SW	-0.16	0.50	0.90	-0.12	0.54	0.97
		AW	0.18	0.47	0.90	-0.17	0.39	0.97
		PW	0.34	0.16	0.90	0.18	0.36	0.97
	L IFG	SW	-0.15	0.54	0.90	-0.12	0.54	0.97
		AW	0.24	0.32	0.90	-0.01	0.97	0.97
		PW	-0.17	0.49	0.90	0.09	0.65	0.97
	L Motor	SW	-0.04	0.86	0.99	-0.05	0.82	0.97
		AW	-0.001	0.99	0.99	0.21	0.29	0.97
		PW	-0.30	0.21	0.90	0.09	0.64	0.97
700-1000	L IFG	SW	-0.005	0.99	0.99	-0.23	0.25	0.97
		AW	0.11	0.65	0.90	0.02	0.90	0.97
		PW	-0.20	0.42	0.90	0.30	0.12	0.97
	R Motor	SW	-0.03	0.92	0.99	-0.09	0.64	0.97
		AW	-0.11	0.65	0.90	0.03	0.88	0.97
		PW	0.15	0.55	0.90	0.28	0.15	0.97

Supplemental Table 1.8 ANOVA comparisons of theta power and BOLD signal in sample with outliers removed

Note: 2 x 3 ANOVA tests looked at the effect of group (ASD, TD) and word condition (SW, AW, PW) and the interaction on event-related theta power and BOLD beta coefficients in both set of ROIs, after the removal of outliers. An outlier was defined as 1.5*interquartile range (IQR) below the first quartile or above the third quartile for theta power and BOLD signal beta coefficients. Group differences in theta power were observed across multiple regions for both sets of ROIs. One group difference in BOLD signal was observed. The interaction was significant for theta power in MEG-derived ROI L motor for the 700-1000 ms time window and fMRI-derived ROI L IFG for the 700-1000 ms time window. The interaction was significant for BOLD signal in MEG-derived ROI L fusiform. * denotes $p \leq .05$, ** $p \leq .01$, *** $p \leq .001$

ASD = autism spectrum disorder
AW = animal word
L IFG = left inferior frontal gyri
L IFGop = left inferior frontal gyrus pars opercularis
L IFGtri = left inferior frontal gyrus pars triangularis
L IFS = left inferior frontal sulcus
L LTC = left lateral temporal cortex
L MTG = left middle temporal gyrus
L SMA/MCC = left SMA and middle cingulate cortices
L SPL/IPL/MOG = left superior parietal, inferior parietal, and middle occipital cortices
ms = millisecond
PW = pseudoword
R ACC = right anterior cingulate cortex
R AG = right angular gyrus
ROI = region-of-interest
SW = standard word
TD = typically developing

Theta Power in aMEG-derived ROIs							
Time Window (ms)	**ROI**	**Group**		**Condition**		**Group x Condition**	
		***F*(df)**	***p***	***F*(df)**	***p***	***F*(df)**	***p***
150-200	L Fusiform	1.64 (1,155)	0.20	0.69 (2,155)	0.50	0.66 (2,155)	0.52
250-350	L LTC	2.14 (1,160)	0.15	1.05 (2,160)	0.35	0.49 (2,160)	0.62
450-650	L IFGop	1.34 (1,161)	0.25	6.67 (2,161)	0.002**	1.29 (2,161)	0.28
	L IFGtri	1.96 (1,159)	0.16	9.92 (1,159)	<0.0001***	0.94 (1,159)	0.39
	L LTC	0.05 (1,157)	0.82	9.35 (1,157)	0.0001***	1.31 (1,157)	0.27
700-1000	R ACC	2.53 (1,150)	0.11	3.49 (1,150)	0.03*	1.40 (1,150)	0.25
	L IFGop	6.47 (1,158)	0.01**	1.35 (1,158)	0.26	0.87 (1,158)	0.42
	L IFGtri	6.29 (1,161)	0.01**	1.02 (1,161)	0.36	2.60 (1,161)	0.08
	L Motor	9.36 (1,155)	0.003**	2.42 (1,155)	0.09	3.66 (1,155)	0.03*

Theta Power in fMRI-derived ROIs							
Time Window (ms)	**ROI**	**Group**		**Condition**		**Group x Condition**	
		***F*(df)**	***p***	***F*(df)**	***p***	***F*(df)**	***p***
110-170	L SPL/IPL/MOG	2.73 (1,158)	0.10	0.14 (1,158)	0.87	0.07 (1,158)	0.93
	R AG	6.39 (1,161)	0.01**	0.65 (1,161)	0.52	0.20 (1,161)	0.82
250-350	L IFG	0.49(1,162)	0.48	0.94 (1,162)	0.39	0.69 (1,162)	0.50
	L MTG	9.00 (1,157)	0.003**	0.22 (1,157)	0.81	0.33 (1,157)	0.72
450-650	L IFS	2.71 (1,155)	0.10	9.27 (1,155)	0.0002***	0.89 (1,155)	0.41
	L SMA/MCC	3.51 (1,158)	0.06	5.63 (1,158)	0.004**	0.49 (1,158)	0.61
	L IFG	4.24 (1,156)	0.04*	3.41 (1,156)	0.04*	0.71 (1,156)	0.49
	L Motor	1.08 (1,162)	0.30	5.93 (1,162)	0.003**	1.14 (1,162)	0.32
700-1000	L IFG	14.08 (1,158)	0.0002***	4.24 (1,158)	0.02*	3.38 (1,158)	0.04*
	R Motor	0.89 (1,158)	0.35	25.72 (1,158)	<0.0001***	0.32 (1,158)	0.73

BOLD Signal in aMEG-derived ROIs							
ROI	**Group**		**Condition**		**Group x Condition**		
	***F*(df)**	***p***	***F*(df)**	***p***	***F*(df)**	***p***	
L Fusiform	0.09 (1,156)	0.77	29.40 (1,156)	<0.0001***	4.30 (1,156)	0.02*	
L LTC	1.84 (1,156)	0.18	10.73 (1,156)	<0.0001***	0.94 (1,156)	0.39	
L IFGop	0.33 (1,156)	0.57	9.84 (1,156)	<0.0001***	0.52 (1,156)	0.59	
L IFGtri	1.11 (1,153)	0.29	5.53 (1,153)	0.005**	2.30 (1,153)	0.10	
R ACC	3.79 (1,158)	0.05*	2.30 (1,158)	0.10	0.63 (1,158)	0.53	
L Motor	0.59 (1,159)	0.44	11.13 (1,159)	<0.0001***	0.04 (1,159)	0.96	

BOLD Signal in fMRI-derived ROIs						
ROI	**Group**		**Condition**		**Group x Condition**	
	***F*(df)**	***p***	***F*(df)**	***p***	***F*(df)**	***p***
L SPL/IPL/MOG	0.10 (1,160)	0.76	11.06 (1,160)	<0.0001***	1.97 (1,160)	0.14
R AG	0.003 (1,153)	0.96	6.80 (1,153)	0.004**	0.94 (1,153)	0.39
L IFG	0.01(1,159)	0.94	7.79 (1,159)	0.0006***	0.004 (1,159)	0.996
L MTG	2.13 (1,161)	0.15	12.22 (1,161)	<0.0001***	1.04 (1,161)	0.36
L IFS	0.43 (1,155)	0.52	9.16 (1,155)	0.0002**	2.47 (1,155)	0.09
L SMA/MCC	0.14 (1,158)	0.71	29.93 (1,158)	<0.0001***	1.09 (1,158)	0.34
L Motor	0.10 (1,158)	0.75	11.77 (1,158)	<0.0001***	0.23 (1,158)	0.80
R Motor	0.0001 (1,156)	0.99	88.28 (1,156)	<0.0001***	0.69 (1,156)	0.50

Supplemental Table 1.9 Pearson partial correlations for BOLD signal and theta power in aMEG-derived ROIs in sample with outliers removed

Note: Pearson partial correlations between event-related theta power and BOLD beta coefficients, after removal of outliers, controlling for root mean square difference (RMSD; motion) and age by group. Correlations were insignificant after FDR-adjustment, in both positive and negative directions for autism spectrum disorder (ASD) and typically developing (TD) adolescents. ** $p \leq .01$

AW = animal word
L IFGop = left inferior frontal gyrus pars opercularis
L IFGtri = left inferior frontal gyrus pars triangularis
L LTC = left lateral temporal cortex
ms = millisecond
PW = pseudoword
R ACC = right anterior cingulate cortex
ROI = region-of-interest
SW = standard word

Theta Time Window (ms)	ROI	Word Condition	TD			ASD		
			r	*p*	FDR-adjusted	*r*	*p*	FDR-adjusted
150-200	L Fusiform	SW	0.15	0.54	0.74	-0.03	0.89	0.96
		AW	-0.18	0.45	0.74	0.09	0.68	0.96
		PW	0.14	0.60	0.76	0.23	0.31	0.96
250-350	L LTC	SW	-0.19	0.42	0.74	0.15	0.48	0.96
		AW	-0.56	0.02	0.41	0.07	0.73	0.96
		PW	-0.27	0.27	0.72	-0.30	0.15	0.96
450-650	L IFGop	SW	-0.19	0.45	0.74	0.10	0.63	0.96
		AW	0.21	0.40	0.74	-0.32	0.11	0.96
		PW	0.09	0.74	0.87	-0.10	0.63	0.96
	L IFGtri	SW	0.16	0.50	0.74	-0.17	0.43	0.96
		AW	0.26	0.29	0.72	-0.05	0.81	0.96
		PW	-0.35	0.16	0.64	-0.08	0.71	0.96
	L LTC	SW	-0.07	0.78	0.88	-0.26	0.19	0.96
		AW	-0.33	0.19	0.64	-0.14	0.55	0.96
		PW	-0.13	0.62	0.76	-0.08	0.69	0.96
700-1000	R ACC	SW	-0.34	0.15	0.64	0.01	0.98	0.98
		AW	0.04	0.89	0.93	-0.03	0.89	0.96
		PW	0.28	0.24	0.72	0.17	0.42	0.96
	L IFGop	SW	0.15	0.55	0.74	-0.01	0.97	0.98
		AW	0.32	0.19	0.64	-0.04	0.86	0.96
		PW	-0.17	0.50	0.74	0.14	0.48	0.96
	L IFGtri	SW	0.004	0.99	0.99	-0.03	0.88	0.96
		AW	0.35	0.16	0.64	0.24	0.28	0.96
		PW	-0.44	0.07	0.64	0.05	0.81	0.96
	L Motor	SW	-0.05	0.84	0.91	0.28	0.17	0.96
		AW	-0.16	0.54	0.74	-0.13	0.57	0.96
		PW	0.42	0.07	0.64	0.27	0.18	0.96

Supplemental Table 1.10 Pearson partial correlations for BOLD signal and theta power in fMRI-derived ROIs in sample with outliers removed

Note: Pearson partial correlations between event-related theta power and BOLD beta coefficients controlling for RMSD and age by group in sample with outliers removed. Correlations were mostly insignificant, in both positive and negative directions for both autism spectrum disorder (ASD) and typically developing (TD) adolescents. ** denotes $p \leq .01$

AW = animal word
L IFG = left inferior frontal gyri
L IFS = left inferior frontal sulcus
L MTG = left middle temporal gyrus
L SMA/MCC = left SMA and middle cingulate cortices
L SPL/IPL/MOG = left superior parietal, inferior parietal, and middle occipital cortices
ms = millisecond
PW = pseudoword
R AG = right angular gyrus
ROI = region-of-interest
SW = standard word

Theta Time Window (ms)	ROI	Word Condition	TD			ASD		
			r	*p*	FDR-adjusted	*r*	*p*	FDR-adjusted
110-170	L SPL/IPL/ MOG	SW	-0.38	0.11	0.87	0.01	0.98	0.98
		AW	0.03	0.92	0.99	-0.04	0.85	0.97
		PW	0.09	0.70	0.99	-0.14	0.50	0.97
	R AG	SW	-0.29	0.23	0.87	0.06	0.77	0.97
		AW	-0.01	0.97	0.99	0.34	0.11	0.92
		PW	0.08	0.75	0.99	-0.06	0.78	0.97
250-350	L IFG	SW	-0.10	0.67	0.99	0.13	0.51	0.97
		AW	0.09	0.72	0.99	-0.06	0.78	0.97
		PW	-0.02	0.92	0.99	0.11	0.59	0.97
	L MTG	SW	-0.32	0.18	0.87	0.16	0.45	0.97
		AW	-0.62	0.004**	0.13	0.13	0.54	0.97
		PW	-0.30	0.22	0.87	0.04	0.84	0.97
450-650	L IFS	SW	-0.11	0.66	0.99	-0.12	0.57	0.97
		AW	0.31	0.21	0.87	-0.35	0.12	0.92
		PW	0.10	0.71	0.99	0.05	0.80	0.97
	L SMA/MCC	SW	-0.16	0.50	0.99	0.03	0.90	0.97
		AW	0.18	0.47	0.99	-0.23	0.27	0.97
		PW	0.34	0.16	0.87	0.24	0.27	0.97
	L IFG	SW	-0.15	0.54	0.99	-0.12	0.57	0.97
		AW	0.12	0.65	0.99	-0.01	0.97	0.98
		PW	-0.04	0.88	0.99	0.09	0.65	0.97
	L Motor	SW	-0.04	0.86	1.00	0.07	0.75	0.97
		AW	-0.001	0.99	1.00	-0.03	0.87	0.97
		PW	-0.30	0.21	0.87	0.17	0.41	0.97
700-1000	L IFG	SW	-0.005	0.99	0.99	-0.11	0.60	0.97
		AW	0.11	0.65	0.99	0.16	0.44	0.97
		PW	-0.22	0.38	0.99	0.30	0.12	0.92
	R Motor	SW	-0.03	0.92	0.99	-0.24	0.30	0.97
		AW	-0.03	0.90	0.99	0.26	0.20	0.97
		PW	0.15	0.55	0.99	0.34	0.10	0.92

Supplemental Table 1.11 Participant demographics in motion-matched sample

Note: Means, standard deviations (SD), and ranges for each group. Chi-square tests (gender, handedness) and *t*-tests were performed to determine if groups were significantly different on demographic variables in a motion-matched sample. While motion during fMRI scans (RMSD) was low across both groups, it was slightly but significantly higher in the ASD than TD group (Table 1). In addition to advanced motion denoising, these supplementary analyses were conducted in a smaller subsample with tightly matched motion. Non-standard degrees of freedom are attributed to Levene's test for homogeneity of variance, and thus reject the null hypothesis of equal variance. * denotes $p \leq .05$, ** $p \leq .01$

ASD = autism spectrum disorder
RMSD = root mean square difference
TD = typically developing

	ASD (n=29)		**TD (n=21)**			**χ2 (df)**	***p***
Gender	20 male, 9 female		17 male, 4 female			.91 (1)	.34
Handedness	28 right, 1 left		19 right, 2 left			.80 (1)	.37
	Mean (SD)	**Range**	**Mean (SD)**	**Range**	**Cohen's d**	***t*-stat (df)**	***p***
Age (years)	15.64 (2.22)	12.25-20	15.28 (2.03)	12.33-21.42	.17	.59 (48)	.56
MRI Task Accuracy (%)	88 (8)	71-99	94 (4)	85-99	-.91	3.30 (40.33)	.002**
MEG Task Accuracy (%)	87 (9)	68-99	92 (6)	70-98	-.63	1.98 (48)	.05*
MRI RMSD	.07 (.02)	.03-.10	.06 (.02)	.03-.13	.50	1.10 (48)	.28
WASI-II							
Full Scale IQ	107.34 (18.71)	59-136	112.05 (13.52)	88-135	-.28	.98 (48)	.33
Verbal IQ	105.52 (17.28)	68-134	110.81 (13.63)	85-135	-.33	1.16 (48)	.25
Non-Verbal IQ	109.45 (22.74)	54-156	110.29 (12.90)	80-128	-.04	.16 (45.76)	.87
ADOS-2							
Total	11.31 (3.51)	6-20	--	--	--	--	--

Supplemental Table 1.12 ANOVA comparisons of theta power and BOLD signal in motion-matched sample

Note: 2 x 3 ANOVA tests looked at the effect of group (ASD, TD) and word condition (SW, AW, PW) and the interaction on event-related theta power and BOLD beta coefficients in both set of ROIs, in a motion-matched sample. Group differences in theta power were observed across multiple regions for both sets of ROIs. One group difference in BOLD signal was observed. The interaction was nonsignificant across all measurements. * denotes $p \leq .05$, ** $p \leq .01$, *** $p \leq .001$

ASD = autism spectrum disorder
AW = animal word
L IFG = left inferior frontal gyri
L IFGop = left inferior frontal gyrus pars opercularis
L IFGtri = left inferior frontal gyrus pars triangularis
L IFS = left inferior frontal sulcus
L LTC = left lateral temporal cortex
L MTG = left middle temporal gyrus
L SMA/MCC = left SMA and middle cingulate cortices
L SPL/IPL/MOG = left superior parietal, inferior parietal, and middle occipital cortices
ms = millisecond
PW = pseudoword
R ACC = right anterior cingulate cortex
R AG = right angular gyrus
ROI = region-of-interest
SW = standard word
TD = typically developing

Theta Power in aMEG-derived ROIs							
Time Window (ms)	**ROI**	**Group**		**Condition**		**Group x Condition**	
		***F*(1,147)**	***p***	***F*(2,147)**	***p***	***F*(2,147)**	***p***
150-200	L Fusiform	9.28	0.003**	0.05	0.95	0.09	0.91
250-350	L LTC	0.83	0.36	0.90	0.41	0.56	0.57
450-650	L IFGop	1.73	0.19	8.19	0.0004***	2.23	0.11
	L IFGtri	4.98	0.03*	11.62	<0.0001***	1.65	0.19
	L LTC	0.15	0.70	6.68	0.002**	2.40	0.09
700-1000	R ACC	5.35	0.02*	1.50	0.23	0.67	0.51
	L IFGop	12.28	0.0006***	1.51	0.22	1.05	0.35
	L IFGtri	9.11	0.003**	1.06	0.35	2.00	0.14
	L Motor	2.48	0.12	1.98	0.14	0.71	0.49

Theta Power in fMRI-derived ROIs							
Time Window (ms)	**ROI**	**Group**		**Condition**		**Group x Condition**	
		***F*(1,147)**	***p***	***F*(2,147)**	***p***	***F*(2,147)**	***p***
110-170	L SPL/IPL/MOG	5.65	0.02*	0.07	0.93	0.03	0.97
	R AG	5.09	0.03*	0.57	0.57	0.24	0.78
250-350	L IFG	1.25	0.26	0.50	0.61	0.66	0.52
	L MTG	2.42	0.12	0.47	0.63	0.16	0.85
450-650	L IFS	4.02	0.05*	11.70	<0.0001***	2.07	0.13
	L SMA/MCC	0.22	0.64	5.30	0.01**	0.31	0.73
	L IFG	6.73	0.01**	5.33	0.01**	0.40	0.67
	L Motor	2.49	0.12	6.48	0.002**	1.45	0.24
700-1000	L IFG	15.03	0.0002***	4.33	0.01**	2.81	0.06
	R Motor	2.26	0.14	18.44	<0.0001***	0.48	0.62

BOLD Signal in aMEG-derived ROIs						
ROI	**Group**		**Condition**		**Group x Condition**	
	***F*(1,147)**	***p***	***F*(2,147)**	***p***	***F*(2,147)**	***p***
L Fusiform	0.08	0.78	29.26	<0.0001***	2.54	0.08
L LTC	2.01	0.16	10.45	<0.0001***	1.00	0.37
L IFGop	0.88	0.35	9.77	0.0001***	1.01	0.37
L IFGtri	1.65	0.20	5.35	0.01**	1.94	0.15
R ACC	5.71	0.02*	1.30	0.28	0.84	0.43
L Motor	1.02	0.31	6.98	0.001**	0.29	0.75

BOLD Signal in fMRI-derived ROIs						
ROI	**Group**		**Condition**		**Group x Condition**	
	***F*(1,147)**	***p***	***F*(2,147)**	***p***	***F*(2,147)**	***p***
L SPL/IPL/MOG	0.31	0.58	12.81	<0.0001***	1.67	0.19
R AG	0.30	0.59	4.41	0.01**	0.88	0.42
L IFG	0.09	0.77	7.53	0.0007***	0.02	0.98
L MTG	4.27	0.04	11.42	<0.0001***	1.01	0.37
L IFS	0.68	0.41	11.52	<0.0001***	2.70	0.07
L SMA/MCC	1.23	0.27	27.59	<0.0001***	0.77	0.47
L Motor	0.08	0.78	10.77	<0.0001***	0.20	0.82
R Motor	0.39	0.53	75.71	<0.0001***	0.67	0.52

Supplemental Table 1.13 Pearson partial correlations for BOLD signal and theta power in aMEG-derived ROIs in motion-matched sample

Note: Pearson partial correlations between event-related theta power and BOLD beta coefficients controlling for root mean square difference (RMSD; motion) and age by group in a motion-matched sample. Correlations were insignificant in both positive and negative directions for both autism spectrum disorder (ASD) and typically developing (TD) adolescents.

AW = animal word
L IFGop = left inferior frontal gyrus pars opercularis
L IFGtri = left inferior frontal gyrus pars triangularis
L LTC = left lateral temporal cortex
ms = millisecond
PW = pseudoword
R ACC = right anterior cingulate cortex
ROI = region-of-interest
SW = standard word

Theta Time Window (ms)	ROI	Word Condition	TD			ASD		
			r	*p*	FDR-adjusted	*r*	*p*	FDR-adjusted
150-200	L Fusiform	SW	0.10	0.69	0.99	0.02	0.92	0.99
		AW	-0.15	0.57	0.99	0.13	0.52	0.95
		PW	-0.16	0.53	0.99	-0.11	0.61	0.95
250-350	L LTC	SW	-0.0005	1.00	0.99	-0.02	0.94	0.99
		AW	-0.33	0.19	0.94	-0.09	0.66	0.95
		PW	-0.32	0.21	0.94	-0.26	0.20	0.78
450-650	L IFGop	SW	-0.05	0.83	0.99	0.07	0.74	0.95
		AW	0.17	0.52	0.99	-0.27	0.20	0.78
		PW	-0.14	0.58	0.99	-0.07	0.74	0.95
	L IFGtri	SW	-0.01	0.98	0.99	0.003	0.99	0.99
		AW	0.11	0.69	0.99	-0.11	0.61	0.95
		PW	0.05	0.85	0.99	-0.34	0.10	0.78
	L LTC	SW	-0.05	0.85	0.99	-0.26	0.20	0.78
		AW	-0.42	0.09	0.94	-0.07	0.74	0.95
		PW	-0.12	0.63	0.99	-0.05	0.82	0.97
700-1000	R ACC	SW	-0.37	0.14	0.94	-0.08	0.70	0.95
		AW	0.07	0.78	0.99	0.15	0.48	0.95
		PW	-0.20	0.44	0.99	0.44	0.03	0.76
	L IFGop	SW	0.15	0.57	0.99	0.01	0.97	0.99
		AW	0.34	0.19	0.94	0.05	0.83	0.97
		PW	-0.21	0.42	0.99	0.09	0.66	0.95
	L IFGtri	SW	-0.18	0.50	0.99	0.17	0.42	0.95
		AW	0.35	0.17	0.94	0.22	0.28	0.95
		PW	-0.004	0.99	0.99	-0.14	0.52	0.95
	L Motor	SW	-0.09	0.72	0.99	0.28	0.18	0.78
		AW	-0.04	0.88	0.99	0.08	0.70	0.95
		PW	0.28	0.27	0.99	0.28	0.17	0.78

Supplemental Table 1.14 Pearson partial correlations for BOLD signal and theta power in fMRI-derived ROIs in motion-matched sample

Note: Pearson partial correlations between event-related theta power and BOLD beta coefficients, controlling for root mean square difference (RMSD; motion) and age by group. Correlations were insignificant after FDR-adjustment, in both positive and negative directions for both autism spectrum disorder (ASD) and typically developing (TD) adolescents.

AW = animal word
L IFG = left inferior frontal gyrus
L IFS = left inferior frontal sulcus
L MTG = left middle temporal gyrus
L SMA/MCC = left supplementary motor area/middle cingulate cortex
L SPL/IPL/MOG = left superior parietal lobule/inferior parietal lobule/middle occipital gyrus
ms = millisecond
PW = pseudoword
R AG = right angular gyrus
ROI = region-of-interest
SW = standard word

Theta Time Window (ms)	ROI	Word Condition	TD			ASD		
			r	*p*	FDR-adjusted	*r*	*p*	FDR-adjusted
110-170	L SPL/IPL/ MOG	SW	-0.30	0.25	0.82	0.08	0.70	0.94
		AW	0.31	0.23	0.82	0.06	0.77	0.94
		PW	0.06	0.81	0.91	-0.19	0.35	0.90
	R AG	SW	-0.29	0.26	0.82	0.03	0.89	0.94
		AW	0.06	0.81	0.91	0.28	0.17	0.90
		PW	0.05	0.86	0.91	-0.29	0.16	0.90
250-350	L IFG	SW	-0.15	0.56	0.91	0.10	0.63	0.90
		AW	-0.06	0.82	0.91	-0.23	0.27	0.90
		PW	-0.05	0.85	0.91	0.03	0.90	0.94
	L MTG	SW	-0.21	0.41	0.82	0.12	0.58	0.90
		AW	-0.38	0.13	0.82	-0.12	0.55	0.90
		PW	-0.30	0.24	0.82	-0.47	0.02*	0.57
450-650	L IFS	SW	-0.35	0.17	0.82	-0.15	0.46	0.90
		AW	0.05	0.84	0.91	-0.10	0.63	0.90
		PW	-0.22	0.39	0.82	0.05	0.82	0.94
	L SMA/MCC	SW	-0.24	0.35	0.82	-0.12	0.56	0.90
		AW	0.24	0.36	0.82	-0.23	0.28	0.90
		PW	0.38	0.13	0.82	0.23	0.27	0.90
	L IFG	SW	-0.22	0.39	0.82	-0.15	0.48	0.90
		AW	0.10	0.69	0.91	-0.18	0.40	0.90
		PW	-0.29	0.26	0.82	0.02	0.91	0.94
	L Motor	SW	-0.10	0.69	0.91	-0.11	0.61	0.90
		AW	-0.14	0.60	0.91	0.05	0.81	0.94
		PW	-0.30	0.24	0.82	0.21	0.31	0.90
700-1000	L IFG	SW	-0.07	0.80	0.91	-0.36	0.08	0.90
		AW	0.02	0.94	0.94	-0.05	0.80	0.94
		PW	-0.24	0.36	0.82	0.27	0.20	0.90
	R Motor	SW	-0.04	0.88	0.91	-0.14	0.50	0.90
		AW	-0.17	0.52	0.91	0.01	0.97	0.97
		PW	-0.04	0.87	0.91	0.29	0.15	0.90

Supplemental Table 1.15 Participant demographics in sample with <150-day scan interval

Note: Means, standard deviations (SD), and ranges for each group. Chi-square tests (gender, handedness) and *t*-tests were performed to determine if groups were significantly different on demographic variables in a sample of individuals who completed MEG and fMRI scans ≥150 days apart. Non-standard degrees of freedom are attributed to Levene's test for homogeneity of variance, and thus reject the null hypothesis of equal variance. ** $p \leq .01$

ASD = autism spectrum disorder
RMSD = root mean square difference
TD = typically developing

	ASD (n=31)		**TD (n=22)**			**χ2 (df)**	***p***
Gender	23 male, 8 female		17 male, 5 female			.07 (1)	.80
Handedness	29 right, 1 left		20 right, 2 left			.77 (1)	.38
	Mean (SD)	**Range**	**Mean (SD)**	**Range**	**Cohen's d**	***t*-stat (df)**	***p***
Age (years)	15.83 (2.20)	12.25-20	15.41 (1.88)	12.33-21.42	.20	.74 (51)	.46
MRI Task Accuracy (%)	89 (8)	71-99	94 (4)	85-99	-.75	3.33 (43.58)	.002**
MEG Task Accuracy (%)	88 (8)	68-99	91 (6)	70-98	-.63	1.69 (51)	.10
MRI RMSD	.07 (.03)	.03-.14	.06 (.02)	.03-.13	.50	2.19 (51)	.03*
WASI-II							
Full Scale IQ	108.81 (15.96)	77-136	111.64 (12.77)	88-135	-.0002	.69 (51)	.49
Verbal IQ	106.52 (15.59)	76-134	110.82 (13.21)	85-135	-.29	1.05 (51)	.30
Non-Verbal IQ	111.10 (19.54)	75-156	109.50 (11.97)	80-127	.10	.37 (50.10)	.71
ADOS-2							
Total	11 (3.44)	6-20	--	--	--	--	--

Supplemental Table 1.16 ANOVA comparisons of theta power and BOLD signal in sample with <150-day scan interval

Note: 2 x 3 ANOVA tests looked at the effect of group (ASD, TD) and word condition (SW, AW, PW) and the interaction on event-related theta power and BOLD beta coefficients in both set of ROIs, in a sample of individuals who completed MEG and fMRI scans ≥150 days apart. Group differences in theta power were observed across multiple regions for both sets of ROIs. One group difference in BOLD signal was observed. The interaction was mostly nonsignificant, except for BOLD signal in fMRI-derived ROI L fusiform. * denotes $p \leq .05$, ** $p \leq .01$, *** $p \leq .001$

ASD = autism spectrum disorder
AW = animal word
L IFG = left inferior frontal gyri
L IFGop = left inferior frontal gyrus pars opercularis
L IFGtri = left inferior frontal gyrus pars triangularis
L IFS = left inferior frontal sulcus
L LTC = left lateral temporal cortex
L MTG = left middle temporal gyrus
L SMA/MCC = left SMA and middle cingulate cortices
L SPL/IPL/MOG = left superior parietal, inferior parietal, and middle occipital cortices
ms = millisecond
PW = pseudoword
R ACC = right anterior cingulate cortex
R AG = right angular gyrus
ROI = region-of-interest
SW = standard word
TD = typically developing

Theta Power in aMEG-derived ROIs							
Time Window (ms)	**ROI**	**Group**		**Condition**		**Group x Condition**	
		***F*(1,153)**	***p***	***F*(2,153)**	***p***	***F*(2,153)**	***p***
150-200	L Fusiform	2.64	0.11	0.13	0.87	0.19	0.83
250-350	L LTC	3.28	0.07	0.97	0.38	0.46	0.63
450-650	L IFGop	0.71	0.40	7.17	0.001**	1.65	0.20
	L IFGtri	2.12	0.15	8.74	0.0003***	1.10	0.34
	L LTC	0.16	0.69	4.25	0.02**	1.36	0.26
700-1000	R ACC	3.24	0.07	1.23	0.29	0.87	0.42
	L IFGop	6.23	0.01*	1.57	0.21	1.12	0.33
	L IFGtri	6.24	0.01*	1.18	0.31	2.49	0.09
	L Motor	2.33	0.13	2.06	0.13	0.94	0.39

Theta Power in fMRI-derived ROIs							
Time Window (ms)	**ROI**	**Group**		**Condition**		**Group x Condition**	
		***F*(1,147)**	***p***	***F*(2,147)**	***p***	***F*(2,147)**	***p***
110-170	L SPL/IPL/MOG	1.23	0.27	0.03	0.97	0.05	0.95
	R AG	5.49	0.02*	0.62	0.54	0.03	0.97
250-350	L IFG	0.46	0.50	1.25	0.29	0.88	0.42
	L MTG	7.85	0.01**	0.64	0.53	0.24	0.78
450-650	L IFS	2.13	0.15	10.69	<0.0001***	1.88	0.16
	L SMA/MCC	1.53	0.22	4.58	0.01**	0.33	0.72
	L IFG	4.33	0.04*	4.74	0.01**	0.31	0.73
	L Motor	0.65	0.42	5.46	0.01**	1.24	0.29
700-1000	L IFG	11.62	0.0008***	3.98	0.02*	2.75	0.07
	R Motor	2.28	0.13	20.05	<0.0001***	0.34	0.72

BOLD Signal in aMEG-derived ROIs						
ROI	**Group**		**Condition**		**Group x Condition**	
	***F*(1,147)**	***p***	***F*(2,147)**	***p***	***F*(2,147)**	***p***
L Fusiform	0.45	0.50	24.57	<0.0001***	4.10	0.02*
L LTC	0.90	0.34	9.36	0.0001***	0.69	0.50
L IFGop	0.94	0.33	8.31	0.0004***	1.45	0.24
L IFGtri	0.95	0.33	3.36	0.04*	1.90	0.15
R ACC	7.45	0.01**	1.47	0.23	0.90	0.41
L Motor	1.87	0.17	8.15	0.0004***	0.15	0.86

BOLD Signal in fMRI-derived ROIs						
ROI	**Group**		**Condition**		**Group x Condition**	
	***F*(1,147)**	***p***	***F*(2,147)**	***p***	***F*(2,147)**	***p***
L SPL/IPL/MOG	0.08	0.77	9.72	0.0001***	1.41	0.25
R AG	0.30	0.58	4.20	0.02*	1.12	0.33
L IFG	0.12	0.73	6.16	0.003**	0.13	0.88
L MTG	2.02	0.16	11.18	<0.0001***	0.74	0.48
L IFS	0.10	0.75	7.23	0.001**	2.90	0.06
L SMA/MCC	0.58	0.45	22.13	<0.0001***	1.28	0.28
L Motor	0.20	0.66	10.59	<0.0001***	0.02	0.98
R Motor	0.03	0.85	64.86	<0.0001***	0.79	0.45

Supplemental Table 1.17 Pearson partial correlations for BOLD signal and theta power in MEG-derived ROIs in sample with <150-day scan interval

Note: Pearson partial correlations between event-related theta power and BOLD beta coefficients controlling for root mean square difference (RMSD; motion) and age by group in 150-day sample. Correlations were insignificant in both positive and negative directions for both autism spectrum disorder (ASD) and typically developing (TD) adolescents after FDR-adjustment. ** denotes $p \leq .01$

AW = animal word
L IFGop = left inferior frontal gyrus pars opercularis
L IFGtri = left inferior frontal gyrus pars triangularis
L LTC = left lateral temporal cortex
ms = millisecond
PW = pseudoword
R ACC = right anterior cingulate cortex
ROI = region-of-interest
SW = standard word

Theta Time Window (ms)	ROI	Word Condition	TD			ASD		
			r	*p*	FDR-adjusted	*r*	*p*	FDR-adjusted
150-200	L Fusiform	SW	0.19	0.44	0.96	0.08	0.69	0.97
		AW	-0.20	0.44	0.96	0.28	0.15	0.87
		PW	0.01	0.96	0.97	0.12	0.56	0.89
250-350	L LTC	SW	-0.18	0.46	0.96	0.05	0.80	0.98
		AW	-0.42	0.09	0.73	-0.03	0.89	0.98
		PW	-0.22	0.39	0.96	0.17	0.40	0.87
450-650	L IFGop	SW	0.07	0.79	0.97	0.17	0.40	0.87
		AW	0.25	0.32	0.96	-0.17	0.41	0.87
		PW	0.04	0.88	0.97	-0.01	0.95	0.98
	L IFGtri	SW	0.17	0.51	0.97	0.13	0.53	0.89
		AW	0.21	0.40	0.96	0.12	0.56	0.89
		PW	0.07	0.79	0.97	-0.18	0.38	0.87
	L LTC	SW	-0.08	0.76	0.97	-0.01	0.94	0.98
		AW	-0.36	0.14	0.75	0.08	0.68	0.97
		PW	-0.01	0.97	0.97	0.25	0.21	0.87
700-1000	R ACC	SW	-0.41	0.09	0.73	-0.0007	0.99	1.00
		AW	-0.01	0.96	0.97	0.16	0.42	0.87
		PW	-0.11	0.67	0.97	0.47	0.01**	0.39
	L IFGop	SW	0.08	0.76	0.97	0.06	0.76	0.98
		AW	0.30	0.23	0.96	0.02	0.91	0.98
		PW	-0.15	0.56	0.97	0.13	0.52	0.89
	L IFGtri	SW	0.02	0.94	0.97	0.24	0.23	0.87
		AW	0.39	0.11	0.73	0.33	0.10	0.87
		PW	-0.01	0.96	0.97	0.02	0.94	0.98
	L Motor	SW	-0.26	0.30	0.96	0.26	0.19	0.87
		AW	-0.11	0.66	0.97	0.16	0.42	0.87
		PW	0.44	0.07	0.73	0.30	0.13	0.87

Supplemental Table 1.18 Pearson partial correlations for BOLD signal and theta power in fMRI-derived ROIs in sample with <150-day scan interval

Note: Pearson partial correlations between event-related theta power and BOLD beta coefficients, controlling for root mean square difference (RMSD; motion) and age by group. Correlations were insignificant, in both positive and negative directions for both autism spectrum disorder (ASD) and typically developing (TD) adolescents. ** denotes $p \leq .01$

AW = animal word
L IFG = left inferior frontal gyrus
L IFS = left inferior frontal sulcus
L MTG = left middle temporal gyrus
L SMA/MCC = left supplementary motor area/middle cingulate cortex
L SPL/IPL/MOG = left superior parietal lobule/inferior parietal lobule/middle occipital gyrus
ms = millisecond
PW = pseudoword
R AG = right angular gyrus
ROI = region-of-interest
SW = standard word

Theta Time Window (ms)	ROI	Word Condition	TD			ASD		
			r	*p*	FDR-adjusted	*r*	*p*	FDR-adjusted
110-170	L SPL/IPL/ MOG	SW	-0.36	0.14	0.93	0.16	0.43	0.94
		AW	0.16	0.53	0.93	0.04	0.83	0.94
		PW	0.12	0.63	0.93	-0.10	0.61	0.94
	R AG	SW	-0.30	0.22	0.93	0.01	0.96	0.96
		AW	-0.09	0.71	0.93	0.20	0.33	0.94
		PW	0.08	0.76	0.94	-0.24	0.25	0.94
250-350	L IFG	SW	-0.002	0.99	0.99	0.30	0.14	0.94
		AW	0.16	0.53	0.93	-0.08	0.69	0.94
		PW	-0.22	0.39	0.93	0.21	0.30	0.94
	L MTG	SW	-0.30	0.23	0.93	0.10	0.63	0.94
		AW	-0.57	0.01**	0.39	-0.08	0.69	0.94
		PW	-0.26	0.29	0.93	-0.10	0.62	0.94
450-650	L IFS	SW	-0.15	0.55	0.93	-0.08	0.70	0.94
		AW	0.10	0.70	0.93	-0.07	0.73	0.94
		PW	-0.10	0.70	0.93	0.06	0.79	0.94
	L SMA/MCC	SW	-0.13	0.60	0.93	-0.17	0.41	0.94
		AW	0.21	0.41	0.93	-0.13	0.52	0.94
		PW	0.33	0.18	0.93	0.20	0.32	0.94
	L IFG	SW	-0.13	0.60	0.93	-0.08	0.71	0.94
		AW	0.28	0.26	0.93	-0.03	0.87	0.94
		PW	-0.13	0.62	0.93	0.14	0.50	0.94
	L Motor	SW	-0.05	0.85	0.98	0.04	0.85	0.94
		AW	-0.01	0.96	0.99	0.22	0.28	0.94
		PW	-0.28	0.26	0.93	0.24	0.23	0.94
700-1000	L IFG	SW	0.01	0.98	0.99	-0.22	0.28	0.94
		AW	0.06	0.82	0.98	0.03	0.90	0.94
		PW	-0.22	0.37	0.93	0.30	0.13	0.94
	R Motor	SW	-0.03	0.89	0.99	-0.09	0.65	0.94
		AW	-0.20	0.44	0.93	0.02	0.91	0.94
		PW	0.14	0.57	0.93	0.34	0.09	0.94

Supplemental Figure 1.1 Group means of theta power

Note. Mean percent change from baseline in event-related theta power for each word condition by group for MEG-derived (top) and fMRI-derived (bottom) ROIs. Theta power was significantly increased in ASD group compared to TD group for both SW (p = .03) and AW (p =.02) conditions in L IFG for the 700-1000ms time window (bottom).

ASD = autism spectrum disorder
AW = animal word
L IFG = left inferior frontal gyri
L IFGop = left inferior frontal gyrus pars opercularis
L IFGtri = left inferior frontal gyrus pars triangularis
L IFS = left inferior frontal sulcus
L LTC = left lateral temporal cortex
L MTG = left middle temporal gyrus
L SMA/MCC = left SMA and middle cingulate cortices
L SPL/IPL/MOG = left superior parietal, inferior parietal, and middle occipital cortices
ms = millisecond
PW = pseudoword
R ACC = right anterior cingulate cortex
R AG = right angular gyrus
ROI = region-of-interest
SW = standard word
TD = typically developing

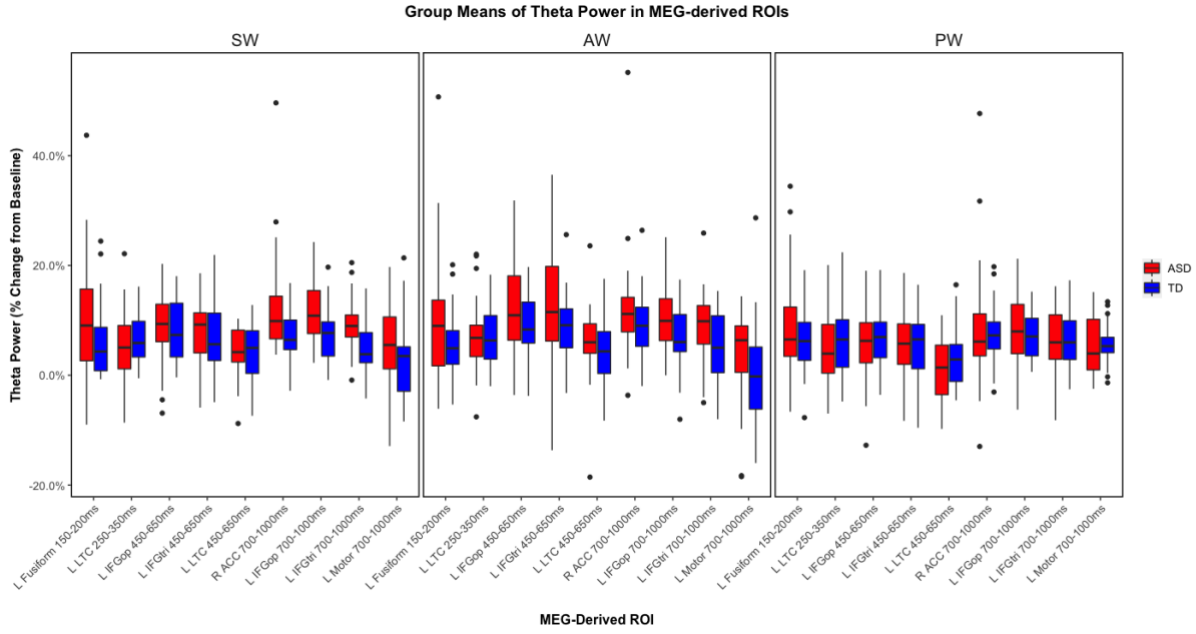
Group Means of Theta Power in MEG-derived ROIs
SW
AW
PW
Theta Power (% Change from Baseline)
40.0%
20.0%
0.0%
-20.0%
L Fusiform 150-200ms
L LTC 250-350ms
L IFGop 450-650ms
L IFGtri 450-650ms
L LTC 450-650ms
R ACC 700-1000ms
L IFGop 700-1000ms
L IFGtri 700-1000ms
L Motor 700-1000ms
ASD
TD
MEG-Derived ROI

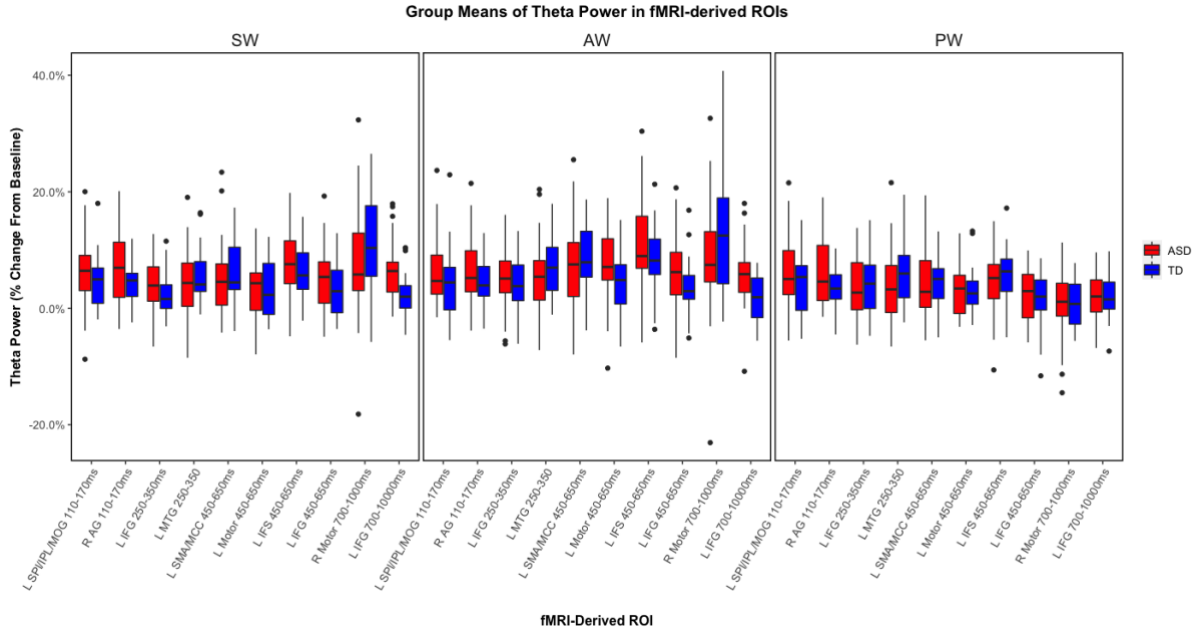
Group Means of Theta Power in fMRI-derived ROIs
SW
AW
PW
Theta Power (% Change From Baseline)
40.0%
20.0%
0.0%
-20.0%
L SPl/IPL/MOG 110-170ms
R AG 110-170ms
L IFG 250-350ms
L MTG 250-350
L SMA/MCC 450-650ms
L Motor 450-650ms
L IFS 450-650ms
L IFG 450-650ms
R Motor 700-1000ms
L IFG 700-1000ms
ASD
TD
fMRI-Derived ROI

Supplemental Figure 1.2 Group means of BOLD signal

Note. Mean of BOLD signal beta coeffcients for each word condition by group for MEG-derived (top) and fMRI-derived (bottom) ROIs. No significant group differences were identified for SW, AW, or PW conditions.

ASD = autism spectrum disorder
AW = animal word
L IFG = left inferior frontal gyri
L IFGop = left inferior frontal gyrus pars opercularis
L IFGtri = left inferior frontal gyrus pars triangularis
L IFS = left inferior frontal sulcus
L LTC = left lateral temporal cortex
L MTG = left middle temporal gyrus
L SMA/MCC = left SMA and middle cingulate cortices
L SPL/IPL/MOG = left superior parietal, inferior parietal, and middle occipital cortices
ms = millisecond
PW = pseudoword
R ACC = right anterior cingulate cortex
R AG = right angular gyrus
ROI = region-of-interest
SW = standard word
TD = typically developing

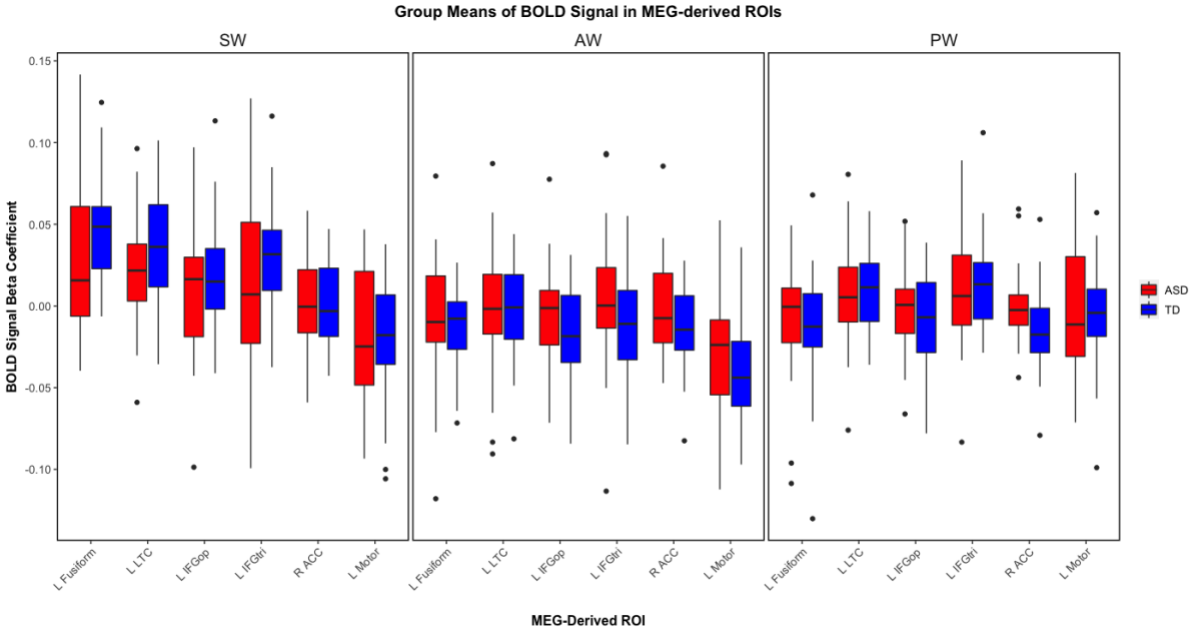
Group Means of BOLD Signal in MEG-derived ROIs
SW
AW
PW
BOLD Signal Beta Coefficient
0.15
0.10
0.05
0.00
-0.05
-0.10
L Fusiform
L LTC
L IFGop
L IFGtri
R ACC
L Motor
ASD
TD
MEG-Derived ROI

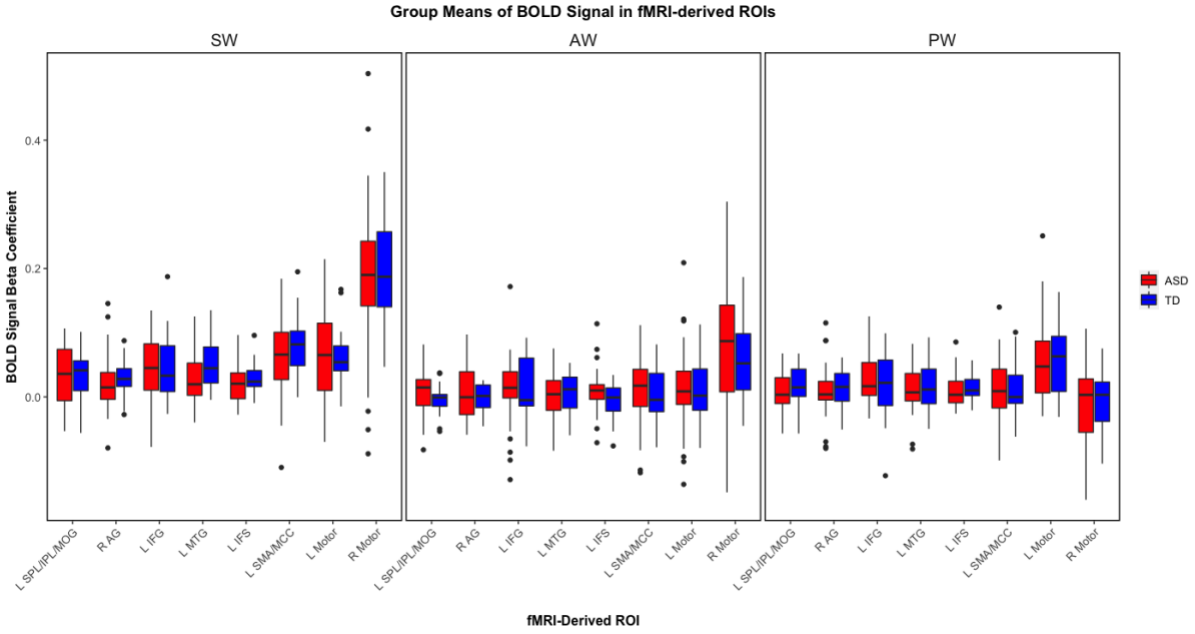
Group Means of BOLD Signal in fMRI-derived ROIs
SW
AW
PW
BOLD Signal Beta Coefficient
0.4
0.2
0.0
L SPL/IPL/MOG
R AG
L IFG
L MTG
L IFS
L SMA/MCC
L Motor
R Motor
ASD
TD
fMRI-Derived ROI

Supplemental Figure 1.3 Theta power and BOLD signal correlations

Note. Plots depicts zero-order correlation of ROI and word condition for each group. Significant partial correlations in TD adolescents between event-related theta power and BOLD signal beta coefficient (Supplementary Tables S1.6-1.7) are shown for L LTC for the 250-350 ms time window for AW condition (left) and left middle temporal gyrus (MTG) between 250-350 ms for animal words (AW) condition (right). ASD group is shown for reference. Significant partial correlation in ASD group between theta power and BOLD signal is shown for R ACC for the 700-1000 ms time window for PW condition (bottom). TD group is shown for reference. Partial correlations controlled for age and RMSD, and were nonsignificant after FDR-adjustment (Supplementary Tables S1.6-1.7).

ASD = autism spectrum disorder
AW = animal words
L LTC = left lateral temporal cortex
L MTG = left middle temporal gyrus
ms = millisecond
PW = pseudoword condition
R ACC = right anterior cingulate cortex
TD = typically developing

L LTC 250-350ms, Animal Words

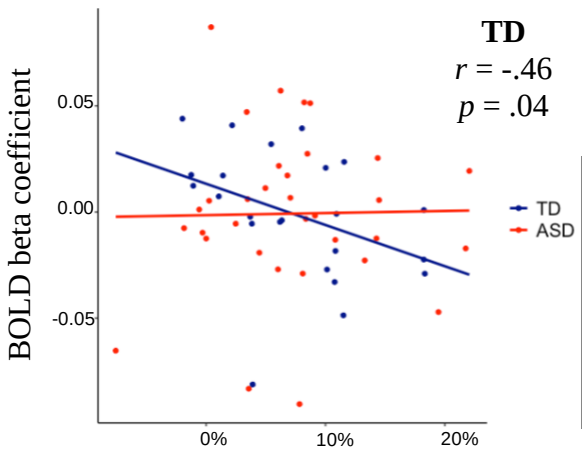

Theta power (% change from baseline)

L MTG 250-350ms, Animal Words

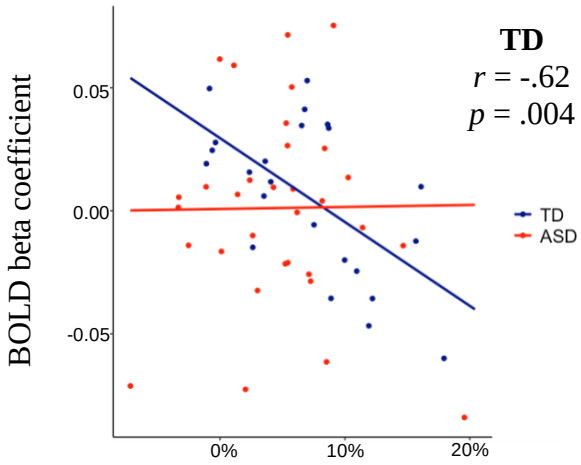

Theta power (% change from baseline)

R ACC 700-1000ms, Pseudowords

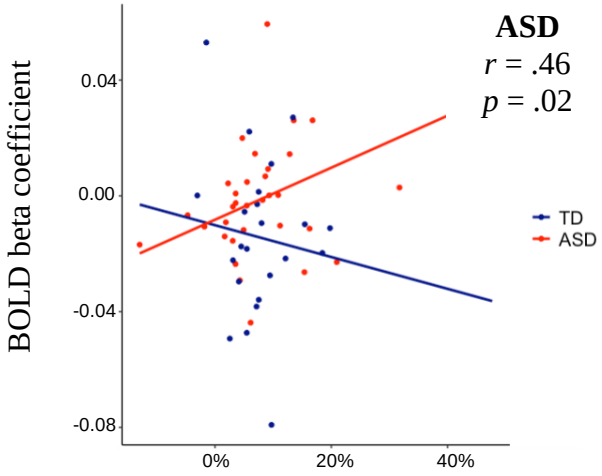

Supplemental Figure 1.4 Group means of theta power in sample with outliers removed

Note. Mean percent change from baseline in event-related theta power for each word condition by group for MEG-derived (top) and fMRI-derived (bottom) ROIs in sample with outliers removed. Theta power was significantly increased in ASD group compared to TD group for AW in L motor for the 700-1000 ms time window (p =.01; top) and in L IFG for the 700-1000 ms time window (p =.004; bottom).

ASD = autism spectrum disorder
AW = animal word
L IFG = left inferior frontal gyri
L IFGop = left inferior frontal gyrus pars opercularis
L IFGtri = left inferior frontal gyrus pars triangularis
L IFS = left inferior frontal sulcus
L LTC = left lateral temporal cortex
L MTG = left middle temporal gyrus
L SMA/MCC = left SMA and middle cingulate cortices
L SPL/IPL/MOG = left superior parietal, inferior parietal, and middle occipital cortices
ms = millisecond
PW = pseudoword
R ACC = right anterior cingulate cortex
R AG = right angular gyrus
ROI = region-of-interest
SW = standard word
TD = typically developing

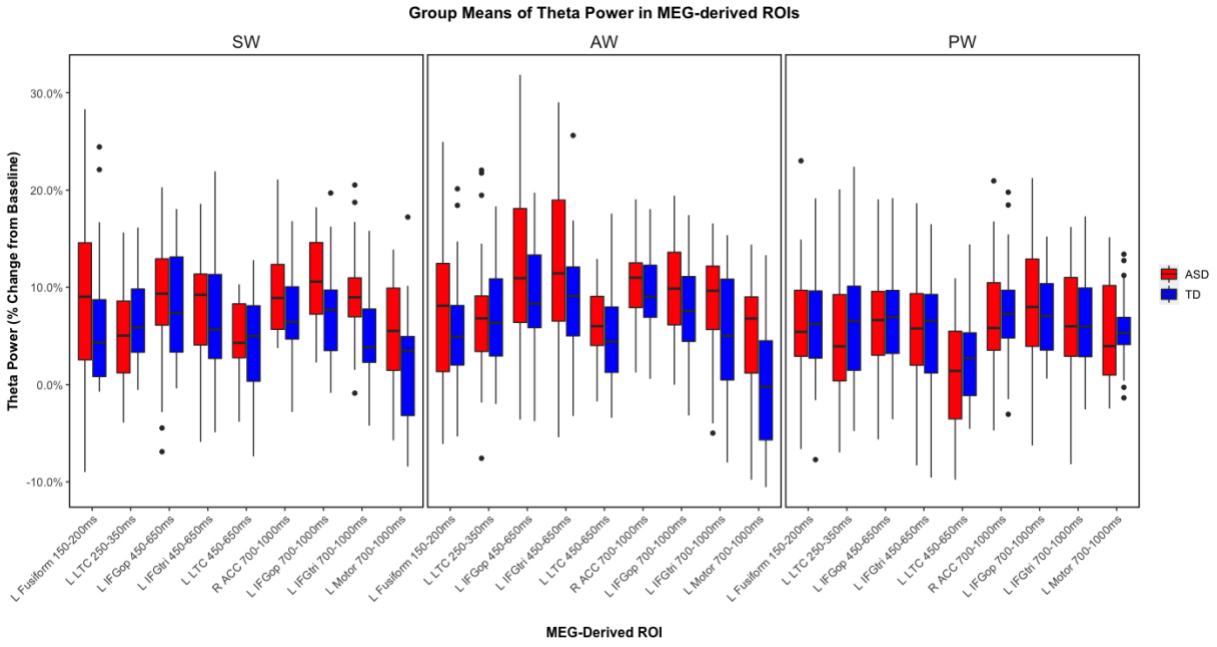
Group Means of Theta Power in MEG-derived ROIs
SW
AW
PW
Theta Power (% Change from Baseline)
30.0%
20.0%
10.0%
0.0%
-10.0%
L Fusiform 150-200ms
L LTC 250-350ms
L IFGop 450-650ms
L IFGtri 450-650ms
L LTC 450-650ms
R ACC 700-1000ms
L IFGop 700-1000ms
L IFGtri 700-1000ms
L Motor 700-1000ms
ASD
TD
MEG-Derived ROI

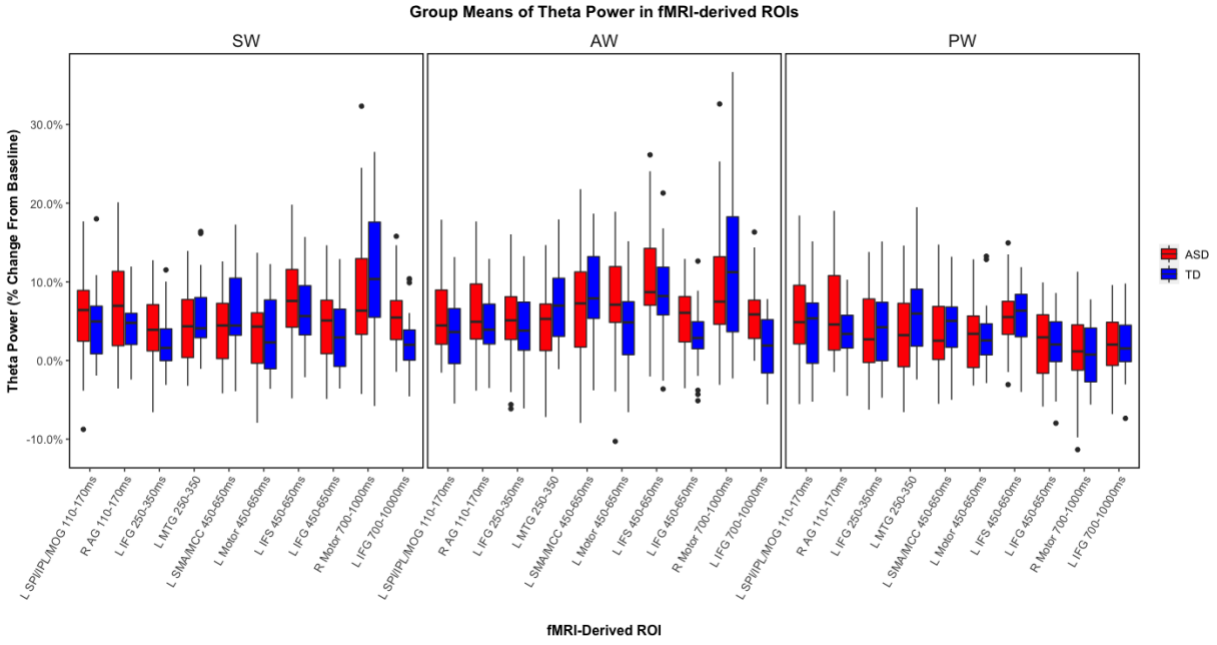
Group Means of Theta Power in fMRI-derived ROIs
SW
AW
PW
Theta Power (% Change From Baseline)
30.0%
20.0%
10.0%
0.0%
-10.0%
L SPl/IPL/MOG 110-170ms
R AG 110-170ms
L IFG 250-350ms
L MTG 250-350
L SMA/MCC 450-650ms
L Motor 450-650ms
L IFS 450-650ms
L IFG 450-650ms
R Motor 700-1000ms
L IFG 700-1000ms
ASD
TD
fMRI-Derived ROI

Supplemental Figure 1.5 Group means of BOLD signal in sample with outliers removed

Note. Mean of BOLD signal beta coeffcients for each word condition by group for MEG-derived (top) and fMRI-derived (bottom) ROIs. No significant group differences were identified for SW, AW, or PW conditions.

ASD = autism spectrum disorder
AW = animal word
L IFG = left inferior frontal gyri
L IFGop = left inferior frontal gyrus pars opercularis
L IFGtri = left inferior frontal gyrus pars triangularis
L IFS = left inferior frontal sulcus
L LTC = left lateral temporal cortex
L MTG = left middle temporal gyrus
L SMA/MCC = left SMA and middle cingulate cortices
L SPL/IPL/MOG = left superior parietal, inferior parietal, and middle occipital cortices
ms = millisecond
PW = pseudoword
R ACC = right anterior cingulate cortex
R AG = right angular gyrus
ROI = region-of-interest
SW = standard word
TD = typically developing

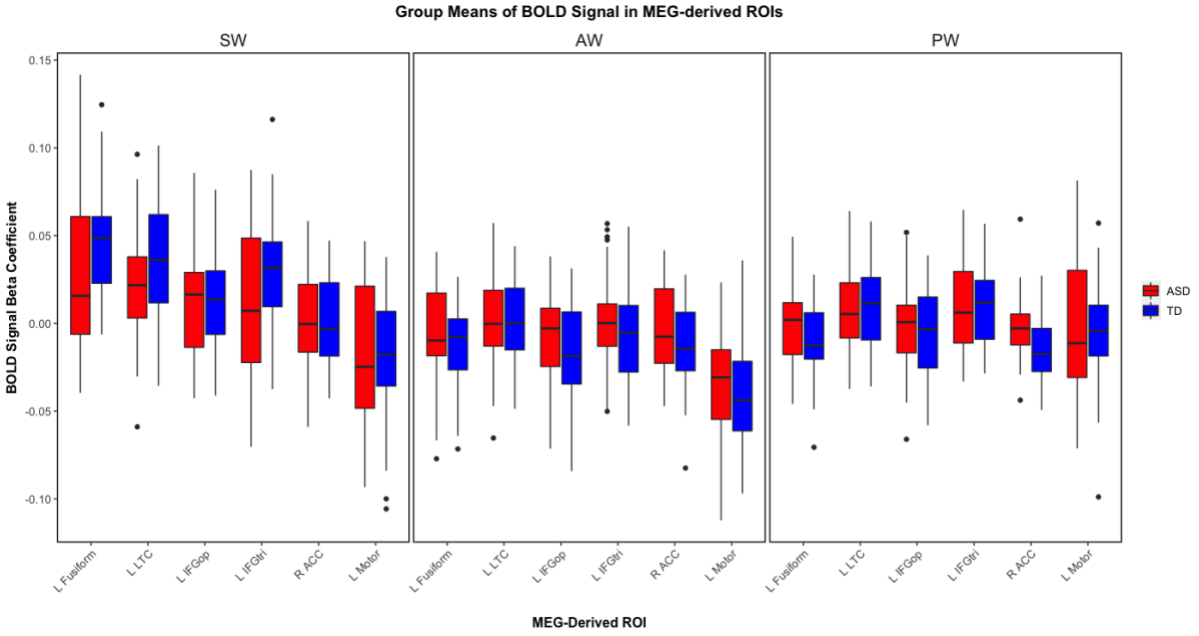
Group Means of BOLD Signal in MEG-derived ROIs
SW
AW
PW
BOLD Signal Beta Coefficient
0.15
0.10
0.05
0.00
-0.05
-0.10
L Fusiform
L LTC
L IFGop
L IFGtri
R ACC
L Motor
MEG-Derived ROI
ASD
TD

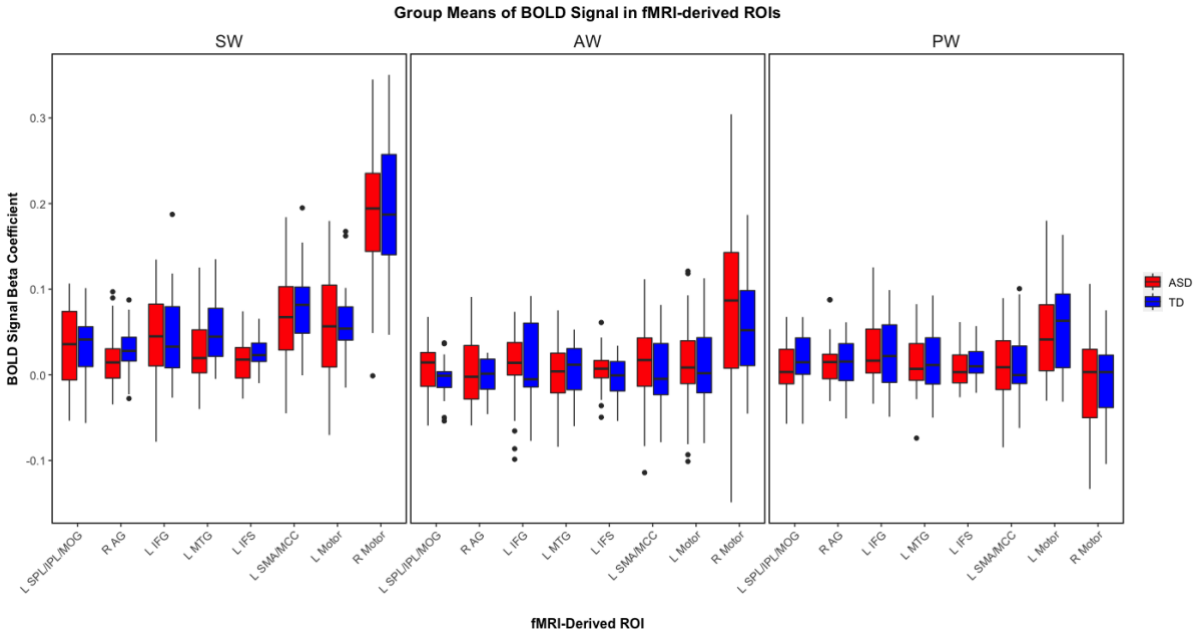
Group Means of BOLD Signal in fMRI-derived ROIs
SW
AW
PW
BOLD Signal Beta Coefficient
0.3
0.2
0.1
0.0
-0.1
L SPL/IPL/MOG
R AG
L IFG
L MTG
L IFS
L SMA/MCC
L Motor
R Motor
fMRI-Derived ROI
ASD
TD

Supplemental Figure 1.6 Group means of theta power in motion-matched sample

Note. Mean percent change from baseline in event-related theta power for each word condition by group for MEG-derived (top) and fMRI-derived (bottom) ROIs in motion-matched sample. There were no significant group differences for any of the word conditions.

ASD = autism spectrum disorder
AW = animal word
L IFG = left inferior frontal gyri
L IFGop = left inferior frontal gyrus pars opercularis
L IFGtri = left inferior frontal gyrus pars triangularis
L IFS = left inferior frontal sulcus
L LTC = left lateral temporal cortex
L MTG = left middle temporal gyrus
L SMA/MCC = left SMA and middle cingulate cortices
L SPL/IPL/MOG = left superior parietal, inferior parietal, and middle occipital cortices
ms = millisecond
PW = pseudoword
R ACC = right anterior cingulate cortex
R AG = right angular gyrus
ROI = region-of-interest
SW = standard word
TD = typically developing

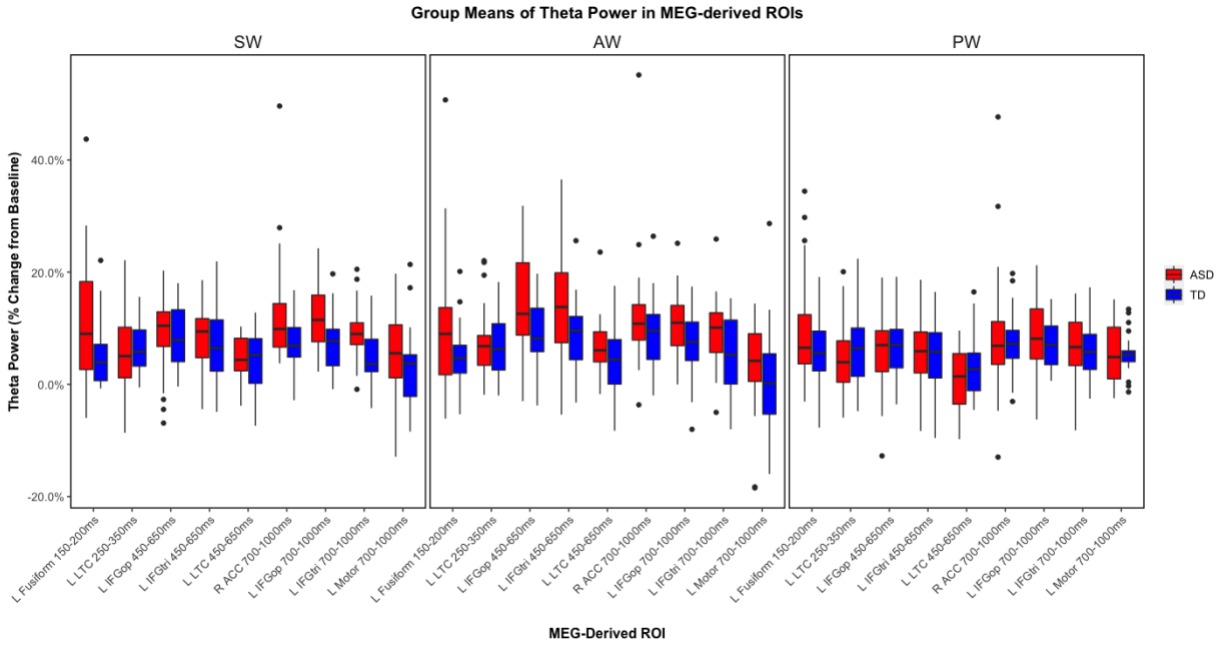
Group Means of Theta Power in MEG-derived ROIs
SW
AW
PW
Theta Power (% Change from Baseline)
40.0%
20.0%
0.0%
-20.0%
L Fusiform 150-200ms
L LTC 250-350ms
L IFGop 450-650ms
L IFGtri 450-650ms
L LTC 450-650ms
R ACC 700-1000ms
L IFGop 700-1000ms
L IFGtri 700-1000ms
L Motor 700-1000ms
ASD
TD
MEG-Derived ROI

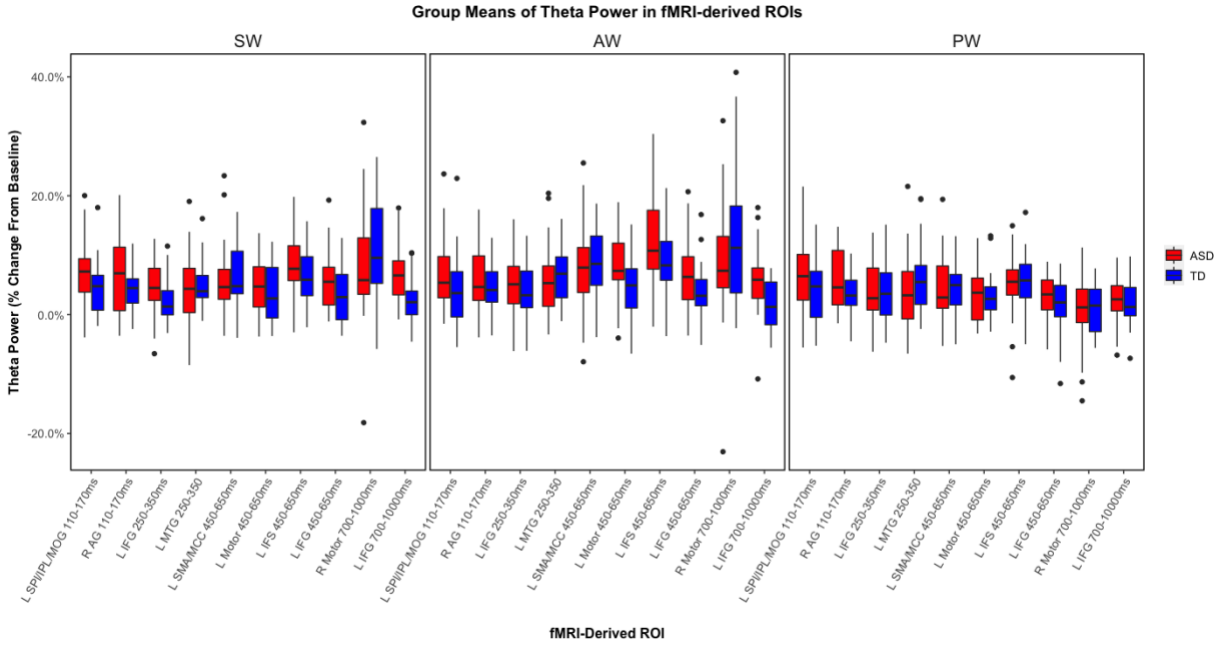
Group Means of Theta Power in fMRI-derived ROIs
SW
AW
PW
Theta Power (% Change From Baseline)
40.0%
20.0%
0.0%
-20.0%
L SPl/IPL/MOG 110-170ms
R AG 110-170ms
L IFG 250-350ms
L MTG 250-350
L SMA/MCC 450-650ms
L Motor 450-650ms
L IFS 450-650ms
L IFG 450-650ms
R Motor 700-1000ms
L IFG 700-10000ms
ASD
TD
fMRI-Derived ROI

Supplemental Figure 1.7 Group means of BOLD signal in motion-matched sample

Note. Mean of BOLD signal beta coeffcients for each word condition by group for MEG-derived (top) and fMRI-derived (bottom) ROIs in motion-matched sample. No significant group differences were identified for SW, AW, or PW conditions.

ASD = autism spectrum disorder
AW = animal word
L IFG = left inferior frontal gyri
L IFGop = left inferior frontal gyrus pars opercularis
L IFGtri = left inferior frontal gyrus pars triangularis
L IFS = left inferior frontal sulcus
L LTC = left lateral temporal cortex
L MTG = left middle temporal gyrus
L SMA/MCC = left SMA and middle cingulate cortices
L SPL/IPL/MOG = left superior parietal, inferior parietal, and middle occipital cortices
ms = millisecond
PW = pseudoword
R ACC = right anterior cingulate cortex
R AG = right angular gyrus
ROI = region-of-interest
SW = standard word
TD = typically developing

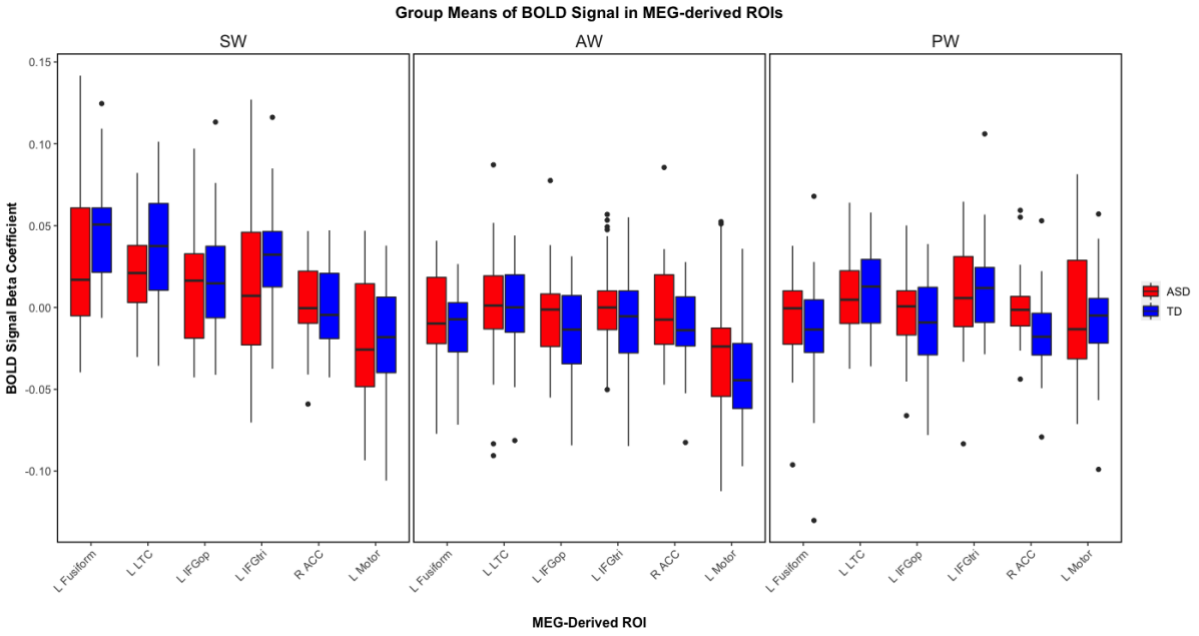
Group Means of BOLD Signal in MEG-derived ROIs
SW
AW
PW
BOLD Signal Beta Coefficient
0.15
0.10
0.05
0.00
-0.05
-0.10
L Fusiform
L LTC
L IFGop
L IFGtri
R ACC
L Motor
ASD
TD
MEG-Derived ROI

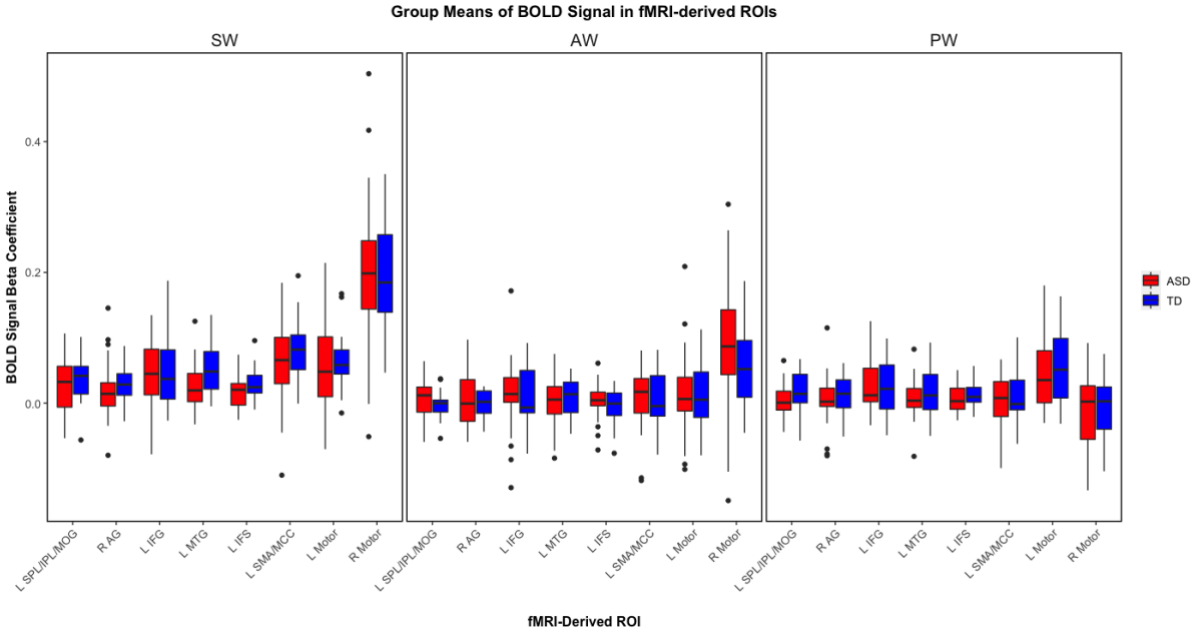
Group Means of BOLD Signal in fMRI-derived ROIs
SW
AW
PW
BOLD Signal Beta Coefficient
0.4
0.2
0.0
L SPL/IPL/MOG
R AG
L IFG
L MTG
L IFS
L SMA/MCC
L Motor
R Motor
ASD
TD
fMRI-Derived ROI

Supplemental Figure 1.8 Group means of theta power in sample with <150-day scan interval

Note. Mean percent change from baseline in event-related theta power for each word condition by group for MEG-derived (top) and fMRI-derived (bottom) ROIs. There were no significant group differences for any of the word conditions.

ASD = autism spectrum disorder
AW = animal word
L IFG = left inferior frontal gyri
L IFGop = left inferior frontal gyrus pars opercularis
L IFGtri = left inferior frontal gyrus pars triangularis
L IFS = left inferior frontal sulcus
L LTC = left lateral temporal cortex
L MTG = left middle temporal gyrus
L SMA/MCC = left SMA and middle cingulate cortices
L SPL/IPL/MOG = left superior parietal, inferior parietal, and middle occipital cortices
ms = millisecond
PW = pseudoword
R ACC = right anterior cingulate cortex
R AG = right angular gyrus
ROI = region-of-interest
SW = standard word
TD = typically developing

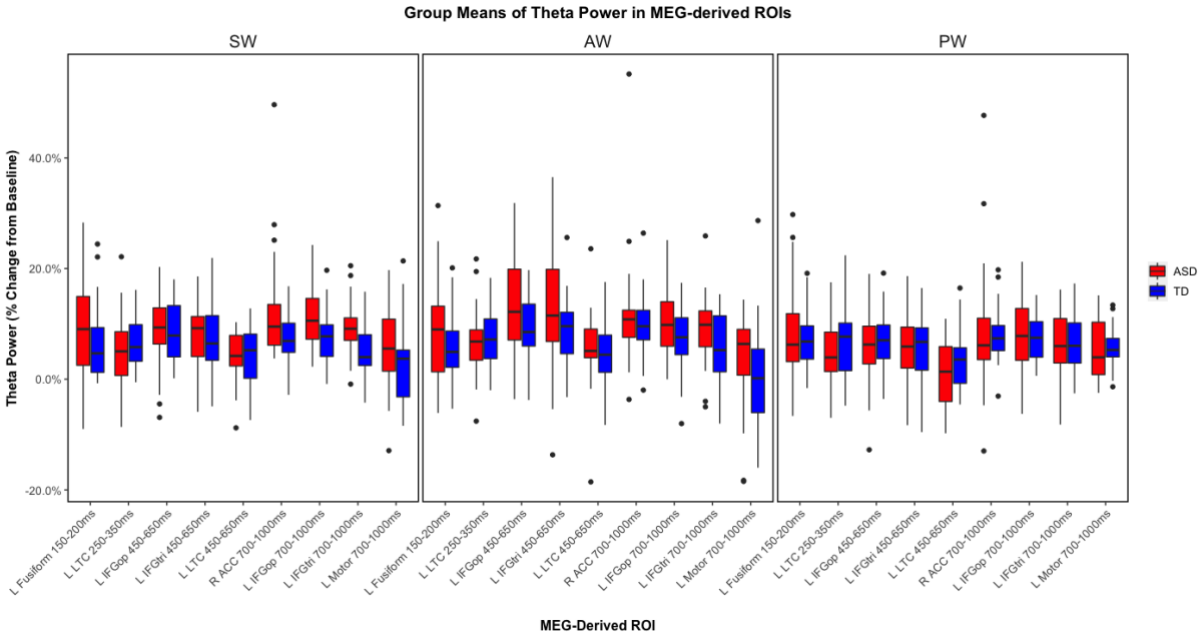
Group Means of Theta Power in MEG-derived ROIs
SW
AW
PW
Theta Power (% Change from Baseline)
40.0%
20.0%
0.0%
-20.0%
L Fusiform 150-200ms
L LTC 250-350ms
L IFGop 450-650ms
L IFGtri 450-650ms
L LTC 450-650ms
R ACC 700-1000ms
L IFGop 700-1000ms
L IFGtri 700-1000ms
L Motor 700-1000ms
ASD
TD
MEG-Derived ROI

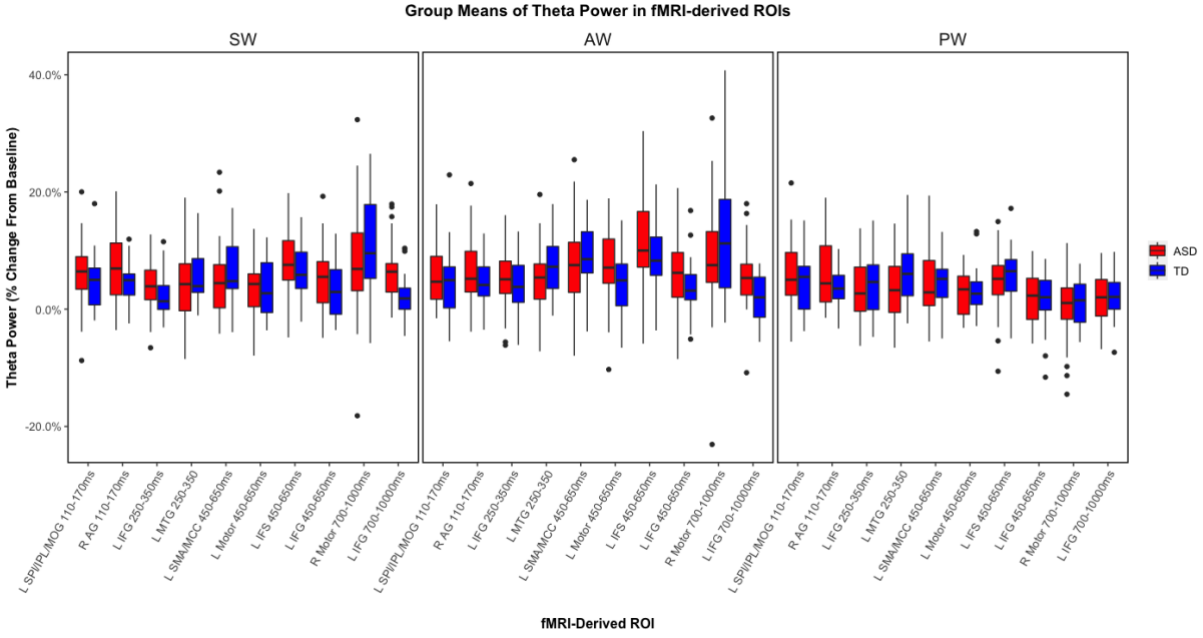
Group Means of Theta Power in fMRI-derived ROIs
SW
AW
PW
Theta Power (% Change From Baseline)
40.0%
20.0%
0.0%
-20.0%
L SPl/IPL/MOG 110-170ms
R AG 110-170ms
L IFG 250-350ms
L MTG 250-350
L SMA/MCC 450-650ms
L Motor 450-650ms
L IFS 450-650ms
L IFG 450-650ms
R Motor 700-1000ms
L IFG 700-10000ms
ASD
TD
fMRI-Derived ROI

Supplemental Figure 1.9 Group means of BOLD signal in sample with <150-day scan interval

Note. Mean of BOLD signal beta coeffcients for each word condition by group for MEG-derived (top) and fMRI-derived (bottom) ROIs in sample with <150-day scan interval. No significant group differences were identified for SW, AW, or PW conditions. No significant gorup differences were identified for any of the word conditions.

ASD = autism spectrum disorder
AW = animal word
L IFG = left inferior frontal gyri
L IFGop = left inferior frontal gyrus pars opercularis
L IFGtri = left inferior frontal gyrus pars triangularis
L IFS = left inferior frontal sulcus
L LTC = left lateral temporal cortex
L MTG = left middle temporal gyrus
L SMA/MCC = left SMA and middle cingulate cortices
L SPL/IPL/MOG = left superior parietal, inferior parietal, and middle occipital cortices
ms = millisecond
PW = pseudoword
R ACC = right anterior cingulate cortex
R AG = right angular gyrus
ROI = region-of-interest
SW = standard word
TD = typically developing

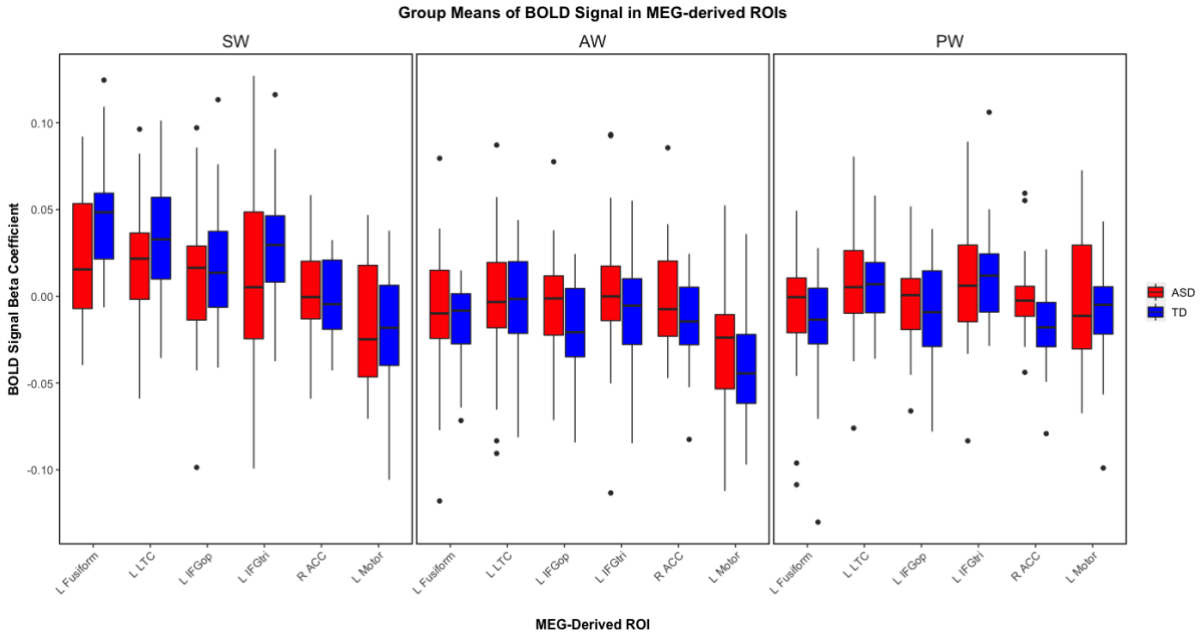
Group Means of BOLD Signal in MEG-derived ROIs
SW
AW
PW
BOLD Signal Beta Coefficient
0.10
0.05
0.00
-0.05
-0.10
L Fusiform
L LTC
L IFGop
L IFGtri
R ACC
L Motor
ASD
TD
MEG-Derived ROI

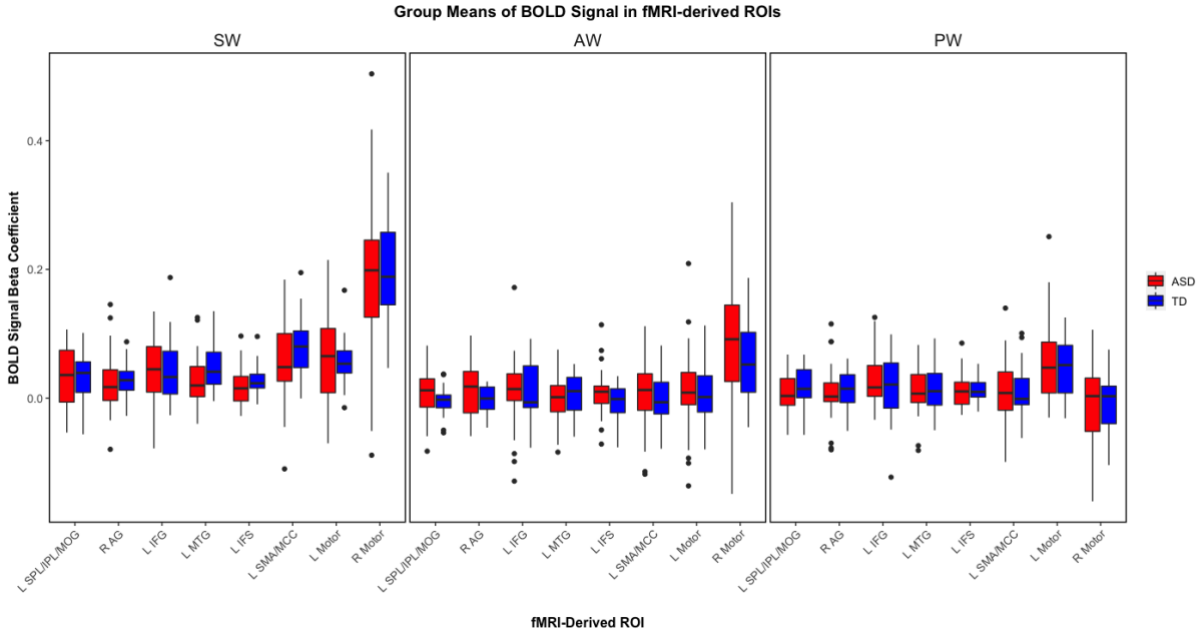
Group Means of BOLD Signal in fMRI-derived ROIs
SW
AW
PW
BOLD Signal Beta Coefficient
0.4
0.2
0.0
L SPL/IPL/MOG
R AG
L IFG
L MTG
L IFS
L SMA/MCC
L Motor
R Motor
ASD
TD
fMRI-Derived ROI

Chapter 2 Study 2

Links between fMRI and MEG indices of lexicosemantic processing in autism

Wilkinson, M.[a,b], Linke, A.C.[a,b], You, Y.[c], Marinkovic, K.[a,c,d], Müller, R-A.[a,b], Jao Keehn, R.J.[a,b]

[a]San Diego State University/University of California San Diego Joint Doctoral Program in Clinical Psychology, San Diego, CA, United States

[b]Brain Development Imaging Laboratories, Department of Psychology, San Diego State University, San Diego, CA, United States

[c]Spatiotemporal Brain Imaging Laboratory, Department of Psychology, San Diego State University, San Diego, CA, United States

[d]Radiology Department, University of California at San Diego, CA, United States

Abstract

Autism spectrum disorder (ASD) is often accompanied by delayed or atypical language development. However, imaging studies of language in ASD have predominantly relied on a single neuroimaging modality. While each neuroimaging method has its strengths and weaknesses, unimodal studies may miss aspects of brain function or structure that can be detected through other methods. The present study combined data from anatomically-constrained magnetoencephalography (aMEG) and functional magnetic resonance imaging (fMRI). The aims of the current study were to: 1) assess language activity and lateralization utilizing aMEG metrics of lexicosemantic processing (N250m and N400m) and fMRI blood oxygen-level dependent (BOLD) signal in adolescents with and without ASD, and 2) analyze the relationship between fMRI BOLD signal and aMEG N250m and N400m during language processing. Thirty adolescents with ASD and 20 typically developing (TD) peers participated in a lexicosemantic decision task during aMEG and fMRI scans, responding differentially to visually presented words and pseudowords. Regions-of-interest (ROIs) were derived for left and right hemispheres based on task-related effects observed across groups during N250m and N400m time windows. N250m, N400m, and BOLD signals were measured for each ROI for each participant. Based on their task performance, ASD participants were divided into “low performers” (L-ASD) and “high performers” (H-ASD), who performed as well as TD peers. Results revealed greater N250m in the inferior frontal region for the H-ASD group, decreased N400m in inferior frontal and temporal regions for the L-ASD group, and greater bilateral N400m in the H-ASD group for inferior frontal and temporal regions. fMRI BOLD signal did not reflect significant group differences revealed by MEG measures. MEG and fMRI activation measures were not found to be correlated for the TD group, while positive correlations were noted across inferior frontal, temporal, and parietal regions in the L-ASD group. These findings suggest a tendency toward

bilateral hemispheric engagement in the H-ASD group that is not present in the L-ASD group, which may indicate potential compensatory mechanisms. This study underscores the significance of integrating multimodal methods such as aMEG and fMRI data to examine patterns in language processing amongst autistic adolescents.

Keywords: Functional magnetic resonance imaging (fMRI), magnetoencephalography (MEG), multimodal integration, autism spectrum disorder (ASD), adolescents, lexicosemantic processing, BOLD signal, N250m, N400m

Introduction

Autism spectrum disorder (ASD) is a neurodevelopmental disorder defined by impaired social communication and the presence of restricted and/or repetitive behaviors (American Psychiatric Association, 2013). Recent reports highlight the increasing prevalence rate, with 1 in 36 children having a diagnosis of ASD (Maenner et al., 2023). Along with social communication and restricted, repetitive behaviors, many individuals with ASD present with language delay and/or impairments, such as lexicosemantic difficulties (Boucher, 2012; Condouris et al., 2003; Haebig et al., 2015; Henderson et al., 2011; Kamio et al., 2007; Löfkvist et al., 2014; Naigles & Tek, 2017; Salem et al., 2021). Lexicosemantic processing involves understanding word meaning and integrating it into the current context. Studies of language in ASD report smaller expressive and receptive vocabularies (Löfkvist et al., 2014), greater lexicosemantic impairment (Naigles & Tek, 2017), and lower performance on neuropsychological assessments of lexicosemantics (Condouris et al., 2003). Lexicosemantic abilities and deficits vary across ages and functioning levels of the ASD population (Boucher, 2012).

Individuals with ASD have shown atypical activation patterns in functional magnetic resonance imaging (fMRI) studies of lexicosemantic processing, such as abnormally increased activity in visual regions (Gaffrey et al., 2007; Herringshaw et al., 2016; Shen et al., 2012) and decreased connectivity between frontal and temporal language regions (Y. Lee et al., 2017). Atypical language laterality more generally is a consistently replicated finding in ASD neuroimaging research based on both functional and structural imaging studies (Gage et al., 2009; Herringshaw et al., 2016; Jouravlev et al., 2020; Kleinhans et al., 2008; Knaus et al., 2008, 2010; Lindell & Hudry, 2013; Mody et al., 2013; Nielsen et al., 2014; Takeuchi et al., 2004). Individuals with ASD commonly exhibit rightward or bilateral activity in language tasks, in contrast to the strong leftward lateralization often observed in TD individuals, although these

findings may be task-dependent. For example, one study identified similar laterality patterns in adolescents with and without ASD in response to a category fluency task, while the same ASD group showed atypically increased activity in right frontal and temporal language areas during a letter fluency task (Kleinhans et al., 2008). Differences in language laterality can also be seen early in development; in 12-to-48-month-old toddlers with ASD, Eyler and colleagues showed decreased left hemisphere activity in response to speech sounds during natural sleep (Eyler et al., 2012b). Furthermore, rightward lateralization in the temporal cortex increases with age, with the strongest effects observed in 3-to-4-year-old autistic children. While the presence of atypical language lateralization is one of the most extensively reproduced results in neuroimaging studies of individuals with ASD, there remains a dearth of conclusive evidence regarding whether this lateralization arises from decreased activity in the left hemisphere, increased activity in the right hemisphere, or a combination of both (Jouravlev et al., 2020).

fMRI has long been the preferred method for investigating task-related brain activity, offering robust spatial resolution while facing limitations in temporal resolution due to reliance on a slow hemodynamic response. Despite its prominence and generally robust findings of atypical language lateralization in ASD, fMRI studies, including those researching language, have also yielded inconsistent results (Hull et al., 2018; Picci et al., 2016; Uddin et al., 2013). For instance, variations in patterns have been reported, such as findings of both increases and decreases in activity and connectivity within the frontal and temporal language areas. These discrepancies may stem from several factors, including participant age, the nature of the task, ASD symptomology, and methodological differences in fMRI procedures and analyses. Resolving these inconsistencies is essential for comprehensive understanding of lexicosemantic

processing in ASD, which may significantly impact diagnosis, biomarker identification, intervention strategies, and an understanding of neural activity within ASD.

Other neuroimaging techniques, such as electroencephalography (EEG) and magnetoencephalography (MEG), have also been used to investigate lexicosemantic processing. The N250 and N400, and their magnetic counterparts, N250m and N400m, are considered crucial markers of language processing: N250(m) has been linked to lexical access, and N400(m) has been linked to semantic processing and integration (Carreiras et al., 2014; Halgren et al., 2002; Kotchoubey, 2002; Kutas & Federmeier, 2000; Kutas & Hillyard, 1980; Leminen et al., 2019; Marinkovic, 2004a; Marinkovic et al., 2014; Parkes et al., 2016; Pylkkänen & Marantz, 2003). N250(m) has received much less attention in ASD language studies compared to N400(m) and conflicting findings from the very limited number of studies highlight the need for further investigation. One such study reported an absence of group differences in N250 during an auditory speech task (Galilee et al., 2017), while findings from an earlier study suggested a) greater N250 (described as "pre-N4") in autistic participants in response to congruous vs. incongruous words, b) longer persisting N250 in response to incongruous vs. congruous words in autistic participants, and c) similar N250 amplitudes between the two word categories in neurotypical participants (Braeutigam et al., 2008).

In contrast, extensive studies on N400(m) in ASD individuals have consistently highlighted atypicalities, including increased latency, reduced amplitude, or complete lack of the N400(m) effect, also known as the priming effect, which has been used as a measure of incongruous stimulus processing with greater N400(m) responses reported for incongruous compared to congruous stimuli (Cantiani et al., 2016; DiStefano et al., 2019; Dunn et al., 1999; Dunn & Bates, 2005; Fishman et al., 2011; McCleery et al., 2010; McFadden & Rojas, 2013;

Pijnacker et al., 2010; Russo et al., 2012). Specific language tasks, such as idiom recognition or semantic processing, have also demonstrated a lack of typical N400 activity that correlates with poor language skills or task performance in ASD (Gold et al. 2010; Strandburg et al., 1993). Even during passive listening tasks, such as listening to words of two different categories, findings have indicated a lack of the N400 effect (i.e., greater N400 amplitude in response to words of two different categories compared to the N400 amplitude in response to a pair of words within the same category) in children with ASD (Dunn & Bates, 2005). These reported atypicalities in the N400(m) response underscore the need for further examination of this effect in order to better understand how 'oddball' processing may influence overall language in autism.

In line with fMRI results, findings from EEG and MEG studies support atypical language lateralization in individuals with ASD (Braeutigam et al., 2008; Curl & Coderre, 2022; Flagg et al., 2005; Liang et al., 2021; Matsuzaki et al., 2020; Yoshimura et al., 2013). For instance, Yoshimura and colleagues (2013) revealed a notable reduction in leftward lateralization for children with ASD in P50m during a passive listening task in comparison to TD peers. Another study reported increased theta coherence in the right hemisphere in autistic participants when processing related words; this phenomenon was not observed in TD participants (Curl & Coderre, 2022). In addition, Flagg and colleagues (2005) reported a distinctive pattern in a small sample MEG study in which the ASD group exhibited an increasing rightward dominance with age during a passive auditory task, while TD children displayed a contrasting increasing leftward dominance with age. A similar right hemisphere dominance, particularly in the anterior temporal cortex, was also observed in a study of adults with ASD in N400 activity in response to incongruous sentences; this rightward lateralization was not observed in neurotypical adults (Braeutigam et al., 2008).

A multimodal approach combining aMEG and fMRI offers a unique perspective for understanding lexicosemantic processing differences in individuals with ASD. The current study extends the findings from our first set of papers, which examined event-related theta power and fMRI BOLD signal during the lexicosemantic task described below (M. Wilkinson et al., 2022; You et al., 2021), as well as our most recent unimodal MEG paper, which examined N250m and N400m during a lexicosemantic task in adolescents with and without ASD (You et al., 2023). The current study includes a partially overlapping sample of the previous studies and investigates activation in both fMRI and MEG during a lexicosemantic task. This study expands on our previous work by examining fMRI BOLD signal during lexicosemantic decision making, specifically in high and low performing ASD adolescents in comparison to TD peers, and the relationship between BOLD signal and aMEG measures of activation (i.e., N250m and N400m) in adolescents with and without ASD. This is the first study to directly compare N250m and N400m with BOLD signal, adding to the multimodal literature an understanding of the relationship between two imaging methods.

Methods

Participants

From a total of 156 ASD and 120 TD adolescents screened, 30 ASD and 22 TD participants (aged 12-21 years) fulfilled all inclusionary criteria for the current study (see supplement for specific details regarding exclusions and data loss). ASD diagnoses were determined using DSM-5 criteria (American Psychiatric Association, 2013), the Autism Diagnostic Observation Schedule, 2nd Edition (ADOS-2) (Lord et al., 2012), the Autism Diagnostic Interview-Revised (ADI-R) (Rutter et al., 2003), and expert clinical judgment. To better understand neural differences with respect to varying linguistic abilities within the autism spectrum, the ASD group was split into two subgroups – high and low performers (Table 2.2).

fMRI and MEG task performance was averaged for each individual. The median of the averages for the TD group was 86.69%. High performers (H-ASD) were defined as individuals with ASD whose average task performance across both fMRI and MEG scans was equal to or greater than 86.69%. Low performers (L-ASD) were individuals in the ASD group with a task average below 86.69%. Two TD individuals who performed below 86.69% were removed from further analysis, resulting in a final sample of 30 ASD and 20 TD participants. The two groups did not differ on gender, handedness, age, or IQ (Table 1). The two ASD subgroups (15 H-ASD, 15 L-ASD) did not differ on gender, handedness, age, fMRI RMSD (measurement of in-scanner motion), or ADOS-2 total score (Table 2.2). The current study sample partially overlaps with You et al. (2023). 27 ASD and 15 TD participants were included in both You et al. (2023) and the current study. 12 ASD and 6 TD participants were included in You et al. (2023), but not in the current study. 3 ASD and 5 TD participants were new to the current study. It is important to note that the previous paper used the same method for determining a cut-off between H-ASD and L-ASD groups (i.e., the median of the TD group), however it only incorporated MEG task performance as it was a unimodal study. The median of the TD group's performance on the task completed during the MEG scan was 80%. Of the 27 ASD participants in both studies, 4 individuals were placed in different subgroups due to the different cut-off for H-ASD and L-ASD groups. Twelve ASD participants were currently taking psychotropic medications (Wilkinson et al., 2022). Fourteen ASD individuals reported comorbidities: 4 with attention-deficit/hyperactivity, 7 with anxiety, and 5 with depression; 2 of these participants reported multiple comorbidities (Wilkinson et al., 2022).

Experimental design

Once participants passed the initial screening and were inducted into the study, their reading level was evaluated using the Word Reading subtest of the Wechsler Individual Achievement Test, 3rd Edition (WIAT-III) (Wechsler, 2009). Participants who scored below a 6th-grade reading level (standard score: 80) were excluded from the study due to the reading level requirements for appropriately engaging in the lexicosemantic task, particularly during neuroimaging scans. Those who scored at a 6th-grade reading level or above continued with the remainder of the assessments, including the Edinburgh Handedness Inventory (Oldfield, 1971), Wechsler Abbreviated Scale of Intelligence, 2nd Edition (WASI-II) (Wechsler, 2011), Beery-Buktenica Developmental Test of Visual-Motor Integration, 6th Edition (Beery VMI-6) (Beery et al., 2010), and Clinical Evaluation of Language Fundamentals, 5th Edition (CELF-5) (Semel et al., 2013). Prior to undergoing the MRI scan, participants completed a mock scan to become familiar with the MR environment and lexicosemantic task. Unique sets of word stimuli were presented during the lexicosemantic task for the mock, MRI, and MEG scans. The MEG and MRI scans were completed during two separate sessions; the order of the scans was counterbalanced across participants. For the majority of participants, both MEG and MRI scans were completed within 150 days or less of one another, with the exception of 1 TD participant (252 days) and 2 ASD participants (174 and 184 days). To increase comfort, participants were provided earplugs, cushions, and a blanket during MRI scans. MRI operators checked in with the participants throughout the scan. Participant comfort was similarly taken into account during MEG scans.

The lexicosemantic task was completed during both MRI and MEG scans. Participants differentially responded to three conditions: real non-animal standard words (SW), animal words

(AW), and pseudowords (PW). Words in the PW condition were orthographically and phonologically legal letter strings with no word meaning (e.g., “blont”). This lexicosemantic task was originally used in previous aMEG studies on neurotypical adults (Marinkovic et al., 2012, 2014) and has been adapted accordingly for our recent studies (Wilkinson et al., 2022; You et al., 2021, 2023).

Participants used their left hand for lexicosemantic task responses on a 2-button fiber optic response pad (Cambridge Research Systems Ltd., Rochester, UK, https://www.crsltd.com). They were directed to press the button beneath their index finger for SW, to press the button beneath their middle finger for AW, and to refrain from pressing any button for PW. There were no significant differences among word conditions in terms of word length or syllable count, and there were no differences between SW and AW conditions in frequency of occurrence (based on the Zipf scale; Brysbaert & New, 2009; van Heuven et al., 2014) or in the age-of-acquisition rating (Kuperman et al., 2012).

During the task portion of the fMRI scan, each word was displayed visually for a duration of 500 ms, followed by a 1500 ms fixation string (“xxxxxx”) to account for the insertion of additional null trials in fMRI (as explained below). Task stimuli were presented across two 7-minute runs, with a 3-minute break between each run. Each run included 90 SW, 30 AW, and 30 PW trials. During the task portion of the MEG scan, words were presented for 500 ms each and followed by a 2000 ms fixation string (“xxxxxx”) without jitter. Task stimuli were presented in a randomized order over an approximately 25-minute run, featuring brief breaks every 4 minutes. Each word condition included 100 trials. For the SW condition, 180 additional words were presented as filler to establish a prepotent response tendency. Presentation® software (Version 22.1, Neurobehavioral Systems, Inc., Berkeley, CA, www.neurobs.com) was used to present

stimuli in white lowercase letters on a black background. The trial sequence was uniform for all participants, except 2 ASD and 2 TD individuals who underwent a second scan due to technical issues. A separate trial sequence was used to avoid practice effects. Distinct stimuli sets were utilized during MEG and fMRI scans.

The trial sequence used in the fMRI event-related design was established using RSFgen, a random stimulus function generator within Analysis of Functional NeuroImages (AFNI, https://afni.nimh.nih.gov) (Cox, 1996). A fixation string ("xxxxxx") was presented during null trials (specific to fMRI). Each run included 124 one-second null trials.

MRI acquisition and processing

MRI scans were conducted at the UCSD Center for fMRI on a General Electric Discovery MR750 3.0 Tesla Scanner (GE Healthcare, Milwaukee, WI) paired with a Nova Medical 32-channel head coil. Structural scans used a Fast Spoiled Gradient Recalled T1-weighted sequence (TR: 8.136 ms; TE: 3.172 ms; flip angle: 8°, FOV: 25.6 cm; acquisition matrix: 256x256; slices: 172; voxel size: 1 mm^3, duration: 5 min). Functional scans were obtained using a multi-echo simultaneous multi-slice (MESMS) T2*-weighted echo planar imaging (EPI) sequence (volumes: 340; TR: 1250 ms; TEs: 13.2, 30.3, 47.4 ms; flip angle: 60°, FOV: 21.6 cm; acquisition matrix: 72x36; acceleration factor[R]: 2; slices: 54; voxel size: 3 mm^3). To allow for magnetization equilibrium, the initial 9 volumes were discarded. The MESMS protocol incorporates the simultaneous acquisition of multiple slices at various echo times and enhances the signal-to-noise ratio (Kundu et al., 2012, 2013; Olafsson et al., 2015). Scans collected during the early stages of the study followed a slightly different protocol, which used a smaller FOV; all parameters were identical except the number of volumes (386), TR (1100 ms), and number of slices (45). This difference impacted 8 of the initial TD participants.

The preprocessing and analysis of fMRI data were carried out using AFNI (Version 19.0.00), FSL (Version 5.0), and Matlab (2013b). For each echo time, EPI underwent correction for susceptibility-induced distortions using FSL's TOPUP tool, a technique involving two spin-echo acquisitions with opposing phase encoding directions (S. M. Smith et al., 2004). AFNI was used for rigid-body realignment for each functional volume to the middle volume. Head motion was quantified as the root mean square difference (RMSD) derived from the six motion parameters of the 30.3 ms echo time data. Optimal combination of EPIs was implemented following the methodology introduced in Kundu et al. (2013). Data denoising was conducted with multi-echo ICA (ME-ICA) (Olafsson et al., 2015) using meica.py, accessible on GitHub (https://github.com/ME-ICA/me-ica). ME-ICA, recognized for its superiority over conventional denoising methods (Lynch et al., 2020), was used to facilitate the removal of artifacts (non-BOLD components) from the BOLD signal (Kundu et al., 2013). FSL FLIRT was utilized for co-registering functional and structural scans, while FNIRT was applied to reorient images to MNI-152 space. Spatial smoothing, employing a Gaussian kernel of 6mm FWHM, was carried out in AFNI's 3dBlurToFWHM, and the data were scaled to percent signal change. Functional data from the two runs were concatenated for each participant and temporally filtered using a high pass filter ($f > 0.008$ Hz; AFNI's 3dBandPass function) for analysis.

The functional data underwent ordinary least squares (OLS) regression using 3dDeconvolve. The regressors incorporated the three conditions (SW, AW, and PW). A statistical parametric mapping (SPM) gamma variate basis function, characterized by a two-parameter model, was employed to approximate the canonical hemodynamic response function. To account for the residuals in the time series, a residual maximum likelihood estimation was performed using 3dREMLfit. This estimation utilized an autoregressive moving average

(ARMA[1,1]) model and was executed on a voxel-wise basis for each participant through a generalized least squares time series fit. The resulting beta coefficients, representing the estimates of effect size, were then extracted and utilized for group comparisons.

MEG acquisition and processing

MEG scans were acquired at the UCSD Radiology Imaging Laboratory with a whole-head Neuromag Vectorview system (Elekta AB, Stockholm, Sweden), using 204 planar gradiometers (102 pairs). Acquisition and processing steps described below are also accessible in additional detail in previous papers (You et al., 2021, 2023). To align MEG with structural MRI scans, fiduciary points (nasion and periauricular points), head position indicator coils, and various random points on the scalp were digitized using a 3Space Isotrak II (Polhemus Inc., Colchester, VT). Continuous signal acquisition was carried out at a sampling rate of 1000 Hz with minimal filtering (0.1 to 300 Hz). Data processing and analysis of MEG data were performed using Matlab scripts (Mathworks Inc., Natick, MA, USA), incorporating EEGLab (Delorme & Makeig, 2004), Fieldtrip (Oostenveld et al., 2011), and MNE (Gramfort et al., 2013). Specific processing and analysis details have been detailed in previous publications (Beaton et al., 2018; Correas et al., 2019; Kovacevic et al., 2012; Marinkovic et al., 2012, 2019; Rosen et al., 2016; You et al., 2021, 2023). The data were downsampled to 250 Hz, bandpass filtered (0.1 to 30 Hz), epoched from -300 to 1100 ms for stimulus-locked analysis, and baseline-corrected using the prestimulus period (-300 to 0 ms). Artifacts were removed with threshold-based rejection (Oostenveld et al., 2011), followed by an independent-component analysis (ICA) to remove eyeblinks, heartbeats, and other stationary artifactual activity (Delorme & Makeig, 2004). Data were visually inspected for any remaining artifacts. Data analyses were conducted in time domain and included trials with accurate task responses. An anatomically-constrained MEG

(aMEG) approach was used to address the lower spatial resolution of MEG. aMEG combines distributed source modeling of the MEG signal with structural MRI, providing insight into spatiotemporal stages of processing (Dale et al., 2000; Marinkovic et al., 2003, 2019).

ROI identification

ROIs were adopted from You et al. (2023) and consisted of regions from MEG scans with significant power based on an average of all participants and word conditions in the left and right hemispheres. Surface ROIs for each hemisphere were transformed into volumetric space using FreeSurfer to be used with fMRI data (Dale et al., 1999) (Figure 2.1). For measurement of the laterality index (LI), after the transformation from surface space to volumetric space, fMRI left hemisphere ROIs were flipped to obtain the homologous region in the right hemisphere.

Data extraction and analysis

N250m and N400m were measured for each participant in left (LH) and right hemisphere (RH) ROIs for each word condition. N250m was measured during the 210-260 ms time window, and N400m was quantified during the 350-550 ms and 400-600 ms time windows. BOLD beta coefficients were extracted for each participant, ROI, and word condition (compared to baseline). As the goal of the current study was to examine group differences in activation and asymmetry, data were averaged across all conditions in primary analyses. Secondary analyses did not reveal significant Group-by-Condition effects. This also served to minimize the number of statistical tests given the limited sample size. The LI for MEG and fMRI measures of activation was calculated using the following equation: (LH – RH) / (LH + RH). The LI ranges from -1 to 1, with negative LI representing greater right hemisphere activity, positive LI representing greater left hemisphere activity, and 0 representing equal activity across hemispheres. Unlike N250m and N400m measures from MEG, fMRI BOLD signal can be negative. To account for this,

BOLD signal beta coefficients were normalized to positive values prior to calculating LI. Normalized BOLD signal was only used for LI; positive and negative BOLD signal values were used for all other analyses. Two (Hemisphere: LH vs. RH) x 2 (Group: ASD vs. TD) and 2 (Hemisphere: LH vs. RH) x 3 (Group: H-ASD, L-ASD, vs. TD) analyses of variance (ANOVA) were used to test for the effects of group, hemisphere, and the interaction of group and hemisphere for N250m, N400m, and BOLD signal. Significant results from the ANOVAs were followed up with Tukey post-hoc analyses to examine pairwise comparisons. Pearson partial correlations, controlling for age and fMRI RMSD, were used to analyze the relationship between MEG and fMRI measures of activation by diagnostic task performance group and hemisphere.

Results

Lexicosemantic task performance

Performance on the lexicosemantic task was significantly lower for the L-ASD group compared to the H-ASD group [$t(28) = 7.77$, $p < 0.0001$] and the TD group [$t(19.66) = 8.80$, $p < 0.0001$]. There were no significant differences between the TD and H-ASD groups [$t(33) = 0.68$, $p = 0.50$] (Supplemental Figure S2.1). Task performance was significantly positively correlated with full-scale IQ [$r(48) = 0.59$, $p < 0.0001$], verbal IQ [$r(48) = 0.31$, $p = 0.03$], and non-verbal IQ [$r(48) = 0.53$, $p < 0.0001$] scores as measured by the WASI-II, as well as the WIAT Word Reading subtest score [$r(48) = 0.65$, $p < 0.0001$]. Performance was not correlated with any other variables, such as motion, gender, handedness, age, ADOS-2 total or severity scores, or comorbidities. There were no group-by-condition interactions for lexicosemantic performance averaged across fMRI and MEG modalities. For fMRI task performance alone, TD and H-ASD groups performed significantly more accurately for SW, AW, and PW word conditions compared to the L-ASD group (Supplemental Figure S2.1). A similar trend was observed for the MEG task performance, but it failed to reach significance.

aMEG measure of activation – N250m

When N250m was compared between TD and ASD groups and hemispheres for all ROIs, 2 x 2 ANOVAs revealed no significant effects (Figure 2.2), nor were there were significant laterality effects between TD and ASD groups for all regions (Figure 2.3).

A 2 x 3 ANOVA analyzing TD, H-ASD, and L-ASD groups across both hemispheres revealed a significant main effect of Group in IFGorb, with greater activity in the H-ASD group compared to L-ASD ($p = 0.03$) and TD ($p = 0.02$) groups [$F(2,96) = 4.63$, $p = 0.01$] (Figure 2.2). There were no significant effects across the IFGop, IPL, or MTG regions. There were no significant differences in laterality between TD, H-ASD, and L-ASD groups across all ROIs (Figure 2.3).

Correlations between N250m and measures of intelligence, word reading, and autism symptomology were further analyzed. N250m was not correlated with any of these variables.

aMEG measure of activation – N400m

When comparing N400m in TD and ASD groups across both hemispheres, a 2 x 2 ANOVA revealed a significant main effect of Group in IFGop, with increased activity in the TD group compared to the ASD group [$F(1,97) = 4.70$, $p = 0.03$] (Figure 2.2). In the IPL, a 2 x 2 ANOVA revealed a significant main effect of Hemisphere, with increased activity in the left hemisphere compared to the right hemisphere [$F(1,97) = 7.73$, $p = 0.007$]. A 2 x 2 ANOVA revealed a main effect of Hemisphere in the MTG, with the left hemisphere demonstrating more activity compared to the right hemisphere [$F(1,96) = 6.87$, $p = 0.01$] (Figure 2). There was also a marginal Group effect, with the TD group showing greater activation than the ASD group in the MTG [$F(1,96) = 2.91$, $p = 0.09$]. There was a significant Group-by-Hemisphere interaction in the MTG [$F(1,96) = 5.64$, $p = 0.02$], with increased activity in the left hemisphere of the TD group

compared to the left hemisphere of the ASD group [$t(96) = 2.89$, $p = 0.005$]. Additionally, the TD group had increased activity in the left hemisphere compared to the right hemisphere [$t(96) = 3.50$, $p = 0.0007$]. There was a significant group difference in laterality in the MTG, with a greater LI in the TD group, demonstrating greater leftward asymmetry compared to the ASD group, which did not show any laterality effect [$t(48) = 2.24$, $p = 0.03$] (Figure 3). There were no significant group or hemisphere effects for the IFGorb, nor were there any significant laterality effects in the IFGorb, IFGop, or IPL.

The pattern of findings for N400m remained largely similar when the ASD group was split into high- and low-performers (Figure 2.2). A 2 x 3 ANOVA revealed a main effect of Group in the IFGop [$F(2,96) = 3.95$, $p = 0.02$], with the TD group showing more activity than the L-ASD group. In the IPL, a 2 x 3 ANOVA revealed greater activation in the left hemisphere compared to the right hemisphere [$F(1,96) = 7.75$, $p = 0.006$]. A 2 x 3 ANOVA revealed a main effect of Group in the MTG, with the TD group showing more activation than the L-ASD group [$F(2,94) = 4.10$, $p = 0.02$]. There was also greater activation in the left hemisphere than the right [$F(1,94) = 7.11$, $p = 0.009$]. A significant Group-by-Hemisphere interaction showed greater MTG left hemisphere activity compared to the right hemisphere in the TD group [$F(2,94) = 2.98$, $p = 0.008$]. There was a marginal Group-by-Hemisphere interaction in the MTG [$F(2,94) = 2.98$, $p = 0.06$], with increased activity in the left hemisphere of the TD group compared to the left hemisphere of the L-ASD group [$t(94) = 3.204$, $p = 0.005$]. A one-way ANOVA revealed a marginal group difference in LI in the MTG, with the TD group showing a greater LI than the H-ASD group, which indicates greater leftward asymmetry [$F(2,47) = 2.66$, $p = 0.08$] (Figure 2.3). There were no significant group, hemisphere, or laterality effects for the IFGop, nor were there laterality effects for the IFGorb or IPL.

Relationships between N400m and cognitive and diagnostic measures were also analyzed. Overall word reading ability, as measured by the WIAT Word Reading subtest, in the ASD and TD groups combined was positively correlated with N400m in the R MTG [$r(48) = 0.36$, $p = 0.01$].

fMRI measure of activation – BOLD signal

When comparing the BOLD signal between TD and ASD groups across both hemispheres, a 2 x 2 ANOVA revealed a significant main effect of Group in the IFGorb, such that the TD group showed greater activity than the ASD group [$F(1,97 = 4.26$, $p = 0.04$] (Figure 2.2). 2 x 2 ANOVAs revealed a significant main effect of Hemisphere in the IFGop [$F(1,97) = 8.49$, $p = 0.0004$] and the MTG [$F(1,97) = 5.48$, $p = 0.02$], with greater activity shown in the left hemisphere than the right hemisphere. There were no significant group or hemisphere effects for the IPL, nor were there group differences in the LI across all ROIs (Figure 2.3).

When comparing BOLD signal between TD, H-ASD, and L-ASD groups, 2 x 3 ANOVAs revealed a significant main effect of Hemisphere in the IFGop [$F(1,96) = 8.62$, $p = 0.004$] and MTG [$F(1,96) = 5.57$, $p = 0.02$], with greater activity in the left hemisphere compared to the right. A 2 x 3 ANOVA revealed a marginal effect of Group in the IPL [$F(2,96) = 2.73$, $p = 0.07$], with the L-ASD group showing more activation than the H-ASD group ($p = 0.10$). There were no significant differences for group or hemisphere in the IFGorb. No group differences in LI were observed across all ROIs (Figure 2.3).

The relationship between BOLD signal and cognitive and diagnostic measures was analyzed in the ASD and TD participants combined. Verbal IQ, as measured by the WASI-II, was correlated with BOLD signal in the L MTG [$r(48) = -0.30$, $p = 0.04$], R MTG [$r(48) = -0.29$, $p = 0.04$], and R IPL [$r(48) =$, $p = 0.05$]. L IFGorb BOLD signal was negatively correlated with

nonverbal IQ [$r(48) = -0.28$, $p = 0.05$]. BOLD signal in the L IPL [$r(48) = -0.33$, $p = 0.02$] and R IFGop [$r(48) =$, $p = 0.02$] was negatively correlated with word reading ability.

MEG-fMRI correlations

Partial correlations, controlling for fMRI RMSD and age, were used to compare N250m and BOLD signal, and N400m and BOLD signal. While no partial correlations survived FDR-adjustment (alpha = 0.5; Benjamini & Hochberg, 1995), the following results describe correlations at the uncorrected threshold with medium to large effect sizes (Table 2.3). Graphs displaying significant correlations at the uncorrected threshold can be found in the supplement (Supplemental Figures S2.2-S2.3).

Correlations between MEG measures and BOLD signal were predominantly observed in the left hemisphere. For N250m, positive correlations were found in the ASD group in L IFGop [$r(26) = 0.50$, $p = 0.006$] and in the LI for IFGorb [$r(26) = 0.39$, $p = 0.04$] (Supplemental Figure S2.2). When testing ASD subgroups, the L-ASD group showed a positive correlation in the L IFGorb [$r(11) = 0.61$, $p = 0.03$] (Supplemental Figure S2.3). The H-ASD group showed positive correlations in L IFGop [$r(11) = 0.67$, $p = 0.01$] and in the LI for IFGorb [$r(11) = 0.57$, $p = 0.04$]. (Supplemental Figure S2.3). No N250m and BOLD signal correlations were found in the right hemisphere.

For N400m and BOLD signal, positive correlations were observed for the ASD group in the L IFGop [$r(26) = 0.46$, $p = 0.01$] and L IPL [$r(26) = 0.47$, $p = 0.01$] and for the TD group in the R MTG [$r(16) = 0.58$, $p = 0.01$] (Supplemental Figure S2.2). When examining ASD subgroups, there were positive correlations for the L-ASD group in the L IFGorb [$r(11) = 0.62$, $p = 0.02$], L IFGop [$r(11) = 0.59$, $p = 0.03$], L IPL [$r(11) = 0.63$, $p = 0.02$], and L MTG [$r(11) =$

0.57, $p = 0.04$] (Supplemental Figure S2.3). No correlations were observed for N400m LI and BOLD signal LI.

Discussion

The present study aimed to investigate lexicosemantic processing in individuals with ASD using a multimodal approach combining aMEG and fMRI as a follow-up study to the unimodal analyses by You and colleagues (2023). In their paper, N250m and N400m were examined during a lexicosemantic task in adolescents with and without ASD. The ASD group was divided into high and low performers, such that high performers completed the lexicosemantic task similarly to the TD group (i.e., task accuracy was equal to or greater than the median of the TD group), and low performers were those who received lower scores on the task than the TD group median. Their findings revealed greater bilateral engagement of the frontal and temporal regions in the ASD group, driven by greater involvement of the right hemisphere. When examined at the subgroup level, the high performers showed greater activity in the right prefrontal and bilateral temporal regions compared to the low performers. The low performers presented with a significantly decreased N400m in the left prefrontal region compared to TD peers. In the current study, MEG-based indices (N250m and N400m) and fMRI BOLD signal revealed activation differences between ASD and TD samples, as well as between ASD subgroups distinguished by low vs. high performance on a lexicosemantic task. Comparisons of TD and ASD groups yielded significant differences in the middle temporal region for N400m, and the inferior frontal region for both N400m and BOLD signal, with greater activity in the TD group compared to the ASD group. When the ASD group was split into groups based on task performance, findings further revealed significant differences, highlighting that detection of neural differences may require testing of behaviorally similar samples rather than considering ASD individuals as one group.

Impact of language ability on neural activity and lateralization

N250m: The N250m reflects the early stages of lexicosemantic processing that involve lexical access and orthographic processing. N250m has been found to be larger in children than adults, suggesting that increased N250m may be related to more immature, more effortful, less efficient word form processing (Eddy et al., 2014). In the present study, the N250m component did not reveal significant differences between the full ASD cohort and the TD group. However, subgroup analysis of the ASD cohort showed a significant group difference in the IFGorb, with greater activity in the H-ASD group compared to both L-ASD and TD groups. This finding may suggest that high performance in some autistic individuals may be related to more effortful, less efficient processing during lexical access stages. An increased N250m may indicate that participants in the H-ASD group required greater neural processing at this early stage to perform equally as well as TD individuals, or alternatively, that these participants performed better than the L-ASD group due to the greater neural effort at this stage. The H-ASD group performed similarly to the TD group on the task, while the L-ASD group, whose N250m appeared similar to the TD group, performed significantly worse. These findings suggest that efficient processing and high task performance in ASD adolescents requires more neural effort, whereas in L-ASD adolescents, failure to have a heightened neural response may be contributing to lower performance. An understanding of the differences in neural processing within the ASD group in relation to lexicosemantics is critical for autism interventions and supports.

As previously noted, the literature on N250(m) as it relates to language in ASD is severely limited. Previous studies have noted a lack of group differences for children with ASD in response to an auditory task of speech and non-speech sounds (Galilee et al., 2017), as well as differential responses to congruous and incongruous words; specifically, increased amplitude

was observed for congruous words, while increased duration was reported for incongruous words in individuals with ASD (Braeutigam et al., 2008). This is unsurprising, as the current study also showed a lack of group differences when comparing all ASD participants to TD peers. The current findings extend the limited literature on language-related N250(m) in ASD. The results reveal distinct neural responses during lexical access, particularly when comparing a high-performing subgroup of autistic individuals to TD adolescents. Specifically, participants in the H-ASD group showed recruitment of potential compensatory mechanisms, such as increased engagement of the lexical access circuitry reflected in a greater N250m, to perform equivalently to TD peers, while participants in the L-ASD group did not show similar development of alternative mechanisms for efficient lexical access. The N250m in the L-ASD group showed no significant difference from the TD group, yet they performed much poorer on the task.

N400m: N400(m) is considered a crucial index in measuring lexicosemantic processing, and has frequently been studied in response to semantic incongruity (Cantiani et al., 2016; DiStefano et al., 2019; M. Dunn et al., 1999; M. A. Dunn & Bates, 2005; Fishman et al., 2011; Marinkovic et al., 2003; McCleery et al., 2010; McFadden & Rojas, 2013; Pijnacker et al., 2010; Russo et al., 2012). The N400m provides information on how well individuals comprehend and integrate semantic information into context. While the N250m is representative of basic phonological knowledge and word reading, the N400m represents an individual's ability to understand the presented word within the context of a task (Carreiras et al., 2014; Halgren et al., 2002; Kotchoubey, 2002; Kutas & Federmeier, 2000; Kutas & Hillyard, 1980; Leminen et al., 2019; Marinkovic, 2004b; Marinkovic et al., 2014; Parkes et al., 2016; Pylkkänen & Marantz, 2003). In the present study, participants were required to respond differently depending on word category. Notable differences between the ASD and TD groups were observed in the N400m

component. The ASD group exhibited reduced activity in the IFGop, IPL, and MTG, with a more bilateral pattern compared to the predominantly left hemisphere engagement seen in the TD group. Further analysis of the ASD group highlighted that these differences were driven by distinctive patterns between high vs. low performers. N400m was diminished in the L-ASD group compared to the TD group in the IFGop, with a marginal effect in the left hemisphere. Thus, decreased N400m in the L-ASD subgroup may suggest reduced task engagement as well as lower ability to comprehend the category to which a presented word may belong. With regard to laterality, the TD group showed marginally greater leftward asymmetry than the H-ASD group, whose laterality index was close to 0 (suggesting bilateral engagement). This bilateral N400m activity in the H-ASD subgroup may reflect potential compensatory mechanisms that allow these individuals to reach performance levels similar to those seen in the TD group.

Previous research has largely focused on the N400(m) effect (i.e., greater N400(m) in response to incongruent stimuli than to congruent stimuli) (Cantiani et al., 2016; DiStefano et al., 2019; Dunn et al., 1999; Dunn & Bates, 2005; Fishman et al., 2011; McCleery et al., 2010; McFadden & Rojas, 2013; Pijnacker et al., 2010; Russo et al., 2012). Phan and colleagues (2023) measured the N400 amplitude in children with ASD during an auditory word paradigm and reported that the N400 was present in children with ASD, however, without an N400 incongruity effect. Additionally, they found that the N400 amplitude predicted language abilities in autistic children who had average language abilities, but not in TD peers or those with ASD who had lower language abilities. This may suggest that average-to-high-performing autistic individuals have alternative neural mechanisms for processing language than their typically developing and lower-performing autistic peers. Taken together, these findings underscore the importance of

taking language abilities in autistic individuals into consideration when examining measures of neural activity.

It is widely accepted that language activation is more prominent in the left hemisphere (Josse & Tzourio-Mazoyer, 2004; Patrick, 2010; Szaflarski et al., 2006; Tzourio-Mazoyer et al., 2017), with atypical patterns seen in individuals with ASD (Braeutigam et al., 2008; Cermak et al., 2022; Curl & Coderre, 2022; Eyler et al., 2012b; Flagg et al., 2005; Jouravlev et al., 2020; Kleinhans et al., 2008; Larson et al., 2023; Liang et al., 2021; Lindell & Hudry, 2013; Matsuzaki et al., 2020; Pijnacker et al., 2010; Preslar et al., 2014; Yoshimura et al., 2013; You et al., 2023). Findings have indicated that individuals with ASD may perform worse on language tasks that are strongly left lateralized in TD individuals, such as letter fluency (Kleinhans et al., 2008). A previous study examined the N400 effect in response to semantic stimuli, and found that N400 was greater in the right hemisphere compared to the left for individuals with ASD, specifically in individuals diagnosed with Asperger's (a previous diagnostic category) (Pijnacker et al., 2010). Bilaterality or right hemisphere lateralization was not observed in neurotypical adults or those labeled 'high-functioning ASD' (IQ $\geq$ 100). In the current study, differences in N400m laterality patterns were observed between the ASD and TD groups, as well as between performance-based ASD subgroups. The H-ASD group showed a more bilateral N400m in the MTG compared to the TD group, which is consistent with previous ASD findings of increased right hemisphere activity during language tasks (Braeutigam et al., 2008; Liang et al., 2021), reduced language lateralization (Jouravlev et al., 2020; Kleinhans et al., 2008; Larson et al., 2023; Preslar et al., 2014), and better language performance being tied to bilateral representation of the arcuate fasciculus (Cermak et al., 2022). In contrast, the L-ASD group showed diminished N400m overall compared to the TD group, significantly in the IFGop and MTG, which is consistent with

previous ASD findings of decreased left temporal N400 activity (Braeutigam et al., 2008), decreased language network connectivity in those with ASD plus a language impairment (Verly et al., 2014), reduced N400 being correlated with difficulties in semantic processing and integration (Curl & Coderre, 2022), and greater ASD symptomology being correlated with decreased N400 (O'Rourke & Coderre, 2021). These findings indicate that individuals with ASD who are able to perform similarly on language tasks to TD peers appear functionally different at the neural activation level than individuals with ASD who are unable to complete language tasks as well as TD peers. Lower-performing ASD individuals appear more similar to their TD peers, suggesting a lack of compensatory mechanisms that are present in the H-ASD group. The differences in lateralization and activation in higher-performing autistic individuals may have been established early on in development, thus allowing these individuals to process language more efficiently. Our findings of distinct patterns in N400m activity associated with language task levels nevertheless provide improved understanding of language processing variability within the ASD population.

BOLD Signal: In addition to MEG indices of activation, fMRI BOLD signal was used to measure activation during the lexicosemantic task across corresponding ROIs. Similar to EEG and MEG research, fMRI studies have generated strong evidence for both atypical language activation and lateralization in individuals with ASD across a variety of study paradigms at the functional and structural levels (Boddaert et al., 2004; Cermak et al., 2022; Eyler et al., 2012a; Gage et al., 2009; Harris et al., 2006; Herringshaw et al., 2016; Jouravlev et al., 2020; Kleinhans et al., 2008; Knaus et al., 2008, 2010; Larson et al., 2023; Y. Lee et al., 2017; Lindell & Hudry, 2013; Nielsen et al., 2014; Shen et al., 2012). In the current study, the L-ASD group showed marginally greater activation in the IPL than the H-ASD group (which was similar to the TD

group). This may suggest more effortful task performance in the L-ASD group; however, greater activation beyond levels observed in the TD and H-ASD groups was not effective in lifting task performance. For the remainder of the ROIs (IFGorb, IFGop, and MTG), no group differences were detected. These findings are inconsistent with previous studies that have suggested alterations in functional activity as measured by fMRI during language-based tasks. This may be due to a number of reasons. It may suggest that group differences are dependent on the type of task. It may also be due to the specific regions selected as part of this study. The major goal of the current study was to directly compare activation in fMRI and MEG in the same set of participants, while completing the same task. In order to examine similarities and differences in activity measured by each modality, it was critical to compare the same regions. Therefore, the ROIs in the current analysis were selected based on significant activation across all participants for the MEG measures, N250m and N400m. It is important to note, however, that our previous research has indicated that regions with significant activity as measured by MEG do not necessarily correlate with regions that are significantly activated as measured by fMRI (M. Wilkinson et al., 2022). Relatedly, other regions of the brain outside of the typical language network may have been recruited by the ASD group during the language task. Thus, examination of these four ROIs bilaterally may not capture regions with significant differences in activity (Gaffrey et al., 2007; Y. Gao et al., 2019; Shen et al., 2012). Additionally, different regions may show greater activation based on fMRI data that are not significantly activated in the MEG setting (Billingsley-Marshall et al., 2007; M. Wilkinson et al., 2022).

When considering laterality, findings from the TD group support previous evidence of typical left hemisphere language lateralization (Josse & Tzourio-Mazoyer, 2004; Patrick, 2010; Szaflarski et al., 2006; Tzourio-Mazoyer et al., 2017). While not statistically significant, the H-

ASD group showed a trend of decreased left hemisphere activity compared to the TD group, suggesting increased bilateral or right hemisphere engagement during lexicosemantic processing. This trend in decreased left hemisphere activity in the high performing ASD group is consistent with results within the current study, namely that the H-ASD group showed greater bilateral engagement of the N400m in the MTG. These findings overall are consistent with the atypical lateralization pattern found in individuals with ASD, especially with regard to language. Notably, the L-ASD group did not show a consistent pattern; in some brain areas they showed greater left hemisphere activity than the TD group, while in other areas they showed less activity, suggesting inefficient lexicosemantic processing, likely contributing to poor task performance.

Relationship between fMRI and MEG measures of language activity

Individual measures from each neuroimaging modality can provide valuable information about language processing in ASD and its relationship to language abilities, as well as the relationship between the two modalities. While correlations did not remain significant after FDR-correction, uncorrected significant correlations between fMRI and MEG measures of activation were all positive, and mostly found within the L-ASD group. Positive correlations between N250m and BOLD signal were identified in the L IFGop for the H-ASD group and the L IFGorb for the L-ASD group. Interestingly, the L-ASD group showed positive correlations between N400m and BOLD signal within all four regions. N400m and BOLD signal were positively correlated in the TD group for the R MTG. Considering the number of regions that were examined for a relationship between fMRI BOLD signal and both N250m and N400m, however, there is an overall lack of a clear relationship between fMRI and MEG measures of activation.

Similar to previous studies comparing various measurements from fMRI and MEG, there was a notable absence of significant correlations between MEG N250m and N400m and fMRI BOLD signal in the TD group. Previous research demonstrated a complex and partly negative relationship between MEG theta power and BOLD signal during a lexicosemantic task (M. Wilkinson et al., 2022). In this previous study, a negative relationship was not unexpected based on the few previous studies examining the relationship between event-related theta power and BOLD signal (Meltzer et al., 2007; Scheeringa et al., 2009b; K. D. Singh et al., 2002; Winterer et al., 2007). Surprisingly, in the current study, robust positive correlations were almost exclusively detected in the ASD group, with more correlations seen for the L-ASD group compared to the H-ASD group. Positive correlations with BOLD signal were observed in the left hemisphere for both N250m and N400m in the two ASD groups. The N250m and the BOLD signal in the L IFGop were positively correlated in the L-ASD group, while the N400m and BOLD signal were positively correlated within all four left hemisphere ROIs in the L-ASD group. Different neural events associated with activity changes, grossly fast electrophysiological and slow hemodynamic activity, coincide more consistently in the ASD group than TD peers, overall. This may suggest processing inefficiency, especially considering the higher number of correlations in the L-ASD group. Unlike activation analyses described above, the H-ASD group appears more similar to the TD group with regard to correlations between modalities, whereas the L-ASD group shows strong correlations unseen in the other groups. This may provide support for an underdeveloped lexicosemantic processing ability in comparison to the H-ASD and TD groups.

The desire to combine fMRI and MEG datasets is largely based on their complementary nature and ability to study spatiotemporal patterns – fMRI with its superior spatial resolution, and MEG with its precise temporal resolution (Babiloni et al., 2004; Belyaeva et al., 2024; B. He

& Liu, 2008; Ullsperger & Debener, 2010). Additionally, each modality measures neural activation distinctly and at different time scales. The fMRI BOLD signal measures activation indirectly through the hemodynamic response and reflects increases in neural activity (Arthurs & Boniface, 2002; Dale & Halgren, 2001), while MEG signals, which are more direct in comparison, are largely based on synaptic current flow that creates the magnetic field properties being measured (Dale & Halgren, 2001). It has been thought that a common link underlying both fMRI and MEG measures of activity may be postsynaptic potentials (Babajani-Feremi et al., 2008; E. L. Hall et al., 2014), such that the number of active potentials contributes to each modality's measurement of activation.

Despite a suggested common underlying component, the few activation studies directly comparing participants who have undergone both fMRI and MEG scans shed light on a lack of a clear relationship between the two, which is concordant with the findings of the current study. Positive correlations were mostly identified within the L-ASD group, between N400m and BOLD signal, but there was otherwise a lack of correlation between the two measures. Correspondingly, a previous study described no relationship between fMRI BOLD signal and the MEG M20 component in the primary sensory area during a stimulation study of 10 adults after a stroke (Altamura et al., 2007). A study of 13 neurotypical adults completing a word recognition task in fMRI and MEG scans found that fMRI demonstrated activity across more brain regions than MEG (Billingsley-Marshall et al., 2007). Similar to the current study, a positive correlation between fMRI BOLD signal and MEG activity was reported in the left frontal lobe, yet there were no correlations between the LI for any ROI (Billingsley-Marshall et al., 2007). Differences in regional activation, as well as hemispheric differences, across modalities have been reported in other studies as well (Liljeström et al., 2009; Vartiainen et al., 2011). Similarly, no significant

voxel-wise correlations were observed between fMRI and MEG in adults watching a movie (Lankinen et al., 2018).

Correlations between fMRI and MEG data have also been examined in other measurements, such as resting-state functional connectivity and MEG oscillations. Vallinoja and colleagues (2024) demonstrated weak correlations between fMRI and MEG functional connectivity values in youth with and without cerebral palsy. The same study reported a lack of similarity between fMRI and MEG networks, such that group differences in interhemispheric connectivity were revealed only in MEG and not by fMRI. Other studies have described a heterogeneous pattern to fMRI-MEG correlations, such that a relationship may be location- , time-, frequency- and/or task-dependent (Furey et al., 2006; Kujala et al., 2014; McDonald et al., 2010; Robitaille et al., 2010; Schulz et al., 2004; Shafiei et al., 2022). For example, one study of the visual cortex showed negative correlations between fMRI BOLD signal and lower frequencies and positive correlations between fMRI BOLD signal and higher frequencies (Zumer et al., 2010). Another study of the language network revealed positive correlations in frontotemporal regions, but differences in laterality of the superior temporal gyrus, with MEG showing the traditional leftward lateralization and fMRI showing bilateral activity (Youssofzadeh & Babajani-Feremi, 2019). While not MEG, a study employing simultaneous EEG-fMRI in 15 adults found a significant N400 effect, yet no significant differences in BOLD signal, in the context of a semantic priming task (Geukes et al., 2013).

The overall research on the relationship between fMRI and MEG is limited and its use in psychopathology is even smaller. Previous studies describe the utility of multimodal neuroimaging in clinical populations, such that the integration of neuroimaging data can support a more complete understanding of psychological disorders that are not yet fully understood at the

neural level (Calhoun & Sui, 2016; Cetin et al., 2016; Gawne et al., 2020). Interestingly, Gawne and colleagues (2020) found a positive relationship between fMRI BOLD signal during an inhibitory task and MEG resting state low frequency activity in a combined group of individuals with psychosis and neurotypical controls. However, this was not in a specific brain region, but an average across eight different regions. To our knowledge, this is the first study specifically examining the relationship of MEG N250m and N400m with fMRI BOLD signal, and one of very few studies to examine the fMRI-MEG relationship in participants with ASD.

Limitations and future directions

The current study is the first to directly compare MEG N250m and N400m with fMRI BOLD signal, though there are several limitations to note. First, the sample size was relatively limited with 50 total participants and only 15 adolescents in each of the ASD subgroups. Only a small fraction of inducted participants were able to fully cooperate with consistently minimal movement in both neuroimaging scans, thereby limiting the number of participants included in analyses. Nevertheless, the meager body of literature comparing fMRI and MEG has been predominantly based on studies with a very small total number of participants (i.e., less than 15). As such, the current study is one of the larger studies directly comparing the two modalities. Second, even though the study examined high- and low- performing individuals with respect to task performance, a 6th-grade reading level was required for appropriate engagement in the task. Our findings may therefore not generalize to the entire spectrum of the ASD population. The current results underscore the need to consider heterogeneity within an ASD sample and provide further evidence that distinguishing behaviorally defined subgroups can be beneficial for teasing out neural differences, both within the spectrum and from TD peers. Future studies may benefit from a longitudinal design to understand differential developmental patterns across ASD

subgroups and the impact of interventions on lexicosemantic processing, as it is unclear from the current study whether greater lexicosemantic processing or alternative neural activation and lateralization precedes the other.

Conclusion

The current study is among the first to directly compare fMRI and MEG in ASD, specifically addressing activation and laterality during lexicosemantic processing, focusing on the N250m and N400m from MEG, and the BOLD signal from fMRI in ASD and TD adolescents. Correlations between fMRI and MEG were notably absent across regions for the TD and H-ASD group, while significant positive correlations were revealed across multiple regions in the L-ASD group. Group differences were identified in MEG N250m and N400m, with increased bilateral frontotemporal activity in the H-ASD group. Although MEG and fMRI scans were performed using the same task in identical participant samples, no corresponding group differences were detected for the BOLD signal. This suggests that multimodal neuroimaging analyses reveal complementary, yet minimally correlated, information. Moreover, the observed subgroup differences highlight the heterogeneity within the ASD population, emphasizing the need for specific approaches in understanding and addressing language processing differences amongst autistic individuals.

Acknowledgements

Chapter 2, in full, is being prepared for submission for publication. Wilkinson, M., Linke, A.C., You, Y., Marinkovic, K., Müller, R.-A. & Jao Keehn, R. J. The dissertation author was the primary investigator and author of this paper.

Table 2.1 Participant demographics

Note: Means, standard deviations (SD), and ranges for each group. Chi-square tests (gender, handedness) and t-tests were performed to determine if groups were significantly different on demographic variables. Non-standard degrees of freedom are attributed to Levene's test for homogeneity of variance and thus reject the null hypothesis of equal variance. * denotes $p \leq .05$, ** $p \leq .01$, *** $p \leq .001$

ASD = autism spectrum disorder
RMSD = root mean square difference; a measure of motion during fMRI scans
TD = typically developing

	ASD (n=30)		**TD (n=20)**			**$\chi 2$ (df)**	***p***
Gender	23 male, 7 female		15 male, 5 female			0.02 (1)	0.89
Handedness	29 right, 1 left		18 right, 2 left			0.95 (1)	0.33
	Mean (SD)	**Range**	**Mean (SD)**	**Range**	**Hedges' g**	***t*-stat (df)**	***p***
Age (years)	15.89 (2.42)	12.25-20	15.37 (1.95)	12.50-21.42	0.23	0.82 (48)	0.42
MRI RMSD	0.07 (0.02)	0.03-0.13	0.06 (0.03)	0.03-0.13	0.76	2.69 (48)	0.01**
Total Task Accuracy (%)	87.18 (7.81)	69.35-99.08	94.23 (2.79)	87.08-98.25	1.10	4.53 (39.02)	<0.0001***
MRI Task Accuracy (%)	87.80 (7.96)	71.00-99.00	95.00 (2.92)	85.00-99.00	1.10	4.52 (39.44)	<0.0001***
MEG Task Accuracy (%)	86.56 (8.24)	67.71-99.17	93.46 (3.13)	86.25-97.50	1.01	4.16 (40.04)	<0.0001***
WASI-II							
Full Scale IQ	107.57 (18.68)	59-136	114.25 (11.47)	93-135	0.41	1.57 (47.76)	0.12
Verbal IQ	105.40 (17.09)	68-134	113.25 (12.24)	85-135	0.51	1.77 (48)	0.08
Non-Verbal IQ	109.90 (22.77)	54-156	111.55 (10.34)	90-128	0.09	0.35 (43.37)	0.73
ADOS-2							
Total	11.07 (3.29)	6-20	--	--	--	--	--

Table 2.2 Demographics of high and low performers

Note: Means, standard deviations (SD), and ranges for each ASD group. Chi-square tests (gender, handedness) and *t*-tests were performed to determine if groups were significantly different on demographic variables. Non-standard degrees of freedom are attributed to Levene's test for homogeneity of variance and thus reject the null hypothesis of equal variance. It is important to note that while one participant in the ASD group had a low IQ (FSIQ = 59), they met the reading requirements for the task and thus were included in the study. * denotes $p \leq .05$, ** $p \leq .01$, *** $p \leq .001$

H-ASD = high-performing ASD
L-ASD = low-performing ASD
RMSD = root mean square difference; a measure of motion during fMRI scans

	H-ASD (n=15)		**L-ASD (n=15)**			**$\chi 2$ (df)**	***p***
Gender	12 male, 3 female		11 male, 4 female			0.19 (1)	0.67
Handedness	14 right, 1 left		15 right, 0 left			1.03 (1)	0.31
	Mean (SD)	**Range**	**Mean (SD)**	**Range**	**Hedges' g**	***t*-stat (df)**	***p***
Age (years)	16.01 (2.84)	12.25-20.00	15.78 (2.01)	13.17-20	0.09	0.25 (28)	0.81
MRI RMSD	0.07 (0.03)	0.03-0.13	0.07 (0.02)	0.04-0.10	0.04	0.10 (28)	0.92
Total Task Accuracy (%)	93.52 (3.33)	86.85-99.08	80.84 (5.37)	69.35-86.52	2.84	7.77 (23.39)	<0.0001***
MRI Task Accuracy (%)	94.13 (3.64)	87.00-99.00	81.47 (5.66)	71.00-88.00	2.66	7.29 (28)	<0.0001***
MEG Task Accuracy (%)	92.92 (4.33)	82.71-99.17	80.21 (5.96)	67.71-88.54	2.44	6.68 (28)	<0.0001***
WASI-II							
Full Scale IQ	118.47 (10.26)	95-136	94.80 (16.06)	59-123	1.76	4.81 (23.80)	<0.0001***
Verbal IQ	116.80 (8.17)	107-134	93.60 (15.51)	68-119	1.87	5.13 (21.21)	<0.0001***
Non-Verbal IQ	116.20 (19.30)	79-156	100.00 (20.21)	54-131	0.82	2.25 (28)	0.03*
ADOS-2							
Total	11.40 (2.75)	8-16	10.73 (3.83)	6-20	0.20	0.55 (28)	0.59

Table 2.3 Pearson partial correlations for fMRI and MEG indices of activation

Note: Pearson partial correlations between MEG N250m and N400m and fMRI BOLD beta coefficients controlling for RMSD and age by group. * denotes $p \leq .05$

ASD = autism spectrum disorder group
H-ASD = high-performing ASD group
IFGop = inferior frontal gyrus opercularis
IFGorb = inferior frontal gyrus orbitalis
IPL = inferior parietal lobule
L = left hemisphere
L-ASD = low-performing ASD group
LI = laterality index
MTG = middle temporal gyrus
R = right hemisphere
TD = typically developing group

ROI	TD		ASD		H-ASD		L-ASD	
	r	***p***	***r***	***p***	***r***	***p***	***r***	***p***
N250m & BOLD Signal								
L IFGorb	-0.01	0.980	0.35	0.070	0.30	0.326	0.61	0.026*
R IFGorb	0.09	0.723	0.12	0.549	0.50	0.081	-0.32	0.287
LI IFGorb	-0.11	0.673	0.39	0.042	0.57	0.017*	0.32	0.282
L IFGop	0.09	0.720	0.50	0.006**	0.67	0.013*	0.53	0.060
R IFGop	-0.21	0.392	-0.12	0.544	0.14	0.639	0.03	0.915
LI IFGop	-0.09	0.726	-0.26	0.190	-0.30	0.317	-0.11	0.711
L IPL	0.17	0.498	0.27	0.172	0.29	0.344	0.29	0.331
R IPL	0.28	0.265	0.01	0.969	0.01	0.971	0.03	0.910
LI IPL	-0.12	0.630	0.16	0.426	0.35	0.248	-0.36	0.232
L MTG	-0.14	0.588	0.09	0.664	0.49	0.088	-0.05	0.873
R MTG	0.33	0.184	0.20	0.312	0.54	0.055	0.08	0.805
LI MTG	0.15	0.565	0.02	0.915	0.05	0.876	-0.03	0.920
N400m & BOLD Signal								
L IFGorb	0.09	0.720	0.32	0.096	0.11	0.726	0.62	0.023*
R IFGorb	-0.10	0.698	0.13	0.520	0.21	0.499	0.36	0.224
LI IFGorb	-0.21	0.397	0.15	0.439	0.13	0.671	0.26	0.395
L IFGop	0.23	0.360	0.45	0.014*	0.45	0.119	0.59	0.033*
R IFGop	0.43	0.074	0.07	0.719	0.24	0.432	0.30	0.311
LI IFGop	0.05	0.852	0.10	0.629	0.15	0.625	0.13	0.679
L IPL	0.33	0.181	0.47	0.013*	0.42	0.150	0.63	0.020*
R IPL	0.26	0.305	0.08	0.704	0.17	0.589	0.15	0.618
LI IPL	-0.11	0.656	0.17	0.399	0.12	0.702	0.27	0.370
L MTG	0.20	0.429	0.27	0.170	0.14	0.637	0.57	0.044*
R MTG	0.58	0.011*	-0.05	0.795	0.04	0.885	-0.13	0.668
LI MTG	0.16	0.522	-0.32	0.101	-0.42	0.148	-0.20	0.513

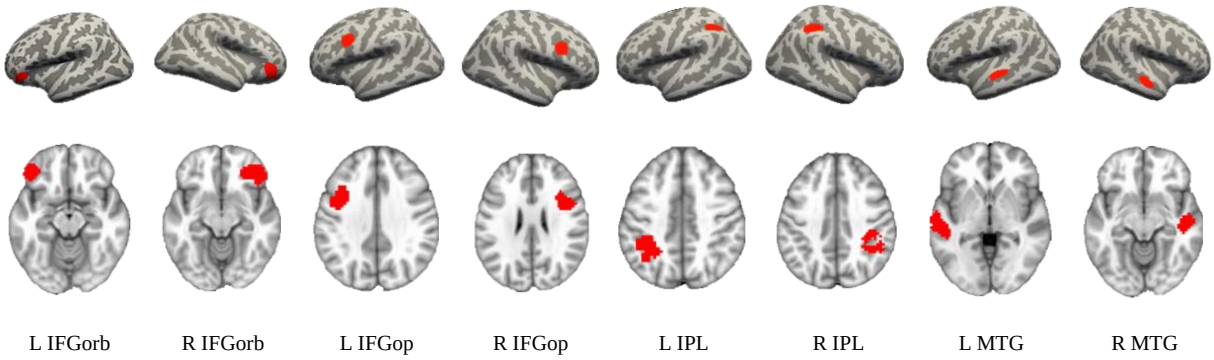

Figure 2.1 ROIs in surface and volumetric space

Note: Surface space ROIs are depicted in the top row, and volumetric ROIs in the second row. ROIs from left to right: left inferior frontal gyrus orbitalis (L IFGorb), right inferior frontal gyrus orbitalis (R IFGorb), left inferior frontal gyrus opercularis (L IFGop), right inferior frontal gyrus opercularis (R IFGop), left inferior parietal lobule (L IPL), right inferior parietal lobule (R IPL), left middle temporal gyrus (L MTG), and right middle temporal gyrus (R MTG)

Figure 2.2 fMRI and MEG measures of activation in TD and ASD groups

Note: Top panel depicts ASD and TD group comparison of MEG N250m, MEG N400m, and fMRI BOLD signal for each hemisphere. Bottom panel depicts H-ASD, L-ASD, and TD group comparison. * denotes $p \leq .05$, ** $p \leq .01$, *** $p \leq .001$

ASD = autism spectrum disorder group
H-ASD = high-performing ASD group
IFGop = inferior frontal gyrus opercularis
IFGorb = inferior frontal gyrus orbitalis
IPL = inferior parietal lobule
L-ASD = low-performing ASD group
MTG = middle temporal gyrus
TD = typically developing group

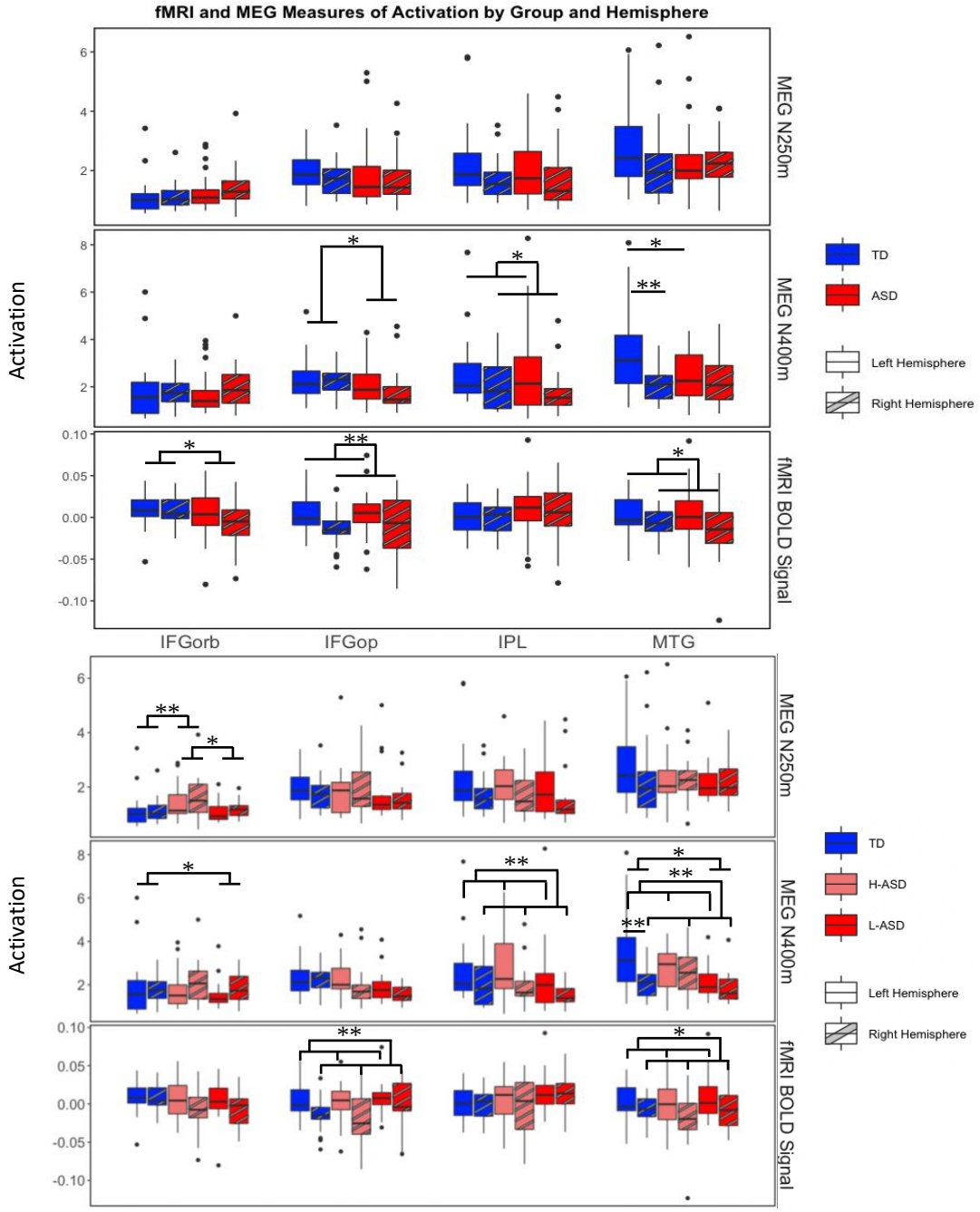
fMRI and MEG Measures of Activation by Group and Hemisphere
Activation
MEG N250m
MEG N400m
fMRI BOLD Signal
IFGorb
IFGop
IPL
MTG
TD
ASD
H-ASD
L-ASD
Left Hemisphere
Right Hemisphere

Figure 2.3 fMRI and MEG laterality index in TD and ASD groups

Note: Top panel depicts ASD and TD group comparison of laterality indices for MEG N250m, MEG N400m, and fMRI BOLD signal. Bottom panel depicts H-ASD, L-ASD, and TD group comparison. * denotes $p \leq .05$, ** $p \leq .01$, *** $p \leq .001$

ASD = autism spectrum disorder group
H-ASD = high-performing ASD group
IFGop = inferior frontal gyrus opercularis
IFGorb = inferior frontal gyrus orbitalis
IPL = inferior parietal lobule
L-ASD = low-performing ASD group
MTG = middle temporal gyrus
TD = typically developing group

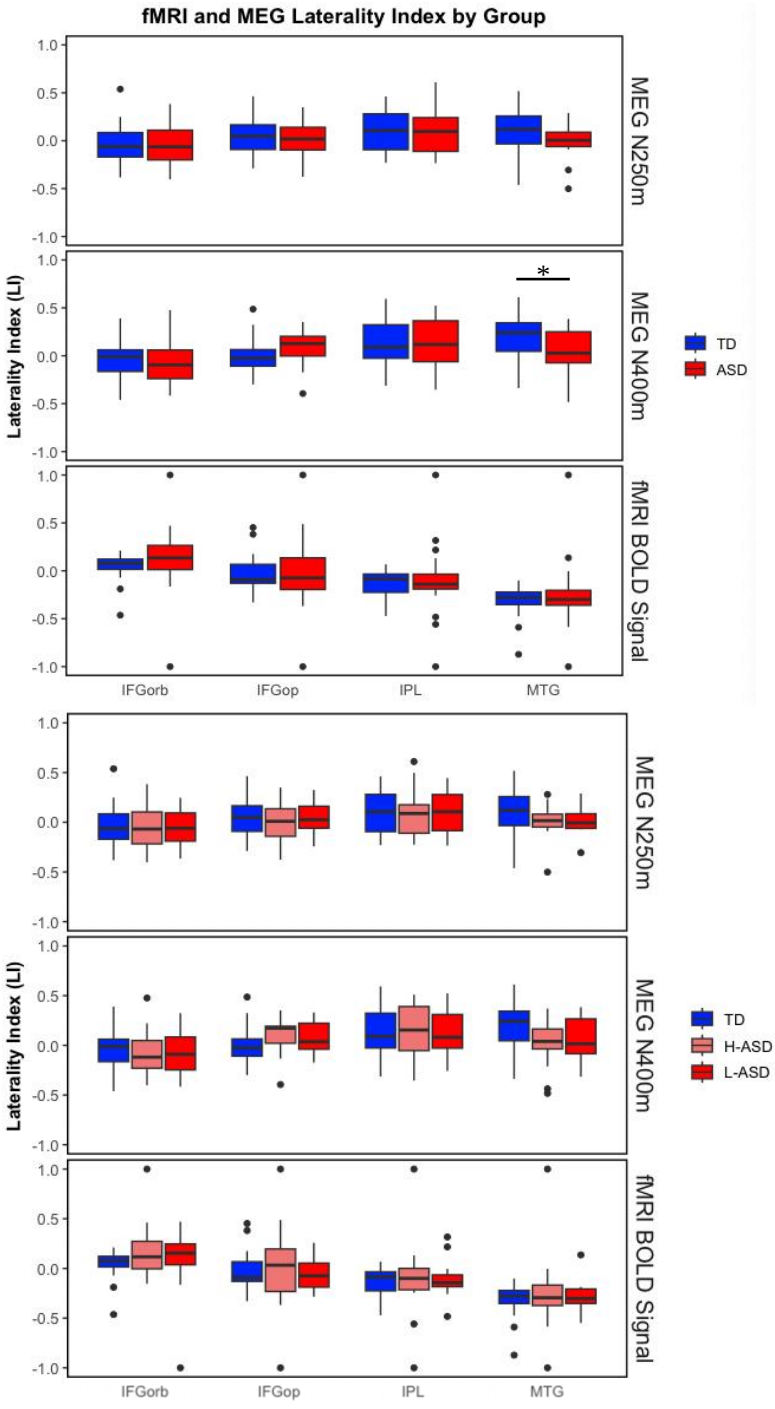
fMRI and MEG Laterality Index by Group
Laterality Index (LI)
MEG N250m
MEG N400m
fMRI BOLD Signal
*
TD
ASD
H-ASD
L-ASD
IFGorb
IFGop
IPL
MTG

Supplemental Materials

Participants

A total of 276 adolescents (156 ASD, 120 TD) were screened. Seventy-nine ASD and 62 TD adolescents were not invited to participate in the study due to contraindications preventing them from having an MRI/MEG scan (e.g., braces, permanent retainer), having additional medical conditions (e.g., Fragile X syndrome, tuberous sclerosis, epilepsy), being exposed to another language before age 5, if they were a TD adolescent with a personal or family history of developmental, neurological, or psychological disorders. Of those invited to join the study after the screening, 16 ASD and 11 TD participants dropped out or were unable to be reached for scheduling. Sixty-one ASD and 47 TD adolescents entered the study; of these participants, 13 ASD and 12 TD adolescents were excluded throughout the study due to one or more of the following reasons: lack of cooperation during neuropsychological testing (ASD: 1, TD: 0), reading skills below a 6th-grade level (ASD: 2, TD: 0), score of 60% or lower on the lexicosemantic task during a practice session (ASD: 5, TD: 2), difficulty following lexicosemantic task directions (ASD: 2, TD: 0), large head size preventing MRI/MEG scanning (ASD: 1, TD: 2), becoming hospitalized for psychiatric care (ASD: 1, TD: 0), only completed one scan (ASD: 2, TD: 4), and inability to continue study due to the COVID-19 research shutdown in March 2020 (ASD: 1, TD: 8). A total of 46 ASD and 31 TD participants completed all components of the study. Unexpected data loss, scanner malfunction, brain abnormalities, excessive head motion, and unusable data impacted 16 ASD and 9 TD individuals.

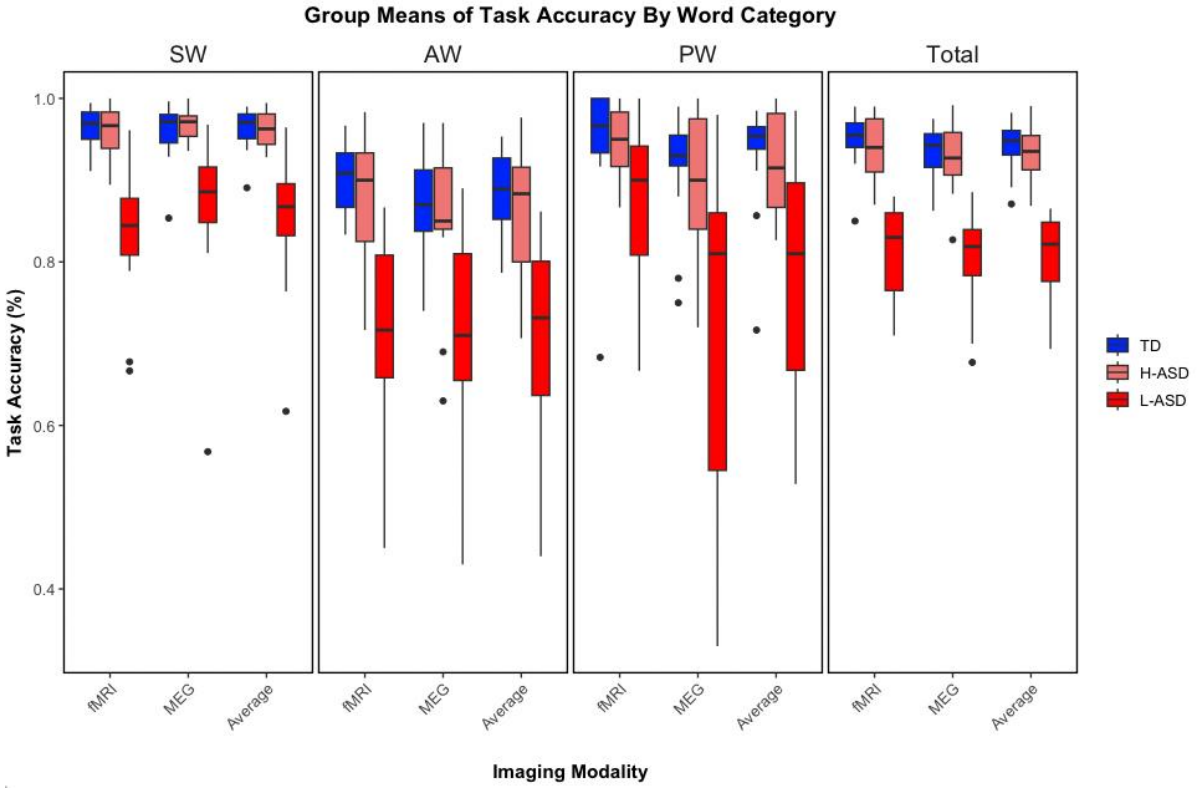

Supplemental Figure 2.1 Lexicosemantic task performance by group for fMRI and MEG scans

Note: Task performance depicted for TD, H-ASD, and L-ASD groups by word category (SW, AW, PW) and total average for each imaging modality (fMRI, MEG), and averaged across both modalities.

ASD = autism spectrum disorder
AW = animal word
H-ASD = high-performing ASD group
L-ASD = low-performing ASD group
PW = pseudoword
SW = standard word
TD = typically developing group

Supplemental Figure 2.2 Pearson partial correlations for ASD and TD groups for MEG N250m, N400m, and fMRI BOLD signal

Note. Uncorrected significant correlations between MEG (N250m, N400m) and fMRI measures of activation (BOLD signal) for ASD and TD groups. Uncorrected Pearson partial correlations, controlling for fMRI RMSD and age, shown in each graph for the group with a significant correlation.

ASD = autism spectrum disorder group
IFGorb = inferior frontal gryus orbitalis
IFGop = inferior frontal gyrus opercularis
IPL = inferior parietal lobule
L = left hemisphere
LI = laterality index
MTG = middle temporal gyrus
R = right hemisphere
TD = typically developing group

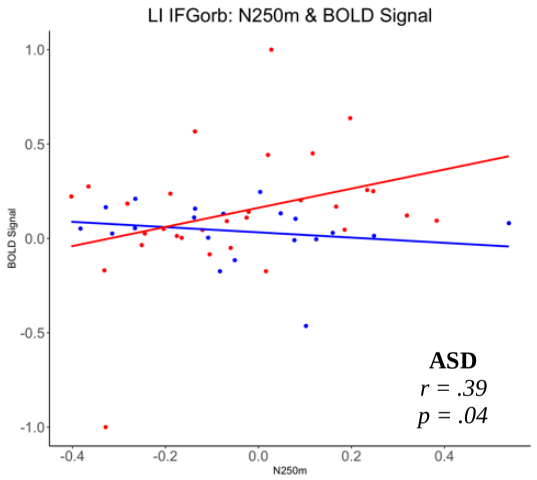
LI IFGorb: N250m & BOLD Signal
BOLD Signal
N250m
ASD
r = .39
p = .04

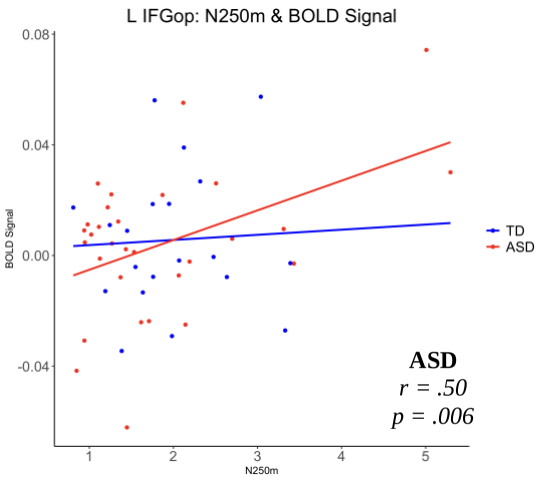
L IFGop: N250m & BOLD Signal
BOLD Signal
N250m
TD
ASD
ASD
r = .50
p = .006

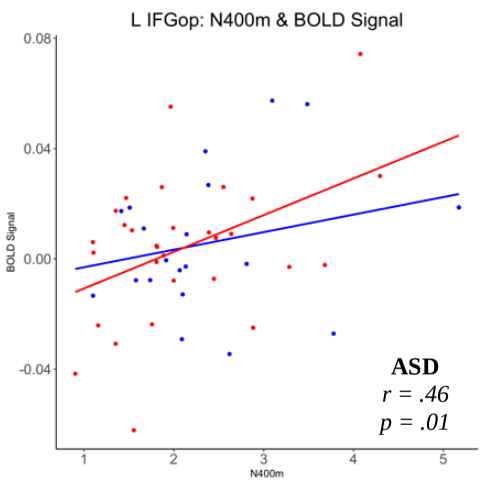
L IFGop: N400m & BOLD Signal
BOLD Signal
N400m
ASD
r = .46
p = .01

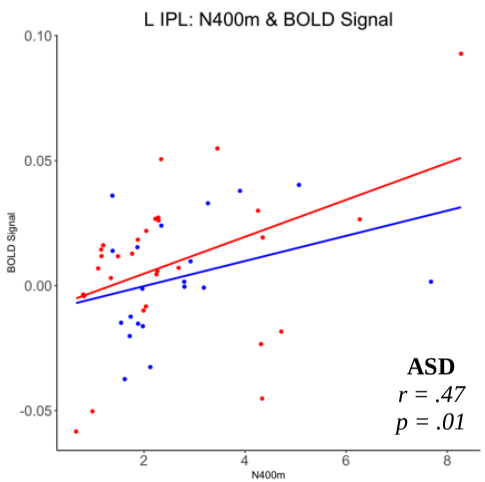
L IPL: N400m & BOLD Signal
BOLD Signal
N400m
ASD
r = .47
p = .01

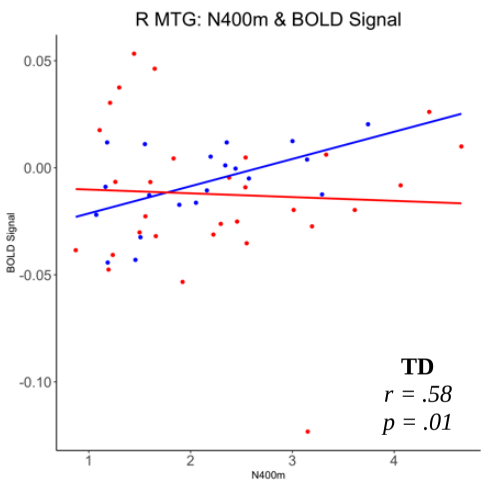
R MTG: N400m & BOLD Signal
BOLD Signal
N400m
TD
r = .58
p = .01

Supplemental Figure 2.3 Pearson partial correlations for H-ASD and L-ASD subgroups for MEG N250m, N400m, and fMRI BOLD signal

Note. Uncorrected significant correlations between MEG (N250m, N400m) and fMRI measures of activation (BOLD signal) for H-ASD and L-ASD subgroups. The TD group (blue) is shown for reference. Top row: N250m and BOLD signal correlations. Bottom row: N400m and BOLD signal correlations.

ASD = autism spectrum disorder group
H-ASD = high-performing ASD group
IFGorb = inferior frontal gryus orbitalis
IFGop = inferior frontal gyrus opercularis
IPL = inferior parietal lobule
L = left hemisphere
L-ASD = low-performing ASD group
LI = laterality index
MTG = middle temporal gyrus
R = right hemisphere
TD = typically developing group

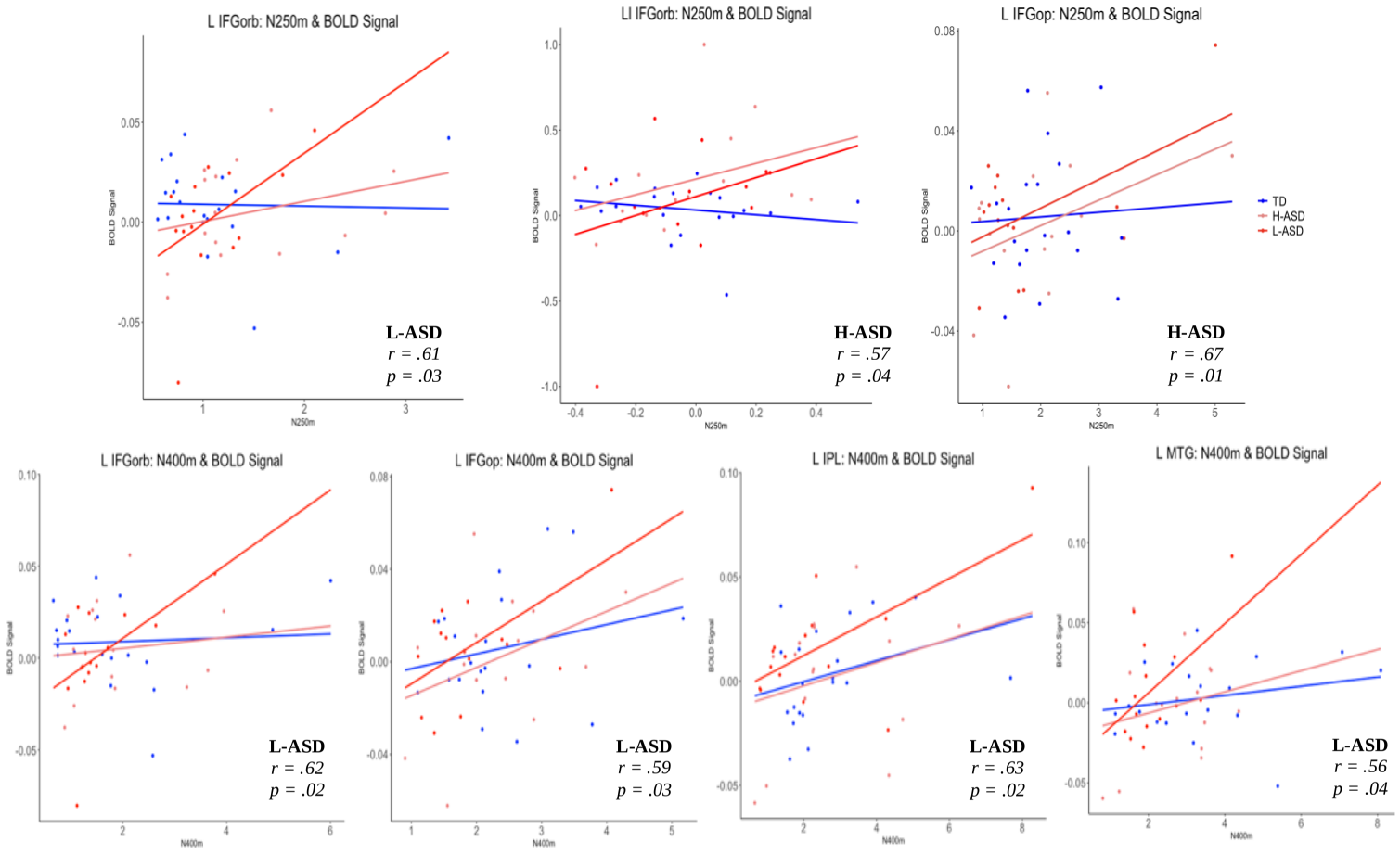
L IFGorb: N250m & BOLD Signal
BOLD Signal
N250m
L-ASD
r = .61
p = .03
LI IFGorb: N250m & BOLD Signal
H-ASD
r = .57
p = .04
L IFGop: N250m & BOLD Signal
H-ASD
r = .67
p = .01
TD
H-ASD
L-ASD
L IFGorb: N400m & BOLD Signal
N400m
L-ASD
r = .62
p = .02
L IFGop: N400m & BOLD Signal
L-ASD
r = .59
p = .03
L IPL: N400m & BOLD Signal
L-ASD
r = .63
p = .02
L MTG: N400m & BOLD Signal
L-ASD
r = .56
p = .04

Chapter 3 Study 3

Comparison of non-invasive measures of excitation-inhibition ratios in autism: fMRI Hurst exponent and MEG aperiodic exponent

Wilkinson, M.[a,b], Jao Keehn, R.J.[b], You, Y.[c], Preston, M.[d], Marinkovic, K.[a,c,e], Müller, R-A.[a,b], Voytek, B.[d], Linke, A.C.[b]

[a]San Diego State University/University of California San Diego Joint Doctoral Program in Clinical Psychology, San Diego, CA, United States

[b]Brain Development Imaging Laboratories, Department of Psychology, San Diego State University, San Diego, CA, United States

[c]Spatiotemporal Brain Imaging Laboratory, Department of Psychology, San Diego State University, San Diego, CA, United States

[d]Department of Cognitive Science, University of California San Diego, CA, United States

[e]Radiology Department, University of California San Diego, CA, United States

Abstract

The excitation-inhibition (E:I) ratio reflects excitatory and inhibitory neuronal activity in the brain and has been found to be atypical in neurodevelopmental conditions such as autism spectrum disorder (ASD). Quantifying the E:I ratio is a critical aspect for understanding the neurobiological profile of individuals with ASD, yet it has been difficult to study non-invasively. The current study investigates two non-invasive measures, the Hurst exponent (HE) from resting-state fMRI (rs-fMRI) and the aperiodic exponent (AE) from resting-state MEG (rs-MEG), and is the first to directly compare these two E:I measures, one derived from a hemodynamic source and the other electrophysiologically. In a group of 34 ASD adolescents and 24 typically developing (TD) peers, rs-fMRI HE was found to be significantly altered in the ASD group, with mostly regional increases, and a few decreases compared to the TD group. In a group of 33 ASD adolescents and 22 TD peers, rs-MEG AE was consistently greater in the ASD compared to the TD group. rs-fMRI HE showed mixed Group-by-Age interactions, increasing and decreasing with age in the ASD group, while rs-MEG AE consistently decreased with age in the ASD group. AE also showed consistent positive correlations with ASD symptoms. A group of 28 ASD adolescents and 20 TD peers with usable data from both fMRI and MEG scans was used for correlational analyses. No clear pattern was observed with regard to a relationship between HE and AE. Although both the HE and AE are thought to reflect the E:I ratio in the respective literatures, no clear pattern of correlation emerged, suggesting that two indices reflective of the E:I ratio may be representative of different, yet complementary components of neuronal activity.

Keywords: Functional magnetic resonance imaging (fMRI), magnetoencephalography (MEG), multimodal integration, autism spectrum disorder (ASD), Hurst exponent, aperiodic exponent, excitation-inhibition (E:I) activity

Introduction

Autism spectrum disorder (ASD) is characterized by challenges in social communication and the display of restricted and/or repetitive behaviors (American Psychiatric Association, 2013). Current reports estimate that 1 in 36 children have a diagnosis of ASD (Maenner et al., 2023). ASD is diagnosed based on behavioral measures of social communication and restricted, repetitive behaviors. To date, there have been no biomarkers identified as a reliable method for diagnosing ASD. Research in the area of diagnostic biomarkers is critical for early diagnosis, but can also be used to develop interventions, monitor intervention progress, and determine long-term outcomes. Noninvasive biomarkers have been difficult to identify due to the broad heterogeneity of the disorder with regard to symptoms, severity, and etiology, as well as a lack of replication studies.

A balance of neuronal excitatory and inhibitory activity is necessary for typical brain development and processing. Excitatory and inhibitory activity rely on glutamate and GABA, respectively, with a balance represented as 2-6 times greater inhibitory compared to excitatory activity (Alvarez & Destexhe, 2004; Xue et al., 2014). Balance is achieved through several factors, such as development of excitatory and inhibitory synapses, downstream signaling pathways, and cellular abnormalities (Lee et al., 2017). Imbalances in excitation:inhibition (E:I) activity have been linked to neurodevelopmental disorders, such as attention-deficit/hyperactivity disorder (ADHD) (Ferranti et al., 2024; Mamiya et al., 2021), schizophrenia (R. Gao & Penzes, 2015; Y. Liu et al., 2021), and ASD (Bruining et al., 2020; Carter Leno et al., 2022; Dani et al., 2005; R. Gao & Penzes, 2015; Mariani et al., 2015; Rubenstein & Merzenich, 2003; R. X. Smith et al., 2018; Sohal & Rubenstein, 2019; Trakoshis et al., 2020). Studies have found individuals with ASD to have an increased level of excitatory activity, or decreased inhibitory abilities, resulting in an E:I imbalance (Bruining et al., 2020; Smith et al., 2018; Trakoshis et al., 2020).

This imbalance relates to poor functional differentiation and increased noise in the brain, and may result from atypical function at various levels of the nervous system (Rubenstein & Merzenich, 2003; Sohal & Rubenstein, 2019). It is hypothesized that the E:I imbalance in ASD is caused by either increases in glutamatergic activity or decreases in GABAergic neurotransmission (Uzunova et al., 2016). Mouse models of ASD have most frequently been used in studies of E:I imbalance due to the invasive nature of measuring excitatory and inhibitory activity (Lee et al., 2017; Sohal & Rubenstein, 2019). These studies have largely found that E:I imbalances are ameliorated by increasing inhibitory activity (Sohal & Rubenstein, 2019). For example, when neurons in the medial prefrontal cortex were activated, this led to atypical social behavior in the mice, as well as an increase in gamma power (Yizhar et al., 2011). Neuroimaging attempts to measure the E:I ratio in humans have relied mostly on glutamate and GABA measures from magnetic resonance spectroscopy (MRS) or oscillations of the MEG signal, particularly the gamma band (Dickinson et al., 2016; Port et al., 2019; Uzunova et al., 2016). A recent study found that in children with ASD, a higher E:I ratio was correlated with higher symptom severity, as measured by the Social Responsiveness Scale (SRS) (Bruining et al., 2020). E:I imbalance is found to be related to differences in functional connectivity and behavioral symptoms in ASD (Bruining et al., 2020; Hegarty et al., 2018; Nelson & Valakh, 2015; Rubenstein & Merzenich, 2003; Siegel-Ramsay et al., 2021; R. X. Smith et al., 2018; Sohal & Rubenstein, 2019).

Direct measures that have traditionally been used do not allow for studying the E:I ratio in humans, and are typically restricted to studying a specific population of cells rather than E:I activity more globally. Fractal scaling parameters, such as the Hurst exponent (HE), the aperiodic exponent, and the fractal dimension (FD), estimate the irregularity, or randomness, of a

complex process using timeseries data (Lai et al., 2010). These parameters follow a spectral pattern, with power decreasing as a function of frequency (Trakoshis et al., 2020). Previous studies have examined the relationship between fractal scaling parameters and medical conditions, such as heart disease and Alzheimer's. The fractal dimension (FD) was found to have increased significantly more in individuals with end-stage heart disease and those with Alzheimer's disease, compared to adults experiencing typical aging without these additional medical complications (Lai et al., 2010). Significant increases in FD is thought to represent increased regularity of typically complex processes (Lai et al., 2010).

HE is another fractal scaling parameter and is estimated through the equation: FD = 2 – HE. Modeling studies have found that changes in the E:I ratio can alter the spectral components that are measured from timeseries data, thus altering the HE or other spectral parameters (Brunel & Wang, 2003; R. Gao et al., 2017; Lombardi et al., 2017; Mazzoni et al., 2008; Trakoshis et al., 2020). HE can be measured from the fMRI blood-oxygen-level-dependent (BOLD) timeseries, with decreases in HE reflecting increases in the E:I ratio, or a "shift-to-randomness" (Lai et al., 2010; Trakoshis et al., 2020). Lai and colleagues (2010) measured HE in adults with ASD who were matched on age and intellectual ability to neurotypical adults. HE was estimated from rs-fMRI. HE was found to be significantly reduced in ASD participants across the whole brain and in regions related to social function (i.e., amygdala, anterior insula, medial prefrontal cortex, and posterior cingulate cortex) when compared to TD individuals (Lai et al., 2010). They also reported a correlation between HE in multiple brain regions and ASD severity, with reduced HE correlated with increased severity (Lai et al., 2010). Trakoshis and colleagues (2020) followed up on their 2010 study (Lai et al., 2010), and compared HE from rs-fMRI between adults with and without ASD. HE was found to be decreased in the ventromedial prefrontal cortex, suggesting an

increased E:I ratio, in ASD males, but not in females with ASD. Gender differences in HE have also been identified in neurotypical adults (Dong et al., 2018). The fractal dimension, calculated from HE, was also found to be decreased in ASD adults during rs-fMRI, suggesting decreased signal complexity, and was also correlated with ASD symptom severity (Dona et al., 2017).

In addition to HE, there is recent research exploring the relationship of aperiodic neural activity from electroencephalography (EEG) and magnetoencephalography (MEG) to understand excitatory and inhibitory activity in the brain. Neural activity can be separated into two components – periodic and aperiodic (Donoghue et al., 2020; B. J. He, 2014; He et al., 2010). Periodic activity, the more researched of the two, refers to neural oscillations and is measured by the power within frequency bands (e.g., alpha, delta, theta, beta, gamma). Historically the aperiodic component has been largely pushed aside as spontaneous neural noise. Aperiodic neural activity, also referred to as $1/f$ activity, $1/f$ noise, or scale-free activity, follows a $1/f$-like pattern of higher amplitudes at lower frequencies, with exponentially decreasing power with increases in frequency (He, 2014). Recent advances have been made to separate periodic and aperiodic activity in the brain, so that the aperiodic activity can be more easily studied. Donoghue et al. (2020) created a toolbox that analyzes Fourier transforms of raw neural data to explicitly quantify periodic and aperiodic activity. The slope of the $1/f$-like distribution, also known as the aperiodic exponent (AE), in neural data is negative (Donoghue et al., 2020; Podvalny et al., 2015) and is significantly different from true random white noise, which has a flat slope. Studies have found changes in the aperiodic exponent to be related to age, processing of stimuli, memory, and sleep/wake stages (Lendner et al., 2020; Maniscalco et al., 2018; Thuwal et al., 2021; Voytek et al., 2015).

Aperiodic activity is hypothesized to be a reflection of the E:I ratio in the brain (Colombo et al., 2019; R. Gao et al., 2017; Gerster et al., 2022; Lendner et al., 2020; Miskovic et al., 2018; Waschke et al., 2021). Similar to the rs-fMRI HE, aperiodic activity is thought to be a noninvasive measure of E:I, which is thought to be unbalanced in ASD. To determine the relationship between aperiodic activity and the E:I ratio, Gao et al. (2017) used a simulation to alter excitatory and inhibitory activity while measuring aperiodic activity in local field potential (LFP) data. They found that the E:I ratio was positively correlated with the aperiodic slope, and that increasing the E:I ratio resulted in a flatter slope. When exploring the relationship between the aperiodic slope and activity in a rat model, they found that the slope was again correlated with the E:I ratio (measured as excitatory and inhibitory synaptic density) (Gao et al., 2017) . These results support aperiodic activity as a noninvasive measure of E:I ratio in the brain.

There are a few recent studies that have examined aperiodic activity in children with ASD and related neurodevelopmental disorders. One study used resting-state EEG data from a small sample of boys with Fragile X Syndrome (FXS) (Wilkinson & Nelson, 2021). Although not all children with FXS have ASD, it is estimated that 30-54% of males with FXS meet criteria for ASD (Kaufmann et al., 2017). The FXS boys group showed a marginally significant reduction in AE in frontal and central compared to TD boys. The flatter slope was caused by an increase in higher frequencies, such as gamma power. The increased gamma was found to be correlated with better language abilities. The aperiodic offset, another part of the aperiodic component, did not show significant differences between groups. An EEG study of females with Rett Syndrome found a steeper aperiodic slope, with higher power in low frequency bands (delta, theta) and lower power in middle frequency bands, compared to TD girls (Roche et al., 2019). The steeper slope was associated with lower cognitive abilities. Levin et al. (2020) analyzed

resting-state EEG scans about a week apart in ASD and TD children using the toolbox described in Donoghue et al. (2020). While the study generally demonstrates test-retest reliability of the power spectrum and aperiodic activity, they suggest that changes in these measures may arise from individual changes, such as mood, task, and epileptic activity. It is important to note that the slope was stable across the two scans in the ASD participants, but less so in the TD group, without a clear explanation of the cause.

The lack of neural biomarkers limits the understanding of ASD. E:I imbalance is one potential biomarker for ASD and has historically been difficult to study in humans due to lack of non-invasive methods. Recent research has highlighted the potential of HE and AE as measurements of E:I activity. The current study examined HE from rs-fMRI and AE from rs-MEG in ASD and TD adolescents. It was hypothesized that HE and AE would reflect an increase in the E:I ratio in ASD adolescents compared to the TD group. In addition to understanding differences between ASD and TD groups on measures of E:I, the study also aimed to understand the relationship between HE and AE, as well as their relationship with ASD symptoms. We hypothesized HE and AE would be significantly correlated with each other and with measures of ASD symptomology.

Methods

Participants

Individuals with ASD and typically developing peers (aged 12-21 years) were recruited to participate in the current study. A total of 156 ASD and 120 TD individuals were screened. See supplement for information on exclusionary criteria. For fMRI analyses, 34 ASD and 28 TD were included (Table 3.1). Twelve ASD participants were taking psychotropic medications at the time of the study and 14 ASD participants reported additional psychological diagnoses (ADHD: 3; anxiety: 7; depression: 5; multiple comorbidities: 1) (Supplemental Table S3.1). For MEG

analyses, 33 ASD and 22 TD participants were included (Table 3.2). Thirteen ASD participants were taking psychotropic medications and 17 reported additional psychological diagnoses (ADHD: 6; anxiety: 8; depression: 6; multiple comorbidities: 3) (Supplemental Table S3.1). 28 ASD and 20 TD participants were eligible based on all inclusionary criteria and had useable neuroimaging data for both fMRI and MEG scans, and were thus included in fMRI-MEG correlation analyses (Table 3.3). Eleven ASD participants were taking psychotropic medications at the time of the time and 13 reported additional psychological diagnoses (ADHD: 3; anxiety: 6; depression: 6; multiple comorbidities: 2) (Supplemental Table S3.1). Adolescents with ASD diagnoses were evaluated using the Autism Diagnostic Observation Schedule, 2nd Edition (ADOS-2) (Lord et al., 2012) and parents completed the Autism Diagnostic Interview-Revised (ADI-R) (Rutter et al., 2003). Expert clinical judgement was also used to confirm that all adolescents in the ASD group met DSM-5 criteria (American Psychiatric Association, 2013).

Experimental design

Although the current paper focuses on resting-state data, participants were screened and inducted into the research study based on qualifications necessary for completion of a lexicosemantic decision task that was completed during fMRI and MEG task-based scans. Results from fMRI and MEG task scans have been previously reported on (Wilkinson et al., 2022; You et al., 2021, 2023). Participants were required to have at least a 6th-grade reading level based on the Word Reading subtest of the Wechsler Individual Achievement Test, 3rd Edition (WIAT-III) to ensure they could read the words presented as part of the task (Wechsler, 2009). Additional assessments that were completed by all ASD and TD participants include the Edinburgh Handedness Inventory (Oldfield, 1971), Wechsler Abbreviated Scale of Intelligence, 2nd Edition (WASI-II) (Wechsler, 2011), Beery-Buktenica Developmental Test of Visual-Motor

Integration, 6th Edition (Beery VMI-6) (Beery et al., 2010), and Clinical Evaluation of Language Fundamentals, 5th Edition (CELF-5) (Semel et al., 2013).

Participants completed a mock MRI scan to become accustomed to the scanning environment and to help reduce motion during the scan. The environment of the mock and actual MRI scans was set up to reduce motion and make participants as comfortable as possible. Blankets, ear plugs, and cushions were provided. Scan operators frequently checked in with the individuals throughout the scans. The MEG scanning environment was equally attempted to be made as comfortable as possible. After a successful mock MRI scan was completed, participants completed MEG and MRI scans on two different days. The order of MEG and MRI scans were counterbalanced amongst participants. Most participants completed both scans within 150 days (mean = 58.47 days). One ASD and one TD completed scans outside of that time frame (ASD: 174 days, TD: 252 days). During the resting-state fMRI and "eyes open" condition for the resting-state MEG scans, individuals were instructed to stare at a white cross ("+") on a black screen. The fMRI resting-state scan lasted 6-minutes. The MEG resting-state scan alternated between two minutes of eyes open and two minutes of eyes closed activity.

MRI acquisition and processing

MRI scans were completed at the UCSD Center for fMRI on a General Electric Discovery MR750 3.0 Tesla Scanner (GE Healthcare, Milwaukee, WI) paired with a Nova Medical 32-channel head coil. Structural scans used a Fast Spoiled Gradient Recalled T1-weighted sequence (TR: 8.136 ms; TE: 3.172 ms; flip angle: 8°, FOV: 25.6 cm; acquisition matrix: 256x256; slices: 172; voxel size: 1 mm^3, duration: 5 min). Functional scans were acquired using a multi-echo simultaneous multi-slice (MESMS) T2*-weighted echo planar imaging (EPI) sequence (volumes: 340; TR: 1250 ms; TEs: 13.2, 30.3, 47.4 ms; flip angle: 60°,

FOV: 21.6 cm; acquisition matrix: 72x36; acceleration factor[R]: 2; slices: 54; voxel size: 3 mm^3). The first 9 volumes were discarded to allow for equilibrium. The MESMS protocol was utilized to obtain greater signal-to-noise ratio, as it simultaneously acquires slices at multiple echo times (Kundu et al., 2013, 2013; Olafsson et al., 2015). The majority of participants were scanned under 1250 TR protocol. However, 10 of the initial participants were scanned using a different protocol that included 1100 TR and 45 slices. Preprocessing and analysis of rs-fMRI data were completed with AFNI (Version 19.0.00), FSL (Version 5.0), and MATLAB (2013b). For all echo times, EPI was corrected for susceptibility-induced distortions using FSL's TOPUP tool which involves two spin-echo acquisitions with opposing phase encoding directions (Smith et al., 2004). Each functional volume was aligned to the middle volume using rigid-body realignment in AFNI. The root mean square difference (RMSD) of the six motion parameters of the 30.3 ms echo time data was used to calculate head motion. EPIs were optimally combined using previously reported methodology (Kundu et al., 2013). Multi-echo ICA (ME-ICA), a superior denoising metho that removes non-BOLD components from the BOLD signal, was conducted using meica.py (https://github.com/ME-ICA/me-ica). Functional and structural scans were registered with FSL FLIRT. Scans were reoriented to MNI-152 space with FNIRT. 3dBlurToFWHM was used in AFNI for spatial smoothing, using a Gaussian kernel of 6mm FWHM. A Butterworth filter was used in MATLAB with a low-pass filter of 0.008 Hz and a high-pass filter of 0.08 Hz.

MEG acquisition and processing

MEG scans were completed at the UCSD Radiology Imaging Laboratory using a whole-head Neuromag Vectorview system (Elekta AB, Stockholm, Sweden), using 204 planar gradiometers (102 pairs). Fiduciary points (naison and periauricular points), head position

indicator coils, and various random points on the scalp were digitized using a 3Space Isotrak II (Poolhemus Inc., Colchester, VT). Signal acquisition was continuous, at a sampling rate of 1000 Hz with minimal filtering (0.1 to 300 Hz). Source modeling was completed using MNE Python to combine structural MRI data with the MEG signal (Gramfort et al., 2013). BEM surfaces were created from MRI scans using the watershed algorithm (Gramfort et al., 2013). MRI and MEG scans were then coregistered for each participant using MNE Python. Inverse solutions were computed using the dSPM method. Source estimates were morphed to fsaverage space.

Data extraction and analysis

The Human Connectome Project Multi-Modal Parcellation version 1 (HCP-MMP1) parcellation was utilized for both fMRI and MEG scans, which contains 180 regions per hemisphere (Glasser et al., 2016). The HE was calculated from rs-fMRI using the nonfractal toolbox (https://github.com/wonsang/nonfractal) used in Trakoshis et al. (2020). HE is estimated through discrete wavelet transform and uses maximum likelihood estimation on the rs-fMRI timeseries. The aperiodic exponent was calculated from rs-MEG using NeuroDSP and FOOOF packages (Cole et al., 2019; Donoghue et al., 2020). The power spectral density (PSD) was first computed for each HCP atlas region for each participant using NeuroDSP. PSD data were then interpolated to remove line noise artifact. The aperiodic exponents were estimated using FOOOF package for each participant for each HCP region. A generalized linear model (GLM) analysis was used to determine the relationship between HE (dependent variable) and age and group (ASD vs. TD), controlling for rs-fMRI RMSD. A similar GLM analysis was completed for AE; rs-fMRI RMSD was not used as a control variable. Pearson partial correlations, controlling for rs-fMRI RMSD, were used to analyze the relationship between HE and ASD symptomology. Similarly, Pearson correlations were used to analyze the relationship between AE and ASD

symptomology. Lastly, Pearson partial correlations, controlling for age and rs-fMRI RMSD, were used to analyze the relationship between rs-fMRI HE and rs-MEG AE.

Results

rs-fMRI Hurst exponent

A GLM analysis was conducted for each ROI to understand the relationship between the HE (dependent variable) with group (ASD vs. TD) and age, as well as the group-by-age interaction (Table 3.4, Figure 3.1). RMSD was included as a covariate in the model to control for head motion. While none of the Group or Group-by-Age interaction effects remained significant after FDR correction, results reported below are significant pre-correction. The GLM revealed a main effect of Group on HE for left premotor, medial frontal, operculum, superior parietal, superior temporal, and auditory regions and right inferior frontal, operculum, insula, auditory, and inferior parietal regions, with greater HE seen in the ASD group compared to the TD group when age and RMSD were included in the model. The ASD group was found to have a reduced HE compared to the TD group in right medial prefrontal and posterior cingulate regions. Group-by-Age interaction effects were also found as a result of the model across a number of regions, with varied patterns of HE increasing and decreasing with age for ASD and TD groups (Table 3.4, Figure 3.1). HE in the ASD group decreased with age, while HE increased in the TD group, in the left middle frontal and superior parietal regions and right inferior frontal, opercular, auditory, and inferior parietal regions. HE in the ASD group remained stable with age, while HE increased in the TD group in the left superior temporal regions. HE increased with age in the ASD group and decreased in the TD group for the right medial prefrontal region. HE was observed to decrease with age in both groups in the right posterior cingulate, with significantly greater decreases with age in the TD group.

Pearson partial correlations, controlling for rs-fMRI RMSD, were conducted to understand the relationship between rs-fMRI HE and ASD symptomology (Table 3.5). Correlations did not remain significant after FDR correction, but pre-correction results are reported here. The ADOS-2 Total score positively correlated with HE in the left auditory, superior parietal, posterior cingulate, and middle temporal regions, and right premotor, inferior parietal, lateral temporal and superior frontal regions. The ADOS-2 Total score negatively correlated with HE in the left dorsolateral prefrontal and right hippocampal regions. Pearson partial correlations were also examined between HE and the SRS-2 Total score, controlling for rs-fMRI RMSD. The SRS-2 Total score positively correlated with HE in the left frontal opercular and right premotor, superior parietal, frontal opercular, and insular regions. The SRS-2 Total score negatively correlated with HE in the left lateral temporal and right middle cingulate, prefrontal, orbitofrontal, auditory, and superior temporal regions.

MEG aperiodic exponent

A GLM analysis with AE as the dependent variable and group (ASD vs. TD) and age as the independent variables revealed that AE was greater in the ASD group for all regions with a group difference (Table 3.6, Figure 3.1). However, none of the Group or Group-by-Age interaction effects remained significant after FDR correction. Increases in AE are representative of an increasingly flatter slope in the context of the power-frequency spectrum. For all regions with Group-by-Age interaction effects, AE decreased (i.e., flattened) with age in the ASD group, compared to the TD group which displayed variable patterns by region.

Correlations were used to analyze the relationship between rs-MEG AE and ASD symptomology (Table 3.7). The ADOS-2 Total score was positively correlated with AE in the left orbitofrontal, auditory, premotor, prefrontal, inferior frontal, and insular regions and right

prefrontal, anterior cingulate, and visual regions. The SRS-2 Total score was correlated with AE in the left temporal and right posterior cingulate regions. Correlations with neither the ADOS-2 Total score nor the SRS-2 Total score were not significant after FDR correction.

fMRI Hurst exponent & MEG aperiodic exponent correlations

Pearson partial correlations controlling for age and rs-fMRI RMSD were used to understand the relationship between rs-fMRI HE and rs-MEG AE (Table 3.8, Figure 3.2). Pearson partial correlations were conducted at the whole-group level, rather than split by ASD and TD groups. Correlations were in the positive direction for left prefrontal and right intraparietal, insula, and middle temporal regions, and in the negative direction for left prefrontal, orbitofrontal, superior temporal, lateral temporal, and visual regions and the right posterior cingulate, superior parietal, superior temporal, and lateral temporal regions. After FDR correction, the negative correlation between HE and AE in the right superior temporal region remained significant (FDR-adjusted $p = 0.027$).

Supplementary analyses

Supplementary analyses were completed with a male-only subset of the overall dataset due to there not being enough females in the dataset to examine gender differences. The overall pattern remained similar when the females were removed from the group. See Supplementary Materials for additional analyses (Supplemental Tables S3.2-S3.9).

Discussion

The excitation-inhibition (E:I) ratio reflects the balance of excitatory (i.e., glutamate) and inhibitory (i.e., GABA) neurotransmitters in the brain, which is influenced by neurotransmitter quantities, synaptic functioning, and neuronal circuitry in the brain. The E:I ratio is thought to be unbalanced in a variety of psychological disorders including ASD (Bruining et al., 2020; Dani et al., 2005; Mariani et al., 2015; Rubenstein & Merzenich, 2003; Smith et al., 2018; Trakoshis et

al., 2020). Historically it has been difficult to measure E:I due to the invasive nature required to measure neurotransmitter and neural circuity activity. Magnetic resonance spectroscopy (MRS) has been utilized as a method of measuring the E:I ratio, but findings have been inconsistent (Ajram et al., 2019). The use of MRS is also limited in clinical populations, such as ASD, and children due to it being a time consuming neuroimaging method and that it is prone to high levels of variability and artifacts (Weinberg et al., 2021). Recent research has suggested two measures as noninvasive measures of E:I – the Hurst exponent and the aperiodic exponent which can be measured from rs-fMRI and rs-MEG, two imaging methods that are more conducive for measuring neural activity from clinical populations and youth.

Hurst exponent

HE, considered to be a measure of E:I ratio in the brain (Trakoshis et al., 2020), was found to be greater in the ASD group compared to the TD group in the left premotor, medial frontal, operculum, superior parietal, superior temporal, and auditory regions and right inferior frontal, operculum, insula, auditory, and inferior parietal regions. HE showed a trend of being reduced in the ASD group compared to the TD group in the right medial prefrontal and posterior cingulate regions. However, HE group differences were not significant after statistical correction. Group-by-Age interaction effects showed that HE in the ASD group decreased with age, while HE increased in the TD group, in the left middle frontal and superior parietal regions and right inferior frontal, opercular, auditory, and inferior parietal regions. HE in the ASD group remained stable with age, while HE increased in the TD group in the left superior temporal regions. HE increased with age in the ASD group and decreased in the TD group for the right medial prefrontal region. HE was observed to decrease with age in both groups in the right posterior cingulate, with greater decreases with age in the TD group.

While the E:I ratio has been extensively studied in ASD, it has been difficult to measure noninvasively or without the use of animal models. The HE, a more modern approach to evaluating the E:I ratio, allows for a noninvasive measurement of this activity. With regard to the E:I ratio, in typically developing individuals, there is greater inhibitory than excitatory activity. In those with ASD, the E:I ratio is unbalanced and suggested to be driven by an increase in excitatory activity. This is reflected in decreased HE (Trakoshis et al., 2020). A recent rs-fMRI study in adults found that HE was atypically decreased in the ASD male group compared to ASD females in the medial prefrontal cortex, suggesting an imbalanced E:I ratio (Trakoshis et al., 2020). The current study analyzed a group of adolescents with ASD that was mostly male, with male-only analyses included in the supplement (Supplemental Tables S2-S9). Compared to the TD group, the ASD group presented with decreased HE in the right medial prefrontal and posterior cingulate regions, suggesting a greater E:I imbalance than the TD adolescents in these areas. However, there were many more regions that demonstrated greater HE in the ASD group than the TD group, which also suggests an imbalance in the E:I ratio compared to the TD group but in the opposite direction such that inhibitory activity increased or excitatory activity decreased substantially to alter the E:I ratio. Alternatively, the TD group may be producing greater excitatory activity in these regions while the ASD group remained stable. While we cannot determine the exact cause of the HE group differences, we can report that there is a difference across a variety of regions with the ASD presenting with both increased and decreased HE compared to the TD group as measured from rs-fMRI.

With both increases and decreases in HE in the ASD group compared to the TD group, it is unsurprising that HE and ASD symptomology were positively correlated in some brain regions and negatively correlated in others. The ADOS-2 Total score was positively correlated with HE

in left early auditory, superior parietal, posterior cingulate, and middle temporal regions and right premotor, superior parietal, posterior cingulate, premotor, inferior parietal, lateral temporal, and superior frontal regions. The ADOS-2 Total score was negatively correlated with HE in the left prefrontal and right parahippocampal regions, such that greater ASD symptoms were associated with decreased HE (i.e., increased E:I imbalance). The SRS-2 Total score was positively correlated with HE in the left operculum and right premotor, superior parietal, operculum, and insular regions . The SRS-2 Total score was negatively correlated with HE in the left lateral temporal and right middle cingulate, prefrontal, orbitofrontal, prefrontal, auditory, and superior temporal regions.

The current study is the first to report on the pattern of HE derived from rs-fMRI in ASD adolescents, compared to TD peers, in specific regions across the whole brain, so it is unclear whether the pattern of both increased and decreased HE across brain regions would be expected. One study measuring the HE from rs-EEG data in 5-to-21-year old males, found two distinct ASD subtypes, one with increased HE across the whole brain and the other with decreased HE compared to the TD group (Bertelsen et al., 2023). Those in the decreased HE subtype showed greater deviation from TD HE than the increased HE group. Interestingly, the decreased HE subtype, which showed greater differences compared to HE in the TD group, revealed no significant correlation with ASD symptomology (i.e, SRS-2 score). This was in contrast to the increased HE group, which showed positive correlations with HE and ASD symptomology.

Aperiodic exponent

AE was found to be significantly greater (i.e., flatter slope) in the ASD group for all regions with group differences. These areas spanned the left somatosensory, motor, cingulate, premotor, parietal, operculum, auditory, temporal, and visual regions and right somatosensory,

motor, premotor, frontal, parietal, cingulate, auditory, operculum, insula, occipital, temporal, visual, and temporo-parieto-occipital regions. Group-by-Age interaction effects revealed that AE decreased (i.e., had a flatter slope) with age in the ASD group. Regions where AE flattened with age in the ASD group include left middle and posterior cingulate, superior and inferior parietal, and visual regions and right somatosensory, motor, premotor, superior and inferior parietal, posterior cingulate, temporal, auditory, operculum, occipital, visual, insula, and temporo-occipital-parietal regions. Within these regions, it appeared that the younger ASD participants looked more similar to the younger TD participants, with equivalent or greater AE. However, older ASD participants showed decreased AE compared to the older TD participants (i.e., flatter slope than TD). Within the range of this study (12-21-year-olds) AE remained relatively stable in the TD participants, and in some regions showed greater AE in the older participants, whereas in the ASD group AE was lower in older participants. Previous research has suggested AE as a noninvasive measurement of the E:I ratio, with lower AE representing a greater E:I ratio (i.e., greater excitatory activity). The current study suggests that the traditional increase in excitatory activity associated with ASD is more prevalent in the mid-teenager years, as compared to the earlier in adolescence.

AE was also found to be significantly correlated with measures of ASD symptomology. The ADOS-2 Total score was positively correlated with AE in the left orbitofrontal, auditory, premotor, prefrontal, inferior frontal, and insula regions and right prefrontal, anterior cingulate, and visual regions. The SRS-2 Total score was significantly correlated with AE in the left lateral temporal and right posterior cingulate regions.

Relationship between Hurst exponent and aperiodic exponent

It is notable that HE and AE displayed significantly different patterns on analyses of group differences and in their relationships with ASD symptomology. This is the first study to directly examine the relationship between these two measures of E:I activity, rs-fMRI HE and rs-MEG AE, in both typically developing individuals and those with ASD. Overall, AE showed a more consistent pattern – regions with group differences always showed greater AE in the ASD group compared to the TD group. Additionally, in regions with Group-by-Age interactions, AE always decreased with age in the ASD group. Lastly, for all regions that were significantly correlated with measures of ASD symptomology, AE was positively correlated with ASD symptomology. In contrast, HE was more variable. In some regions, HE was greater in the ASD group than the TD group, whereas in others it was smaller. There was also an inconsistent pattern for Group-by-Age interaction effects and correlations with ASD symptomology.

Due to the variability in the HE pattern, it was unsurprising to find both positive and negative correlations depending on brain region between HE and AE. rs-fMRI HE and rs-MEG AE were found to be positively correlated across all participants (ASD and TD groups) in the left prefrontal and right intraparietal, insula, middle temporal and visual regions. HE and AE were negatively correlated in the left prefrontal, orbitofrontal, superior temporal, lateral temporal, and visual and right posterior cingulate, superior parietal, superior temporal, and lateral temporal regions.

HE and AE have both been separately proposed as measures of E:I activity, with the use of animal models to support this. Yet, the current study reveals an unclear relationship between the two, with surprisingly few correlations between the two measures. The E:I ratio reflects activity at the neuronal level of the brain (i.e., neurotransmitters, synapse function, neuronal

circuits). MEG is well suited for detecting activity at the neuronal level, due to its high temporal resolution allowing activity to be measured at the millisecond level, and is thought to be a more direct measurement of cortical neuron activity. On the other hand, fMRI has been a neuroimaging modality of choice in the study of ASD for decades, similar to research on other disorders and across many functional domains. It has excellent spatial resolution, but is limited by the slow hemodynamic response (i.e., BOLD signal) and its susceptibility to motion and neurovascular activity. fMRI BOLD signal may not be best suited for measuring E:I activity, which reflects excitatory and inhibitory activity occurring at the neuron level. A combined approach, such as the in current study, that integrates structural MRI data with functional MEG data to be able to measure activity at specific locations in the brain is superior to critically understanding data that requires temporal and spatial information, such as E:I activity. Limitations presented on fMRI may reflect the inconsistent findings of HE as measured from rs-fMRI, in comparison to the consistent AE pattern revealed from rs-MEG data.

Limitations

The current study is the first to compare two measures of E:I activity from ASD and TD adolescents that completed both rs-fMRI and rs-MEG scans and is thus a substantial contribution to the understanding of how HE and AE relate to ASD pathology, as well as how they relate to one another more generally. However, we recognize that there are limitations to this study. First, the sample used in this study for the correlation analyses consists of 24 ASD and 16 TD individuals. There were many requirements to participating in the study, such that individuals needed to read at a 6^{th}-grade level, and had to complete both fMRI and MEG scans. Additionally, data collection was halted by the COVID-19 pandemic. Due to sample size limitations, gender-based analyses were not possible due to the very small number of females in each group. We

recognize this as a limitation due to the few previous studies looking at E:I ratio noting significant gender-based differences in ASD individuals. To accommodate for the small sample size, male-only analyses were run and are provided in the supplement. The pattern remained similar as the whole-group analyses, however this is likely due to the whole-group analyses consisting largely of males. Future studies should aim to replicate the current analyses with a larger sample, as well as to examine variables by gender. While we studied the relationship between HE and AE measurements with ASD symptomology, we recognize that individuals in our study had to be able to sit through neuropsychological assessments and both MRI and MEG scans which lasted about an hour. The nature of the study allows for a limited range of the autism spectrum to be studied. Attempts were made to include 'lower-functioning' ASD participants in the study with the help of multiple mock scans to aid in familiarity with the scanning environment. While some of the individuals were able to participate in the study, we acknowledge that our ASD sample mostly consists of 'high-functioning' individuals with ASD. The make-up of the ASD group may have influenced correlations with ASD symptomology, such that there are less individuals at the extreme end. We suggest that future studies aim to measure the E:I ratio in individuals with greater ASD severity in order to better understand the relationship of the E:I ratio with ASD symptomology. Lastly, we acknowledge that E:I activity is typically studied in animal models due to the invasive nature to best capture neurotransmitter activity. Use of HE and AE as noninvasive representations of E:I activity is new and there is minimal evidence supporting these measurements. We aim to add to the literature studying these measures in individuals with ASD, but recognize that their relationship to E:I activity is still being understood.

Conclusion

Two measures of E:I activity were compared in the current study using rs-fMRI and rs-MEG. rs-fMRI HE showed both increases and decreases in the ASD group compared to the TD group, and showed mixed correlations with ASD symptomology. rs-MEG AE was greater in the ASD group compared to the TD group and was positively correlated with ASD symptomology. There was a lack of a clear relationship between rs-fMRI HE and rs-MEG AE across brain regions, with very few correlations. Despite HE and AE both measuring E:I activity, there are noteable differences between the two measures as it relates to ASD and TD individuals, suggesting they are measuring neural activity and the E:I ratio differently.

Acknowledgements

Chapter 3, in full, is being prepared for submission for publication. Wilkinson, M., Jao Keehn, R.J., You, Y., Preston, M., Marinkovic, K., Müller, R-A., Voytek, B., Linke, A.C. The dissertation author was the primary investigator and author of this paper.

Table 3.1 Participant demographics for fMRI analyses

Note: Means, standard deviations (SD), and ranges for each group. Chi-square tests (gender, handedness) and *t*-tests were performed to determine if groups were significantly different on demographic variables. Non-standard degrees of freedom are attributed to Levene's test for homogeneity of variance, and thus reject the null hypotheses of equal variance.

ASD = autism spectrum disorder
RMSD = root mean square difference
TD = typically developing

	ASD (n=34)		**TD (n=28)**			**χ2 (df)**	***p***
Gender	24 male, 10 female		21 male, 7 female			0.15 (1)	0.70
Handedness	32 right, 2 left		25 right, 3 left			0.49 (1)	0.49
	Mean (SD)	**Range**	**Mean (SD)**	**Range**	**Hedges' g**	***t*-stat (df)**	***p***
Age (years)	15.92 (2.37)	12.25-20.00	15.12 (1.89)	12.33-21.42	0.36	1.44 (60)	0.16
MRI RMSD	0.08 (0.03)	0.03-0.15	0.07 (0.03)	0.02-0.16	0.40	1.61 (60)	0.11
WASI-II							
Full Scale IQ	104.53 (16.81)	59-136	111.86 (11.96)	88-135	-0.49	1.94 (60)	0.06
Verbal IQ	104.06 (16.59)	68-134	110.82 (12.16)	85-135	-0.45	1.80 (60)	0.08
Non-Verbal IQ	105.32 (19.05)	54-156	109.93 (11.89)	80-128	-0.28	1.16 (56.22)	0.25
ADOS-2							
Total	11.26 (3.78)	6-20	--	--	--	--	--

Table 3.2 Participant demographics for MEG analyses

Note: Means, standard deviations (SD), and ranges for each group. Chi-square tests (gender, handedness) and *t*-tests were performed to determine if groups were significantly different on demographic variables. * denotes $p \leq 0.05$

ASD = autism spectrum disorder
TD = typically developing

	ASD (n=33)		**TD (n=22)**			**χ2 (df)**	***p***
Gender	26 male, 7 female		16 male, 6 female			0.27 (1)	0.60
Handedness	30 right, 2 left, 1 ambidextrous		19 right, 3 left			1.53 (2)	0.47
	Mean (SD)	**Range**	**Mean (SD)**	**Range**	**Hedges' g**	***t*-stat (df)**	***p***
Age (years)	15.58 (2.33)	12.25-20	14.97 (2.00)	12.33-21.42	0.27	1.00 (53)	0.32
WASI-II							
Full Scale IQ	105.61 (13.61)	77-136	113.68 (13.13)	88-140	-0.59	2.19 (53)	0.03*
Verbal IQ	104.45 (14.13)	76-131	112.73 (12.92)	85-135	-0.60	2.20 (53)	0.03*
Non-Verbal IQ	107.12 (16.55)	75-156	111.27 (13.13)	80-138	-0.27	0.99 (53)	0.33
ADOS-2							
Total	10.67 (3.42)	6-20	--	--	--	--	--

Table 3.3 Participant demographics for fMRI-MEG correlations

Note: Means, standard deviations (SD), and ranges for each group. Chi-square tests (gender, handedness) and *t*-tests were performed to determine if groups were significantly different on demographic variables.

ASD = autism spectrum disorder
RMSD = root mean square difference
TD = typically developing

	ASD (n=28)		**TD (n=20)**			**χ2 (df)**	***p***
Gender	21 male, 7 female		15 male, 5 female			0.11 (1)	0.74
Handedness	27 right, 1 left		18 right, 2 left			0.82 (1)	0.36
	Mean (SD)	**Range**	**Mean (SD)**	**Range**	**Hedges' g**	***t*-stat (df)**	***p***
Age (years)	15.95 (2.33)	12.25-20	15.04 (2.07)	12.33-21.42	0.40	1.40 (46)	0.17
MRI RMSD	0.08 (0.03)	0.03-0.15	0.07 (0.03)	0.02-0.16	0.35	1.22 (46)	0.23
WASI-II							
Full Scale IQ	105.32 (14.50)	77-136	111.95 (12.14)	88-132	-0.48	1.67 (46)	0.10
Verbal IQ	104.96 (14.82)	76-131	111.35 (12.44)	85-133	-0.45	1.57 (46)	0.12
Non-Verbal IQ	106.39 (17.67)	75-156	109.50 (12.06)	80-128	-0.20	0.68 (46)	0.50
ADOS-2							
Total	10.36 (3.25)	6-20	--	--	--	--	--

Table 3.4 GLM analysis results for rs-fMRI Hurst exponent

Note: GLM analysis results for ROIs with significant main effect of Group and/or significant Group-by-Age interaction for HE. * denotes $p \leq 0.05$, ** denotes $p \leq 0.01$

ROI		Estimate	SE	*t*	*p*	FDR-adjusted *p*	Estimate	SE	*t*	*p*	FDR-adjusted *p*
		Main Effect of Group					Group x Age Interaction				
L 6v	Premotor	0.189	0.093	2.026	0.048*	0.961	--	--	--	--	--
L 8Av	Middle frontal gyrus	0.233	0.101	2.312	0.024*	0.961	-0.015	0.007	-2.37	0.021*	0.933
L FOP1	Frontal opercular	0.221	0.107	2.067	0.043*	0.961	--	--	--	--	--
L LIPd	Superior parietal	0.269	0.121	2.213	0.039*	0.961	-0.017	0.008	-2.081	0.042*	0.933
L STV	Superior temporal	0.225	0.095	2.357	0.022*	0.961	-0.014	0.006	-2.206	0.031*	0.933
L TA2	Auditory	0.227	0.112	2.036	0.046*	0.961	--	--	--	--	--
R a47r	Inferior frontal	0.173	0.082	2.115	0.039*	0.961	-0.011	0.005	-2.164	0.035*	0.933
R FOP1	Frontal opercular	0.216	0.092	2.343	0.023*	0.961	-0.014	0.006	-2.359	0.022*	0.933
R Ig	Insula	0.240	0.110	2.183	0.033*	0.961	--	--	--	--	--
R OP1	Posterior opercular	0.266	0.112	2.378	0.021*	0.961	-0.016	0.007	-2.186	0.033*	0.933
R PFcm	Early auditory	0.247	0.102	2.379	0.021*	0.961	-0.015	0.007	-2.356	0.022*	0.933
R PFop	Inferior parietal	0.249	0.098	2.550	0.014*	0.961	-0.016	0.006	-2.485	0.016*	0.933
R pOFC	Medial prefrontal	-0.222	0.102	-2.179	0.034*	0.961	0.017	0.007	2.623	0.011*	0.933
R POS2	Posterior cingulate	-0.232	0.105	-2.220	0.030*	0.961	0.015	0.007	2.281	0.026*	0.933
R RI	Early auditory	0.231	0.095	2.429	0.018*	0.961	-0.014	0.006	-2.288	0.026*	0.933
R TA2	Auditory	0.312	0.112	2.794	0.007**	0.961	-0.020	0.007	-2.840	0.006**	0.933

Table 3.5 Pearson partial correlations for rs-fMRI HE and ASD symptomology (ADOS-2 Total & SRS-2 Total)

Note: Significant Pearson partial correlations for rs-fMRI and ADOS-2 Total and SRS-2 Total scores for the ASD group. * denotes $p \leq 0.05$, ** denotes $p \leq 0.01$

	ROI	*r*	*p*	FDR-adjusted *p*
ADOS-2 Total				
L 52	Early auditory	0.345	0.049*	0.873
L 7AL	Superior parietal	0.347	0.048*	0.873
L 9a	Dorsolateral prefrontal	-0.383	0.028*	0.873
L DVT	Posterior cingulate	0.394	0.023*	0.873
L FST	Middle temporal	0.348	0.047*	0.873
L PH	Middle temporal	0.521	0.002**	0.936
R 55b	Premotor	0.431	0.012*	0.873
R 7Am	Superior parietal	0.409	0.018*	0.873
R DVT	Posterior cingulate	0.414	0.017*	0.873
R FEF	Premotor	0.522	0.002**	0.337
R PFt	Inferior parietal	0.351	0.045*	0.873
R PHA1	Parahippocampal	-0.386	0.027*	0.873
R PHT	Lateral temporal	0.377	0.031*	0.873
R SFL	Superior frontal language area	0.359	0.040*	0.873
SRS-2 Total				
L FOP4	Frontal opercular	0.409	0.020*	0.999
L TGv	Lateral temporal	-0.352	0.049*	0.999
R 24dv	Middle cingulate	-0.391	0.027*	0.999
R 6r	Premotor	0.465	0.007**	0.999
R 7PL	Superior parietal	0.456	0.009**	0.999
R d32	Prefrontal	-0.376	0.033*	0.999
R FOP4	Frontal opercular	0.373	0.036*	0.999
R MI	Insula	0.366	0.039*	0.999
R OFC	Orbitofrontal	-0.461	0.008**	0.999
R p32	Prefrontal	-0.400	0.023*	0.999
R STSva	Auditory association	-0.398	0.024*	0.999
R STV	Superior temporal visual area	-0.366	0.040*	0.999

Table 3.6 GLM analysis results for rs-MEG aperiodic exponent

Note: GLM analysis results for ROIs with significant main effect of Group and/or significant Group-by-Age interaction for AE. * denotes $p \leq 0.05$, ** denotes $p \leq 0.01$

ROI		Estimate	SE	*t*	*p*	FDR-adjusted *p*	Estimate	SE	*t*	*p*	FDR-adjusted *p*
		Main Effect of Group					Group x Age Interaction				
L 5L	Middle cingulate	1.639	0.642	2.552	0.014*	0.148	-0.103	0.042	-2.458	0.017*	0.188
L 7PC	Superior parietal	1.294	0.573	2.259	0.028*	0.173	-0.082	0.037	-2.186	0.033*	0.188
L 7PL	Superior parietal	1.726	0.611	2.824	0.007**	0.148	-0.114	0.040	-2.857	0.006**	0.183
L 23c	Posterior cingulate	1.463	0.578	2.532	0.015*	0.149	-0.097	0.039	-2.566	0.013*	0.183
L 24dv	Middle cingulate	1.445	0.621	2.326	0.024*	0.169	-0.094	0.041	-2.313	0.025*	0.189
L 31pv	Posterior cingulate	1.276	0.533	2.395	0.020*	0.162	-0.079	0.035	-2.281	0.027*	0.189
L IP2	Inferior parietal	1.221	0.478	2.552	0.014*	0.148	-0.088	0.031	-2.815	0.007**	0.183
L IPS1	Dorsal visual	1.169	0.474	2.465	0.017*	0.158	-0.077	0.031	-2.484	0.016*	0.183
L LIPd	Superior parietal	1.052	0.480	2.131	0.033*	0.175	-0.070	0.031	-2.237	0.030*	0.189
L LIPv	Intraparietal	1.213	0.545	2.225	0.031*	0.175	-0.077	0.036	-2.170	0.035*	0.189
L MIP	Superior parietal	1.349	0.659	2.046	0.046*	0.188	-0.093	0.043	-2.159	0.036*	0.189
L OP2.3	Posterior opercular	1.218	0.567	2.149	0.036*	0.178	-0.077	0.037	-2.083	0.042*	0.195
L p24pr	Prefrontal	1.173	0.581	2.017	0.049*	0.188	--	--	--	--	--
L PFm	Inferior parietal	1.049	0.517	2.030	0.048*	0.188	-0.073	0.034	-2.148	0.037*	0.189
L PGi	Inferior parietal	1.293	0.585	2.209	0.032*	0.175	-0.080	0.038	-2.092	0.042*	0.195
L PI	Insula	1.267	0.630	2.011	0.050*	0.188	--	--	--	--	--
L PoI1	Insula	1.407	0.692	2.033	0.047*	0.241	--	--	--	--	--
L SCEF	Supplementary / cingulate eye field	1.524	0.640	2.380	0.021*	0.162	-0.099	0.042	-2.369	0.022*	0.189
L STSdp	Superior temporal	1.082	0.536	2.017	0.049*	0.188	--	--	--	--	--
L STSvp	Superior temporal	1.439	0.561	2.564	0.013*	--	-0.087	0.037	-2.387	0.021*	0.189
L V1	Primary visual	1.269	0.527	2.406	0.020*	0.162	-0.086	0.034	-2.511	0.015*	0.183
L V3B	Dorsal visual	1.200	0.556	2.159	0.036*	0.178	-0.083	0.036	-2.275	0.027*	0.189
L V7	Dorsal visual	1.183	0.572	2.070	0.044*	0.188	-0.081	0.037	-2.168	0.035*	0.189
L VIP	Intraparietal	1.319	0.614	2.147	0.037*	0.178	-0.088	0.040	-2.198	0.033*	0.189
R 1	Somatosensory / motor	1.290	0.604	2.134	0.038*	--	--	--	--	--	--
R 2	Somatosensory / motor	1.052	0.505	2.083	0.042*	0.188	--	--	--	--	--
R 3a	Somatosensory / motor	1.726	0.508	3.396	0.001***	0.148	-0.108	0.033	-3.255	0.002**	0.183
R 3b	Primary sensory	1.566	0.551	2.840	0.006**	0.148	-0.099	0.036	-2.754	0.008**	0.183
R 6d	Premotor	1.128	0.561	2.009	0.050*	0.188	--	--	--	--	--
R 6mp	Middle cingulate	1.311	0.619	2.117	0.039*	0.186	--	--	--	--	--
R 6v	Premotor	1.512	0.617	2.452	0.018*	0.159	-0.097	0.040	-2.405	0.020*	0.189
R 7AL	Superior parietal	1.460	0.570	2.561	0.013*	0.148	-0.097	0.037	-2.598	0.012*	0.183
R 7Am	Superior parietal	1.583	0.671	2.359	0.022*	0.162	-0.098	0.044	-2.239	0.030*	0.189
R 7PL	Superior parietal	1.273	0.630	2.021	0.049*	0.188	-0.089	0.041	-2.155	0.036*	0.189

Table 3.6 GLM analysis results for rs-MEG aperiodic exponent, Continued

ROI		Estimate	SE	*t*	*p*	FDR-adjusted *p*	Estimate	SE	*t*	*p*	FDR-adjusted *p*
		Main Effect of Group					Group x Age Interaction				
R 7Pm	Posterior cingulate	1.649	0.608	2.710	0.009**	0.148	-0.111	0.040	-2.809	0.007**	0.183
R 8Av	Dorsolateral prefrontal	1.351	0.602	2.244	0.029*	0.173	-0.084	0.039	-2.144	0.037*	0.189
R 23d	Posterior cingulate	1.260	0.583	2.162	0.035*	0.178	-0.079	0.038	-2.082	0.042*	0.195
R 43	Premotor	1.562	0.531	2.944	0.005**	0.148	-0.093	0.035	-2.672	0.010**	0.183
R 52	Temporal	1.804	0.616	2.927	0.005**	0.148	-0.115	0.040	-2.853	0.006**	0.183
R 55b	Premotor	1.291	0.597	2.161	0.035*	0.178	-0.082	0.039	-2.097	0.041*	0.195
R A1	Primary auditory	1.133	0.428	2.650	0.011*	0.148	-0.065	0.028	-2.324	0.024*	0.189
R A4	Auditory	1.102	0.533	2.070	0.044*	0.188	--	--	--	--	--
R A5	Auditory	1.136	0.557	2.039	0.047*	0.188	--	--	--	--	--
R DVT	Posterior cingulate	1.144	0.526	2.174	0.034*	0.178	-0.076	0.034	-2.222	0.031*	0.189
R FEF	Frontal eye fields	1.587	0.593	2.678	0.010**	0.148	-0.096	0.039	-2.491	0.016*	0.183
R FFC	Ventral visual	1.693	0.708	2.393	0.020*	0.162	-0.104	0.046	-2.245	0.029*	0.189
R FOP1	Frontal operculum	1.267	0.538	2.354	0.023*	0.162	-0.078	0.035	-2.212	0.031*	0.189
R FOP2	Frontal operculum	1.246	0.497	2.507	0.015*	0.150	-0.076	0.032	-2.34	0.023*	0.189
R FST	Lateral occipital	1.717	0.597	2.877	0.006**	0.148	-0.108	0.039	-2.765	0.008*	0.183
R H	Hippocampus	2.107	0.754	2.795	0.007**	0.148	-0.130	0.049	-2.637	0.011*	0.183
R Ig	Insula	1.202	0.510	2.358	0.022*	0.162	-0.073	0.033	-2.203	0.032*	0.189
R IP0	Inferior parietal	1.394	0.512	2.722	0.009**	0.148	-0.089	0.033	-2.651	0.011*	0.183
R IP1	Inferior parietal	1.415	0.507	2.792	0.007**	0.148	-0.092	0.033	-2.777	0.008**	0.183
R IPS1	Dorsal visual	1.079	0.472	2.286	0.026*	0.173	-0.070	0.031	-2.285	0.027*	0.189
R Lbelt	Early auditory	1.086	0.470	2.310	0.025*	0.172	-0.063	0.031	-2.056	0.045*	0.205
R LIPv	Intraparietal	1.221	0.542	2.253	0.029*	0.173	-0.080	0.035	-2.261	0.028*	0.189
R LO2	Lateral occipital	1.481	0.572	2.588	0.013*	0.148	-0.096	0.037	-2.569	0.013*	0.183
R LO3	Lateral occipital	1.134	0.547	2.071	0.043*	0.188	-0.077	0.036	-2.148	0.037*	0.189
R MT	Middle temporal	1.097	0.500	2.195	0.033*	0.175	-0.071	0.033	-2.18	0.034*	0.189
R OP2.3	Posterior operculum	1.008	0.443	2.274	0.027*	0.173	-0.066	0.029	-2.269	0.028*	0.189
R OP4	Posterior operculum	1.036	0.505	2.051	0.046*	0.188	--	--	--	--	--
R Pbelt	Auditory	1.160	0.455	2.546	0.014*	0.148	-0.068	0.030	-2.278	0.027*	0.189
R PCV	Precuneus visual	1.461	0.524	2.787	0.007**	0.148	-0.092	0.034	-2.678	0.01**	0.183
R PFm	Inferior parietal	1.175	0.510	2.304	0.025*	0.172	-0.073	0.033	-2.183	0.034*	0.189
R PGp	Inferior parietal	1.750	0.593	2.950	0.005**	0.148	-0.117	0.039	-3.030	0.004**	0.183
R PGs	Inferior parietal	1.278	0.561	2.276	0.027*	0.173	-0.082	0.037	-2.232	0.030*	0.189
R PH	Middle temporal	1.581	0.705	2.242	0.029*	0.173	-0.097	0.046	-2.097	0.041*	0.195
R PHA1	Parahippocampal	1.584	0.778	2.036	0.047*	0.188	--	--	--	--	--

Table 3.6 GLM analysis results for rs-MEG aperiodic exponent, Continued

ROI		Estimate	SE	*t*	*p*	FDR-adjusted *p*	Estimate	SE	*t*	*p*	FDR-adjusted *p*
		Main Effect of Group					Group x Age Interaction				
R PHA2	Parahippocampal	1.756	0.795	2.208	0.032*	0.175	-0.106	0.052	-2.034	0.047*	0.212
R PHT	Lateral temporal	1.473	0.512	2.879	0.006**	0.148	-0.094	0.033	-2.816	0.007**	0.183
R PI	Insula	1.300	0.580	2.243	0.029*	0.173	--	--	--	--	--
R PoI1	Posterior insula	1.463	0.668	2.190	0.033*	0.175	-0.092	0.044	-2.101	0.041*	0.195
R PreS	Presubiculum	1.811	0.711	2.545	0.014*	0.148	-0.111	0.046	-2.387	0.021*	0.189
R ProS	Prostriate area	1.929	0.703	2.744	0.008**	0.148	-0.121	0.046	-2.63	0.011*	0.183
R RI	Insula	1.165	0.438	2.660	0.010**	0.148	-0.0715	0.029	-2.499	0.016*	0.183
R STSdp	Superior temporal	0.963	0.465	2.069	0.044*	0.188	--	--	--	--	--
R STSvp	Superior temporal	1.438	0.503	2.862	0.006**	0.148	-0.088	0.033	-2.686	0.01*	0.183
R STV	Superior temporal visual	1.388	0.482	2.879	0.006**	0.148	-0.088	0.031	-2.805	0.007**	0.183
R TA2	Superior temporal	1.468	0.519	2.828	0.007**	0.148	-0.080	0.034	-2.374	0.021*	0.189
R TE1m	Lateral temporal	1.454	0.557	2.611	0.012*	0.148	-0.088	0.036	-2.426	0.019*	0.189
R TE1p	Lateral temporal	1.137	0.512	2.222	0.031*	0.175	-0.070	0.033	-2.104	0.040*	0.195
R TE2p	Lateral temporal	1.646	0.657	2.505	0.016*	0.150	-0.101	0.043	-2.356	0.022*	0.189
R TPOJ1	Temporo-parieto- occipital junction	1.244	0.472	2.636	0.011*	0.148	-0.075	0.031	-2.449	0.018*	0.188
R TPOJ2	Temporo-parieto- occipital junction	1.502	0.464	3.238	0.002**	0.148	-0.099	0.030	-3.28	0.002**	0.183
R TPOJ3	Temporo-parieto- occipital junction	1.401	0.506	2.768	0.008**	0.148	-0.089	0.033	-2.684	0.01**	0.183
R V1	Primary visual	1.760	0.530	3.322	0.002**	0.148	-0.114	0.035	-3.306	0.002**	0.183
R V2	Early visual	1.401	0.673	2.083	0.042*	0.188	-0.093	0.044	-2.113	0.040*	0.195
R V3	Early visual	1.351	0.553	2.441	0.018*	0.160	-0.092	0.036	-2.547	0.014*	0.183
R V3B	Dorsal visual	1.339	0.553	2.421	0.019*	0.162	-0.094	0.036	-2.611	0.012*	0.183
R V8	Ventral visual	1.528	0.741	2.062	0.044*	0.188	-0.104	0.048	-2.15	0.036*	0.189
R VIP	Superior parietal	1.718	0.688	2.497	0.016*	0.150	-0.113	0.044	-2.504	0.016*	0.183
R VMV1	Ventral visual	1.663	0.643	2.586	0.013*	0.148	-0.109	0.042	-2.593	0.012*	0.183
R VMV2	Ventral visual	1.886	0.604	3.121	0.003**	0.148	-0.117	0.039	-2.967	0.005**	0.183
R VVC	Ventral visual	1.460	0.615	2.376	0.021*	0.162	-0.086	0.040	-2.154	0.036*	0.189

Table 3.7 Pearson partial correlations between rs-MEG AE and ASD symptomology

Note: Significant Pearson partial correlations for rs-MEG AE and ADOS-2 Total and SRS-2 Total scores for the ASD group. * denotes $p \leq 0.05$, ** denotes $p \leq 0.01$.

	ROI	*r*	*p*	FDR-adjusted *p*
ADOS-2 Total				
L 47s	Orbitofrontal	0.354	0.043*	0.594
L 52	Early auditory	0.398	0.022*	0.594
L 6R	Premotor	0.369	0.023*	0.594
L 9.46d	Dorsolateral prefrontal	0.424	0.014*	0.594
L IFSa	Inferior frontal	0.385	0.03*	0.594
L Ig	Insula	0.388	0.026*	0.594
L p47r	Inferior frontal	0.401	0.021*	0.594
L PoI1	Insula	0.379	0.030*	0.594
L PoI2	Insula	0.399	0.021*	0.594
R 8Ad	Dorsolateral prefrontal	0.359	0.040*	0.594
R 8BL	Dorsolateral prefrontal	0.370	0.034*	0.594
R 9.46d	Dorsolateral prefrontal	0.385	0.027*	0.594
R 9a	Dorsolateral prefrontal	0.372	0.033*	0.594
R 9m	Anterior cingulate	0.466	0.006**	0.594
R 9p	Dorsolateral prefrontal	0.396	0.022*	0.594
R PIT	Ventral visual	0.353	0.04*	0.594
R SCEF	Supplementary cingulate eye field	0.354	0.043*	0.594
R V4	Early visual	0.376	0.031*	0.594
SRS-2 Total				
L TE2p	Lateral temporal	0.361	0.042*	0.987
R ProS	Prostriate area	0.362	0.042*	0.987

Table 3.8 Regions with significant Pearson partial correlations for rs-fMRI HE and rs-MEG AE

Note: Regions with significant Pearson partial correlations between rs-fMRI HE and rs-fMRI AE controlling for fMRI RMSD and age for all individuals (ASD and TD combined). * denotes $p \leq .05$, ** denotes $p \leq .01$

	ROI	***r***	***p***	**FDR-adjusted *p***
L 10r	Prefrontal	-0.311	0.036*	0.885
L 8Ad	Dorsolateral prefrontal	0.369	0.012*	0.674
L a10p	Orbitofrontal	-0.308	0.037*	0.885
L p32	Prefrontal	-0.431	0.003**	0.885
L STGa	Superior temporal	-0.347	0.018*	0.674
L TE2p	Lateral temporal	-0.339	0.021*	0.699
L V8	Ventral visual	-0.440	0.002**	0.330
R 31pv	Posterior cingulate	-0.290	0.050*	0.885
R 7Am	Superior parietal	-0.368	0.012*	0.674
R IP0	Intraparietal	0.355	0.015*	0.674
R PoI1	Posterior insula	0.296	0.046*	0.885
R PoI2	Posterior insula	0.348	0.018*	0.674
R STSva	Superior temporal	-0.550	<0.0001**	0.027*
R STSvp	Superior temporal	-0.357	0.015*	0.674
R TE1p	Lateral temporal	-0.298	0.045*	0.885
R V3CD	Middle temporal	0.333	0.024*	0.712
R VMV2	Ventral visual	0.299	0.044*	0.885

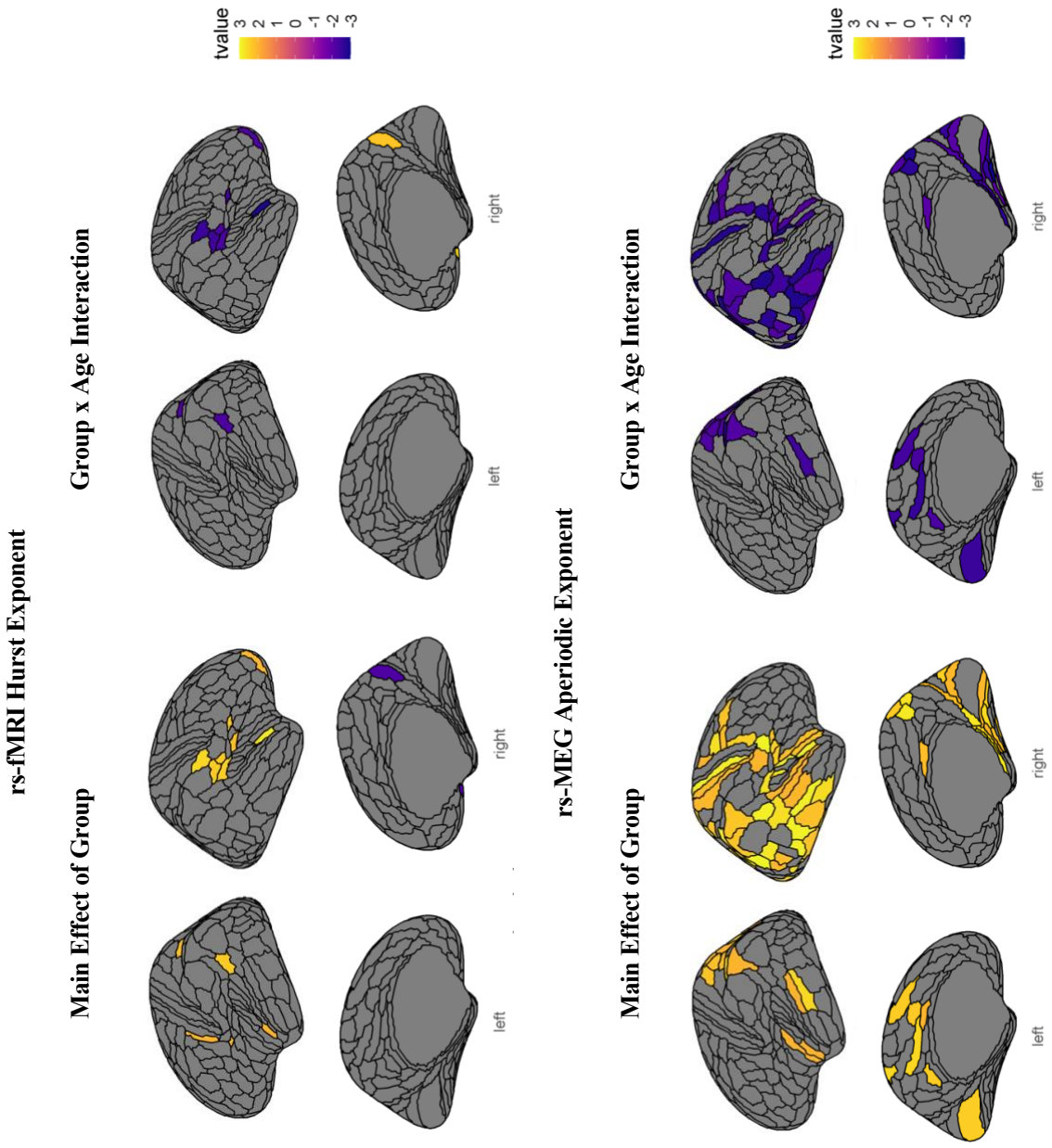

Figure 3.1 Regions with significant group differences for Hurst exponent and aperiodic exponent

Note: Regions with significant group differences for rs-fMRI HE (top panel) and rs-MEG AE (bottom panel). ROIs with significant main effect of Group represented on the lefthand side of the figure, with left and right hemispheres depicted separately. ROIs with significant Group-by-Age interaction effects represented on the righthand side of the figure, with left and right hemispheres depicted separately.

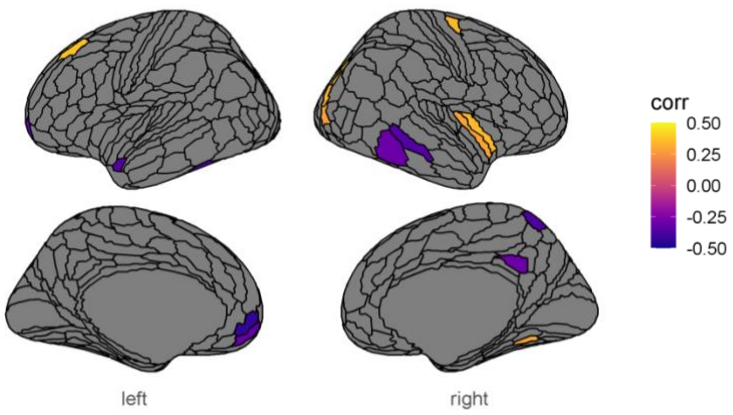

Figure 3.2 Regions with significant correlations between rs-fMRI HE and rs-MEG AE

Note: Regions with significant Pearson partial correlations for rs-fMRI HE and rs-MEG AE, controlling for age and fMRI RMSD.

Supplemental Materials

Participants

A total of 276 adolescents (156 ASD, 120 TD) were screened. Seventy-nine ASD and 62 TD adolescents were not invited to participate in the study due to contraindications preventing them from having an MRI/MEG scan (e.g., braces, permanent retainer), having additional medical conditions (e.g., Fragile X syndrome, tuberous sclerosis, epilepsy), being exposed to another language before age 5, or if they were a TD adolescent with a personal or family history of developmental, neurological, or psychological disorders. Of those invited to join the study after the screening, 16 ASD and 11 TD participants dropped out or were unable to be reached for scheduling. Sixty-one ASD and 47 TD adolescents entered the study; 13 ASD and 12 TD adolescents were excluded throughout the study due to lack of cooperation during neuropsychological testing (ASD: 1, TD: 0), reading skills below a 6^{th}-grade level (ASD: 2, TD: 0), score of 60% or lower on the lexicosemantic task during a practice session (ASD: 5, TD: 2), difficulty following lexicosemantic task directions (ASD: 2, TD: 0), large head size preventing MRI/MEG scanning (ASD: 1, TD: 2), becoming hospitalized for psychiatric care (ASD: 1, TD: 0), only completed one scan (ASD: 2, TD: 4), and inability to continue study due to the COVID-19 research shutdown in March 2020 (ASD: 1, TD: 8). A total of 46 ASD and 31 TD participants completed all components of the study. Unexpected data loss, scanner malfunction, brain abnormalities, excessive head motion, and unusable data impacted 12 ASD and 3 TD individuals.

Supplemental Table 3.1 Medications and psychological conditions

[a]Mood stabilizers include antipsychotics and anticonvulsants
[b]Other includes sympatholytics and an antihistamine (used as an anxiolytic)
Note. Current psychotropic medication and psychological comorbidities for participants in autism spectrum disorder (ASD) group. Analyses each participant was included in denoted in "Analyses" column (correlations refers to fMRI-MEG correlation analyses).

SSRI = selective serotonin reuptake inhibitor
ADHD = attention deficit/hyperactivity disorder

	Analyses	Medications	Stimulants	Mood Stabilizers[a]	SSRI/ Antidepressants	Anxiolytics/ Other[b]	Co-occurring Disorders
1	fMRI	Methylphenidate, Risperidone	+	+			ADHD
2	MEG	Amphetamine/ dextroamphetamine, Risperidone	+	+			ADHD
3	MEG	Lamotrigine		+			ADHD
4	fMRI, MEG, Correlations	Aripiprazole. Escitalopram, Methylphenidate, Mirtazapine	+	+	+		
5	fMRI, MEG, Correlations	Methylphenidate	+				ADHD
6	fMRI, MEG, Correlations	Alprazolam, Aripiprazole, Escitalopram, Guanfacine, Oxcarbazepine		+	+	+	Anxiety, Depression
7	fMRI, MEG, Correlations	Amphetamine/ dextroamphetamine	+				Anxiety
8	fMRI, MEG, Correlations	Propranolol, Ranitidine				+	Anxiety
9	fMRI, MEG, Correlations	Aripiprazole		+			Depression
10	fMRI, MEG, Correlations	Aripiprazole, Buproprion, Guanfacine		+	+	+	
11	fMRI, MEG, Correlations	Aripiprazole, Dextroamphetamine, Fluoxetine, Escitalopram, Lisdexamfetamine	+	+	+		Anxiety
12	fMRI, MEG, Correlations	Fluoxetine, Propranolol			+	+	Depression
13	fMRI, MEG, Correlations	Amantadine, Duloxetine, Prazosin, Quetiapine, Sertraline		+	+	+	Depression
14	fMRI, MEG, Correlations	Aripiprazole, Guanfacine		+		+	ADHD
15	fMRI	None					Anxiety
16	MEG	None					Anxiety
17	MEG	None					ADHD, Anxiety
18	MEG, Correlations	None					ADHD, Depression
19	fMRI, MEG, Correlations	None					Anxiety
20	fMRI, MEG, Correlations	None					Anxiety
21	fMRI, MEG, Correlations	None					Depression
		Total	6	10	6	6	19

Supplemental Table 3.2 Participant demographics for fMRI analyses - Male-only subgroup

Note: Means, standard deviations (SD), and ranges for each group of the male only subgroup. Chi-square test (handedness) and *t*-tests were performed to determine if groups were significantly different on demographic variables.

ASD = autism spectrum disorder
RMSD = root mean square difference
TD = typically developing

	ASD (n=24)		**TD (n=21)**			**$\chi 2$ (df)**	***p***
Handedness	23 right, 1 left		20 right, 1 left			0.40 (1)	0.53
	Mean (SD)	**Range**	**Mean (SD)**	**Range**	**Hedges' g**	***t*-stat (df)**	***p***
Age (years)	15.70 (2.46)	12.25-20.00	14.98 (2.00)	12.33-21.42	0.31	1.06 (43)	0.29
MRI RMSD	0.09 (0.03)	0.04-0.15	0.07 (0.03)	0.02-0.16	0.51	1.73 (43)	0.09
WASI-II							
Full Scale IQ	105.79 (13.25)	84-122	112.33 (13.50)	88-135	-0.48	1.64 (43)	0.11
Verbal IQ	106.00 (14.77)	76-131	111.52 (13.33)	85-135	-0.38	1.31 (43)	0.20
Non-Verbal IQ	105.83 (14.75)	79-132	109.90 (13.40)	80-128	-0.28	0.96 (43)	0.34
ADOS-2							
Total	12.04 (3.76)	6-20	--	--	--	--	--

Supplemental Table 3.3 Participant demographics for MEG analyses – Male-only subgroup

Note: Means, standard deviations (SD), and ranges for each group for male only subgroup. Chi-square tests (gender, handedness) and *t*-tests were performed to determine if groups were significantly different on demographic variables.

ASD = autism spectrum disorder
TD = typically developing

	ASD (n=26)		**TD (n=16)**			**χ2 (df)**	***p***
Handedness	23 right, 2 left, 1 ambidextrous		15 right, 1 left			0.68 (2)	0.41
	Mean (SD)	**Range**	**Mean (SD)**	**Range**	**Hedges' g**	***t*-stat (df)**	***p***
Age (years)	15.36 (2.44)	12.25-20	14.96 (2.25)	12.33-21.42	0.16	0.53 (40)	0.60
WASI-II							
Full Scale IQ	106.35 (12.08)	84-122	112.69 (13.47)	88-132	-0.49	1.58 (40)	0.12
Verbal IQ	105.65(13.71)	76-131	112.13 (13.28)	85-133	-0.47	1.50 (40)	0.14
Non-Verbal IQ	107.27 (14.25)	79-132	109.88 (13.33)	80-128	-0.18	0.59 (40)	0.56
ADOS-2							
Total	11.46 (3.39)	6-20	--	--	--	--	--

Supplemental Table 3.4 Participant demographics for fMRI-MEG correlations – Male-only subgroup

Note: Means, standard deviations (SD), and ranges for each group for male only subgroup. Chi-square tests (gender, handedness) and *t*-tests were performed to determine if groups were significantly different on demographic variables.

ASD = autism spectrum disorder
RMSD = root mean square difference
TD = typically developing

	ASD (n=21)		**TD (n=15)**			**χ2 (df)**	***p***
Handedness	20 right, 1 left		14 right, 1 left			0.06 (1)	0.81
	Mean (SD)	**Range**	**Mean (SD)**	**Range**	**Hedges' g**	***t*-stat (df)**	***p***
Age (years)	15.80 (2.50)	12.25-20	15.07 (2.29)	12.33-21.42	0.30	0.89 (34)	0.38
MRI RMSD	0.09 (0.03)	0.06-0.15	0.08 (0.04)	0.02-0.16	0.45	1.35 (34)	0.19
WASI-II							
Full Scale IQ	106.14 (13.05)	84-122	112.07 (13.70)	88-132	-0.43	1.31 (34)	0.20
Verbal IQ	106.62 (14.47)	76-131	111.73 (13.65)	85-133	-0.35	1.07 (34)	0.29
Non-Verbal IQ	106.33 (15.39)	79-132	109.20 (13.51)	80-128	-0.19	0.58 (34)	0.57
ADOS-2							
Total	11.24 (3.22)	6-20	--	--	--	--	--

Supplemental Table 3.5 GLM analysis results for rs-fMRI Hurst exponent – Male-only subgroup

Note: GLM analysis results for ROIs with significant or main effect of Group and/or Group-by-Age interaction for HE in the male-only subgroup. * denotes $p \leq 0.05$, ** denotes $p \leq 0.01$

ROI		Estimate	SE	*t*	*p*	FDR-adjusted *p*	Estimate	SE	*t*	*p*	FDR-adjusted *p*
		Main Effect of Group					Group x Age Interaction				
L 5m	Middle cingulate	-0.206	0.101	-2.044	0.048*	0.887	--	--	--	--	--
L 6v	Premotor	0.192	0.094	2.034	0.049*	0.887	--	--	--	--	--
L 7Am	Superior parietal	-0.210	0.102	-2.062	0.046*	0.887	0.014	0.007	2.061	0.046*	0.952
L 43	Premotor	0.239	0.114	2.095	0.043*	0.887	--	--	--	--	--
L 47s	Orbitofrontal	0.272	0.129	2.110	0.041*	0.887	-0.017	0.008	-2.036	0.048*	0.952
L AAIC	Insula	0.253	0.118	2.136	0.039*	0.887	--	--	--	--	--
L FOP1	Frontal opercular	0.276	0.114	2.421	0.020*	0.887	-0.017	0.007	-2.332	0.025*	0.952
L STV	Superior temporal	0.235	0.112	2.103	0.042*	0.887	--	--	--	--	--
L VMV1	Ventral visual	0.181	0.088	2.051	0.047*	0.887	-0.014	0.006	-2.402	0.021*	0.952
R 5L	Middle cingulate	-0.232	0.103	-2.255	0.030*	0.887	0.015	0.007	2.299	0.027*	0.952
R 13l	Orbitofrontal	--	--	--	--	--	0.015	0.007	2.036	0.048*	0.952
R 44	Inferior frontal	-0.259	0.126	-2.055	0.047*	0.887	0.018	0.008	2.165	0.036*	0.952
R a47r	Inferior frontal	0.219	0.095	2.298	0.027*	0.887	-0.015	0.006	-2.336	0.025*	0.952
R FOP1	Frontal opercular	0.212	0.099	2.137	0.039*	0.887	-0.014	0.006	-2.188	0.035*	0.952
R Ig	Insula	0.258	0.118	2.176	0.036*	0.887	--	--	--	--	--
R LO3	Lateral occipital	-0.262	0.110	-2.372	0.023*	0.887	0.018	0.007	2.475	0.018*	0.952
R OP2.3	Posterior operculum	0.292	0.124	2.352	0.024*	0.887	--	--	--	--	--
R POS2	Posterior cingulate	-0.276	0.129	-2.147	0.038*	0.887	0.019	0.008	2.241	0.031*	0.952
R RI	Early auditory	0.277	0.100	2.778	0.008**	0.887	-0.016	0.007	-2.519	0.016*	0.952
R TA2	Auditory	0.294	0.130	2.254	0.030*	0.887	-0.020	0.009	-2.310	0.026*	0.952

Supplemental Table 3.6 Pearson partial correlations for rs-fMRI HE and ASD symptomology (ADOS-2 Total & SRS-2 Total) – Male-only subgroup

Note: Significant Pearson partial correlations for rs-fMRI and ADOS-2 Total and SRS-2 Total scores for the male-only ASD group. * denotes $p \leq 0.05$, ** denotes $p \leq 0.01$

	ROI	*r*	*p*	FDR-adjusted *p*
ADOS-2 Total				
L 7AL	Superior parietal	0.494	0.017*	0.962
L 7Pm	Superior parietal	0.523	0.010**	0.962
L 9a	Dorsolateral prefrontal	-0.435	0.038*	0.962
L FST	Middle temporal	0.502	0.015*	0.962
L IPS1	Dorsal visual	-0.424	0.044*	0.962
L LIPd	Superior parietal	0.447	0.033*	0.962
L p47r	Inferior frontal	0.425	0.043*	0.962
L PH	Middle temporal	0.508	0.013*	0.962
L VMV1	Ventral visual	0.456	0.029*	0.962
R 55b	Premotor	0.484	0.019*	0.962
R 5L	Middle cingulate	-0.437	0.037*	0.962
R 8BL	Dorsolateral prefrontal	0.458	0.028*	0.962
R 9p	Dorsolateral prefrontal	-0.431	0.040*	0.962
R DVT	Posterior cingulate	0.463	0.026*	0.962
R FEF	Premotor	0.420	0.046*	0.962
R IPS1	Dorsal visual	-0.517	0.011*	0.962
R STV	Superior temporal visual	-0.415	0.049*	0.962
R V3B	Dorsal visual	-0.426	0.042*	0.962
SRS-2 Total				
L FOP4	Frontal opercular	0.451	0.035*	0.995
L LIPd	Superior parietal	0.453	0.034*	0.995
L LO1	Lateral occipital	-0.468	0.028*	0.995
L TGd	Lateral temporal	0.482	0.023*	0.995
L V7	Dorsal visual	-0.475	0.026*	0.995
R 13l	Orbitofrontal	-0.461	0.031*	0.995
R 6r	Premotor	0.629	0.002**	0.622
R 7PL	Superior parietal	0.516	0.009**	0.995
R 9a	Dorsolateral prefrontal	-0.451	0.035*	0.995
R p32	Prefrontal	-0.503	0.017*	0.995
R V2	Early visual	0.435	0.043*	0.995
R V3	Early visual	0.426	0.048*	0.995

Supplemental Table 3.7 GLM analysis results for rs-MEG aperiodic exponent – Male-only subgroup

Note: GLM analysis results for ROIs with significant main effect and/or Group-by-Age interaction for AE in the male-only subgroup. * denotes $p \leq 0.05$, ** denotes $p \leq 0.01$

ROI		Estimate	SE	*t*	*p*	FDR-adjusted *p*	Estimate	SE	*t*	*p*	FDR-adjusted *p*
		Main Effect of Group					Group x Age Interaction				
L 5L	Middle cingulate	1.573	0.687	2.288	0.028*	0.0348	-0.094	0.045	-2.083	0.440*	0.503
L 6mp	Middle cingulate	1.637	0.728	2.248	0.030*	0.348	-0.097	0.048	-2.027	0.050*	0.503
L 7PL	Superior parietal	1.924	0.609	3.158	0.003**	0.348	-0.119	0.040	-2.991	0.005**	0.503
L 23c	Posterior cingulate	1.451	0.682	2.128	0.040*	0.348	-0.094	0.045	-2.092	0.043*	0.503
L IP2	Inferior parietal	--	--	--	--	--	-0.062	0.030	-2.090	0.043*	0.503
L IPS1	Dorsal visual	1.112	0.514	2.166	0.037*	0.348	-0.071	0.034	-2.119	0.041*	0.503
L LIPd	Superior parietal	1.022	0.504	2.027	0.050*	0.348	--	--	--	--	--
L LIPv	Intraparietal	1.238	0.543	2.277	0.029*	0.348	-0.074	0.036	-2.090	0.043*	0.503
L SCEF	Supplementary / cingulate eye field	1.721	0.705	2.442	0.019*	0.359	-0.105	0.046	-2.280	0.028*	0.503
L V1	Primary visual	1.059	0.502	2.112	0.041*	0.348	-0.068	0.033	-2.066	0.046*	0.503
L VIP	Intraparietal	1.211	0.595	2.034	0.049*	0.348	--	--	--	--	--
R 3a	Somatosensory / motor	1.598	0.553	2.892	0.006**	0.348	-0.094	0.036	-2.593	0.013*	0.503
R 3b	Primary sensory	1.526	0.595	2.566	0.014*	0.348	-0.089	0.039	-2.283	0.028*	0.503
R 6v	Premotor	1.430	0.679	2.108	0.042*	0.348	--	--	--	--	--
R 7AL	Superior parietal	1.379	0.583	2.364	0.023*	0.348	-0.086	0.038	-2.255	0.030*	0.508
R 7Am	Superior parietal	1.630	0.735	2.218	0.033*	0.348	--	--	--	--	--
R 7Pm	Posterior cingulate	1.548	0.658	2.351	0.024*	0.348	-0.100	0.043	-2.323	0.026*	0.503
R 8Av	Dorsolateral prefrontal	1.411	0.650	2.170	0.036*	0.348	--	--	--	--	--
R 43	Premotor	1.404	0.310	2.30	0.027*	0.348	--	--	--	--	--
R 47m	Orbitofrontal	1.725	0.810	2.128	0.040*	0.348	--	--	--	--	--
R 52	Temporal	1.601	0.636	2.524	0.016*	0.348	-0.096	0.042	-2.304	0.027*	0.503
R A1	Primary auditory	1.017	0.459	2.213	0.033*	0.348	--	--	--	--	--
R A4	Auditory	1.097	0.536	2.048	0.048*	0.348	--	--	--	--	--
R FEF	Frontal eye fields	1.546	0.652	2.372	0.023*	0.348	-0.088	0.043	-2.063	0.046*	0.503
R FST	Lateral occipital	1.652	0.657	2.514	0.016*	0.348	-0.100	0.043	-2.320	0.026*	0.503
R H	Hippocampus	1.892	0.748	2.530	0.016*	0.348	-0.109	0.049	-2.220	0.033*	0.503
R IFJa	Inferior frontal	1.163	0.524	2.222	0.032*	0.348	--	--	--	--	--
R IP0	Inferior parietal	1.191	0.550	2.165	0.037*	0.348	-0.073	0.036	-2.025	0.050*	0.503

Supplemental Table 3.7 GLM analysis results for rs-MEG aperiodic exponent – Male-only subgroup, Continued

ROI		Estimate	SE	*t*	*p*	FDR-adjusted *p*	Estimate	SE	*t*	*p*	FDR-adjusted *p*
		Main Effect of Group					Group x Age Interaction				
R IP1	Inferior parietal	1.303	0.510	2.555	0.015*	0.348	-0.081	0.033	-2.422	0.020*	0.503
R LO2	Lateral occipital	1.262	0.623	2.023	0.050*	0.348	--	--	--	--	--
R OP2.3	Posterior operculum	1.034	0.444	2.329	0.025*	0.348	-0.063	0.029	-2.159	0.037*	0.503
R Pbelt	Auditory	1.089	0.490	2.225	0.032*	0.348	--	--	--	--	--
R PCV	Precuneus visual	1.373	0.572	2.403	0.021*	0.348	-0.083	0.037	-2.208	0.033*	0.778
R PGp	Inferior parietal	1.761	0.615	2.863	0.007**	0.348	-0.114	0.040	-2.829	0.007**	0.503
R PHT	Lateral temporal	1.403	0.573	2.447	0.019*	0.348	-0.087	0.038	-2.303	0.027*	0.503
R PreS	Presubiculum	1.571	0.748	2.101	0.042*	0.348	--	--	--	--	--
R ProS	Prostriate area	2.008	0.695	2.889	0.006**	0.348	-0.118	0.046	-2.587	0.014*	0.503
R RI	Insula	0.971	0.472	2.055	0.047*	0.348	--	--	--	--	--
R STSvp	Superior temporal	1.218	0.557	2.187	0.035*	0.348	--	--	--	--	--
R STV	Superior temporal visual	1.107	0.515	2.149	0.038*	0.348	-0.068	0.034	-2.027	0.050*	0.503
R TA2	Superior temporal	1.402	0.553	2.538	0.015*	0.348	--	--	--	--	--
R TE1m	Lateral temporal	1.261	0.604	2.088	0.044*	0.348	--	--	--	--	--
R TPOJ1	Temporo-parieto-occipital junction	1.121	0.496	2.260	0.030*	0.348	--	--	--	--	--
R TPOJ2	Temporo-parieto-occipital junction	1.560	0.507	3.076	0.004**	0.348	-0.099	0.033	-2.979	0.005**	0.503
R TPOJ3	Temporo-parieto-occipital junction	1.235	0.570	2.167	0.037*	0.348	-0.076	0.037	-2.032	0.049*	0.503
R V1	Primary visual	1.698	0.554	3.603	0.004**	0.348	-0.106	0.036	-2.918	0.006**	0.503
R V3	Early visual	1.192	0.577	2.067	0.046*	0.348	-0.077	0.038	-2.037	0.049*	0.503
R V3B	Dorsal visual	--	--	--	--	--	-0.076	0.037	-2.078	0.045*	0.503
R VIP	Superior parietal	1.837	0.739	2.483	0.018*	0.348	-0.114	0.048	-2.361	0.024*	0.503
R VMV1	Ventral visual	1.501	0.630	2.383	0.022*	0.348	-0.089	0.041	-2.167	0.037*	0.503
R VMV2	Ventral visual	1.648	0.599	2.752	0.009**	0.348	-0.097	0.039	-2.479	0.018*	0.503
R VVC	Ventral visual	1.354	0.616	2.198	0.034*	0.348	--	--	--	--	--

Supplemental Table 3.8 Pearson correlations between rs-MEG AE and ASD symptomology – Male-only subgroup

Note: Significant Pearson correlations for rs-MEG AE and ADOS-2 Total and SRS-2 Total scores for the male-only ASD group. * denotes $p \leq 0.05$

	ROI	*r*	*p*	FDR-adjusted *p*
ADOS-2 Total				
R 9m	Anterior cingulate	0.392	0.048*	0.981
R p47r	Inferior frontal	0.396	0.045*	0.981
R V4	Early visual	0.470	0.015*	0.981
SRS-2 Total				
L a47r	Inferior frontal	-0.411	0.042*	0.998
R 25	Anterior cingulate	-0.405	0.044*	0.998
R ProS	Prostriate area	0.417	0.038*	0.998
R s32	Anterior cingulate	-0.396	0.050*	0.998

Supplemental Table 3.9 Regions with significant Pearson partial correlations for rs-fMRI HE and rs-MEG AE – Male-only subgroup

Note: Regions with significant Pearson partial correlations between rs-fMRI HE and rs-fMRI AE controlling for fMRI RMSD and age for all individuals in the male-only subgroup (ASD and TD combined). * denotes $p \leq .05$, ** denotes $p \leq .01$, *** denotes $p \leq .001$

	ROI	***r***	***p***	**FDR-adjusted *p***
L 8Ad	Dorsolateral prefrontal	0.416	0.014*	0.863
L a10p	Orbitofrontal	-0.350	0.042*	0.869
L FST	Middle temporal	0.400	0.019*	0.863
L p32	Prefrontal	-0.562	0.0005***	0.098
L POS1	Posterior cingulate	0.374	0.0291*	0.879
L STGa	Superior temporal	-0.364	0.034*	0.879
L V6	Dorsal visual	0.393	0.022*	0.863
R 10pp	Orbitofrontal	0.341	0.048*	0.946
R 6d	Premotor	0.363	0.035*	0.879
R 7Am	Superior parietal	-0.416	0.014*	0.863
R 7PL	Superior parietal	-0.404	0.018*	0.863
R LO1	Middle temporal	0.413	0.015*	0.863
R Mbelt	Early auditory	0.355	0.039*	0.879
R PoI2	Posterior insula	0.357	0.038*	0.879
R STSva	Superior temporal	-0.589	0.0002***	0.089
R STSvp	Superior temporal	-0.487	0.003**	0.414
R TE1p	Lateral temporal	-0.366	0.033*	0.879
R TGd	Lateral temporal	-0.369	0.032*	0.879

Conclusion

Summary of Findings

This dissertation aimed to compare fMRI and MEG measures of activation to provide a more comprehensive approach to brain function in the context of a clinical population, ASD. The three studies described above investigated the relationship between these two neuroimaging modalities in adolescents who underwent both task and resting-state scans in each modality. In addition to understanding the relationship between the two imaging modalities, activity from adolescents with ASD was compared to that from TD peers.

Paper 1 examined neural activity patterns during lexicosemantic processing in adolescents with ASD and their TD peers, utilizing fMRI BOLD signal and MEG event-related theta power. Regions of interest were identified based on fMRI and MEG data, such that areas that showed significant activation across participants at the whole-group level were then further examined in each modality. Event-related theta power was greater in the ASD group across several time windows and regions, such as frontal and temporal areas, when compared to the TD group. In contrast, BOLD signal was greater in the ASD group in only one region, the anterior cingulate gyrus. BOLD signal and theta power were positively correlated for the anterior cingulate cortex in the ASD group, however this was not significant after correction. Comparisons between the two measures did not reveal a clear pattern. While this first study found no clear relationship between BOLD signal and a time-frequency domain measurement from MEG, it was hypothesized that an investigation between BOLD signal and a time domain measurement from MEG may shed more light on the relationship between the two modalities. Additionally, it was hypothesized that the lack of group differences seen in the fMRI data may be in part attributed to behavioral heterogeneity within the ASD group.

Paper 2 followed up on the analyses presented in Paper 1, by comparing the fMRI BOLD signal to time domain measurements (N250m and N400m) from MEG. Similar to event-related theta power, N250m and N400m are known to be related to language processing and were thus a suitable measure for the current study. Regions of interest were identified based on areas with significant whole-group activation based on MEG N250m and N400m. ASD encompasses a broad spectrum of behavioral and clinical variability, contributing to the large amount of heterogeneity amongst individuals with ASD. Inter-individual heterogeneity at the behavioral level may affect neuroimaging findings, which may contribute to the inconsistencies in the field (Lenroot & Yeung, 2013). While Paper 1 examined the ASD group as a whole and did not find expected group differences in the fMRI data, Paper 2 aimed to examine ASD subgroups. Subgroups were based on lexicosemantic task performance, with one ASD subgroup performing at levels equal to TD peers and the other performing below the TD group. This resulted in a smaller and slightly different set of regions in comparison to Paper 1. With regard to MEG findings, the H-ASD group was found to have greater N250m in the inferior frontal region compared to the TD group and greater bilateral N400m in the inferior frontal and temporal regions. The L-ASD group was found to have decreased N400m in the inferior frontal region. While N250m and N400m revealed group differences supporting differential task performance across subgroups, fMRI BOLD signal did not show significant differences, similar to the overall findings from Paper 1. Also similarly, N250m and N400m were minimally correlated with BOLD signal, with the exception of the L-ASD group which showed positive correlations between N400m and BOLD signal for all four regions examined. Papers 1 and 2 investigated the relationship between fMRI and MEG in task scans, with findings of minimal and/or weak

correlations. We therefore considered whether resting-state data may instead reveal a clearer pattern connecting the two modalities.

Paper 3 studied the relationship between fMRI and MEG through a resting-state analysis, including overlapping participants from Papers 1 and 2. Previous studies describe an imbalance between excitatory and inhibitory neurotransmitters in ASD, although this work stems from invasive methods used on animal models. Recent studies are thought to have found indirect measurements of the excitatory-inhibitory ratio (E:I) – two of which are the HE and the AE, both measurements of the spectral components found in time series data. This study found that the HE, measured from rs-fMRI, was mostly increased in the ASD group compared to the TD group across various regions. Additionally, the ASD and TD groups were found to have differential patterns related to age. In many regions, the ASD group showed a decrease in HE with age, whereas the TD group showed an increase. The HE was also found to be mostly positively correlated with ASD symptomology, as measured by the ADOS-2. HE was mostly positively correlated with ASD symptomology measured by the ADOS-2, while correlations with the SRS-2 were positive for some brain regions and negative for others. Overall, the HE was mostly increased in the ASD group, showed atypical decreases with age, and was both positively and negatively correlated with ASD symptomology. Paper 3 also examined the AE in rs-MEG. AE was found to be significantly increased in many regions across the brain in the ASD group compared to the TD group. Additionally, AE was found to decrease with age in the ASD group, whereas AE in the TD group either increased or remained stable. The AE was positively correlated with ASD symptomology measured by the ADOS-2 and the SRS-2. When considering the relationship between the two E:I ratio measurements, the HE and AE did not reveal a consistent pattern. No clear relationship was revealed between the two exponents, as they were

found to be positively correlated in some brain regions, and negatively correlated in others. While it was hypothesized to reveal a clear relationship between the two measures, Paper 3 instead revealed that there is no clear pattern across the whole brain that shows a relationship between the two measures.

Conclusion

This dissertation is the first to comprehensively examine the relationship between fMRI and MEG for multiple different measurements of activity in a group of individuals with ASD who completed both fMRI and MEG scans. When considering the results of all three papers, a consistent pattern was revealed. In analyses of fMRI data few or no group differences were detected, whereas analyses of MEG data highlighted many more group differences. In Paper 1, there was a lack of group differences in the fMRI BOLD signal, while event-related theta power was found to be significantly greater in the ASD group, compared to TD peers, across multiple brain regions. In Paper 2, N400m was greater in many brain regions in the ASD group whereas fMRI BOLD signal revealed few group differences. Lastly in Paper 3, rs-fMRI HE was significantly increased in the ASD group for many regions, while rs-MEG AE showed increases across many more regions. Additionally, findings revealed that fMRI and MEG lack a clear relationship in both task and resting state scans. Despite the lack of a clear relationship, this dissertation adds to the neuroimaging literature, such that many studies do not take advantage of other methodologies and remain unimodal. Tulay et al. (2019) clearly outlines the necessity of multimodal neuroimaging studies in the context of neurodevelopmental and psychiatric conditions. While each imaging method has its own strengths, there is no single method that can allow for a fully comprehensive analysis at the level that is required to reveal distinct differences in disorders that exist along a spectrum, such as ASD. Neuroimaging studies have the potential

to reveal biomarkers that can be used to diagnose and understand disorders that rely on behavioral diagnostic processes.

This dissertation has revealed that unimodal studies do not capture the entire picture of neural activation, and that patterns observed in data from one imaging method may not replicate in another imaging method. fMRI- and MEG-derived measures such as the BOLD signal, event-related theta power, N250m, and N400m, were not found to correlate well through analyses that directly compared 'activation' from the same individuals. Similarly, two measures that are thought to represent the E:I ratio also did not correlate to the extent that would be expected. Multimodal neuroimaging is critical for understanding aspects relevant to the neural profile of those with and without psychological conditions, as unimodal studies are substantially insufficient.

The current series of papers contributes to the small, but growing literature on multimodal neuroimaging, with multiple studies reporting an unclear relationship between fMRI and MEG. This poor relationship between neuroimaging methods that are considered measures of neural 'activation' is remarkable and requires explanation. It may be hypothesized that either fMRI or MEG, or both, are unreliable measures of activity as some have suggested (Elliott et al., 2020; Kennedy et al., 2022). As pointed out by Kragel and colleagues (2021), when making the conclusion that fMRI is an unreliable source for neural activity, Elliott and colleagues (2020) based their report on studies with small sample sizes and long test-retest windows, which would confound studies of reliability. It is unlikely to be the case that these neuroimaging modalities, which are widely used and have been for decades, are unreliable. fMRI findings show replicability across many studies (Berboth et al., 2021; Buimer et al., 2020; Guo et al., 2012;

Nettekoven et al., 2018; Plichta et al., 2012; Taxali et al., 2021), as do MEG studies (Legget et al., 2017; Martín-Buro et al., 2015).

The more realistic reason behind the lack of correlation between the two is that they are each measuring different components of neural activation. When considering the results of all three papers, the pattern suggests that fMRI data, which have greater spatial resolution, reveal some group differences, but when MEG data are examined, which have greater temporal resolution, many more group differences are observed. In comparison to fMRI BOLD signal in Paper 1, event-related theta power was significantly greater across multiple regions in the ASD group. In paper 2, N400m was greater in many brain regions in the ASD group whereas fMRI BOLD signal revealed few group differences. Lastly in Paper 3, rs-fMRI HE was significantly increased in the ASD group for many regions, while rs-MEG AE showed increases across many more regions.

It is clear that fMRI and MEG do not measure neural activation in the same manner. fMRI relies on the hemodynamic response, whereas MEG measures the magnetic fields that results from changes to the electrical current in the brain. Yet, because they are both measuring neural activity, an initial expectation was that they would produce patterns of similar findings. Previous research studies comparing the two modalities present evidence of the opposite. An early study of multimodal neuroimaging research examined data from fMRI and MEG scans during a visual motion task in neurotypical adults (Ahlfors et al., 1999). While some regions, such as the middle temporal and superior temporal regions, were shown to be activated in both fMRI and MEG scans, activity in the frontal region was only seen in the MEG data and not fMRI. Conversely, activity in the posterior occipital regions was seen only in fMRI and not in MEG data. Another study compared fMRI and MEG data from individuals after a stroke and

found no correlation between activation intensities of the two modalities (Altamura et al., 2007). In a further study, neurotypical adults watched a movie during fMRI and MEG scans. Direct voxel-wise comparisons between the fMRI and MEG data did not reveal significant correlations across the brain (Lankinen et al., 2018). Engemann and colleagues (2020) provide evidence that combining data from both fMRI and MEG improved a machine learning approach to age prediction, suggesting that each contributes critical information to the model. One of the few multimodal neuroimaging studies in a psychiatric population, compared MEG and fMRI data in adults with and without schizophrenia (Sanfratello et al., 2019). Results showed different functional connectivity patterns in each of the modalities. Although EEG is a different methodology than MEG, such that both measure electrical activity, and thus it is important to note that one large study of 1657 neurotypical individuals compared fMRI and EEG (Nentwich et al., 2020). This study found that the spatial patterns of the functional connectivity revealed by each modality were significantly different from the other. The current dissertation supports the hypothesis that fMRI and MEG are complementary measurements, each providing unique information to the understanding of the brain. Previous research studies comparing the two modalities do not do so in the context of ASD or language processing, and are commonly carried out with adult participants. Also, previous studies have been relatively small in comparison to the current study (Ahlfors et al., 1999; Altamura et al., 2007; Babajani-Feremi et al., 2008; Lankinen et al., 2018), including as few as 4 participants.

While the three papers included in this dissertation add to the neuroimaging ASD literature, they are not without limitations. Papers 1 and 2 looked at a select few regions that were identified as being activated at the whole-group level in each of the modalities. Previous studies have found that individuals with ASD may recruit regions that are atypical to the

presented task, and thus we may not have fully captured the expansive profile that the ASD group may show. Paper 3 examined resting-state data in fMRI and MEG. During the MEG scan, both eyes open and eyes closed conditions were used during the scanning procedure. However, during fMRI, only an eyes open protocol was conducted. To ensure that similar neural activity was compared across modalities, the eyes open portion of the MEG scan was used. A previous study of typically developing youth has shown that the eyes closed condition may evoke greater alpha power as measured by MEG in comparison to the eyes open condition (Petro et al., 2022). Across all three papers, a select group of individuals participated in the study. Adolescents were recruited who were able to tolerate fMRI and MEG scans, as well as neuropsychological testing and the lexicosemantic task that was used in Papers 1 and 2. We recognize that these studies represent a specific group of individuals with ASD, and that findings may not apply to those who are unable to participate in neuroimaging studies due to cognitive or sensory differences. Lastly, while this series of papers compared data from fMRI and MEG scans, only correlations were used to understand the general pattern between the modalities. Papers that call for multimodal neuroimaging are increasingly describing methods of data fusion and integration (Belyaeva et al., 2024; Calhoun & Sui, 2016; Jafarian et al., 2020). Future studies should take advantage of novel statistical analyses that utilize novel methods to potentially uncover more complex patterns and relationships between two imaging modalities.

In conclusion, this dissertation is the first to examine the relationship between fMRI and MEG across multiple measurements in a group of individuals with ASD. Analyses examining data from both task- and resting-state scans revealed no clear relationship between the two modalities with regard to measurements of language activation, hemispheric laterality, and spectral properties. This dissertation demonstrates the complexity of understanding the

relationship between two neuroimaging methods, and emphasizes the need for an increase in the studies using multimodal neuroimaging approaches to comprehensively study complex psychological and neurodevelopmental disorders, such as ASD.

References

Ahlfors, S. P., & Mody, M. (2019). Overview of MEG. *Organizational Research Methods*, *22*(1), 95–115. https://doi.org/10.1177/1094428116676344

Ahlfors, S. P., Simpson, G. V., Dale, A. M., Belliveau, J. W., Liu, A. K., Korvenoja, A., Virtanen, J., Huotilainen, M., Tootell, R. b. h., Aronen, H. J., & Ilmoniemi, R. J. (1999). Spatiotemporal Activity of a Cortical Network for Processing Visual Motion Revealed by MEG and fMRI. *Journal of Neurophysiology*, *82*(5), 2545–2555. https://doi.org/10.1152/jn.1999.82.5.2545

Ajram, L. A., Pereira, A. C., Durieux, A. M. S., Velthius, H. E., Petrinovic, M. M., & McAlonan, G. M. (2019). The contribution of [1H] magnetic resonance spectroscopy to the study of excitation-inhibition in autism. *Progress in Neuro-Psychopharmacology and Biological Psychiatry*, *89*, 236–244. https://doi.org/10.1016/j.pnpbp.2018.09.010

Altamura, C., Torquati, K., Zappasodi, F., Ferretti, A., Pizzella, V., Tibuzzi, F., Vernieri, F., Pasqualetti, P., Landi, D., Del Gratta, C., Romani, G.-L., Maria Rossini, P., & Tecchio, F. (2007). fMRI-vs-MEG evaluation of post-stroke interhemispheric asymmetries in primary sensorimotor hand areas. *Experimental Neurology*, *204*(2), 631–639. https://doi.org/10.1016/j.expneurol.2006.12.017

Alvarez, F. P., & Destexhe, A. (2004). Simulating cortical network activity states constrained by intracellular recordings. *Neurocomputing*, *58–60*, 285–290. https://doi.org/10.1016/j.neucom.2004.01.057

Amaral, D. G. (2017). Examining the Causes of Autism. *Cerebrum: The Dana Forum on Brain Science*, *2017*, cer-01-17.

American Psychiatric Association. (2013). *Diagnostic and Statistical Manual of Mental Disorders*. American Psychiatric Association.

Anderson, J. S. (2013). Functional Connectivity MRI in Autism. In *Imaging the Brain in Autism* (1st ed., pp. 325–347). Springer. https://doi.org/10.1007/978-1-4614-6843-1

Arthurs, O. J., & Boniface, S. (2002). How well do we understand the neural origins of the fMRI BOLD signal? *Trends in Neurosciences*, *25*(1), 27–31. https://doi.org/10.1016/S0166-2236(00)01995-0

Arunachalam, S., & Luyster, R. J. (2016). The integrity of lexical acquisition mechanisms in autism spectrum disorders: A research review. *Autism Research*, *9*(8), 810–828. https://doi.org/10.1002/aur.1590

Audrain, S. P., Urbain, C. M., Yuk, V., Leung, R. C., Wong, S. M., & Taylor, M. J. (2020). Frequency-specific neural synchrony in autism during memory encoding, maintenance and recognition. *Brain Communications*, *2*(2), fcaa094. https://doi.org/10.1093/braincomms/fcaa094

Babajani-Feremi, A., Soltanian-Zadeh, H., & Moran, J. E. (2008). Integrated MEG/fMRI Model Validated Using Real Auditory Data. *Brain Topography*, *21*(1), 61–74. https://doi.org/10.1007/s10548-008-0056-3

Babiloni, F., Mattia, D., Babiloni, C., Astolfi, L., Salinari, S., Basilisco, A., Rossini, P. M., Marciani, M. G., & Cincotti, F. (2004). Multimodal integration of EEG, MEG and fMRI data for the solution of the neuroimage puzzle. *Magnetic Resonance Imaging*, *22*(10), 1471–1476. https://doi.org/10.1016/j.mri.2004.10.007

Baillet, S. (2017). Magnetoencephalography for brain electrophysiology and imaging. *Nature Neuroscience*, *20*(3), 327–339. https://doi.org/10.1038/nn.4504

Bakker-Marshall, I., Takashima, A., Schoffelen, J.-M., van Hell, J. G., Janzen, G., & McQueen, J. M. (2018). Theta-band Oscillations in the Middle Temporal Gyrus Reflect Novel Word Consolidation. *Journal of Cognitive Neuroscience*, *30*(5), 621–633. https://doi.org/10.1162/jocn_a_01240

Bastiaansen, M. C. M., Linden, M. V. D., Keurs, M. T., Dijkstra, T., & Hagoort, P. (2005). Theta Responses Are Involved in Lexical—Semantic Retrieval during Language Processing. *Journal of Cognitive Neuroscience*, *17*(3), 530–541. https://doi.org/10.1162/0898929053279469

Bavin, E. L., Prendergast, L. A., Kidd, E., Baker, E., & Dissanayake, C. (2016). Online processing of sentences containing noun modification in young children with high-functioning autism. *International Journal of Language & Communication Disorders*, *51*(2), 137–147. https://doi.org/10.1111/1460-6984.12191

Beaton, L. E., Azma, S., & Marinkovic, K. (2018). When the brain changes its mind: Oscillatory dynamics of conflict processing and response switching in a flanker task during alcohol challenge. *PLoS ONE*, *13*(1), e0191200. https://doi.org/10.1371/journal.pone.0191200

Beery, K. E., Buktenica, N. A., & Beery, N. A. (2010). *The Beery–Buktenica Developmental Test of Visual–Motor Integration: Administration, Scoring, and Teaching Manual* (6th ed.). Pearson.

Begus, K., & Bonawitz, E. (2020). The rhythm of learning: Theta oscillations as an index of active learning in infancy. *Developmental Cognitive Neuroscience*, *45*, 100810. https://doi.org/10.1016/j.dcn.2020.100810

Belyaeva, I., Gabrielson, B., Wang, Y.-P., Wilson, T. W., Calhoun, V. D., Stephen, J. M., & Adali, T. (2024). Learning Spatiotemporal Brain Dynamics in Adolescents via Multimodal MEG and fMRI Data Fusion Using Joint Tensor/Matrix Decomposition. *IEEE Transactions on Biomedical Engineering*, 1–12. https://doi.org/10.1109/TBME.2024.3364704

Benjamini, Y., & Hochberg, Y. (1995). Controlling the false discovery rate: A practical and powerful approach to multiple testing. *Journal of the Royal Statistical Society. Series B (Methodological)*, *57*(1), 289–300.

Berard, N., Loutzenhiser, L., Sevigny, P. R., & Alfano, D. P. (2017). Executive Function, Social Emotional Learning, and Social Competence in School-Aged Boys With Autism Spectrum Disorder. *Canadian Journal of School Psychology*, *32*(3–4), 265–281. https://doi.org/10.1177/0829573517707907

Berboth, S., Windischberger, C., Kohn, N., & Morawetz, C. (2021). Test-retest reliability of emotion regulation networks using fMRI at ultra-high magnetic field. *NeuroImage*, *232*, 117917. https://doi.org/10.1016/j.neuroimage.2021.117917

Bertelsen, N., Vitale, A., Bolis, D., Mandelli, V., & Lombardo, M. V. (2023). *Electrophysiologically-defined excitation-inhibition autism neurosubtypes* (p. 2023.11.22.23298729). medRxiv. https://doi.org/10.1101/2023.11.22.23298729

Best, J. R., & Miller, P. H. (2010). A developmental perspective on executive function. *Child Development*, *81*(6), 1641–1660. https://doi.org/10.1111/j.1467-8624.2010.01499.x

Billingsley-Marshall, R. L., Clear, T., Mencl, W. E., Simos, P. G., Swank, P. R., Men, D., Sarkari, S., Castillo, E. M., & Papanicolaou, A. C. (2007). A comparison of functional MRI and magnetoencephalography for receptive language mapping. *Journal of Neuroscience Methods*, *161*(2), 306–313. https://doi.org/10.1016/j.jneumeth.2006.10.020

Bloy, L., Shwayder, K., Blaskey, L., Roberts, T. P. L., & Embick, D. (2019). A Spectrotemporal Correlate of Language Impairment in Autism Spectrum Disorder. *Journal of Autism and Developmental Disorders*, *49*(8), 3181–3190. https://doi.org/10.1007/s10803-019-04040-x

Blumenfeld, H. K., Booth, J. R., & Burman, D. D. (2006). Differential prefrontal–temporal neural correlates of semantic processing in children. *Brain and Language*, *99*(3), 226–235. https://doi.org/10.1016/j.bandl.2005.07.004

Boddaert, N., Chabane, N., Belin, P., Bourgeois, M., Royer, V., Barthelemy, C., Mouren-Simeoni, M.-C., Philippe, A., Brunelle, F., Samson, Y., & Zilbovicius, M. (2004). Perception of complex sounds in autism: Abnormal auditory cortical processing in children. *American Journal of Psychiatry*, *161*(11), 2117–2120. https://doi.org/10.1176/appi.ajp.161.11.2117

Bolton, T. A. W., Morgenroth, E., Preti, M. G., & Van De Ville, D. (2020). Tapping into Multi-Faceted Human Behavior and Psychopathology Using fMRI Brain Dynamics. *Trends in Neurosciences*, *43*(9), 667–680. https://doi.org/10.1016/j.tins.2020.06.005

Boucher, J. (2003). Language development in autism. *International Journal of Pediatric Otorhinolaryngology*, *67*, S159–S163. https://doi.org/10.1016/j.ijporl.2003.08.016

Boucher, J. (2012). Research Review: Structural language in autistic spectrum disorder - characteristics and causes. *Journal of Child Psychology & Psychiatry*, *53*(3), 219–233. https://doi.org/10.1111/j.1469-7610.2011.02508.x

Braconnier, M. L., & Siper, P. M. (2021). Neuropsychological Assessment in Autism Spectrum Disorder. *Current Psychiatry Reports*, *23*(10), 63. https://doi.org/10.1007/s11920-021-01277-1

Braeutigam, S., Swithenby, S. J., & Bailey, A. J. (2008). Contextual integration the unusual way: A magnetoencephalographic study of responses to semantic violation in individuals with autism spectrum disorders. *European Journal of Neuroscience*, *27*(4), 1026–1036. https://doi.org/10.1111/j.1460-9568.2008.06064.x

Bruining, H., Hardstone, R., Juarez-Martinez, E. L., Sprengers, J., Avramiea, A.-E., Simpraga, S., Houtman, S. J., Poil, S.-S., Dallares, E., Palva, S., Oranje, B., Matias Palva, J., Mansvelder, H. D., & Linkenkaer-Hansen, K. (2020). Measurement of excitation-inhibition ratio in autism spectrum disorder using critical brain dynamics. *Scientific Reports*, *10*(1), Article 1. https://doi.org/10.1038/s41598-020-65500-4

Brunel, N., & Wang, X.-J. (2003). What Determines the Frequency of Fast Network Oscillations With Irregular Neural Discharges? I. Synaptic Dynamics and Excitation-Inhibition Balance. *Journal of Neurophysiology*, *90*(1), 415–430. https://doi.org/10.1152/jn.01095.2002

Brysbaert, M., & New, B. (2009). Moving beyond Kučera and Francis: A critical evaluation of current word frequency norms and the introduction of a new and improved word frequency measure for American English. *Behavior Research Methods*, *41*(4), 977–990. https://doi.org/10.3758/BRM.41.4.977

Buimer, E. E. L., Pas, P., Brouwer, R. M., Froeling, M., Hoogduin, H., Leemans, A., Luijten, P., van Nierop, B. J., Raemaekers, M., Schnack, H. G., Teeuw, J., Vink, M., Visser, F., Hulshoff Pol, H. E., & Mandl, R. C. W. (2020). The YOUth cohort study: MRI protocol and test-retest reliability in adults. *Developmental Cognitive Neuroscience*, *45*, 100816. https://doi.org/10.1016/j.dcn.2020.100816

Buxton, R. B. (2009). *Introduction to Functional Magnetic Resonance Imaging: Principles and Techniques* (2nd ed.). Cambridge University Press.

Cabeza, R., & Nyberg, L. (2000). Imaging Cognition II: An Empirical Review of 275 PET and fMRI Studies. *Journal of Cognitive Neuroscience*, *12*(1), 1–47. https://doi.org/10.1162/08989290051137585

Calhoun, V. D., & Sui, J. (2016). Multimodal fusion of brain imaging data: A key to finding the missing link(s) in complex mental illness. *Biological Psychiatry : Cognitive Neuroscience and Neuroimaging*, *1*(3), 230–244. https://doi.org/10.1016/j.bpsc.2015.12.005

Cantiani, C., Choudhury, N. A., Yu, Y. H., Shafer, V. L., Schwartz, R. G., & Benasich, A. A. (2016). From Sensory Perception to Lexical-Semantic Processing: An ERP Study in Non-Verbal Children with Autism. *PLoS ONE*, *11*(8), e0161637. https://doi.org/10.1371/journal.pone.0161637

Cardinale, R. C., Shih, P., Fishman, I., Ford, L. M., & Müller, R.-A. (2013). Pervasive Rightward Asymmetry Shifts of Functional Networks in Autism Spectrum Disorder. *JAMA Psychiatry*, *70*(9), 975–982. https://doi.org/10.1001/jamapsychiatry.2013.382

Carper, R. A., Solders, S., Treiber, J. M., Fishman, I., & Müller, R.-A. (2015). Corticospinal Tract Anatomy and Functional Connectivity of Primary Motor Cortex in Autism. *Journal of the American Academy of Child and Adolescent Psychiatry*, *54*(10), 859–867. https://doi.org/10.1016/j.jaac.2015.07.007

Carreiras, M., Armstrong, B. C., Perea, M., & Frost, R. (2014). The what, when, where, and how of visual word recognition. *Trends in Cognitive Sciences*, *18*(2), 90–98. https://doi.org/10.1016/j.tics.2013.11.005

Carter, C. S., & Van Veen, V. (2007). Anterior cingulate cortex and conflict detection: An update of theory and data. *Cognitive, Affective, & Behavioral Neuroscience*, *7*(4), 367–379. https://doi.org/10.3758/CABN.7.4.367

Carter Leno, V., Begum-Ali, J., Goodwin, A., Mason, L., Pasco, G., Pickles, A., Garg, S., Green, J., Charman, T., Johnson, M. H., Jones, E. J. H., Vassallo, G., Burkitt-Wright, E., Eelloo, J., Gareth Evans, D., West, S., Hupton, E., Lewis, L., Robinson, L., … STAARS Teams. (2022). Infant excitation/inhibition balance interacts with executive attention to predict autistic traits in childhood. *Molecular Autism*, *13*(1), 46. https://doi.org/10.1186/s13229-022-00526-1

Cavanagh, J. F., & Frank, M. J. (2014). Frontal theta as a mechanism for cognitive control. *Trends in Cognitive Sciences*, *18*(8), 414–421. https://doi.org/10.1016/j.tics.2014.04.012

Cermak, C. A., Arshinoff, S., Ribeiro de Oliveira, L., Tendera, A., Beal, D. S., Brian, J., Anagnostou, E., & Sanjeevan, T. (2022). Brain and Language Associations in Autism Spectrum Disorder: A Scoping Review. *Journal of Autism and Developmental Disorders*, *52*(2), 725–737. https://doi.org/10.1007/s10803-021-04975-0

Cetin, M. S., Houck, J. M., Rashid, B., Agacoglu, O., Stephen, J. M., Sui, J., Canive, J., Mayer, A., Aine, C., Bustillo, J. R., & Calhoun, V. D. (2016). Multimodal Classification of Schizophrenia Patients with MEG and fMRI Data Using Static and Dynamic Connectivity Measures. *Frontiers in Neuroscience*, *10*. https://doi.org/10.3389/fnins.2016.00466

Chen, G., Saad, Z. S., Nath, A. R., Beauchamp, M. S., & Cox, R. W. (2012). FMRI group analysis combining effect estimates and their variances. *NeuroImage*, *60*(1), 747–765. https://doi.org/10.1016/j.neuroimage.2011.12.060

Chou, T.-L., Booth, J. R., Burman, D. D., Bitan, T., Bigio, J. D., Lu, D., & Cone, N. E. (2006). Developmental changes in the neural correlates of semantic processing. *NeuroImage*, *29*(4), 1141–1149. https://doi.org/10.1016/j.neuroimage.2005.09.064

Ciric, R., Nomi, J. S., Uddin, L. Q., & Satpute, A. B. (2017). Contextual connectivity: A framework for understanding the intrinsic dynamic architecture of large-scale functional

brain networks. *Scientific Reports*, *7*(1), 6537. https://doi.org/10.1038/s41598-017-06866-w

Cole, S., Donoghue, T., Gao, R., & Voytek, B. (2019). NeuroDSP: A package for neural digital signal processing. *Journal of Open Source Software*, *4*(36), 1272. https://doi.org/10.21105/joss.01272

Colombo, M. A., Napolitani, M., Boly, M., Gosseries, O., Casarotto, S., Rosanova, M., Brichant, J.-F., Boveroux, P., Rex, S., Laureys, S., Massimini, M., Chieregato, A., & Sarasso, S. (2019). The spectral exponent of the resting EEG indexes the presence of consciousness during unresponsiveness induced by propofol, xenon, and ketamine. *NeuroImage*, *189*, 631–644. https://doi.org/10.1016/j.neuroimage.2019.01.024

Condouris, K., Meyer, E., & Tager-Flusberg, -Flusberg Helen. (2003). The relationship between standardized measures of language and measures of spontaneous speech in children With autism. *American Journal of Speech-Language Pathology*, *12*(3), 349–358. https://doi.org/10.1044/1058-0360(2003/080)

Correas, A., López-Caneda, E., Beaton, L., Rodríguez Holguín, S., García-Moreno, L., Antón-Toro, L., Cadaveira, F., Maestú, F., & Marinkovic, K. (2019). Decreased event-related theta power and phase-synchrony in young binge drinkers during target detection: An anatomically-constrained MEG approach. *Journal of Psychopharmacology*, *33*(3), 335–346. https://doi.org/10.1177/0269881118805498

Cox, R. W. (1996). AFNI: Software for Analysis and Visualization of Functional Magnetic Resonance Neuroimages. *Computers and Biomedical Research*, *29*(3), 162–173. https://doi.org/10.1006/cbmr.1996.0014

Craig, F., Margari, F., Legrottaglie, A. R., Palumbi, R., de Giambattista, C., & Margari, L. (2016). A review of executive function deficits in autism spectrum disorder and attention-deficit/hyperactivity disorder. *Neuropsychiatric Disease and Treatment*, *12*, 1191–1202. https://doi.org/10.2147/NDT.S104620

Curl, A., & Coderre, E. L. (2022). The time-locked neurodynamics of semantic processing in autism spectrum disorder: An EEG study. *Cognitive Neurodynamics*, *16*(1), 43–72. https://doi.org/10.1007/s11571-021-09697-8

Dale, A. M., Fischl, B., & Sereno, M. I. (1999). Cortical Surface-Based Analysis: I. Segmentation and Surface Reconstruction. *NeuroImage*, *9*(2), 179–194. https://doi.org/10.1006/nimg.1998.0395

Dale, A. M., & Halgren, E. (2001). Spatiotemporal mapping of brain activity by integration of multiple imaging modalities. *Current Opinion in Neurobiology*, *11*(2), 202–208. https://doi.org/10.1016/S0959-4388(00)00197-5

Dale, A. M., Liu, A. K., Fischl, B. R., Buckner, R. L., Belliveau, J. W., Lewine, J. D., & Halgren, E. (2000). Dynamic Statistical Parametric Mapping: Combining fMRI and MEG

for High-Resolution Imaging of Cortical Activity. *Neuron*, *26*(1), 55–67. https://doi.org/10.1016/S0896-6273(00)81138-1

Dani, V. S., Chang, Q., Maffei, A., Turrigiano, G. G., Jaenisch, R., & Nelson, S. B. (2005). Reduced Cortical Activity Due to a Shift in the Balance between Excitation and Inhibition in a Mouse Model of Rett Syndrome. *Proceedings of the National Academy of Sciences of the United States of America*, *102*(35), 12560–12565.

Davis, M. H., & Gaskell, M. G. (2009). A complementary systems account of word learning: Neural and behavioural evidence. *Philosophical Transactions of the Royal Society B: Biological Sciences*, *364*(1536), 3773–3800. https://doi.org/10.1098/rstb.2009.0111

Delorme, A., & Makeig, S. (2004). EEGLAB: An open source toolbox for analysis of single-trial EEG dynamics including independent component analysis. *Journal of Neuroscience Methods*, *134*(1), 9–21. https://doi.org/10.1016/j.jneumeth.2003.10.009

Demetriou, E. A., DeMayo, M. M., & Guastella, A. J. (2019). Executive Function in Autism Spectrum Disorder: History, Theoretical Models, Empirical Findings, and Potential as an Endophenotype. *Frontiers in Psychiatry*, *10*, 753. https://doi.org/10.3389/fpsyt.2019.00753

Devonshire, I. M., Papadakis, N. G., Port, M., Berwick, J., Kennerley, A. J., Mayhew, J. E. W., & Overton, P. G. (2012). Neurovascular coupling is brain region-dependent. *NeuroImage*, *59*(3), 1997–2006. https://doi.org/10.1016/j.neuroimage.2011.09.050

Dickinson, A., Jones, M., & Milne, E. (2016). Measuring neural excitation and inhibition in autism: Different approaches, different findings and different interpretations. *Brain Research*, *1648*, 277–289. https://doi.org/10.1016/j.brainres.2016.07.011

DiStefano, C., Senturk, D., & Jeste, S. S. (2019). ERP evidence of semantic processing in children with ASD. *Developmental Cognitive Neuroscience*, *36*, 100640. https://doi.org/10.1016/j.dcn.2019.100640

Doesburg, S. M., Tingling, K., MacDonald, M. J., & Pang, E. W. (2015). *Development of Network Synchronization Predicts Language Abilities*. *28*(1).

Doesburg, S. M., Vidal, J., & Taylor, M. J. (2013). Reduced Theta Connectivity during Set-Shifting in Children with Autism. *Frontiers in Human Neuroscience*, *7*. https://doi.org/10.3389/fnhum.2013.00785

Dona, O., Hall, G. B., & Noseworthy, M. D. (2017). Temporal fractal analysis of the rs-BOLD signal identifies brain abnormalities in autism spectrum disorder. *PLOS ONE*, *12*(12), e0190081. https://doi.org/10.1371/journal.pone.0190081

Dong, J., Jing, B., Ma, X., Liu, H., Mo, X., & Li, H. (2018). Hurst Exponent Analysis of Resting-State fMRI Signal Complexity across the Adult Lifespan. *Frontiers in Neuroscience*, *12*, 34. https://doi.org/10.3389/fnins.2018.00034

Donoghue, T., Haller, M., Peterson, E. J., Varma, P., Sebastian, P., Gao, R., Noto, T., Lara, A. H., Wallis, J. D., Knight, R. T., Shestyuk, A., & Voytek, B. (2020). Parameterizing neural power spectra into periodic and aperiodic components. *Nature Neuroscience*, *23*(12), 1655–1665. https://doi.org/10.1038/s41593-020-00744-x

Dunn, M. A., & Bates, J. C. (2005). Developmental change in neutral processing of words by children with autism. *Journal of Autism and Developmental Disorders*, *35*(3), 361–376. https://doi.org/10.1007/s10803-005-3304-3

Dunn, M., Vaughan Jr., H., Kreuzer, J., & Kurtzberg, D. (1999). Electrophysiologic Correlates of Semantic Classification in Autistic and Normal Children. *Developmental Neuropsychology*, *16*(1), 79. https://doi.org/10.1207/S15326942DN160105

Eddy, M. D., Grainger, J., Holcomb, P. J., Mitra, P., & Gabrieli, J. D. E. (2014). Masked priming and ERPs dissociate maturation of orthographic and semantic components of visual word recognition in children. *Psychophysiology*, *51*(2), 136–141. https://doi.org/10.1111/psyp.12164

Edgar, J. C., Dipiero, M., McBride, E., Green, H. L., Berman, J., Ku, M., Liu, S., Blaskey, L., Kuschner, E., Airey, M., Ross, J. L., Bloy, L., Kim, M., Koppers, S., Gaetz, W., Schultz, R. T., & Roberts, T. P. L. (2019). Abnormal maturation of the resting-state peak alpha frequency in children with autism spectrum disorder. *Human Brain Mapping*, *40*(11), 3288–3298. https://doi.org/10.1002/hbm.24598

Eigsti, I.-M., Stevens, M. C., Schultz, R. T., Barton, M., Kelley, E., Naigles, L., Orinstein, A., Troyb, E., & Fein, D. A. (2015). Language comprehension and brain function in individuals with an optimal outcome from autism. *NeuroImage : Clinical*, *10*, 182–191. https://doi.org/10.1016/j.nicl.2015.11.014

Ekstrom, A., Suthana, N., Millett, D., Fried, I., & Bookheimer, S. (2009). Correlation Between BOLD fMRI and Theta-Band Local Field Potentials in the Human Hippocampal Area. *Journal of Neurophysiology*, *101*(5), 2668–2678. https://doi.org/10.1152/jn.91252.2008

Elder, J., Kreider, C., Brasher, S., & Ansell, M. (2017). Clinical impact of early diagnosis of autism on the prognosis and parent-child relationships. *Psychology Research and Behavior Management*, *Volume 10*, 283–292. https://doi.org/10.2147/PRBM.S117499

Elliott, M. L., Knodt, A. R., Ireland, D., Morris, M. L., Poulton, R., Ramrakha, S., Sison, M. L., Moffitt, T. E., Caspi, A., & Hariri, A. R. (2020). What Is the Test-Retest Reliability of Common Task-Functional MRI Measures? New Empirical Evidence and a Meta-Analysis. *Psychological Science*, *31*(7), 792–806. https://doi.org/10.1177/0956797620916786

Engemann, D. A., Kozynets, O., Sabbagh, D., Lemaître, G., Varoquaux, G., Liem, F., & Gramfort, A. (2020). Combining magnetoencephalography with magnetic resonance imaging enhances learning of surrogate-biomarkers. *eLife*, *9*, e54055. https://doi.org/10.7554/eLife.54055

Eyler, L. T., Pierce, K., & Courchesne, E. (2012a). A failure of left temporal cortex to specialize for language is an early emerging and fundamental property of autism. *Brain*, *135*(3), 949–960. https://doi.org/10.1093/brain/awr364

Eyler, L. T., Pierce, K., & Courchesne, E. (2012b). A failure of left temporal cortex to specialize for language is an early emerging and fundamental property of autism. *Brain*, *135*(3), 949–960. https://doi.org/10.1093/brain/awr364

Ferranti, A. S., Luessen, D. J., & Niswender, C. M. (2024). Novel pharmacological targets for GABAergic dysfunction in ADHD. *Neuropharmacology*, *249*, 109897. https://doi.org/10.1016/j.neuropharm.2024.109897

Fiebach, C. J., Friederici, A. D., Müller, K., & Cramon, D. Y. V. (2002). fMRI Evidence for Dual Routes to the Mental Lexicon in Visual Word Recognition. *Journal of Cognitive Neuroscience*, *14*(1), 11–23. https://doi.org/10.1162/089892902317205285

Fischl, B., Sereno, M. I., & Dale, A. M. (1999). *Cortical surface-based analysis: II. Inflation, flattening, and a surface-based coordinate system. 9*(2), 195–207. https://doi.org/doi.org/10.1006/nimg.1998.0396

Fishman, I., Yam, A., Bellugi, U., Lincoln, A., & Mills, D. (2011). Contrasting patterns of language-associated brain activity in autism and Williams syndrome. *Social Cognitive and Affective Neuroscience*, *6*(5), 630–638. https://doi.org/10.1093/scan/nsq075

Flagg, E. J., Cardy, J. E. O., Roberts, W., & Roberts, T. P. L. (2005). Language lateralization development in children with autism: Insights from the late field magnetoencephalogram. *Neuroscience Letters*, *386*(2), 82–87. https://doi.org/10.1016/j.neulet.2005.05.037

Fogassi, L., & Luppino, G. (2005). Motor functions of the parietal lobe. *Current Opinion in Neurobiology*, *15*(6), 626–631. https://doi.org/10.1016/j.conb.2005.10.015

Fox, M. D., & Raichle, M. E. (2007). Spontaneous fluctuations in brain activity observed with functional magnetic resonance imaging. *Nature Reviews Neuroscience*, *8*(9), 700–711. https://doi.org/10.1038/nrn2201

Friedman, L., & Sterling, A. (2019). A review of language, executive function, and intervention in autism spectrum disorder. *Seminars in Speech and Language*, *40*(04), 291–304. https://doi.org/10.1055/s-0039-1692964

Furey, M. L., Tanskanen, T., Beauchamp, M. S., Avikainen, S., Uutela, K., Hari, R., & Haxby, J. V. (2006). Dissociation of face-selective cortical responses by attention. *Proceedings of the National Academy of Sciences*, *103*(4), 1065–1070. https://doi.org/10.1073/pnas.0510124103

Gaffrey, M. S., Kleinhans, N. M., Haist, F., Akshoomoff, N., Campbell, A., Courchesne, E., & Müller, R.-A. (2007). A typical participation of visual cortex during word processing in autism: An fMRI study of semantic decision. *Neuropsychologia*, *45*(8), 1672–1684. https://doi.org/10.1016/j.neuropsychologia.2007.01.008

Gage, N. M., Juranek, J., Filipek, P. A., Osann, K., Flodman, P., Isenberg, A. L., & Spence, M. A. (2009). Rightward hemispheric asymmetries in auditory language cortex in children with autistic disorder: An MRI investigation. *Journal of Neurodevelopmental Disorders*, *1*(3), 205–214. https://doi.org/10.1007/s11689-009-9010-2

Galilee, A., Stefanidou, C., & McCleery, J. P. (2017). Atypical speech versus non-speech detection and discrimination in 4- to 6- yr old children with autism spectrum disorder: An ERP study. *PLoS ONE*, *12*(7), e0181354. https://doi.org/10.1371/journal.pone.0181354

Gao, R., & Penzes, P. (2015). Common Mechanisms of Excitatory and Inhibitory Imbalance in Schizophrenia and Autism Spectrum Disorders. *Current Molecular Medicine*, *15*(2), 146–167.

Gao, R., Peterson, E. J., & Voytek, B. (2017). Inferring synaptic excitation/inhibition balance from field potentials. *NeuroImage*, *158*, 70–78. https://doi.org/10.1016/j.neuroimage.2017.06.078

Gao, Y., Linke, A., Jao Keehn, R. J., Punyamurthula, S., Jahedi, A., Gates, K., Fishman, I., & Müller, R.-A. (2019). The language network in autism: Atypical functional connectivity with default mode and visual regions. *Autism Research*, *12*(9), 1344–1355. https://doi.org/10.1002/aur.2171

Gaudet, I., Hüsser, A., Vannasing, P., & Gallagher, A. (2020). Functional Brain Connectivity of Language Functions in Children Revealed by EEG and MEG: A Systematic Review. *Frontiers in Human Neuroscience*, *14*. https://doi.org/10.3389/fnhum.2020.00062

Gawne, T. J., Overbeek, G. J., Killen, J. F., Reid, M. A., Kraguljac, N. V., Denney, T. S., Ellis, C. A., & Lahti, A. C. (2020). A multimodal magnetoencephalography 7 T fMRI and 7 T proton MR spectroscopy study in first episode psychosis. *Npj Schizophrenia*, *6*(1), 1–9. https://doi.org/10.1038/s41537-020-00113-4

Gerster, M., Waterstraat, G., Litvak, V., Lehnertz, K., Schnitzler, A., Florin, E., Curio, G., & Nikulin, V. (2022). Separating Neural Oscillations from Aperiodic 1/f Activity: Challenges and Recommendations. *Neuroinformatics*, *20*(4), 991–1012. https://doi.org/10.1007/s12021-022-09581-8

Geukes, S., Huster, R. J., Wollbrink, A., Junghöfer, M., Zwitserlood, P., & Dobel, C. (2013). A Large N400 but No BOLD Effect – Comparing Source Activations of Semantic Priming in Simultaneous EEG-fMRI. *PLOS ONE*, *8*(12), e84029. https://doi.org/10.1371/journal.pone.0084029

Glasser, M. F., Coalson, T. S., Robinson, E. C., Hacker, C. D., Harwell, J., Yacoub, E., Ugurbil, K., Andersson, J., Beckmann, C. F., Jenkinson, M., Smith, S. M., & Van Essen, D. C. (2016). A multi-modal parcellation of human cerebral cortex. *Nature*, *536*(7615), 171–178. https://doi.org/10.1038/nature18933

Glover, G. H. (2011). Overview of functional magnetic resonance imaging. *Neurosurgery Clinics of North America*, *22*(2), 133–139. https://doi.org/10.1016/j.nec.2010.11.001

Goense, J., Merkle, H., & Logothetis, N. K. (2012). High-Resolution fMRI Reveals Laminar Differences in Neurovascular Coupling between Positive and Negative BOLD Responses. *Neuron*, *76*(3), 629–639. https://doi.org/10.1016/j.neuron.2012.09.019

Gold, R., Faust, M., & Goldstein, A. (2010). Semantic integration during metaphor comprehension in Asperger syndrome. *Brain and Language*, *113*(3), 124–134. https://doi.org/10.1016/j.bandl.2010.03.002

Gollo, L. L. (2018). Exploring atypical timescales in the brain. *eLife*, *8*, e45089. https://doi.org/10.7554/eLife.45089

Gowen, E., & Hamilton, A. (2013). Motor Abilities in Autism: A Review Using a Computational Context. *Journal of Autism and Developmental Disorders*, *43*(2), 323–344. https://doi.org/10.1007/s10803-012-1574-0

Gramfort, A., Luessi, M., Larson, E., Engemann, D. A., Strohmeier, D., Brodbeck, C., Goj, R., Jas, M., Brooks, T., Parkkonen, L., & Hämäläinen, M. (2013). MEG and EEG data analysis with MNE-Python. *Frontiers in Neuroscience*, *7*, 267. https://doi.org/10.3389/fnins.2013.00267

Green, H. L., Edgar, J. C., Matsuzaki, J., & Roberts, T. P. L. (2020). Magnetoencephalography Research in Pediatric Autism Spectrum Disorder. *Neuroimaging Clinics of North America*, *30*(2), 193–203. https://doi.org/10.1016/j.nic.2020.01.001

Groen, W., Zwiers, M., Vandergaag, R., & Buitelaar, J. (2008). The phenotype and neural correlates of language in autism: An integrative review. *Neuroscience & Biobehavioral Reviews*, *32*(8), 1416–1425. https://doi.org/10.1016/j.neubiorev.2008.05.008

Guo, C. C., Kurth, F., Zhou, J., Mayer, E. A., Eickhoff, S. B., Kramer, J. H., & Seeley, W. W. (2012). One-year test–retest reliability of intrinsic connectivity network fMRI in older adults. *NeuroImage*, *61*(4), 1471–1483. https://doi.org/10.1016/j.neuroimage.2012.03.027

Guo, X., Dominick, K. C., Minai, A. A., Li, H., Erickson, C. A., & Lu, L. J. (2017). Diagnosing Autism Spectrum Disorder from Brain Resting-State Functional Connectivity Patterns Using a Deep Neural Network with a Novel Feature Selection Method. *Frontiers in Neuroscience*, *11*. https://www.frontiersin.org/journals/neuroscience/articles/10.3389/fnins.2017.00460

Gurney, J. G., McPheeters, M. L., & Davis, M. M. (2006). Parental Report of Health Conditions and Health Care Use Among Children With and Without Autism: National Survey of Children's Health. *Archives of Pediatrics & Adolescent Medicine*, *160*(8), 825–830. https://doi.org/10.1001/archpedi.160.8.825

Haebig, E., Kaushanskaya, M., & Ellis Weismer, S. (2015). Lexical processing in school-age children with autism spectrum disorder and children with specific language impairment: The role of semantics. *Journal of Autism and Developmental Disorders*, *45*(12), 4109–4123. https://doi.org/10.1007/s10803-015-2534-2

Halgren, E., Dhond, R. P., Christensen, N., Van Petten, C., Marinkovic, K., Lewine, J. D., & Dale, A. M. (2002). N400-like Magnetoencephalography Responses modulated by semantic context, word frequency, and lexical class in sentences. *NeuroImage*, *17*(3), 1101–1116. https://doi.org/10.1006/nimg.2002.1268

Halgren, E., Kaestner, E., Marinkovic, K., Cash, S. S., Wang, C., Schomer, D. L., Madsen, J. R., & Ulbert, I. (2015). Laminar profile of spontaneous and evoked theta: Rhythmic modulation of cortical processing during word integration. *Neuropsychologia*, *76*, 108–124. https://doi.org/10.1016/j.neuropsychologia.2015.03.021

Hall, E. L., Robson, S. E., Morris, P. G., & Brookes, M. J. (2014). The relationship between MEG and fMRI. *NeuroImage*, *102*, 80–91. https://doi.org/10.1016/j.neuroimage.2013.11.005

Hall, J., McGregor, K. K., & Oleson, J. (2017). Weaknesses in lexical-semantic knowledge among college students with specific learning disabilities: Evidence from a semantic fluency task. *Journal of Speech, Language, and Hearing Research*, *60*(3), 640–653. https://doi.org/10.1044/2016_JSLHR-L-15-0440

Hari, R., & Salmelin, R. (2012). Magnetoencephalography: From SQUIDs to neuroscience. *NeuroImage*, *61*(2), 386–396. https://doi.org/10.1016/j.neuroimage.2011.11.074

Harris, G. J., Chabris, C. F., Clark, J., Urban, T., Aharon, I., Steele, S., McGrath, L., Condouris, K., & Tager-Flusberg, H. (2006). Brain activation during semantic processing in autism spectrum disorders via functional magnetic resonance imaging. *Brain and Cognition*, *61*(1), 54–68. https://doi.org/10.1016/j.bandc.2005.12.015

Hau, J., Baker, A., Chaaban, C., Kohli, J. S., Jao Keehn, R. J., Linke, A. C., Mash, L. E., Wilkinson, M., Kinnear, M. K., Müller, R.-A., & Carper, R. A. (2022). Reduced asymmetry of the hand knob area and decreased sensorimotor u-fiber connectivity in middle-aged adults with autism. *Cortex*, *153*, 110–125. https://doi.org/10.1016/j.cortex.2022.04.004

He, B. J. (2014). Scale-free brain activity: Past, present and future. *Trends in Cognitive Sciences*, *18*(9), 480–487. https://doi.org/10.1016/j.tics.2014.04.003

He, B. J., Zempel, J. M., Snyder, A. Z., & Raichle, M. E. (2010). The Temporal Structures and Functional Significance of Scale-free Brain Activity. *Neuron*, *66*(3), 353–369. https://doi.org/10.1016/j.neuron.2010.04.020

He, B., & Liu, Z. (2008). Multimodal Functional Neuroimaging: Integrating Functional MRI and EEG/MEG. *IEEE Reviews in Biomedical Engineering*, *1*(2008), 23–40. https://doi.org/10.1109/RBME.2008.2008233

Hegarty, J. P., Weber, D. J., Cirstea, C. M., & Beversdorf, D. Q. (2018). Cerebro-Cerebellar Functional Connectivity is Associated with Cerebellar Excitation–Inhibition Balance in Autism Spectrum Disorder. *Journal of Autism and Developmental Disorders*, *48*(10), 3460–3473. https://doi.org/10.1007/s10803-018-3613-y

Heilbronner, S. R., & Hayden, B. Y. (2016). Dorsal Anterior Cingulate Cortex: A Bottom-Up View. *Annual Review of Neuroscience*, *39*(1), 149–170. https://doi.org/10.1146/annurev-neuro-070815-013952

Henderson, L. M., Clarke, P. J., & Snowling, M. J. (2011). Accessing and selecting word meaning in autism spectrum disorder. *Journal of Child Psychology & Psychiatry*, *52*(9), 964–973. https://doi.org/10.1111/j.1469-7610.2011.02393.x

Herringshaw, A. J., Ammons, C. J., DeRamus, T. P., & Kana, R. K. (2016). Hemispheric differences in language processing in autism spectrum disorders: A meta-analysis of neuroimaging studies. *Autism Research*, *9*(10), 1046–1057. https://doi.org/10.1002/aur.1599

Hill, E. L. (2004). Executive dysfunction in autism☆. *Trends in Cognitive Sciences*, *8*(1), 26–32. https://doi.org/10.1016/j.tics.2003.11.003

Hillman, E. M. C. (2014). Coupling Mechanism and Significance of the BOLD Signal: A Status Report. *Annual Review of Neuroscience*, *37*(1), 161–181. https://doi.org/10.1146/annurev-neuro-071013-014111

Hiraishi, H., Kikuchi, M., Yoshimura, Y., Kitagawa, S., Hasegawa, C., Takahashi, T., Suzuki, M., Higashida, H., Asada, M., & Minabe, Y. (2015). Unusual developmental pattern of brain lateralization in young boys with autism spectrum disorder: Power analysis with child-sized magnetoencephalography. *Psychiatry and Clinical Neurosciences*, *69*, 153–160. https://doi.org/10.1111/pcn.12261

Holland, S. K., Vannest, J., Mecoli, M., Jacola, L. M., Tillema, J.-M., Karunanayaka, P. R., Schmithorst, V. J., Yuan, W., Plante, E., & Byars, A. W. (2007). Functional MRI of language lateralization during development in children. *International Journal of Audiology*, *46*(9), 533–551. https://doi.org/10.1080/14992020701448994

Holroyd, C. B., & Umemoto, A. (2016). The research domain criteria framework: The case for anterior cingulate cortex. *Neuroscience & Biobehavioral Reviews*, *71*, 418–443. https://doi.org/10.1016/j.neubiorev.2016.09.021

Hornung, T., Chan, W.-H., Müller, R.-A., Townsend, J., & Keehn, B. (2019). Dopaminergic hypo-activity and reduced theta-band power in autism spectrum disorder: A resting-state EEG study. *International Journal of Psychophysiology*, *146*, 101–106. https://doi.org/10.1016/j.ijpsycho.2019.08.012

Huang, J., Zhu, Z., Zhang, J. X., Wu, M., Chen, H.-C., & Wang, S. (2012). The role of left inferior frontal gyrus in explicit and implicit semantic processing. *Brain Research*, *1440*, 56–64. https://doi.org/10.1016/j.brainres.2011.11.060

Hull, J. V., Dokovna, L. B., Jacokes, Z. J., Torgerson, C. M., Irimia, A., Van Horn, J. D., & the GENDAAR Research Consortium. (2018). Corrigendum: Resting-State Functional Connectivity in Autism Spectrum Disorders: A Review. *Frontiers in Psychiatry*, *9*, 268. https://doi.org/10.3389/fpsyt.2018.00268

Hutchison, R. M., Womelsdorf, T., Allen, E. A., Bandettini, P. A., Calhoun, V. D., Corbetta, M., Della Penna, S., Duyn, J. H., Glover, G. H., Gonzalez-Castillo, J., Handwerker, D. A., Keilholz, S., Kiviniemi, V., Leopold, D. A., de Pasquale, F., Sporns, O., Walter, M., & Chang, C. (2013). Dynamic functional connectivity: Promise, issues, and interpretations. *NeuroImage*, *80*, 360–378. https://doi.org/10.1016/j.neuroimage.2013.05.079

Hutchison, S. M., Müller, U., & Iarocci, G. (2020). Parent Reports of Executive Function Associated with Functional Communication and Conversational Skills Among School Age Children With and Without Autism Spectrum Disorder. *Journal of Autism and Developmental Disorders*, *50*(6), 2019–2029. https://doi.org/10.1007/s10803-019-03958-6

Jafarian, A., Litvak, V., Cagnan, H., Friston, K. J., & Zeidman, P. (2020). Comparing dynamic causal models of neurovascular coupling with fMRI and EEG/MEG. *NeuroImage*, *216*, 116734. https://doi.org/10.1016/j.neuroimage.2020.116734

Jansiewicz, E. M., Goldberg, M. C., Newschaffer, C. J., Denckla, M. B., Landa, R., & Mostofsky, S. H. (2006). Motor Signs Distinguish Children with High Functioning Autism and Asperger's Syndrome from Controls. *Journal of Autism and Developmental Disorders*, *36*(5), 613–621. https://doi.org/10.1007/s10803-006-0109-y

Jochaut, D., Lehongre, K., Saitovitch, A., Devauchelle, A.-D., Olasagasti, I., Chabane, N., Zilbovicius, M., & Giraud, A.-L. (2015). Atypical coordination of cortical oscillations in response to speech in autism. *Frontiers in Human Neuroscience*, *9*. https://doi.org/10.3389/fnhum.2015.00171

Joseph, R. M., McGrath, L. M., & Tager-Flusberg, H. (2005). Executive dysfunction and its relation to language ability in verbal school-age children with autism. *Developmental Neuropsychology*, *27*(3), 361–378. https://doi.org/10.1207/s15326942dn2703_4

Josse, G., & Tzourio-Mazoyer, N. (2004). Hemispheric specialization for language. *Brain Research Reviews*, *44*(1), 1–12. https://doi.org/10.1016/j.brainresrev.2003.10.001

Jouravlev, O., Kell, A. J. E., Mineroff, Z., Haskins, A. J., Ayyash, D., Kanwisher, N., & Fedorenko, E. (2020). Reduced language lateralization in autism and the broader autism phenotype as assessed with robust individual-subjects analyses. *Autism Research*, *13*(10), 1746–1761. https://doi.org/10.1002/aur.2393

Just, M. A., Cherkassky, V. L., Keller, T. A., & Minshew, N. J. (2004). Cortical activation and synchronization during sentence comprehension in high-functioning autism: Evidence of underconnectivity. *Brain*, *127*(8), 1811–1821. https://doi.org/10.1093/brain/awh199

Kamio, Y., Robins, D., Kelley, E., Swainson, B., & Fein, D. (2007). Atypical lexical/semantic processing in high-functioning autism spectrum disorders without early language delay. *Journal of Autism and Developmental Disorders*, *37*(6), 1116–1122. https://doi.org/10.1007/s10803-006-0254-3

Kana, R. K., Keller, T. A., Cherkassky, V. L., Minshew, N. J., & Just, M. A. (2006). Sentence comprehension in autism: Thinking in pictures with decreased functional connectivity. *Brain : A Journal of Neurology*, *129*(0 9), 2484–2493. https://doi.org/10.1093/brain/awl164

Kaufmann, W. E., Kidd, S. A., Andrews, H. F., Budimirovic, D. B., Esler, A., Haas-Givler, B., Stackhouse, T., Riley, C., Peacock, G., Sherman, S. L., Brown, W. T., & Berry-Kravis, E. (2017). Autism Spectrum Disorder in Fragile X Syndrome: Cooccurring Conditions and Current Treatment. *Pediatrics*, *139*(Supplement_3), S194–S206. https://doi.org/10.1542/peds.2016-1159F

Kaushanskaya, M., Park, J. S., Gangopadhyay, I., Davidson, M. M., & Weismer, S. E. (2017). The relationship between executive functions and language abilities in children: A latent variables approach. *Journal of Speech, Language, and Hearing Research*, *60*(4), 912–923. https://doi.org/10.1044/2016_JSLHR-L-15-0310

Kennedy, J. T., Harms, M. P., Korucuoglu, O., Astafiev, S. V., Barch, D. M., Thompson, W. K., Bjork, J. M., & Anokhin, A. P. (2022). Reliability and stability challenges in ABCD task fMRI data. *NeuroImage*, *252*, 119046. https://doi.org/10.1016/j.neuroimage.2022.119046

Kleinhans, N. M., Müller, R.-A., Cohen, D. N., & Courchesne, E. (2008). Atypical functional lateralization of language in autism spectrum disorders. *Brain Research*, *1221*, 115–125. https://doi.org/10.1016/j.brainres.2008.04.080

Klimesch, W. (1999). EEG alpha and theta oscillations reflect cognitive and memory performance: A review and analysis. *Brain Research Reviews*, *29*(2–3), 169–195. https://doi.org/10.1016/S0165-0173(98)00056-3

Knaus, T. A., Burns, C., Kamps, J., & Foundas, A. L. (2017). Atypical activation of action-semantic network in adolescents with autism spectrum disorder. *Brain and Cognition*, *117*, 57–64. https://doi.org/10.1016/j.bandc.2017.06.004

Knaus, T. A., Silver, A. M., Kennedy, M., Lindgren, K. A., Dominick, K. C., Siegel, J., & Tager-Flusberg, H. (2010). Language laterality in autism spectrum disorder and typical controls: A functional, volumetric, and diffusion tensor MRI study. *Brain and Language*, *112*(2), 113–120. https://doi.org/10.1016/j.bandl.2009.11.005

Knaus, T. A., Silver, A. M., Lindgren, K. A., Hadjikhani, N., & Tager-Flusberg, H. (2008). fMRI activation during a language task in adolescents with ASD. *Journal of the International Neuropsychological Society*, *14*(6), 967–979. https://doi.org/10.1017/S1355617708081216

Kotchoubey, B. (2002). Do event-related brain potentials reflect mental (cognitive) operations? *Journal of Psychophysiology*, *16*(3), 129–149. https://doi.org/10.1027//0269-8803.16.3.129

Kouijzer, M. E. J., Van Schie, H. T., De Moor, J. M. H., Gerrits, B. J. L., & Buitelaar, J. K. (2010). Neurofeedback treatment in autism. Preliminary findings in behavioral, cognitive,

and neurophysiological functioning. *Research in Autism Spectrum Disorders*, *4*(3), 386–399. https://doi.org/10.1016/j.rasd.2009.10.007

Kovacevic, S., Azma, S., Irimia, A., Sherfey, J., Halgren, E., & Marinkovic, K. (2012). Theta oscillations are sensitive to both early and late conflict processing stages: Effects of alcohol intoxication. *PLoS ONE*, *7*(8), e43957. https://doi.org/10.1371/journal.pone.0043957

Kragel, P. A., Han, X., Kraynak, T. E., Gianaros, P. J., & Wager, T. D. (2021). Functional MRI Can Be Highly Reliable, but It Depends on What You Measure: A Commentary on Elliott et al. (2020). *Psychological Science*, *32*(4), 622–626. https://doi.org/10.1177/0956797621989730

Kujala, J., Sudre, G., Vartiainen, J., Liljeström, M., Mitchell, T., & Salmelin, R. (2014). Multivariate analysis of correlation between electrophysiological and hemodynamic responses during cognitive processing. *NeuroImage*, *92*, 207–216. https://doi.org/10.1016/j.neuroimage.2014.01.057

Kundu, P., Brenowitz, N. D., Voon, V., Worbe, Y., Vértes, P. E., Inati, S. J., Saad, Z. S., Bandettini, P. A., & Bullmore, E. T. (2013). Integrated strategy for improving functional connectivity mapping using multiecho fMRI. *Proceedings of the National Academy of Sciences of the United States of America*, *110*(40), 16187–16192.

Kundu, P., Inati, S. J., Evans, J. W., Luh, W.-M., & Bandettini, P. A. (2012). Differentiating BOLD and non-BOLD signals in fMRI time series using multi-echo EPI. *NeuroImage*, *60*(3), 1759–1770. https://doi.org/10.1016/j.neuroimage.2011.12.028

Kuperman, V., Stadthagen-Gonzalez, H., & Brysbaert, M. (2012). Age-of-acquisition ratings for 30,000 English words. *Behavior Research Methods*, *44*(4), 978–990. https://doi.org/10.3758/s13428-012-0210-4

Kutas, M., & Federmeier, K. D. (2000). Electrophysiology reveals semantic memory use in language comprehension. *Trends in Cognitive Sciences*, *4*(12), 463–470. https://doi.org/10.1016/S1364-6613(00)01560-6

Kutas, M., & Hillyard, S. A. (1980). Reading Senseless sentences: Brain potentials reflect semantic incongruity. *Science*, *207*(4427), 203–205.

Lachaux, J., Rodriguez, E., Martinerie, J., & Varela, F. J. (1999). Measuring phase synchrony in brain signals. *Human Brain Mapping*, *8*(4), 194–208. https://doi.org/10.1002/(SICI)1097-0193(1999)8:4<194::AID-HBM4>3.0.CO;2-C

Lai, M.-C., Lombardo, M. V., Chakrabarti, B., Sadek, S. A., Pasco, G., Wheelwright, S. J., Bullmore, E. T., Baron-Cohen, S., & Suckling, J. (2010). A Shift to Randomness of Brain Oscillations in People with Autism. *Biological Psychiatry*, *68*(12), 1092–1099. https://doi.org/10.1016/j.biopsych.2010.06.027

Lajiness-O'Neill, R., Bowyer, S. M., Moran, J. E., Zillgitt, A., Richard, A. E., & Boutros, N. N. (2014). Neurophysiological findings from magnetoencephalography in autism spectrum disorder: A comprehensive review. *Future Neurology*.

Lankinen, K., Saari, J., Hlushchuk, Y., Tikka, P., Parkkonen, L., Hari, R., & Koskinen, M. (2018). Consistency and similarity of MEG- and fMRI-signal time courses during movie viewing. *NeuroImage, 173*, 361–369. https://doi.org/10.1016/j.neuroimage.2018.02.045

Larrain-Valenzuela, J., Zamorano, F., Soto-Icaza, P., Carrasco, X., Herrera, C., Daiber, F., Aboitiz, F., & Billeke, P. (2017). Theta and Alpha Oscillation Impairments in Autistic Spectrum Disorder Reflect Working Memory Deficit. *Scientific Reports, 7*, 14328. https://doi.org/10.1038/s41598-017-14744-8

Larson, C., Thomas, H. R., Crutcher, J., Stevens, M. C., & Eigsti, I.-M. (2023). Language Networks in Autism Spectrum Disorder: A systematic review of connectivity-based fMRI studies. *Review Journal of Autism and Developmental Disorders*. https://doi.org/10.1007/s40489-023-00382-6

Lee, E., Lee, J., & Kim, E. (2017). Excitation/Inhibition Imbalance in Animal Models of Autism Spectrum Disorders. *Biological Psychiatry*, *81*(10), 838–847. https://doi.org/10.1016/j.biopsych.2016.05.011

Lee, Y., Park, B., James, O., Kim, S.-G., & Park, H. (2017). Autism spectrum disorder related functional connectivity changes in the language network in children, adolescents and adults. *Frontiers in Human Neuroscience*, *11*, 418. https://doi.org/10.3389/fnhum.2017.00418

Legget, K. T., Hild, A. K., Steinmetz, S. E., Simon, S. T., & Rojas, D. C. (2017). MEG and EEG demonstrate similar test-retest reliability of the 40 Hz auditory steady-state response. *International Journal of Psychophysiology*, *114*, 16–23. https://doi.org/10.1016/j.ijpsycho.2017.01.013

Lehto, J. E., Juujärvi, P., Kooistra, L., & Pulkkinen, L. (2003). Dimensions of executive functioning: Evidence from children. *British Journal of Developmental Psychology*, *21*(1), 59–80. https://doi.org/10.1348/026151003321164627

Leminen, A., Smolka, E., Duñabeitia, J. A., & Pliatsikas, C. (2019). Morphological processing in the brain: The good (inflection), the bad (derivation) and the ugly (compounding). *Cortex*, *116*, 4–44. https://doi.org/10.1016/j.cortex.2018.08.016

Lendner, J. D., Helfrich, R. F., Mander, B. A., Romundstad, L., Lin, J. J., Walker, M. P., Larsson, P. G., & Knight, R. T. (2020). An electrophysiological marker of arousal level in humans. *eLife*, *9*, e55092. https://doi.org/10.7554/eLife.55092

Lenroot, R. K., & Yeung, P. K. (2013). Heterogeneity within Autism Spectrum Disorders: What have We Learned from Neuroimaging Studies? *Frontiers in Human Neuroscience, 7*. https://doi.org/10.3389/fnhum.2013.00733

Levin, A. R., Naples, A. J., Scheffler, A. W., Webb, S. J., Shic, F., Sugar, C. A., Murias, M., Bernier, R. A., Chawarska, K., Dawson, G., Faja, S., Jeste, S., Nelson, C. A., McPartland, J. C., Şentürk, D., & Trials, and the A. B. C. for C. (2020). Day-to-Day Test-Retest Reliability of EEG Profiles in Children With Autism Spectrum Disorder and Typical Development. *Frontiers in Integrative Neuroscience*, *14*. https://doi.org/10.3389/fnint.2020.00021

Liang, A., Wu, H., Ma, Y., Liang, X., Jia, Y., Gao, Y., Ning, X., & Fang, J. (2021). Whole-Head Magnetoencephalogram and Its Application in Developmental Communication Disorders Research: A Review. *IEEE Access*, *9*, 42515–42532. https://doi.org/10.1109/ACCESS.2021.3063054

Liljeström, M., Hultén, A., Parkkonen, L., & Salmelin, R. (2009). Comparing MEG and fMRI views to naming actions and objects. *Human Brain Mapping*, *30*(6), 1845–1856. https://doi.org/10.1002/hbm.20785

Lindell, A. K., & Hudry, K. (2013). Atypicalities in cortical structure, handedness, and functional lateralization for language in autism spectrum disorders. *Neuropsychology Review*, *23*(3), 257–270. https://doi.org/10.1007/s11065-013-9234-5

Liss, M., Harel, B., Fein, D., Allen, D., Dunn, M., Feinstein, C., Morris, R., Waterhouse, L., & Rapin, I. (2001). *Predictors and Correlates of Adaptive Functioning in Children with Developmental Disorders*.

Liu, S., Cai, W., Liu, S., Zhang, F., Fulham, M., Feng, D., Pujol, S., & Kikinis, R. (2015). Multimodal neuroimaging computing: A review of the applications in neuropsychiatric disorders. *Brain Informatics*, *2*(3), 167–180. https://doi.org/10.1007/s40708-015-0019-x

Liu, Y., Ouyang, P., Zheng, Y., Mi, L., Zhao, J., Ning, Y., & Guo, W. (2021). A Selective Review of the Excitatory-Inhibitory Imbalance in Schizophrenia: Underlying Biology, Genetics, Microcircuits, and Symptoms. *Frontiers in Cell and Developmental Biology*, *9*, 664535. https://doi.org/10.3389/fcell.2021.664535

Lo, Y.-C., Chou, T.-L., Fan, L.-Y., Gau, S. S.-F., Chiu, Y.-N., & Tseng, W.-Y. I. (2013). Altered Structure–Function Relations of Semantic Processing in Youths with High-Functioning Autism: A Combined Diffusion and Functional MRI Study. *Autism Research*, *6*(6), 561–570. https://doi.org/10.1002/aur.1315

Löfkvist, U., Almkvist, O., Lyxell, B., & Tallberg, I.-M. (2014). Lexical and semantic ability in groups of children with cochlear implants, language impairment and autism spectrum disorder. *International Journal of Pediatric Otorhinolaryngology*, *78*(2), 253–263. https://doi.org/10.1016/j.ijporl.2013.11.017

Lombardi, F., Herrmann, H. J., & de Arcangelis, L. (2017). Balance of excitation and inhibition determines 1/f power spectrum in neuronal networks. *Chaos: An Interdisciplinary Journal of Nonlinear Science*, *27*(4), 047402. https://doi.org/10.1063/1.4979043

Lombardo, M. V., Lai, M.-C., & Baron-Cohen, S. (2019). Big data approaches to decomposing heterogeneity across the autism spectrum. *Molecular Psychiatry*, *24*(10), 1435–1450. https://doi.org/10.1038/s41380-018-0321-0

Lord, C., Elsabbagh, M., Baird, G., & Veenstra-Vanderweele, J. (2018). Autism spectrum disorder. *The Lancet*, *392*(10146), 508–520. https://doi.org/10.1016/S0140-6736(18)31129-2

Lord, C., Rutter, M., DiLavore, P. C., Risi, S., Gotham, K., & Bishop, S. (2012). *Autism Diagnostic Observation Schedule* (Second). Western Psychological Services. https://www.wpspublish.com/ados-2-autism-diagnostic-observation-schedule-second-edition

Loucas, T., Charman, T., Pickles, A., Simonoff, E., Chandler, S., Meldrum, D., & Baird, G. (2008). Autistic symptomatology and language ability in autism spectrum disorder and specific language impairment. *Journal of Child Psychology and Psychiatry*, *49*(11), 1184–1192. https://doi.org/10.1111/j.1469-7610.2008.01951.x

Lütkenhöner, B. (2003). Magnetoencephalography and its Achilles' heel. *Journal of Physiology-Paris*, *97*(4–6), 641–658. https://doi.org/10.1016/j.jphysparis.2004.01.020

Luu, P., & Tucker, D. M. (2001). Regulating action: Alternating activation of midline frontal and motor cortical networks. *Clinical Neurophysiology*, *112*(7), 1295–1306. https://doi.org/10.1016/S1388-2457(01)00559-4

Lv, H., Wang, Z., Tong, E., Williams, L. M., Zaharchuk, G., Zeineh, M., Goldstein-Piekarski, A. N., Ball, T. M., Liao, C., & Wintermark, M. (2018). Resting-State Functional MRI: Everything That Nonexperts Have Always Wanted to Know. *AJNR: American Journal of Neuroradiology*, *39*(8), 1390–1399. https://doi.org/10.3174/ajnr.A5527

Lynch, C. J., Power, J. D., Scult, M. A., Dubin, M., Gunning, F. M., & Liston, C. (2020). Rapid precision functional mapping of individuals using multi-echo fMRI. *Cell Reports*, *33*(12). https://doi.org/10.1016/j.celrep.2020.108540

Maenner, M. J., Warren, Z., Williams, A. R., Amoakohene, E., Bakian, A. V., Bilder, D. A., Durkin, M. S., Fitzgerald, R. T., Furnier, S. M., Hughes, M. M., Ladd-Acosta, C. M., McArthur, D., Pas, E. T., Salinas, A., Vehorn, A., Williams, S., Esler, A., Grzybowski, A., Hall-Lande, J., … Shaw, K. A. (2023). Prevalence and characteristics of autism spectrum disorder among children aged 8 years—Autism and Developmental Disabilities Monitoring Network, 11 sites, United States, 2020. *MMWR Surveillance Summaries*, *72*(SS-2), 1–14. http://dx.doi.org/10.15585/mmwr.ss7202a1

Mamiya, P. C., Arnett, A. B., & Stein, M. A. (2021). Precision Medicine Care in ADHD: The Case for Neural Excitation and Inhibition. *Brain Sciences*, *11*(1), 91. https://doi.org/10.3390/brainsci11010091

Maniscalco, B., Lee, J. L., Abry, P., Lin, A., Holroyd, T., & He, B. J. (2018). Neural Integration of Stimulus History Underlies Prediction for Naturalistically Evolving Sequences.

Journal of Neuroscience, *38*(6), 1541–1557. https://doi.org/10.1523/JNEUROSCI.1779-17.2017

Mariani, J., Coppola, G., Zhang, P., Abyzov, A., Provini, L., Tomasini, L., Amenduni, M., Szekely, A., Palejev, D., Wilson, M., Gerstein, M., Grigorenko, E. L., Chawarska, K., Pelphrey, K. A., Howe, J. R., & Vaccarino, F. M. (2015). FOXG1-Dependent Dysregulation of GABA/Glutamate Neuron Differentiation in Autism Spectrum Disorders. *Cell*, *162*(2), 375–390. https://doi.org/10.1016/j.cell.2015.06.034

Marinkovic, K. (2004a). Spatiotemporal dynamics of word processing in the human cortex. *The Neuroscientist*, *10*(2), 142–152. https://doi.org/10.1177/1073858403261018

Marinkovic, K. (2004b). Spatiotemporal dynamics of word processing in the human cortex. *The Neuroscientist*, *10*(2), 142–152. https://doi.org/10.1177/1073858403261018

Marinkovic, K., Beaton, L. E., Rosen, B. Q., Happer, J. P., & Wagner, L. C. (2019). Disruption of frontal lobe neural synchrony during cognitive control by alcohol intoxication. *Journal of Visualized Experiments*, *144*, e58839. https://doi.org/10.3791/58839

Marinkovic, K., Dhond, R. P., Dale, A. M., Glessner, M., Carr, V., & Halgren, E. (2003). Spatiotemporal Dynamics of Modality-Specific and Supramodal Word Processing. *Neuron*, *38*(3), 487–497. https://doi.org/10.1016/S0896-6273(03)00197-1

Marinkovic, K., Rosen, B. Q., Cox, B., & Hagler, D. J. (2014). Spatio-temporal processing of words and nonwords: Hemispheric laterality and acute alcohol intoxication. *Brain Research*, *1558*, 18–32. https://doi.org/10.1016/j.brainres.2014.02.030

Marinkovic, K., Rosen, B. Q., Cox, B., & Kovacevic, S. (2012). Event-related theta power during lexical-semantic retrieval and decision conflict is modulated by alcohol intoxication: Anatomically constrained MEG. *Frontiers in Psychology*, *3*, 121. https://doi.org/10.3389/fpsyg.2012.00121

Martín-Buro, M. C., Garcés, P., & Maestú, F. (2015). Test-retest reliability of resting-state magnetoencephalography power in sensor and source space. *Human Brain Mapping*, *37*(1), 179–190. https://doi.org/10.1002/hbm.23027

Mash, L. E., Reiter, M. A., Linke, A. C., Townsend, J., & Müller, R. (2018). Multimodal approaches to functional connectivity in autism spectrum disorders: An integrative perspective. *Developmental Neurobiology*, *78*(5), 456–473. https://doi.org/10.1002/dneu.22570

Masi, A., DeMayo, M. M., Glozier, N., & Guastella, A. J. (2017). An Overview of Autism Spectrum Disorder, Heterogeneity and Treatment Options. *Neuroscience Bulletin*, *33*(2), 183–193. https://doi.org/10.1007/s12264-017-0100-y

Matson, J. L., Kozlowski, A. M., & Matson, M. M. (2012). Speech deficits in persons with autism: Etiology and symptom presentation. *Research in Autism Spectrum Disorders*, *6*(2), 573–577. https://doi.org/10.1016/j.rasd.2011.10.009

Matsuzaki, J., Berman, J. I., Blaskey, L., Kuschner, E. S., Gaetz, L., Mukherjee, P., Buckner, R. L., Nagarajan, S. S., Chung, W. K., Sherr, E. H., & Roberts, T. P. L. (2020). Abnormal Auditory Mismatch Fields in Children and Adolescents With 16p11.2 Deletion and 16p11.2 Duplication. *Biological Psychiatry: Cognitive Neuroscience and Neuroimaging*, *5*(10), 942–950. https://doi.org/10.1016/j.bpsc.2019.11.005

Maximo, J., Keown, C., Nair, A., & Müller, R.-A. (2013). Approaches to local connectivity in autism using resting state functional connectivity MRI. *Frontiers in Human Neuroscience*, *7*. https://www.frontiersin.org/articles/10.3389/fnhum.2013.00605

May, K. E., & Kana, R. K. (2020). Frontoparietal Network in Executive Functioning in Autism Spectrum Disorder. *Autism Research*, *13*(10), 1762–1777. https://doi.org/10.1002/aur.2403

May, T., Rinehart, N., Wilding, J., & Cornish, K. (2013). The Role of Attention in the Academic Attainment of Children with Autism Spectrum Disorder. *Journal of Autism and Developmental Disorders*, *43*(9), 2147–2158. https://doi.org/10.1007/s10803-013-1766-2

Mazzoni, A., Panzeri, S., Logothetis, N. K., & Brunel, N. (2008). Encoding of Naturalistic Stimuli by Local Field Potential Spectra in Networks of Excitatory and Inhibitory Neurons. *PLoS Computational Biology*, *4*(12), e1000239. https://doi.org/10.1371/journal.pcbi.1000239

McCleery, J. P., Ceponiene, R., Burner, K. M., Townsend, J., Kinnear, M., & Schreibman, L. (2010). Neural correlates of verbal and nonverbal semantic integration in children with autism spectrum disorders. *Journal of Child Psychology and Psychiatry*, *51*(3), 277–286. https://doi.org/10.1111/j.1469-7610.2009.02157.x

McDonald, C. R., Thesen, T., Carlson, C., Blumberg, M., Girard, H. M., Trongnetrpunya, A., Sherfey, J. S., Devinsky, O., Kuzniecky, R., Dolye, W. K., Cash, S. S., Leonard, M. K., Hagler, D. J., Dale, A. M., & Halgren, E. (2010). Multimodal imaging of repetition priming: Using fMRI, MEG, and intracranial EEG to reveal spatiotemporal profiles of word processing. *NeuroImage*, *53*(2), 707–717. https://doi.org/10.1016/j.neuroimage.2010.06.069

McFadden, K. L., & Rojas, D. C. (2013). Electrophysiology of Autism. In M. Fitzgerald (Ed.), *Recent Advances in Autism Spectrum Disorders* (Vol. 2). IntechOpen. https://directory.doabooks.org/handle/20.500.12854/66450

McGregor, K. K., Berns, A. J., Owen, A. J., Michels, S. A., Duff, D., Bahnsen, A. J., & Lloyd, M. (2012). Associations Between Syntax and the Lexicon Among Children With or Without ASD and Language Impairment. *Journal of Autism and Developmental Disorders*, *42*(1), 35–47. https://doi.org/10.1007/s10803-011-1210-4

Meltzer, J. A., Negishi, M., Mayes, L. C., & Constable, R. T. (2007). Individual differences in EEG theta and alpha dynamics during working memory correlate with fMRI responses across subjects. *Clinical Neurophysiology: Official Journal of the International*

Federation of Clinical Neurophysiology, *118*(11), 2419–2436. https://doi.org/10.1016/j.clinph.2007.07.023

Ming, X., Brimacombe, M., & Wagner, G. C. (2007). Prevalence of motor impairment in autism spectrum disorders. *Brain and Development*, *29*(9), 565–570. https://doi.org/10.1016/j.braindev.2007.03.002

Miskovic, V., MacDonald, K. J., Rhodes, L. J., & Cote, K. A. (2018). Changes in EEG multiscale entropy and power-law frequency scaling during the human sleep cycle. *Human Brain Mapping*, *40*(2), 538–551. https://doi.org/10.1002/hbm.24393

Mody, M., Manoach, D. S., Guenther, F. H., Kenet, T., Bruno, K. A., McDougle, C. J., & Stigler, K. A. (2013). Speech and language in autism spectrum disorder: A view through the lens of behavior and brain imaging. *Neuropsychiatry*, *3*(2), 223–233. https://doi.org/10.2217/npy.13.19

Molina, J. L., Voytek, B., Thomas, M. L., Joshi, Y. B., Bhakta, S. G., Talledo, J. A., Swerdlow, N. R., & Light, G. A. (2020). Memantine effects on EEG measures of putative excitatory/inhibitory balance in schizophrenia. *Biological Psychiatry. Cognitive Neuroscience and Neuroimaging*, *5*(6), 562–568. https://doi.org/10.1016/j.bpsc.2020.02.004

Moore-Parks, E. N., Burns, E. L., Bazzill, R., Levy, S., Posada, V., & Müller, R.-A. (2010). An fMRI study of sentence-embedded lexical-semantic decision in children and adults. *Brain and Language*, *114*(2), 90–100. https://doi.org/10.1016/j.bandl.2010.03.009

Moseley, R. L., Mohr, B., Lombardo, M. V., Baron-Cohen, S., Hauk, O., & Pulvermüller, F. (2013). Brain and behavioral correlates of action semantic deficits in autism. *Frontiers in Human Neuroscience*, *7*. https://doi.org/10.3389/fnhum.2013.00725

Mostofsky, S. H., & Ewen, J. B. (2011). Altered Connectivity and Action Model Formation in Autism Is Autism. *The Neuroscientist : A Review Journal Bringing Neurobiology, Neurology and Psychiatry*, *17*(4), 437–448. https://doi.org/10.1177/1073858410392381

Naigles, L., & Tek, S. (2017). 'Form is easy, meaning is hard' revisited: (Re) characterizing the strengths and weaknesses of language in children with autism spectrum disorder—Naigles—2017—WIREs Cognitive Science—Wiley Online Library. *WIREs: Cognitive Science*, *8:e1438*. https://doi.org/10.1002/wcs.1438

Nebel, M. B., Joel, S. E., Muschelli, J., Barber, A. D., Caffo, B. S., Pekar, J. J., & Mostofsky, S. H. (2014). Disruption of functional organization within the primary motor cortex in children with autism. *Human Brain Mapping*, *35*(2), 567–580. https://doi.org/10.1002/hbm.22188

Nelson, S. B., & Valakh, V. (2015). Excitatory/Inhibitory Balance and Circuit Homeostasis in Autism Spectrum Disorders. *Neuron*, *87*(4), 684–698. https://doi.org/10.1016/j.neuron.2015.07.033

Nentwich, M., Ai, L., Madsen, J., Telesford, Q. K., Haufe, S., Milham, M. P., & Parra, L. C. (2020). Functional connectivity of EEG is subject-specific, associated with phenotype, and different from fMRI. *NeuroImage*, *218*, 117001. https://doi.org/10.1016/j.neuroimage.2020.117001

Nettekoven, C., Reck, N., Goldbrunner, R., Grefkes, C., & Weiß Lucas, C. (2018). Short- and long-term reliability of language fMRI. *NeuroImage*, *176*, 215–225. https://doi.org/10.1016/j.neuroimage.2018.04.050

Nielsen, J. A., Zielinski, B. A., Fletcher, P. T., Alexander, A. L., Lange, N., Bigler, E. D., Lainhart, J. E., & Anderson, J. S. (2014). Abnormal lateralization of functional connectivity between language and default mode regions in autism. *Molecular Autism*, *5*, 8. https://doi.org/10.1186/2040-2392-5-8

Norbury, C. F., Griffiths, H., & Nation, K. (2010). Sound before meaning: Word learning in autistic disorders. *Neuropsychologia*, *48*(14), 4012–4019. https://doi.org/10.1016/j.neuropsychologia.2010.10.015

Olafsson, V., Kundu, P., Wong, E. C., Bandettini, P. A., & Liu, T. T. (2015). Enhanced identification of BOLD-like components with multi-echo simultaneous multi-slice (MESMS) fMRI and multi-echo ICA. *NeuroImage*, *112*, 43–51. https://doi.org/10.1016/j.neuroimage.2015.02.052

Oldfield, R. C. (1971). The assessment and analysis of handedness: The Edinburgh inventory. *Neuropsychologia*, *9*(1), 97–113. https://doi.org/10.1016/0028-3932(71)90067-4

Oostenveld, R., Fries, P., Maris, E., & Schoffelen, J.-M. (2011). FieldTrip: Open source software for advanced analysis of MEG, EEG, and invasive electrophysiological data. *Computational Intelligence and Neuroscience*, *2011*, 156869. https://doi.org/10.1155/2011/156869

O'Reilly, C., Lewis, J. D., & Elsabbagh, M. (2017). Is functional brain connectivity atypical in autism? A systematic review of EEG and MEG studies. *PLoS ONE*, *12*(5), e0175870. https://doi.org/10.1371/journal.pone.0175870

O'Rourke, E., & Coderre, E. L. (2021). Implicit semantic processing of linguistic and non-linguistic stimuli in adults with autism spectrum disorder. *Journal of Autism and Developmental Disorders*, *51*(8), 2611–2630. https://doi.org/10.1007/s10803-020-04736-5

Ortiz-Mantilla, S., Cantiani, C., Shafer, V. L., & Benasich, A. A. (2019). Minimally-verbal children with autism show deficits in theta and gamma oscillations during processing of semantically-related visual information. *Scientific Reports*, *9*(1), 5072. https://doi.org/10.1038/s41598-019-41511-8

Padmanabhan, P., Nedumaran, A. M., Mishra, S., Pandarinathan, G., Archunan, G., & Gulyás, B. (2017). The Advents of Hybrid Imaging Modalities: A New Era in Neuroimaging

Applications. *Advanced Biosystems*, *1*(8), 1700019. https://doi.org/10.1002/adbi.201700019

Parkes, L., Perry, C., & Goodin, P. (2016). Examining the N400m in affectively negative sentences: A magnetoencephalography study. *Psychophysiology*, *53*(5), 689–704. https://doi.org/10.1111/psyp.12601

Patrick, G. (2010). Evolutionary Depth of Human Brain Language Areas. In *The Two Halves of the Brain*. The MIT Press.

Petro, N. M., Ott, L. R., Penhale, S. H., Rempe, M. P., Embury, C. M., Picci, G., Wang, Y.-P., Stephen, J. M., Calhoun, V. D., & Wilson, T. W. (2022). Eyes-closed versus eyes-open differences in spontaneous neural dynamics during development. *NeuroImage*, *258*, 119337. https://doi.org/10.1016/j.neuroimage.2022.119337

Phan, L., Tariq, A., Lam, G., Mirza, M., Paiva, D., Lazic, M., Emami, Z., Anagnostou, E., Gordon, K. A., & Pang, E. W. (2023). Children with autism spectrum disorder who demonstrate normal language scores use a bottom-up semantic processing strategy: Evidence from N400 recordings. *Brain and Behavior*, *13*(9), e3158. https://doi.org/10.1002/brb3.3158

Picci, G., Gotts, S. J., & Scherf, K. S. (2016). A theoretical rut: Revisiting and critically evaluating the generalized under/over-connectivity hypothesis of autism. *Developmental Science*, *19*(4), 524–549. https://doi.org/10.1111/desc.12467

Pierce, K., Gazestani, V. H., Bacon, E., Barnes, C. C., Cha, D., Nalabolu, S., Lopez, L., Moore, A., Pence-Stophaeros, S., & Courchesne, E. (2019). Evaluation of the Diagnostic Stability of the Early Autism Spectrum Disorder Phenotype in the General Population Starting at 12 Months. *JAMA Pediatrics*, *173*(6), 578–587. https://doi.org/10.1001/jamapediatrics.2019.0624

Pijnacker, J., Geurts, B., van Lambalgen, M., Buitelaar, J., & Hagoort, P. (2010). Exceptions and anomalies: An ERP study on context sensitivity in autism. *Neuropsychologia*, *48*(10), 2940–2951. https://doi.org/10.1016/j.neuropsychologia.2010.06.003

Plichta, M. M., Schwarz, A. J., Grimm, O., Morgen, K., Mier, D., Haddad, L., Gerdes, A. B. M., Sauer, C., Tost, H., Esslinger, C., Colman, P., Wilson, F., Kirsch, P., & Meyer-Lindenberg, A. (2012). Test–retest reliability of evoked BOLD signals from a cognitive–emotive fMRI test battery. *NeuroImage*, *60*(3), 1746–1758. https://doi.org/10.1016/j.neuroimage.2012.01.129

Podvalny, E., Noy, N., Harel, M., Bickel, S., Chechik, G., Schroeder, C. E., Mehta, A. D., Tsodyks, M., & Malach, R. (2015). A unifying principle underlying the extracellular field potential spectral responses in the human cortex. *Journal of Neurophysiology*, *114*(1), 505–519. https://doi.org/10.1152/jn.00943.2014

Port, R. G., Oberman, L. M., & Roberts, T. P. (2019). Revisiting the excitation/inhibition imbalance hypothesis of ASD through a clinical lens. *The British Journal of Radiology*, *92*(1101), 20180944. https://doi.org/10.1259/bjr.20180944

Posner, M. I., Rothbart, M. K., Sheese, B. E., & Tang, Y. (2007). The anterior cingulate gyrus and the mechanism of self-regulation. *Cognitive, Affective, & Behavioral Neuroscience*, *7*(4), 391–395. https://doi.org/10.3758/CABN.7.4.391

Preslar, J., Kushner, H. I., Marino, L., & Pearce, B. (2014). Autism, lateralisation, and handedness: A review of the literature and meta-analysis: Laterality. *Laterality*, *19*(1), 64–95. https://doi.org/10.1080/1357650X.2013.772621

Price, C. J. (2010). The anatomy of language: A review of 100 fMRI studies published in 2009. *Annals of the New York Academy of Sciences*, *1191*(1), 62–88. https://doi.org/10.1111/j.1749-6632.2010.05444.x

Pu, Y., Cheyne, D., Sun, Y., & Johnson, B. W. (2020). Theta oscillations support the interface between language and memory. *NeuroImage*, *215*, 116782. https://doi.org/10.1016/j.neuroimage.2020.116782

Pylkkänen, L., & Marantz, A. (2003). Tracking the time course of word recognition with MEG. *Trends in Cognitive Sciences*, *7*(5), 187–189. https://doi.org/10.1016/S1364-6613(03)00092-5

Rajan, A., Siegel, S. N., Liu, Y., Bengson, J., Mangun, G. R., & Ding, M. (2019). Theta Oscillations Index Frontal Decision-Making and Mediate Reciprocal Frontal–Parietal Interactions in Willed Attention. *Cerebral Cortex*, *29*(7), 2832–2843. https://doi.org/10.1093/cercor/bhy149

Rane, P., Cochran, D., Hodge, S. M., Haselgrove, C., Kennedy, D., & Frazier, J. A. (2015). Connectivity in Autism: A review of MRI connectivity studies. *Harvard Review of Psychiatry*, *23*(4), 223–244. https://doi.org/10.1097/HRP.0000000000000072

Reynell, C., & Harris, J. J. (2013). The BOLD signal and neurovascular coupling in autism. *Developmental Cognitive Neuroscience*, *6*, 72–79. https://doi.org/10.1016/j.dcn.2013.07.003

Robinson, S., Goddard, L., Dritschel, B., Wisley, M., & Howlin, P. (2009). Executive functions in children with Autism Spectrum Disorders. *Brain and Cognition*, *71*(3), 362–368. https://doi.org/10.1016/j.bandc.2009.06.007

Robitaille, N., Marois, R., Todd, J., Grimault, S., Cheyne, D., & Jolicœur, P. (2010). Distinguishing between lateralized and nonlateralized brain activity associated with visual short-term memory: fMRI, MEG, and EEG evidence from the same observers. *NeuroImage*, *53*(4), 1334–1345. https://doi.org/10.1016/j.neuroimage.2010.07.027

Roche, K. J., LeBlanc, J. J., Levin, A. R., O'Leary, H. M., Baczewski, L. M., & Nelson, C. A. (2019). Electroencephalographic spectral power as a marker of cortical function and

disease severity in girls with Rett syndrome. *Journal of Neurodevelopmental Disorders*, *11*(1), 15. https://doi.org/10.1186/s11689-019-9275-z

Rosen, B. Q., Padovan, N., & Marinkovic, K. (2016). Alcohol hits you when it is hard: Intoxication, task difficulty, and theta brain oscillations. *Alcoholism: Clinical and Experimental Research*, *40*(4), 743–752. https://doi.org/10.1111/acer.13014

Rubenstein, J. L. R., & Merzenich, M. M. (2003). Model of autism: Increased ratio of excitation/inhibition in key neural systems. *Genes, Brain, and Behavior*, *2*(5), 255–267.

Ruff, I., Blumstein, S. E., Myers, E. B., & Hutchison, E. (2008). Recruitment of anterior and posterior structures in lexical–semantic processing: An fMRI study comparing implicit and explicit tasks. *Brain and Language*, *105*(1), 41–49. https://doi.org/10.1016/j.bandl.2008.01.003

Russo, N., Mottron, L., Burack, J. A., & Jemel, B. (2012). Parameters of semantic multisensory integration depend on timing and modality order among people on the autism spectrum: Evidence from event-related potentials. *Neuropsychologia*, *50*(9), 2131–2141. https://doi.org/10.1016/j.neuropsychologia.2012.05.003

Rutter, M., LeCouteur, A., & Lord, C. (2003). *Autism Diagnostic Interview-Revised Manual*. Western Psychological Services.

Sahyoun, C. P., Belliveau, J. W., Soulières, I., Schwartz, S., & Mody, M. (2010). Neuroimaging of the functional and structural networks underlying visuospatial vs. Linguistic reasoning in high-functioning autism. *Neuropsychologia*, *48*(1), 86–95. https://doi.org/10.1016/j.neuropsychologia.2009.08.013

Salem, A. C., MacFarlane, H., Adams, J. R., Lawley, G. O., Dolata, J. K., Bedrick, S., & Fombonne, E. (2021). Evaluating atypical language in autism using automated language measures. *Scientific Reports*, *11*(1), Article 1. https://doi.org/10.1038/s41598-021-90304-5

Sanfratello, L., Houck, J. M., & Calhoun, V. D. (2019). Dynamic Functional Network Connectivity in Schizophrenia with Magnetoencephalography and Functional Magnetic Resonance Imaging: Do Different Timescales Tell a Different Story? *Brain Connectivity*, *9*(3), 251–262. https://doi.org/10.1089/brain.2018.0608

Schaefer, A., Kong, R., Gordon, E. M., Laumann, T. O., Zuo, X.-N., Holmes, A. J., Eickhoff, S. B., & Yeo, B. T. T. (2018). Local-Global Parcellation of the Human Cerebral Cortex from Intrinsic Functional Connectivity MRI. *Cerebral Cortex*, *28*(9), 3095–3114. https://doi.org/10.1093/cercor/bhx179

Scheeringa, R., & Fries, P. (2019). Cortical layers, rhythms and BOLD signals. *NeuroImage*, *197*, 689–698. https://doi.org/10.1016/j.neuroimage.2017.11.002

Scheeringa, R., Petersson, K. M., Oostenveld, R., Norris, D. G., Hagoort, P., & Bastiaansen, M. C. M. (2009a). Trial-by-trial coupling between EEG and BOLD identifies networks

related to alpha and theta EEG power increases during working memory maintenance. *NeuroImage*, *44*(3), 1224–1238. https://doi.org/10.1016/j.neuroimage.2008.08.041

Scheeringa, R., Petersson, K. M., Oostenveld, R., Norris, D. G., Hagoort, P., & Bastiaansen, M. C. M. (2009b). Trial-by-trial coupling between EEG and BOLD identifies networks related to alpha and theta EEG power increases during working memory maintenance. *NeuroImage*, *44*(3), 1224–1238. https://doi.org/10.1016/j.neuroimage.2008.08.041

Schulz, M., Chau, W., Graham, S. J., McIntosh, A. R., Ross, B., Ishii, R., & Pantev, C. (2004). An integrative MEG–fMRI study of the primary somatosensory cortex using cross-modal correspondence analysis. *NeuroImage*, *22*(1), 120–133. https://doi.org/10.1016/j.neuroimage.2003.10.049

Seghier, M. L. (2013). The Angular Gyrus. *The Neuroscientist*, *19*(1), 43–61. https://doi.org/10.1177/1073858412440596

Semel, E., Wiig, E., & Secord, W. A. (2013). *Clinical Evaluation of Language Fundamentals.* (5th ed.). Pearson.

Shafiei, G., Baillet, S., & Misic, B. (2022). Human electromagnetic and haemodynamic networks systematically converge in unimodal cortex and diverge in transmodal cortex. *PLOS Biology*, *20*(8), e3001735. https://doi.org/10.1371/journal.pbio.3001735

Shen, M. D., Shih, P., Öttl, B., Keehn, B., Leyden, K. M., Gaffrey, M. S., & Müller, R.-A. (2012). Atypical lexicosemantic function of extrastriate cortex in autism spectrum disorder: Evidence from functional and effective connectivity. *NeuroImage*, *62*(3), 1780–1791. https://doi.org/10.1016/j.neuroimage.2012.06.008

Siegel-Ramsay, J. E., Romaniuk, L., Whalley, H. C., Roberts, N., Branigan, H., Stanfield, A. C., Lawrie, S. M., & Dauvermann, M. R. (2021). Glutamate and functional connectivity—Support for the excitatory-inhibitory imbalance hypothesis in autism spectrum disorders. *Psychiatry Research: Neuroimaging*, *313*, 111302. https://doi.org/10.1016/j.pscychresns.2021.111302

Singh, K. D., Barnes, G. R., Hillebrand, A., Forde, E. M. E., & Williams, A. L. (2002). Task-Related Changes in Cortical Synchronization Are Spatially Coincident with the Hemodynamic Response. *NeuroImage*, *16*(1), 103–114. https://doi.org/10.1006/nimg.2001.1050

Singh, S. P. (2014). Magnetoencephalography: Basic principles. *Annals of Indian Academy of Neurology*, *17*(Suppl 1), S107. https://doi.org/10.4103/0972-2327.128676

Smith, R. X., Jann, K., Dapretto, M., & Wang, D. J. J. (2018). Imbalance of Functional Connectivity and Temporal Entropy in Resting-State Networks in Autism Spectrum Disorder: A Machine Learning Approach. *Frontiers in Neuroscience*, *12*. https://www.frontiersin.org/journals/neuroscience/articles/10.3389/fnins.2018.00869

Smith, S. M., Jenkinson, M., Woolrich, M. W., Beckmann, C. F., Behrens, T. E. J., Johansen-Berg, H., Bannister, P. R., De Luca, M., Drobnjak, I., Flitney, D. E., Niazy, R. K., Saunders, J., Vickers, J., Zhang, Y., De Stefano, N., Brady, J. M., & Matthews, P. M. (2004). Advances in functional and structural MR image analysis and implementation as FSL. *NeuroImage*, *23*, S208–S219. https://doi.org/10.1016/j.neuroimage.2004.07.051

Sohal, V. S., & Rubenstein, J. L. R. (2019). Excitation-inhibition balance as a framework for investigating mechanisms in neuropsychiatric disorders. *Molecular Psychiatry*, *24*(9), Article 9. https://doi.org/10.1038/s41380-019-0426-0

Strandburg, R. J., Marsh, J. T., Brown, W. S., Asarnow, R. F., Guthrie, D., & Higa, J. (1993). Event-related potentials in high-functioning adult autistics: Linguistic and nonlinguistic visual information processing tasks. *Neuropsychologia*, *31*(5), 413–434. https://doi.org/10.1016/0028-3932(93)90058-8

Szaflarski, J. P., Holland, S. K., Schmithorst, V. J., & Byars, A. W. (2006). fMRI study of language lateralization in children and adults. *Human Brain Mapping*, *27*(3), 202–212. https://doi.org/10.1002/hbm.20177

Tager-Flusberg, H. (2000). Understanding the language and communicative impairments in autism. In L. M. Glidden (Ed.), *Autism* (pp. 185–205). Academic Press.

Takeuchi, M., Harada, M., Matsuzaki, K., Nishitani, H., & Mori, K. (2004). Difference of signal change by a language task on autistic patients using functional MRI. *The Journal of Medical Investigation*, *51*(1–2), 59–62. https://doi.org/10.2152/jmi.51.59

Taxali, A., Angstadt, M., Rutherford, S., & Sripada, C. (2021). Boost in Test–Retest Reliability in Resting State fMRI with Predictive Modeling. *Cerebral Cortex*, *31*(6), 2822–2833. https://doi.org/10.1093/cercor/bhaa390

Tesink, C. M. J. Y., Buitelaar, J. K., Petersson, K. M., Van Der Gaag, R. J., Teunisse, J.-P., & Hagoort, P. (2011). Neural correlates of language comprehension in autism spectrum disorders: When language conflicts with world knowledge. *Neuropsychologia*, *49*(5), 1095–1104. https://doi.org/10.1016/j.neuropsychologia.2011.01.018

Thuwal, K., Banerjee, A., & Roy, D. (2021). Aperiodic and Periodic Components of Ongoing Oscillatory Brain Dynamics Link Distinct Functional Aspects of Cognition across Adult Lifespan. *eNeuro*, *8*(5). https://doi.org/10.1523/ENEURO.0224-21.2021

Trakoshis, S., Martínez-Cañada, P., Rocchi, F., Canella, C., You, W., Chakrabarti, B., Ruigrok, A. N., Bullmore, E. T., Suckling, J., Markicevic, M., Zerbi, V., MRC AIMS Consortium, Baron-Cohen, S., Gozzi, A., Lai, M.-C., Panzeri, S., & Lombardo, M. V. (2020). Intrinsic excitation-inhibition imbalance affects medial prefrontal cortex differently in autistic men versus women. *eLife*, *9*, e55684. https://doi.org/10.7554/eLife.55684

Tsujimoto, T., Shimazu, H., & Isomura, Y. (2006). Direct Recording of Theta Oscillations in Primate Prefrontal and Anterior Cingulate Cortices. *Journal of Neurophysiology*, *95*(5), 2987–3000. https://doi.org/10.1152/jn.00730.2005

Tulay, E. E., Metin, B., Tarhan, N., & Arıkan, M. K. (2019). Multimodal Neuroimaging: Basic Concepts and Classification of Neuropsychiatric Diseases. *Clinical EEG and Neuroscience*, *50*(1), 20–33. https://doi.org/10.1177/1550059418782093

Tzourio-Mazoyer, N., Perrone-Bertolotti, M., Jobard, G., Mazoyer, B., & Baciu, M. (2017). Multi-factorial modulation of hemispheric specialization and plasticity for language in healthy and pathological conditions: A review. *Cortex*, *86*, 314–339. https://doi.org/10.1016/j.cortex.2016.05.013

Uddin, L., Supekar, K., & Menon, V. (2013). Reconceptualizing functional brain connectivity in autism from a developmental perspective. *Frontiers in Human Neuroscience*, *7*. https://www.frontiersin.org/articles/10.3389/fnhum.2013.00458

Ullsperger, M., & Debener, S. (Eds.). (2010). *Simultaneous EEG and fMRI: Recording, analysis, and application*. Oxford University Press.

Uzunova, G., Pallanti, S., & Hollander, E. (2016). Excitatory/inhibitory imbalance in autism spectrum disorders: Implications for interventions and therapeutics. *The World Journal of Biological Psychiatry*, *17*(3), 174–186. https://doi.org/10.3109/15622975.2015.1085597

Valdizán, J. R., Abril-Villalba, B., Méndez-García, M., Sans-Capdevila, O., Pablo, M. J., Peralta, P., Lasierra, Y., & Bernal-Lafuente, M. (2003). Cognitive evoked potentials in autistic children. *Neurologique*, *36*(5), 425–428.

Vallinoja, J., Nurmi, T., Jaatela, J., Wens, V., Bourguignon, M., Mäenpää, H., & Piitulainen, H. (2024). Functional connectivity of sensorimotor network is enhanced in spastic diplegic cerebral palsy: A multimodal study using fMRI and MEG. *Clinical Neurophysiology*, *157*, 4–14. https://doi.org/10.1016/j.clinph.2023.10.014

van Heuven, W. J. B., Mandera, P., Keuleers, E., & Brysbaert, M. (2014). Subtlex-UK: A new and improved word frequency database for British English. *Quarterly Journal of Experimental Psychology*, *67*(6), 1176–1190. https://doi.org/10.1080/17470218.2013.850521

Vartiainen, J., Liljeström, M., Koskinen, M., Renvall, H., & Salmelin, R. (2011). Functional Magnetic Resonance Imaging Blood Oxygenation Level-Dependent Signal and Magnetoencephalography Evoked Responses Yield Different Neural Functionality in Reading. *Journal of Neuroscience*, *31*(3), 1048–1058. https://doi.org/10.1523/JNEUROSCI.3113-10.2011

Verly, M., Verhoeven, J., Zink, I., Mantini, D., Oudenhove, L. V., Lagae, L., Sunaert, S., & Rommel, N. (2014). Structural and functional underconnectivity as a negative predictor for language in autism. *Human Brain Mapping*, *35*(8), 3602–3615. https://doi.org/10.1002/hbm.22424

Verstynen, T., Diedrichsen, J., Albert, N., Aparicio, P., & Ivry, R. B. (2005). Ipsilateral Motor Cortex Activity During Unimanual Hand Movements Relates to Task Complexity. *Journal of Neurophysiology*, *93*(3), 1209–1222. https://doi.org/10.1152/jn.00720.2004

Voytek, B., Kramer, M. A., Case, J., Lepage, K. Q., Tempesta, Z. R., Knight, R. T., & Gazzaley, A. (2015). Age-Related Changes in 1/f Neural Electrophysiological Noise. *Journal of Neuroscience*, *35*(38), 13257–13265. https://doi.org/10.1523/JNEUROSCI.2332-14.2015

Wang, J., Barstein, J., Ethridge, L. E., Mosconi, M. W., Takarae, Y., & Sweeney, J. A. (2013). Resting state EEG abnormalities in autism spectrum disorders. *Journal of Neurodevelopmental Disorders*, *5*(1), 24. https://doi.org/10.1186/1866-1955-5-24

Waschke, L., Donoghue, T., Fiedler, L., Smith, S., Garrett, D. D., Voytek, B., & Obleser, J. (2021). Modality-specific tracking of attention and sensory statistics in the human electrophysiological spectral exponent. *eLife*, *10*, e70068. https://doi.org/10.7554/eLife.70068

Watanabe, T., Rees, G., & Masuda, N. (2019). Atypical intrinsic neural timescale in autism. *eLife*, *8*, e42256. https://doi.org/10.7554/eLife.42256

Wechsler, D. (2009). *Wechsler Individual Achievement Test* (3rd ed.). Psychological Corporation.

Wechsler, D. (2011). *Wechsler Abbreviated Scale of Intelligence* (2nd ed.). NCS Pearson.

Weinberg, B. D., Kuruva, M., Shim, H., & Mullins, M. E. (2021). Clinical applications of magnetic resonance spectroscopy (MRS) in of brain tumors: From diagnosis to treatment. *Radiologic Clinics of North America*, *59*(3), 349–362. https://doi.org/10.1016/j.rcl.2021.01.004

Weismer, S. E., Kaushanskaya, M., Larson, C., Mathée, J., & Bolt, D. (2018). Executive function skills in school-age children with autism spectrum disorder: Association with language abilities. *Journal of Speech, Language, and Hearing Research*, *61*(11), 2641–2658. https://doi.org/10.1044/2018_JSLHR-L-RSAUT-18-0026

Weng, S.-J., Wiggins, J. L., Peltier, S. J., Carrasco, M., Risi, S., Lord, C., & Monk, C. S. (2010). Alterations of resting state functional connectivity in the default network in adolescents with autism spectrum disorders. *Brain Research*, *1313*, 202–214. https://doi.org/10.1016/j.brainres.2009.11.057

Wilkinson, C. L., Gabard-Durnam, L. J., Kapur, K., Tager-Flusberg, H., Levin, A. R., & Nelson, C. A. (2020). Use of Longitudinal EEG Measures in Estimating Language Development in Infants With and Without Familial Risk for Autism Spectrum Disorder. *Neurobiology of Language*, *1*(1), 33–53. https://doi.org/10.1162/nol_a_00002

Wilkinson, C. L., & Nelson, C. A. (2021). Increased aperiodic gamma power in young boys with Fragile X Syndrome is associated with better language ability. *Molecular Autism*, *12*(1), 17. https://doi.org/10.1186/s13229-021-00425-x

Wilkinson, M., Jao Keehn, R. J., Linke, A. C., You, Y., Gao, Y., Alemu, K., Correas, A., Rosen, B. Q., Kohli, J. S., Wagner, L., Sridhar, A., Marinkovic, K., & Müller, R.-A. (2022). fMRI BOLD and MEG theta power reflect complementary aspects of activity during

lexicosemantic decision in adolescents with ASD. *Neuroimage: Reports*, *2*(4), 100134. https://doi.org/10.1016/j.ynirp.2022.100134

Winterer, G., Carver, F. W., Musso, F., Mattay, V., Weinberger, D. R., & Coppola, R. (2007). Complex relationship between BOLD signal and synchronization/desynchronization of human brain MEG oscillations. *Human Brain Mapping*, *28*(9), 805–816. https://doi.org/10.1002/hbm.20322

Wise, S. P. (1985). The primate premotor cortex: Past, present, and preparatory. A. *Annual Review of Neuroscience*, *8*, 1–9.

Xue, M., Atallah, B. V., & Scanziani, M. (2014). Equalizing excitation–inhibition ratios across visual cortical neurons. *Nature*, *511*(7511), Article 7511. https://doi.org/10.1038/nature13321

Yamagata, B., Itahashi, T., Fujino, J., Ohta, H., Nakamura, M., Kato, N., Mimura, M., Hashimoto, R., & Aoki, Y. (2019). Machine learning approach to identify a resting-state functional connectivity pattern serving as an endophenotype of autism spectrum disorder. *Brain Imaging and Behavior*, *13*(6), 1689–1698. https://doi.org/10.1007/s11682-018-9973-2

Yang, X., Zhang, N., & Schrader, P. (2022). A study of brain networks for autism spectrum disorder classification using resting-state functional connectivity. *Machine Learning with Applications*, *8*, 100290. https://doi.org/10.1016/j.mlwa.2022.100290

Yao, S., Becker, B., & Kendrick, K. M. (2021). Reduced Inter-hemispheric Resting State Functional Connectivity and Its Association With Social Deficits in Autism. *Frontiers in Psychiatry*, *12*. https://www.frontiersin.org/journals/psychiatry/articles/10.3389/fpsyt.2021.629870

Ye, A. X., Leung, R. C., Schäfer, C. B., Taylor, M. J., & Doesburg, S. M. (2014). Atypical resting synchrony in autism spectrum disorder. *Human Brain Mapping*, *35*(12), 6049–6066. https://doi.org/10.1002/hbm.22604

Yerys, B. E., Antezana, L., Weinblatt, R., Jankowski, K. F., Strang, J., Vaidya, C. J., Schultz, R. T., Gaillard, W. D., & Kenworthy, L. (2015). Neural correlates of set-shifting in children with autism. *Autism Research*, *8*(4), 386–397. https://doi.org/10.1002/aur.1454

Yizhar, O., Fenno, L. E., Prigge, M., Schneider, F., Davidson, T. J., O'Shea, D. J., Sohal, V. S., Goshen, I., Finkelstein, J., Paz, J. T., Stehfest, K., Fudim, R., Ramakrishnan, C., Huguenard, J. R., Hegemann, P., & Deisseroth, K. (2011). Neocortical excitation/inhibition balance in information processing and social dysfunction. *Nature*, *477*(7363), 171–178. https://doi.org/10.1038/nature10360

Yoshimura, Y., Kikuchi, M., Shitamichi, K., Ueno, S., Munesue, T., Ono, Y., Tsubokawa, T., Haruta, Y., Oi, M., Niida, Y., Remijn, G. B., Takahashi, T., Suzuki, M., Higashida, H., & Minabe, Y. (2013). Atypical brain lateralisation in the auditory cortex and language performance in 3- to 7-year-old children with high-functioning autism spectrum disorder:

A child-customised magnetoencephalography (MEG) study. *Molecular Autism*, *4*, 38. https://doi.org/10.1186/2040-2392-4-38

You, Y., Correas, A., Jao Keehn, R. J., Wagner, L. C., Rosen, B. Q., Beaton, L. E., Gao, Y., Brocklehurst, W. T., Fishman, I., Müller, R.-A., & Marinkovic, K. (2021). MEG theta during lexico-semantic and executive processing Is altered in high-functioning adolescents with autism. *Cerebral Cortex*, *31*(2), 1116–1130. https://doi.org/10.1093/cercor/bhaa279

You, Y., Correas, A., White, D. R., Wagner, L. C., Jao Keehn, R. J., Rosen, B. Q., Alemu, K., Müller, R.-A., & Marinkovic, K. (2023). Mapping access to meaning in adolescents with autism: Atypical lateralization and spatiotemporal patterns as a function of language ability. *NeuroImage : Clinical*, *39*, 103467. https://doi.org/10.1016/j.nicl.2023.103467

Youssofzadeh, V., & Babajani-Feremi, A. (2019). Mapping critical hubs of receptive and expressive language using MEG: A comparison against fMRI. *NeuroImage*, *201*, 116029. https://doi.org/10.1016/j.neuroimage.2019.116029

Yuk, V., Dunkley, B. T., Anagnostou, E., & Taylor, M. J. (2020). Alpha connectivity and inhibitory control in adults with autism spectrum disorder. *Molecular Autism*, *11*, 95. https://doi.org/10.1186/s13229-020-00400-y

Zhang, Z., Peng, P., & Zhang, D. (2020). Executive function in high-functioning autism spectrum disorder: A meta-analysis of fMRI studies. *Journal of Autism and Developmental Disorders*, *50*(11), 4022–4038. https://doi.org/10.1007/s10803-020-04461-z

Zumer, J. M., Brookes, M. J., Stevenson, C. M., Francis, S. T., & Morris, P. G. (2010). Relating BOLD fMRI and neural oscillations through convolution and optimal linear weighting. *NeuroImage*, *49*(2), 1479–1489. https://doi.org/10.1016/j.neuroimage.2009.09.020